GEOTECHNICAL CONSIDERATIONS FOR ONSHORE WIND TURBINES

Adapting Knowledge and Experience for Founding on South African Pedocretes

BY

MR CHARLES JOHN WARREN-CODRINGTON

SUPERVISED BY DR DENIS KALUMBA

A dissertation submitted in partial fulfilment for the degree of Master of Science in Engineering

University of Cape Town

Department of Civil Engineering

November 2013

PREFACE

This dissertation was submitted in partial fulfilment for the Degree of Master of Science in Engineering, in Civil Engineering, at the University of Cape Town. It is the culmination of two years of research and learning in the field of geotechnical and structural engineering.

The following study stemmed from the rapidly growing interest in wind energy throughout South Africa. The Geotechnical Engineering Research Group at the University of Cape Town recognised a need to apprise South African engineers on the behaviour of wind turbine structures and the geotechnical design thereof, given the novelty of the respective technology and the information void in South Africa. Simultaneously, this thesis was designed to serve as a design aid for any practicing engineer working within South Africa in the field of wind energy, or the field of dynamic-foundation design, as key geological characteristics of pedocrete and associated materials were presented within a framework of dynamic-foundation design.

This dissertation drew on current research and engineering experience in the fields of structural mechanics, dynamics and geotechnical engineering, to provide a consolidated piece of work relating to the design of wind turbine foundations operating within South African geotechnical conditions. In doing so I, Charles Warren-Codrington, declare the following:

1. I am presenting this dissertation in partial fulfilment of the requirements for my degree.
2. I know the meaning of plagiarism and declare that all of the work in the dissertation, save for that which is properly acknowledged, is my own.
3. I hereby grant the University of Cape Town free licence to reproduce for the purpose of research, either the whole or any portion of the contents, in any manner whatsoever of the following dissertation.

Mr Charles John Warren-Codrington

Signature: _____

Date: _____

GEOTECHNICAL CONSIDERATIONS FOR ONSHORE WIND TURBINES:

Adapting Knowledge and Experience for Founding on South African Pedocretes

By

Mr Charles John Warren-Codrington

Supervised by Dr Denis Kalumba

Wind energy has been placed at the centre of the South African Government's Renewable Energy Independent Producer Programme (REIPPP) with the purpose of addressing electricity capacity deficits and poor service delivery. In doing so, substantial wind farm development has been proposed for the Western, Eastern and Northern Cape of South Africa, with several projects already underway.

Wind energy, from a technological standpoint, is regarded as a mature form of renewable energy. However, much of the wind turbine geotechnical experience was gained in the temperate climate of the Northern Hemisphere, where soil conditions differ significantly from those of South Africa. Simultaneously, although mature, wind energy is a novel field in South Africa. Therefore, this study sought the need bridge the gap between local South African soil conditions and international wind energy experience.

It was against this backdrop that the following study was initiated, which aimed to provide insight into the site-specific geotechnical design of foundations for wind turbine structures. In doing so, this major objective was divided into four minor objectives, each contributing a major theme to the study, the key points of which are summarised below. It should be noted that the following study was limited to three-blade wind turbines mounted on conical tubular steel towers with shallow foundations.

Part I: Mechanics, Dynamics and Foundation Behaviour assessed the different components of wind turbine structures and assessed the loading regimes and the response of the structure to those loads with the aim of identifying key loading characteristics requiring resistance by the foundation. The dynamic nature of the structure was deemed critical, where separation of the rotor frequency (1P) and the blade passing frequency (3P) from the natural frequency of the tower-foundation-soil system was the central to the structure's stability. Also, the foundation was shown to reduce the natural frequency of the system. Secondly, the dynamic nature of the structure causes the aerodynamic

loading to be greater than what would be expected from a static structure of equal cross-sectional area. This coupled with the slender nature of wind turbine structures, and their relative low weight, creates a substantial overturning moment.

These considerations were tackled in **Part II: Geotechnical Design of Shallow Foundations** by two approaches: (1) strength and stability considerations and (2) settlement and stiffness considerations. The former addressed the ultimate limit state design of shallow foundations, with emphasis on resisting eccentric loading by means of the generalised bearing capacity theory and the yield surface approach, which showed defined the limiting horizontal and moment loads as $H \approx V_{max}/8$ and $M/2r \approx V_{max}/11$, respectively (Butterfield and Gottardi, 1994). The elastic displacement theory was presented in view of assessing the differential settlement of wind turbine foundations. Critically, it was shown that the stiffening of conventional pad, or gravity foundations, by means of piles was only beneficial if the pile dimensions are proportioned such that they convey the major portion of the foundation load.

Part III: Dynamic Aspects of Wind Turbine Foundations characterised the vibrations generated to be of a long-term nature, inducing low magnitudes of shear strain in the subgrade. Hence, the system was deemed to be elastic in nature. However, the cyclic degradation of soil stiffness due to excessively large number stress cycles was regarded as important, and hence the Ramberg-Osgood and hyperbolic models were presented to model stiffness degradation. Also, the parameters affecting soil stiffness were presented, and chiefly consisted of the confining stress and void ratio for granular materials and the Over Consolidation Ratio (OCR) and time of confinement for cohesive materials. This discourse on the properties of materials under dynamic and cyclic loading was followed by an analysis of dynamically loaded footings on the surface of an elastic half-space. *Lysmer's Analog* was used to bridge the gap between elastic half-space theory and the lumped parameter mode, which revealed interesting points:

1. Flexible foundations are likely to undergo larger amplitudes of vibration;
2. Rigid layers below footing impede the radiation of stress away from the footing, and exacerbate the oscillation of the footing;
3. Coupled rocking and sliding modes of vibration were deemed the most likely for wind turbine foundations, based on the slenderness and dynamic characteristics of the loading.

The concepts and theory dealt with in Parts I-III were consolidated linked back to South African geological conditions prevalent along the western coast and northern interior. Pedocrete materials were of particular interest due to the founding and material testing challenges presented. Thus, **Part IV: Considerations for Founding Wind Turbines on Pedocretes** firstly defined and characterised the engineering properties of pedocretes. The major engineering characteristics of concern included the variable consistency of pedocrete profiles, the contradiction between plasticity and compaction properties, poor grading and changes in engineering characteristics under drying and disturbance.

This was followed by an assessment of the founding challenges presented by the vertical and lateral profile variability and the problems associated with collapsible soil fabrics. The following key points were made:

1. Founding on rigid pedocrete layers should only be done if the thickness and lateral consistency have been evaluated.
2. Anchoring wind turbine foundations into rigid pedocrete layers, or using such layers to produce a rafting effect should also only be done alongside a thorough site investigation process.
3. The collapse potential of pedocretes and associated soils should be assessed to minimise the likelihood of differential settlement, either by collapse of the material, or by an inappropriately selected ground improvement technique.

Therefore, in-situ geophysical methods were regarded as the most appropriate means of assessing the soil stiffness of pedocrete materials and associated collapsible profiles, as these methods would encapsulate the soil variability and test the material under its in-situ stress and drainage conditions. Of the geophysical methods available, Continuous Surface Wave (CSW) tests were deemed most appropriate as the depth of influence may be varied and damping properties may be assessed. Damping and stiffness degradation may also be assessed by means of laboratory tests; however, these require undisturbed samples of the highest quality, advanced laboratory equipment and experienced personnel.

The benefits of integrating the fields of structural and geotechnical engineering during the design of wind turbine structures was emphasised by this study, as it allowed the construction of relationships between soil mechanics and structural mechanics which aided the optimisation of the respective problem.

ACKNOWLEDGEMENTS

This research was made possible through the continuous support of many people, of whom it is important to acknowledge and thank.

Firstly, thank you to my supervisor, Dr Denis Kalumba, who provided valuable support and guidance throughout the period of this work for which I am extremely grateful. I am also appreciative of your boundless energy and positive attitude, which made this study enjoyable and stimulating.

Thank you to Mr Patrick Beales, of *Kantey and Templer Consulting Engineers*, for your willingness to provide guidance and thought provoking advice, which spurred this study on. Not only have you been an integral part of this research, but you have also played a hugely influential role in my development as an engineer and in nurturing my interest in geotechnical engineering.

The advice and resources provided by Dr Peter Day, Prof Gerhard Heymann and Mr Iain Paton with respect to wind turbine foundations and geophysical testing, respectively, is highly appreciated. In addition, I would like to thank Dr Frank Netterberg for his willingness to provide support and advice on the behaviour of pedocrete materials.

My postgraduate studies would not have been possible without the financial support of *SMEC Africa*, for which I am highly appreciative.

Lastly, and most importantly, thank you to my friends and family for your unconditional love and support throughout my studies and research, without which this task would have been insurmountable.

For my parents

CONTENTS

NOTATION

The selection of notation used throughout this dissertation was done based on the standard nomenclature adopted by the International Society of Soil Mechanics and Foundation Engineering (ISSMFE). However, some symbols have been selected to conform to other engineering disciplines incorporated in this dissertation. The distinctions are made clear in the text. Symbols are defined where they first appear in the text. Those which appear several times are listed below. The SI unit convention was utilised.

Acronyms

1P	Rotational frequency
3P	Blade passing frequency
CSW	Continuous Surface Wave Test
ERS	Electrical Resistivity Survey
FEM	Finite Element Method
GRP	Glass-fibre Reinforced Polymer
GW	Giga-watts
HAWT	Horizontal Axis Wind Turbine
IDZ	Industrial Development Zone
iCK	Gestamp iConkrete
IEC	International Electrotechnical Commission
IPP	Independent Power Producer
kWh	Kilowatt Hour
MASW	Multi-channel Analysis of Surface Waves
MW	Megawatt
OCR	Over Consolidation Ratio
PI	Plasticity Index
REIPP	Renewable Energy Independent Power Producer
REFIT	Renewable Energy Feed-in-tariff
R-O	Ramberg-Osgood model
SASW	Spectral Analysis of Surface Waves
SDOF	Single Degree of Freedom
SPT	Standard Penetrometer Test

Geometrical Constants

$A_{footing}$	Plan area of footing
B	Foundation breadth
B', L', A'	Effective base dimensions and area
d	Depth of foundation
L	Foundation length
m	Lumped mass of system
r	Radius
t	Thickness

Coordinate System

x, y, z	Rectangular coordinates
w, u, θ	Vertical, lateral and rotational displacements of footing

Material Parameters

c'	Effective soil cohesion
c_u	Undrained soil cohesion
E	Young's modulus
G	Shear modulus
G_{max}	Small strain shear modulus
ν	Poisson's ratio
ϕ'	Internal angle of friction
I	Second moment of area

Subscripts

c	Critical
dyn	Dynamic parameter
f	Foundation parameter
max	Maximum
p	Pile
s	Soil
β, ς	Flap-wise, edge-wise
x, y, z	Rectangular coordinates

Symbols

$\mathrm{A(z)}$	Cross-sectional area of tower
a'	Effective elliptical area
A_Δ	Area of hysteretic triangle
A_{loop}	Area of hysteretic loop
A_z	Amplitude of steady-state vibration
$\bar{a}_0$	Frequency factoy
B	Breadth of foundation
b_e	Minor axis of ellipse
$\bar{\boldsymbol{B}}$	Mass factor
c	Chord length
C	Slope of Chin (1971) transformation
C_D	Coefficient of drag
C_L	Coefficient of lift
C_Q	Torque coefficient
C_T	Thrust coefficient
C_m	Grain characteristics
c_z	Damping for vertical oscillation
c_x, c_y	Damping for horizontal oscillation
$c_{\varphi x}, c_{\varphi y}$	Damping for rotational oscillation
$c_{\psi x}$	Damping for torsional oscillation
$c_{z,c}$	Critical damping coefficient
$C_{1,2,3,4,\mathrm{n}}$	Constants of differentiation
$\bar{c}_{x1}$	Impedence functions for embedded foundation
$D(z)$	Tower diameter
d	Depth of founding

d_c, d_q, d_γ	Bearing capacity depth factors
$D = 2r$	Diameter of footing
D_p	Diameter of pile
D_r	Relative density
D	Dynamic amplification factor
e_x, e_y	Eccentricity in respective direction
e	Void ratio
e	Eccentricity of rotating mass
F_L	Lift force
F_D	Drag force
$F_W(h)$	Aerodynamic lateral force
F_{YE}	Aerodynamic drag forces acting on the nacelle and rotor
$F_{ZE}(h)$	Load due to the weight of the rotor, nacelle and tower
f_m	Resonant cyclic frequency
g	Gravitational acceleration
H	Tower hub height
h	Reference height
H	Horizontal load applied to footing
H'	Adjusted horizontal load for the effect of torque
H	Thickness of soil layer to bedrock
i'_c, i_q, i_γ	Inclination factors
I_s	Foundation influence factor
I_ψ, I_φ	Mass moment of inertia for rocking and torsional oscillation
K_p	Coefficient of passive earth pressure
k_e	Equivalent stiffness
K_z	Vertical coefficient of stiffness
K_h	Horizontal coefficient of stiffness
K_θ	Rotational coefficient of stiffness
k	Modulus of subgrade reaction
K_{f-s}	Foundation-soil stiffness
K_{p-f}	Stiffness of piled foundation
K_{pg}	Stiffness of pile group
K_f	Stiffness of footing
K_p	Stiffness of pile
K	Bulk modulus
k_z	Stiffness for vertical oscillation
k_x, k_y	Stiffness for horizontal oscillation
k_φ	Stiffness for rocking oscillation
l	Length
M_{max}	Maximum bending moment
$M(x)$	Bending moment
M_β	Flap-wise moment
M_ς	Edge-wise bending moment
$M_X(h)$	Moment due to the aerodynamic forces acting on the rotor
M_Y, M_Z	Moments from the rotation of the rotor
$M_W(h)$	Aerodynamic bending moment
M_x, M_y, M_z	Moment load applied to footing with axis of rotation defined by subscript
m	Lumped mass of system
M	Lumped mass of frequency-dependent forcing
N	Number of loading cycles

P	Power
Q	Mean torque
q	Uniformly applied load
$q(x)$	Subgrade reaction
Q_{p-f}	Load capacity of piled foundation
Q_{pg}	Load capacity of pile group
Q_f	Load capacity of footing
Q_0	Amplitude of sinusoidal force
R	Blade radius
r_γ	Bearing capacity reduction factor for large bases
r	Radius of footing
S_β	Edge-wise shear stress
St	Strouhal number
s_c, s_q, s_γ	Bearing capacity shape factors
s_t	Total settlement
s_i	Immediate settlement
s_c	Consolidation/primary settlement
s_s	Secondary/creep settlement
Δs^*	Normalised differential settlement
S	Degree of saturation
$\bar{s}_{z1}$	Impedence functions for embedded foundation
T	Thrust moment
T_r	Transmissibility index
u	Pore water pressure
Δu	Change in pore water pressure
U	Inflow airstream velocity
t_f	Foundation thickness
t	Geological time
V_f	Ultimate load capacity of footing
$V(z)$	Wind velocity
v_r	Critical wind velocity
V_{max}	Maximum vertical load capacity of footing ignoring overburden effect
V	Vertical load applied to footing
W	Relative inflow wind velocity
w^*	Foundation tilt
$\ddot{x}, \dot{x}, x$	Acceleration, velocity and displacement
$\bar{y}$	Lever arm
z	Depth
z_s	Static deflection
$z_c(t)$	Complementary solution
$z_p(t)$	Particular solution
β	Frequency ratio
γ	Soil unit weight
γ_a	Shear strain at point of inversion in load cycle
γ_r	Reference shear strain
γ_f	Shear strain at failure
γ_{tl}	Shear strain linear elastic threshold
γ_{tv}	Volumetric cyclic threshold
γ_{td}	Degradation threshold
γ_{tf}	Shear strain failure threshold
$\gamma_{0.7}$	Shear strain corresponding to $0.7G_{max}$

γ_c	Cyclic shear strain	ψ	Azimuth angle
γ_{xz}	Shear strain	Ω	Rotor rotational speed
$\delta(x)$	Beam deflection		
ε_z	Vertical normal strain		
ε_x	Lateral normal strain		
	Damping ratio		
ζ_{max}	Maximum damping ratio		
ζ_z	Damping ratio		
ρ	Material density		
ρ_t	Density of tower material		
$\overline{\sigma_0}'$	Effective confining stress		
σ_{max}	Maximum bending stress		
$\sigma_{\beta,max}$	Maximum flap-wise bending stress		
σ_0	Total normal vertical stress		
σ_0'	Effective normal vertical stress		
σ_f'	Ultimate bearing pressure		
$\Delta\sigma_x$	Change in lateral stress		
$\Delta\sigma_z$	Change in vertical stress		
$\tau_{xz} = \tau_{zx}$	Shear stress		
τ_f	Shear strength at failure		
v_S	Shear wave velocity		
v_R	Rayleigh wave velocity		
θ, φ	Phase angles		
ω	Frequency of sinusoidal force		
ω_n	Natural (angular) frequency		
ω_m	Resonant (angular) frequency		
ω_d	Damped natural frequency		

TABLES

FIGURES

1. INTRODUCTION

1.1 BACKGROUND

1.1.1 South Africa's Energy Culture

Two major issues underpin any discussion on energy in South Africa. The first relates to the fact that over a quarter of the population lack access to electricity, as well as other basic services such as water, sanitation, housing and transport. The second is the country's concurrent dependency on fossil fuels for electricity production. This dependency is engrained in the country's *energy culture*, as Philip Duguay (2011) described it. The term *energy culture* encapsulates the notion that the country relies on coal for the majority of its electricity supply, on account of its vast coal reserves and the necessary resources to extract it. Furthermore, this fossil fuel industry provides thousands of jobs as well as the stable supply base upon which South Africa's steel, automotive and mining industries have been founded. Hence, the nation faces the challenge of addressing these socio-economic issues with the added pressure of growing environmental and natural resource constraints.

It is against this backdrop that potential solutions have been debated and developed at government level, one being the implementation of wind energy.

1.1.2 Wind Energy in South Africa

There has been much controversy surrounding the idea of wind energy, which has been placed at the centre of the South African Government's Renewable Energy Independent Power Provider Programme (REIPPP). However, debating the implementation of wind energy in South Africa fell outside of the scope of this study. Instead, South Africa's potential for wind energy development was acknowledged on two grounds. The first was with regard to the country's ever increasing need to need to diversify its energy mix in the face of growing electricity demand, deficits in service delivery and natural resource depletion. The second was based on the country's topographical and meteorological characteristics which, when combined, make the South African coastal regions highly suitable to wind farm development, especially in the Northern, Western and Eastern Cape coastal regions (Szewczuk and Prinsloo, 2010), referred to as the *Southern Cape* and *Northern Interior* from herein.

(a)

(b)

Figure 1.1 **South African wind farms: (a) Darling Wind Farm (Wilkinson, 2008) and (b) Klipheuwel Wind Energy Research Facility (Warrenski, 2010)**

These positive impacts were exemplified by the commissioning of the Klipheuwel Wind Energy Research Facility (Figure 1.1 (a)) in 2003. This was followed by Darling Wind Farm (Figure 1.1 (a)), South Africa's first commercial wind energy facility, and Coega Wind Farm more recently. Darling Wind Farm went online in 2008 and comprised four wind turbines with a total capacity of 5.2 MW.

The Coega Industrial Development Zone (IDZ), to the north of Port Elizabeth, has plans for wind farm of 24 turbines. One turbine was commissioned in 2010 primarily as a pilot project. The sole 1.8 MW turbine was erected in time to supplement Port Elizabeth's energy needs during the 2010 FIFA World Cup, and has done so since. The anticipated wind farm at the Coega IDZ is one of many proposed wind farms for the Southern Cape region. This area has experienced a surge of interest from independent power producers (IPP) since 2009. This has been due to the lucrative Renewable Energy Feed-in-tariff (REFIT) offered to IPPs in South Africa. Hence, there are currently 40 wind farms, incorporating up to 2800 wind turbines, proposed for the Western Cape region (Hartdegen, 2011) and approximately 31 wind farms planned for the Eastern Cape.

It was against this milieu of imminent growth in South Africa's wind energy sector that this study was conducted, to provide insight into one of the fundamental issues facing wind farm development: founding wind turbine structures for site specific conditions.

1.2 FOUNDATION ENGINEERING: ITS IMPORTANCE IN WIND TURBINE DESIGN

Wind turbine structures are designed to convert the kinetic energy of the wind to mechanical energy by means of aerodynamic lift forces acting on a rotor. The mechanical energy is then used to drive a generator to produce electrical energy (Burton et al., 2008). Wind turbines may be placed either onshore or at sea (offshore), each application having its own set of positive and negative attributes. This dissertation was concerned with the design of foundations for onshore wind turbines operating under geological conditions prevalent in South Africa.

The foundation, or *substructure*, is that part of an engineered system that transfers to, and into, the underlying soil or rock any loads emanating from the supported structure (Byrne and Houlsby, 2003). It is critical that the foundation can withstand all the possible loads transferred to it, especially during extreme environmental conditions. What is fundamental to this process is the fact that a foundation provides an interface between the structure and the underlying strata. A thorough understanding of this interface, and the load transfer mechanisms present, are required by the foundation engineer in order to deliver a safe and efficient design. A key consideration concerning wind turbine foundations is the dynamic nature of the loading and resulting soil-structure interaction. This is an inter-disciplinary field which incorporates structural mechanics and dynamics as well as geotechnical engineering. Hence, it is often an interaction which is poorly understood within both fields (Wolf and Song, 2002). The understanding of the soil-structure interface is dependent on the respective geology, and thus, is site specific.

The current trend within the wind energy industry is not to site-optimise wind turbine structures, but rather to produce a selection of standard wind turbines in order to keep manufacturing costs low. The task then is to choose a standard wind turbine from this selection and verify that it is capable of withstanding the required limit states for the given location (DNV/Risø, 2002). However, foundation design is required to be carried out with respect to the specific site conditions, which may vary considerably across a wind farm. This results in two components of wind turbine foundation design which formed the core of the following study:

1. A sound understanding of the structure to be founded, the loading it is subjected to and its response thereof.
2. Experience and knowledge of the local soil and rock conditions prevalent on site as well as the geotechnical processes and practises of the respective area or country.

1.3 THEMES AND OBJECTIVES OF THIS WORK

1.3.1 Thesis Objectives

The major objective of this thesis was to provide insight into the site-specific geotechnical design of foundations for wind turbine structures, within a South African geological context. The major objective was divided into four minor objectives, which aimed to:

1. Give an introduction to the mechanics and dynamics of wind turbine structures with the purpose of conveying an understanding of the nature and type of loads transmitted to the foundation and critical loading cases.
2. Present fundamental principles of foundation engineering and soil mechanics pertaining to the design of foundations for supporting the type and nature of loads transferred from wind turbine structures.
3. Study the problem pertaining to dynamically loaded foundations, including a qualitative assessment of the effects of dynamic loading on soils and the analysis of dynamically loaded foundations.
4. To provide insight into the determination of subgrade stiffness and damping properties against the backdrop of geological characteristics prevalent in South Africa.

1.3.2 Scope and Delimitation

Foundation engineering and principles of soil mechanics formed the centre of this study, which was focussed on providing insight into the structural mechanics of shallow foundations under a combination of monotonic and dynamic loading. More specifically, this study sought to provide key considerations pertaining to the geotechnical design of wind turbine foundations, specifically with regard to the qualitative and quantitative assessment of foundation stability and stiffness. A soil-structure interaction approach, centred on the *lumped parameter model,* was adopted in order to achieve this. Thus, the following subject matter formed the core of this study:

1. Rotor dynamics, with emphasis on the *ideal rigid rotor model;*
2. Structural dynamics of wind turbine towers based on the lumped parameter model;
3. The design of shallow foundations for combined loading, including the yield surface approach;
4. Principles of soil-structure interaction focussed on the problem of dynamic and static stiffness, and;
5. The behaviour of soils under dynamic and cyclic loading within strain levels common to wind turbine structures.

The determination of stiffness and damping parameters using geotechnical field and laboratory techniques were presented within a South African geological context relevant to the Southern Cape Northern Interior of South Africa. In particular, considerations pertaining to founding and the determination of soil stiffness and damping on pedocrete and collapsible soils were presented.

Control and electrical aspects of wind turbine structures were not explored in the following chapters, neither was the design of components which make up the superstructure, such as the rotor, nacelle and tower. Furthermore, although introduced, the following topics were not explored in detail:

1. The design of the connection between the tower and foundation;
2. The structural design of foundations;
3. Grounding of wind turbine structures with respect to electrical resistivity of the foundation and soil.

The environmental conditions and aspects related to durability were not presented. Also, aspects related to the economic, environmental, political and social impact of wind turbines were omitted.

These decisions were made on the basis that this thesis aimed to present information that would supplement that of wind turbine design codes, manuals and specifications instead of re-producing that material. In doing so, it attempted to aid engineers in the geotechnical design and optimisation of wind turbine foundations through a better understanding of the load transfer-mechanisms at hand and the influence of key-geological characteristics of South Africa. This was through constructing relationships between key structural behaviour of these structures, and the qualitative and quantitative response of foundations to combined loading of a static and dynamic nature.

1.3.3 Audience

This thesis was intended for geotechnical engineers working in the wind energy field. An understanding of structural mechanics, geotechnical and structural engineering is required. Furthermore, it provides a base upon which practitioners or researchers may model or analyse wind turbine foundations, or develop an understanding of key aspects of dynamic soil-structure interaction.

1.4 THESIS STRUCTURE

The current chapter provided an introduction to this study, including the aims, scope and structure as well as a background to wind energy in South Africa. These topics fell within Chapter 1: Introduction.

In order to achieve the principle objectives stated in Chapter 1 in a clear and concise manner, the body of this thesis was divided into four parts, the details of which are explained below, and summarised by Figure 1.2.

Part I aimed to present an overview of the key loading and structural response aspects directly related to foundation design. It incorporated Chapter 2: Mechanics and Dynamics of Wind Turbine Structures and Chapter 3: Introduction to Wind Turbine Foundation Behaviour.

Components of shallow foundation design and soil-structure interaction principles were studied in **Part II**, which comprised Chapter 4: Strength and Stability Considerations and Chapter 5: Settlement and Stiffness Considerations.

Part II served the primary purpose of presenting the key considerations pertaining to the stability and displacement of the foundation. **Part III** explored the dynamically loaded foundation problem which was divided into Chapter 6: Behaviour of Foundation-soil Systems under Dynamic and Cyclic Loading and Chapter 7: Analysis of Foundations under Dynamic Loads on Elastic Media.

Part IV related the information presented by the three preceding sections to specific South African soil conditions prevalent in the Southern Cape and interior. This included a discussion on specific problems associated with founding on pedocretes, and associated, materials in Chapter 8: Founding Wind Turbine Structures on Pedocretes. Specific considerations pertaining to the determination of dynamic soil properties were explored in Chapter 9: Assessing the Dynamic Properties of Pedocrete Soils.

Chapter 10: Conclusions summarised the key considerations pertaining to the design of wind turbine foundations on pedocrete soil. This was followed by the list of references and appendices containing key structural dynamics equations.

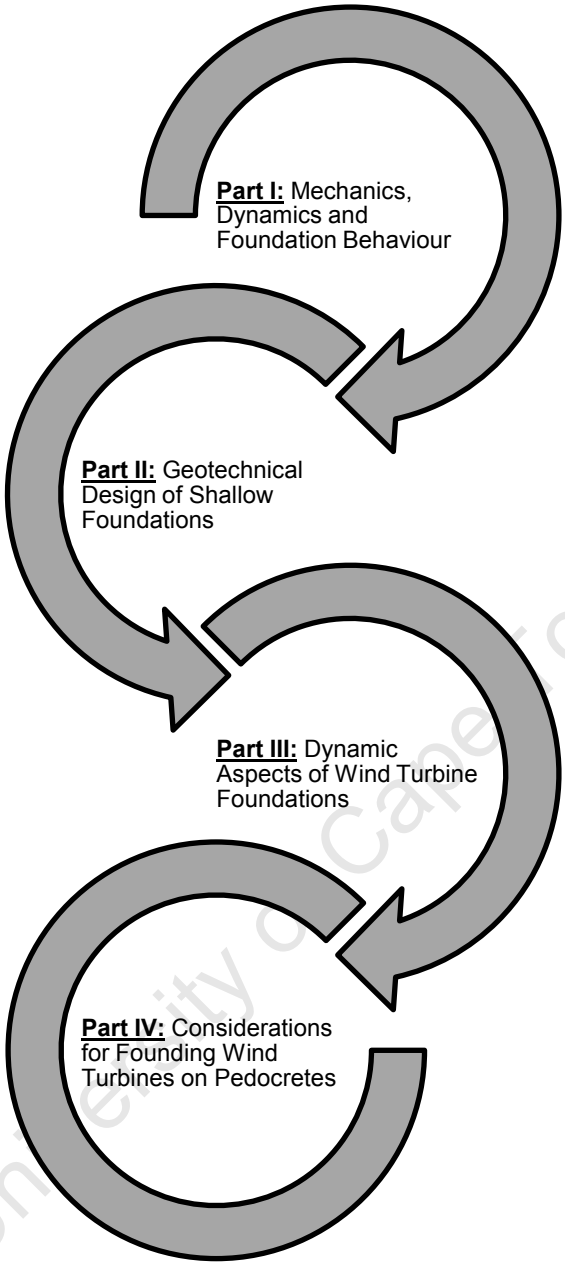

Figure 1.2 **Organisation of dissertation by major theme**

PART I MECHANICS, DYNAMICS AND FOUNDATION BEHAVIOUR

2. MECHANICS AND DYNAMICS OF WIND TURBINE STRUCTURES

2.1 INTRODUCTION

2.1.1 Background

Wind turbine structures are used to convert the kinetic energy of the wind into electrical energy. The concept of drawing electrical energy from the wind has been around for centuries and originated from the use of windmills that derived mechanical energy from the wind to carry out industrial processes (Burton et al., 2008). Over the last few decades wind turbine technologies have received considerable attention aided by improved computing power, industrial processes and development of material sciences, making the re-emergence of wind energy one of the most significant developments of the late 20th and early 21st Century. This has been done in view of; (1) the need for energy coupled with the finiteness of fossil fuels and (2) the potential of wind energy, given that wind may be accessed anywhere in the world, and in some place with great energy density.

With this considerable growth has come increased focus and research into the mechanics of wind turbine structures because the loads experienced by these structures are proportional to their size. This is due to increased aerodynamic loading and weight, as a result of increased height and surface area, as larger energy yields are sought.

2.1.2 Horizontal Axis Wind Turbines

Throughout the 20th Century three fundamental philosophies relating to the design of wind turbines emerged. These essentially related to the way wind turbines resisted operational loads, and included, (1) withstanding loads, (2) shedding or avoiding loads and (3) resisting loads mechanically. This resulted in a wide array of wind turbine designs which varied mainly in terms of the number of blades present, tower structure and the orientation of the rotor axis. Modern wind turbines employ three rotor blades as this has been deemed the optimal configuration between weight considerations and power producing ability. One and two bladed concepts have been tested, but these concepts yielded the need for very large rotors in order to achieve the required power output, and hence the weight-saving characteristics diminished. Furthermore, these concepts resulted in poor fatigue performance due to the high levels of dynamic excitation experienced (Stoddard, 1978).

This study focused on three blade horizontal-axis wind turbines (HAWTs) mounted on a tubular steel tower, as this is presently deemed the most efficient and practical method of constructing wind turbine

structures (DNV/Risø, 2002) with respect to the way the structure sheds and resists loads. The components of a modern HAWT are illustrated by Figure 2.1. The rotor, which includes the rotor blades and hub, is responsible for harnessing the energy of the wind and transferring the mechanical energy to the generator. The generator is housed in the nacelle and connected to the rotor by the drive shaft. The nacelle also houses the gearbox, braking system and other controlling machinery. The tower supports the nacelle and rotor.

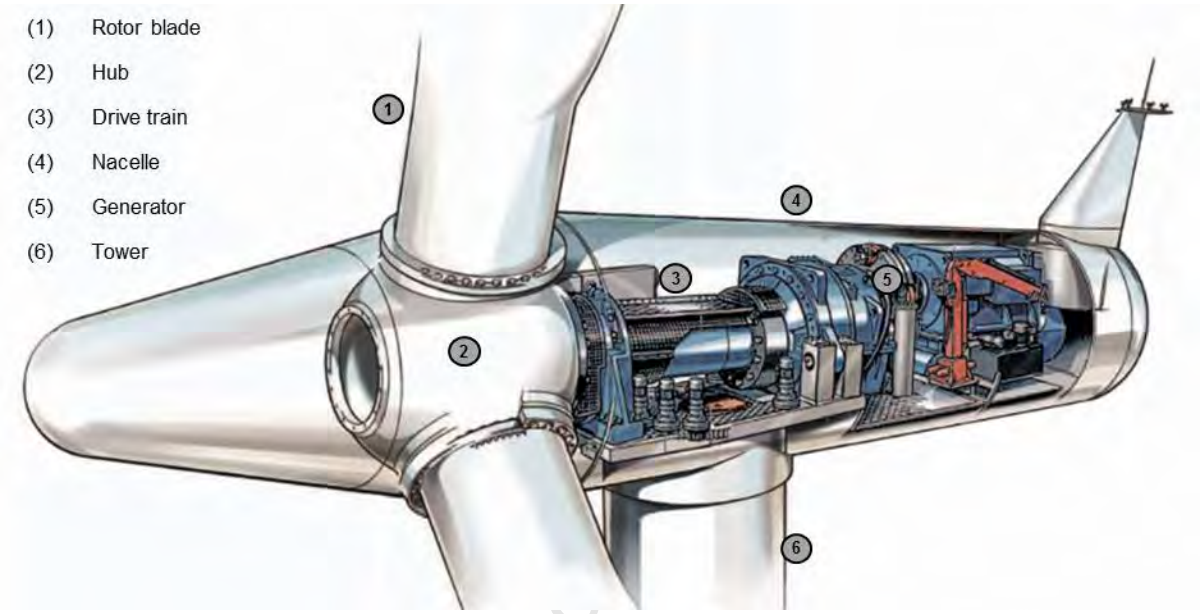

Figure 2.1 **Components of a Horizontal Axis Wind Turbine (HAWT) (Seimens, 2012)**

HAWTs can either have an upwind or downwind configuration. Upwind rotors face the wind in front of the vertical tower and have the advantage of somewhat avoiding the wind shade effect from the presence of the tower, as well as reducing the gyroscopic and fatigue loads experienced by the structure (Manwell et al., 2002). The drawback of upwind rotors is the need for a yawing system to position the rotor into the wind. Downwind rotors operate on the lee side of the tower, meaning they do not require a yawing system, as the nacelle is designed to position the rotors into the downwind position. However, the downwind configuration suffers greatly from the wind tower shadow effect, whereby the rotors experience a loss in lift forces when passing behind the tower.

All of the forces on a turbine must ultimately be transferred to the ground through the tower. This is the backbone of the following chapter, which firstly presents an overview of the wind turbine loads and how they are affected by the operational state of the turbine. This is followed by a study of the wind turbine rotor dynamics and tower loading and response behaviour.

2.2 OVERVIEW OF WIND TURBINE LOADING

Loading is the first point of call when analysing the dynamics and mechanics of wind turbines. The term *load* refers to forces or moments that may act upon the wind turbine structure as a result of (1) its external conditions and (2) the dynamic response of the structure through its mechanical operation and response to time-varying external loads.

2.2.1 Environmental Conditions

Firstly, the environmental conditions govern wind turbine loading, the wind characteristics playing the greatest role. Lightning, snow, frost, fire and rain are also key loading considerations, but mainly affect the durability of the structure. The wind turbine should be designed according to the anticipated external conditions with respect to the IEC 61400[1] standard in conjunction with local design and construction standards. Additionally, guidelines such as DNV/Risø (2002) and AWEA/ASCE (2011) should also be observed. These standards and guidelines will be alluded to in the following chapters, but not explored in detail as they are well established and accessible to any wind turbine designer.

2.2.2 Operational Loading

The loading of wind turbine structures is also dependent on whether the turbine is in operation or parked, and when the turbine is generating energy the loading depends on the nature of operation. The key states of operation include:

1. Parked
2. Normal Operation
3. Start-up and shut-down
4. Extreme environmental conditions
5. Abnormal or fault states

The parked state implies that the rotor is stationary, and therefore no rotation-induced loads are experienced by the structure. Normal operation is the state in which the structure spends most of its service-life, and hence forms the main serviceability consideration. The rotational frequency of the rotor is constant during normal operation and pitch angle of the blades may be altered by the controller to improve efficiency. Start-up and shut-down manoeuvres initiate a change in rotor frequency, from stationary or operational, respectively. The fourth case, extreme environmental conditions, involves events such as extreme gusts of wind, formation of ice, fire and so on. Situations such as rotor over-speeding is characterised as an abnormal scenario.

[1] The International Electrotechnical Commission (IEC) is a non-profit, non-governmental international standards organisation that prepares and publishes International Standards for electrical, electronic and related technologies – collectively known as "electrotechnology"

Wind turbine foundation engineers are in an enviable position, based on the design process of the superstructure. This requires a rigorous approach to determine the most critical load cases based on ultimate and fatigue limit states. Therefore, the foundation engineer generally has a wealth of loading data to draw on in order to conduct the foundation design (Bonnett, 2005). For this reason the calculation of loads is not addressed in the following chapter, but rather an assessment of the nature and types of loading transmitted to the wind turbine foundation is given.

2.3 WIND TURBINE ROTOR DYNAMICS

The response of wind turbine components to the environmental loading as well as the induced loads from the operation of the structure is encapsulated under the theme of *mechanics and dynamics*. With reference to this study, the following section is primarily concerned with the loads emanating from the rotor and tower components, all of which are transferred to the foundation. Thus, the aim of the following section is to provide insight into the nature of the loads which are transferred to the foundation and to provide simplified models of assessment where applicable.

2.3.1 The Wind Turbine Rotor

HAWTs with an upwind configuration have become the international standard for wind energy production. The rotor blades of HAWTs operate on the principle of lift, whereby the rotor blade is designed with an aerofoil profile. Therefore, it is necessary that the rotor blades are sufficiently light without compromising on stiffness, in order to optimise lift and limit centripetal forces (Thresher et al., 2009). This has been achieved by constructing the blades from two glass-fibre reinforced polymer (GRP) shells which are usually fixed by an adhesive (DNV/Risø, 2002). The rotor blades are stiffened by means of webs, to ensure they can withstand the respective loads that they are subjected to under operational loads. The hub is a shell structure which transfers all the loads from the rotor blades to the nacelle and facilitates blade pitch control. Thus, the loads on the hub are directly dependent on the loads acting on the blades, the most significant being: (1) aerodynamic and (2) rotational effects. Hence, the hub acts as the point of fixity for the blades, which are essentially cantilevered structural elements.

2.3.2 Basic Mechanics of Cantilevered Structural Elements

2.3.2.1 Bending Stress

The bending moment distribution, $M(x)$ for a uniform and linear force distribution are given below, respectively. l is the length of the beam, x is the distance from the fixed-end and $P(x)$ is the loading per unit length (force/unit length). P denotes the maximum magnitude of the linearly varying load, which increases from the hub outwards due to the wind velocity profile.

$$M(x) = \frac{P(x)}{2}(l-x)^2 \qquad \textit{Eqn. 2.1}$$

$$M(x) = \frac{P}{3}\left(l^2 + \frac{x^2}{2l}\right) \qquad \textit{Eqn. 2.2}$$

The maximum stress, σ_{max}, experienced by the respective beam occurs at a lever arm of $\bar{y}$ from the centroid to the outermost fibre. This is a function of the moment of inertia, I, and the maximum moment, M_{max}, as is defined by Eqn. 2.3.

$$\sigma_{max} = \frac{M_{max}\,\bar{y}}{I} \qquad \textit{Eqn. 2.3}$$

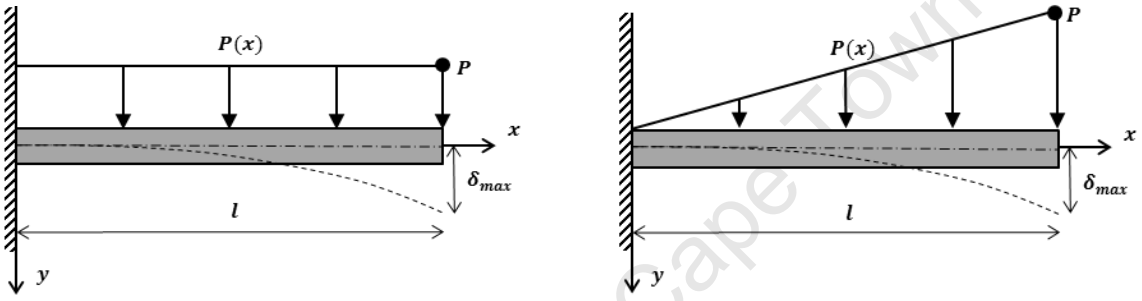

(a) **(b)**

Figure 2.2 **Loading configurations of cantilever beams (a) uniform loading and (b) linear distribution**

2.3.2.2 Deflection of Cantilevered Beams

The deflection of the uniform and triangular loading configurations may be assessed from basic statics principles, resulting in the following expression for a deflection at a distance x from the fixed support, respectively (Kassimali, 2005):

$$\delta(x) = -\frac{Px^2}{24EI}(x^2 + 6l^2 + 4lx) \qquad \textit{Eqn. 2.4}$$

$$\delta(x) = -\frac{Px^2}{120lEI}(20l^3 - 10l^2 - 5lx^2 + x^3) \qquad \textit{Eqn. 2.5}$$

2.3.3 Aerodynamic Loading

An aerodynamic force is exerted on an object as a result of the difference in velocity between the airstream and object. The magnitude of these forces is principally dependent on the cross-sectional area of the object perpendicular to the airstream and the velocity of the airstream. The inflow airstream velocity, U, is reduced by a factor a, to aU, as it passes through the rotor plane to account for axial interference. In addition, as the airstream passes through the rotor plane and intersects the

blades rotating with a frequency of ω, a tangential airstream velocity is introduced. The tangential airstream has a magnitude of $a'\omega r$, where r is the distance from the hub to cross section under consideration. The resulting relative inflow wind velocity is determined by solving these above-defined vectors, as shown in Figure 2.3, and is denoted as W.

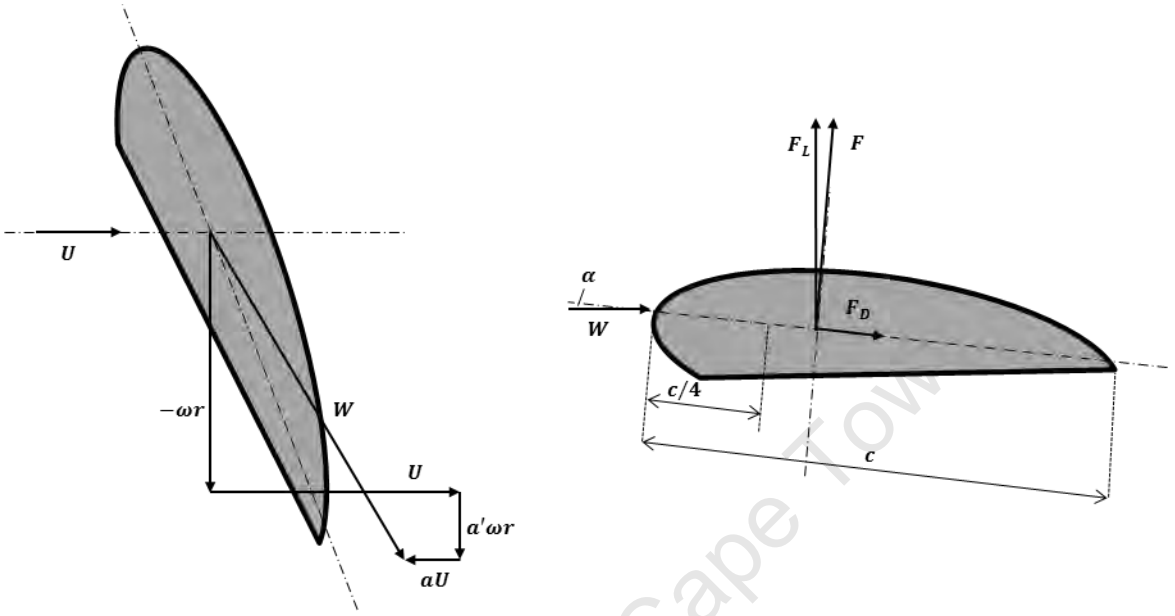

Figure 2.3 **Definition of aerodynamic forces acting on blades: (a) diagram of air velocities acting with respect to blade cross-section, and (b) definition of lift and drag forces acting on aerofoil**

A rotor blade may be viewed as a series of segments, and at an instant in time, each segment is subjected to two aerodynamic forces due to the motion of air over the blade: (1) lift and (2) drag. For a first approximation Eqn. 2.6 and Eqn. 2.7 may be used to calculate lift and drag forces, F_L and F_D, respectively (DNV/Risø, 2002). ρ denotes air density, C_L and C_D are the lift and drag coefficients, respectively, and c the chord length.

$$F_L = 0.5\rho C_L c W^2 \qquad \textit{Eqn. 2.6}$$

$$F_D = 0.5\rho C_D c W^2 \qquad \textit{Eqn. 2.7}$$

A third force, termed *aerodynamic thrust*, acts on the rotor and causes it to rotate. The effects and calculation of this force are detailed in §2.3.5. When the wind turbine is in a parked state the blades are feathered, such that the lift component of the aerodynamic force is significantly less than the drag component. Thus, the horizontal force component acting on the blade when stationary is greater than when the turbine is working, due to the shedding effect that the relationship between lift and drag produces. This emphasises the importance of the pitch angle, which is studied in more detail in §2.4.2.

2.3.4 Rotational Effects: Mass and Inertia Considerations

When stationary, the weight force is constant in magnitude and direction relative to each blade. However, when rotating, the direction of the weight force relative to each blade changes. This means that the effect of the weight force is a function of the azimuth angle, ψ, and may be characterised into a longitudinal component or a lateral component. A centrifugal force is induced in each blade under operation. The centrifugal force is always in the radial direction and outward from the centre of rotation. Hence, it induces an axial load in each blade, the magnitude of which is proportional to the rotational frequency and weight of the respective blade. A third force, inertia, acts on each blade when the rotor is under acceleration. The inertia force acts in a lateral direction and is dependent on the magnitude of acceleration. Hence, this load is important during start-up and shutdown procedures and may reach critical values if the rotor is stopped suddenly. Also, the inertial force bends the blades in the plane of rotation and acts in the opposite direction to rotation during start-up and in the same direction as rotation during shut-down. The relationship between these three force components is depicted in Figure 2.4.

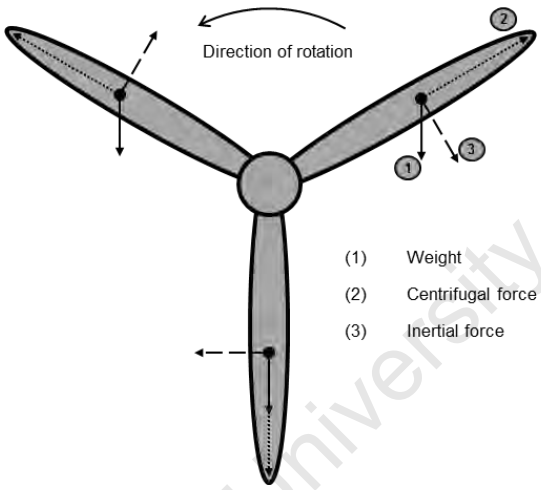

Figure 2.4 **Centrifugal, inertial and weight forces during start-up**

2.3.5 The Ideal Rigid Rotor Model

The effects of the forces thus far studied may be characterised as either:

1. Lateral (inertial and lateral component of the weight force);
2. Longitudinal (centrifugal force and longitudinal component of the weight force).

The blade, therefore, is subjected to a combination of compressive and tensile stresses resulting from the axial loads and bending. Additionally, the drag force acting on the rotor during operation induces another lateral load which acts in the opposite plane to the other lateral loads (Hemami, 2011).

It may be said that the inertial and lateral weight forces act in the plane of rotation and the drag force acts out of plane. Thus, biaxial bending is developed in each rotor blade. These are coupled with torsional and shear effects from the redistribution of weight under bending. These effects are summarised in Figure 2.5.

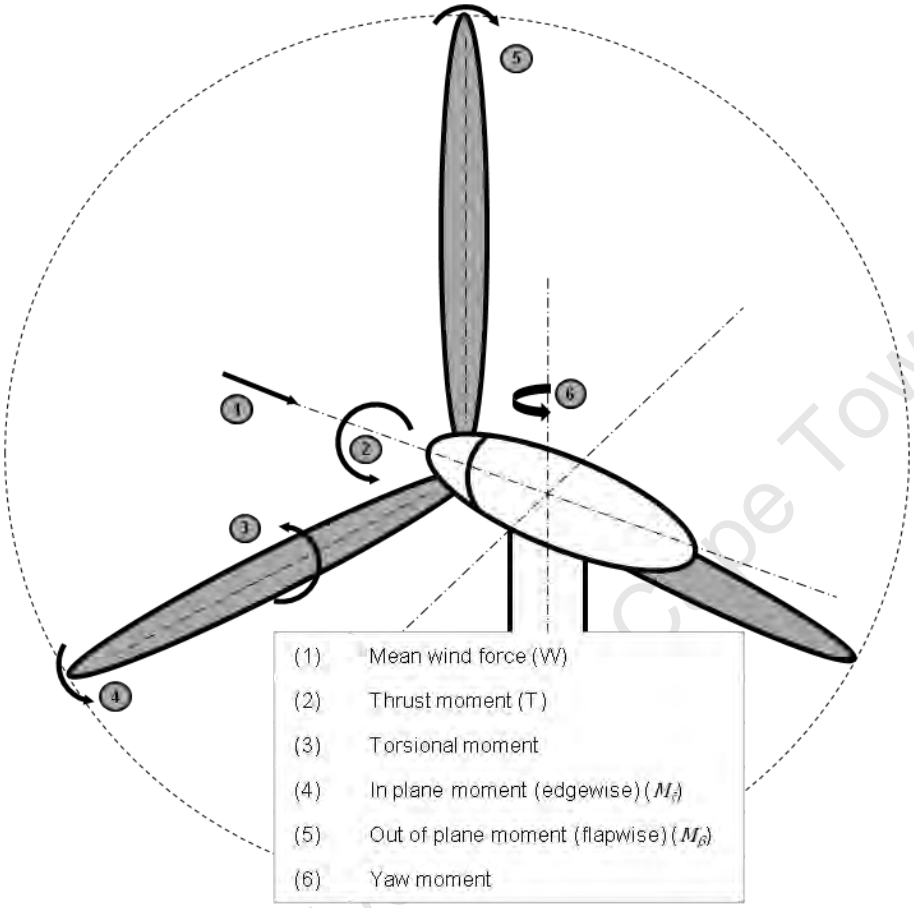

Figure 2.5 **Overview of wind turbine rotor loading**

Thus the interaction of the forces acting on a rotor is complex and may be analysed with varying degrees of accuracy. The *Rigid Rotor Model* (Manwell et al., 2007) is an idealisation of the actual rotor behaviour, but nevertheless a good first approximation and a useful tool for introducing the relevant interactions. For a more detailed model, the reader is referred to the *Hinge-spring Blade Rotor Model* (Manwell et al., 2002). The *Rigid Rotor Model* is centred on describing the in- and out-of plane moments with respect to the rotor thrust, T. T is a function of the thrust coefficient, C_T, as well as the aerodynamic parameters already introduced, such as: the density of the air, ρ, radius of the rotor, R, and free stream velocity, U:

$$T = C_T \frac{1}{2} \rho \pi R^2 U^2 \qquad \textit{Eqn. 2.8}$$

This case assumes the rotor to be aerodynamically ideal, so $C_T = 8/9$, and hence the total thrust varies with the square of the free stream velocity and the radius of the rotor. Blade bending moments are denoted as flap-wise, edge-wise or torsional. Flap-wise (due to lateral forces) moments cause bending in the upwind/downwind plane and edge-wise (due to longitudinal forces) moments cause bending in the plane of rotation. Torsional moments (due to the effects of mass-distribution and force interaction) cause rotation of the blades about the pitch axis.

2.3.5.1 Flap-wise Forces and Moment

The flap-wise bending moment is defined by the product of the thrust force per blade acting at 2/3 of the radius of the rotor. Therefore, considering the rotor to consist of a series of annuli of width dr the flap-wise bending moment, M_β, at the point of fixity for a turbine with n blades is:

$$M_\beta = \frac{1}{n}\int_0^R R(C_T \frac{1}{2}\rho\pi 2RU^2)\, dR = \frac{1}{n}\int_0^R R(T(R))\, dR \qquad \textit{Eqn. 2.9}$$

Upon integrating and gathering terms, noting that $C_T = 8/9$, this becomes:

$$M_\beta = \frac{T}{n}\frac{2}{3}R \qquad \textit{Eqn. 2.10}$$

Hence, the maximum flap-wise stress, $\sigma_{\beta,max}$, is given by Eqn. 2.11. Note that this stems from the theory of cantilever beams, where $\bar{y}$ is the depth from the flap-wise neutral axis I_b is the area moment of inertia of the blade cross-section at the point of fixity.

$$\sigma_{\beta,max} = \frac{M_{\beta,max}\bar{y}}{I_b} \qquad \textit{Eqn. 2.11}$$

The shear force at the point of fixity is defined by the thrust divided by the number of blades i.e.

$$S_\beta = \frac{T}{n} \qquad \textit{Eqn. 2.12}$$

2.3.5.2 Edge-wise Forces and Moments

The edge-wise moment gives rise to the power producing the torque, responsible for the rotation of the blades. The edge-wise moments are generally less significant than the flap-wise moments, and are dependent on the mean torque, Q. The mean torque is defined as the ratio between the power, P, and the rotational speed, Ω.

$$Q = \frac{P}{\Omega} = C_Q \frac{1}{2}\rho\pi R^2 \frac{U^3}{\Omega} \qquad \textit{Eqn. 2.13}$$

It should be stressed that this expression for torque is highly simplified due to its derivation from an ideal rotor. Hence, torque is defined in terms of the torque co-efficient, $C_Q = C_p/\lambda$, which is a function of the power coefficient and the tip speed ratio, λ. Note that torque varies with the square of the wind speed and is not dependent on the blade azimuth, as it is with other models. Now, the edge-wise moment at the root of the blade can be defined as the ratio between torque and the number of blades:

$$M_{\varsigma} = \frac{Q}{n} \qquad \textit{Eqn. 2.14}$$

2.4 WIND TURBINE TOWER LOADING AND RESPONSE

The continued growth of the wind energy market has led to the pursuit of higher energy yields and with that, continuous growth and development in the area. One such technique is to increase the diameter of rotors and hence the height of towers. Wind velocity also increases with altitude and is generally less turbulent, leading to more consistent energy production. This has a crucial impact on the design of wind turbine towers and foundations, which have the primary function of elevating the wind turbine generation unit and ensuring its stability over its operating life (Basu, 2010). The main consideration in this regard is the trade-off between the higher energy yields and the increased cost of stabilising the structure, as the height of the structure increases. Modern wind turbine tower configurations are introduced below.

2.4.1 Tower Configurations

The wind turbine tower has received significant research over the years. This has been primarily due to advancements in material sciences as well as investigations into structural optimisation. Presently, a hollow truncated cone comprising high grade structural steel is used most extensively, but other forms of tower have been used. Common forms of wind turbine towers also include steel lattice towers and concrete or concrete-steel composite towers, as illustrated in Figure 2.6.

2.4.1.1 Tubular Steel Tower

The majority of wind turbine towers are constructed from steel. This is due to several reasons, including (Burton et al., 2008): (1) steel has an excellent strength to weight relationship, (2) tubular towers have the benefit of consistent bending stresses in each direction, (3) construction of towers from steel requires less time than the use of other materials such as reinforced concrete, (4) steel has high torsional resistance and (5) the natural frequency of tubular steel towers can be determined relatively easily and consistently. Furthermore, tubular steel towers have a modest taper to improve stability and load transfer to the foundation. The key parameters for foundation design, therefore, are the diameter at the tower base and wall thickness. The tower top diameter is governed by the size of the yaw bearing and hence the size of the rotor blades and nacelle.

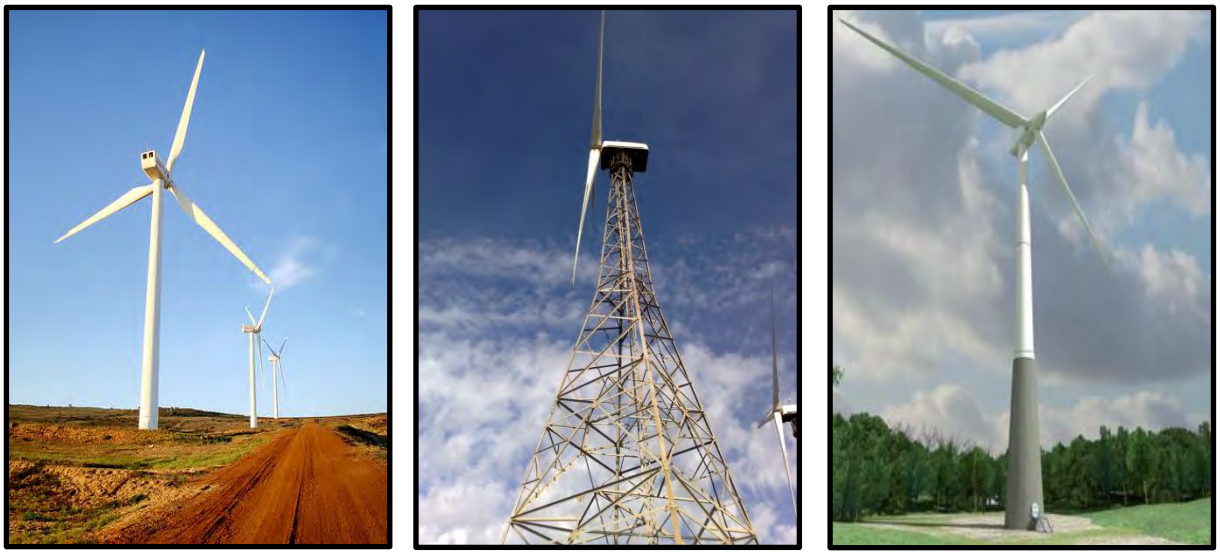

(a) **(b)** **(c)**

Figure 2.6 **Modern wind turbine towers; (a) tubular steel tower (Darling Wind Farm), (b) steel lattice tower (Ruukki, 2013), and (c) conceptual concrete-steel composite tower (Gestamp, 2013)**

Hence, one needs to determine the tower base diameter and wall thickness in terms of buckling of the shell wall in compression, strength under fatigue loading and stiffness required to achieve specific natural frequency-ranges (Hassanzadeh et al., 2012).

Accompanying these key design parameters are practical considerations regarding the transport of steel tubular towers, or sections thereof. The limit with respect to the maximum diameter of the tower is generally between 4.0 m and 4.2 m (Burton et al., 2008), and would be reduced drastically in mountainous areas. This is an important consideration in South Africa and the rugged terrain of the southern cape.

2.4.1.2 Steel Lattice Tower

Steel lattice towers are often assembled from angled sections, with bolting used to attach the bracing members to the legs and splicing the leg sections together. The significant advantage of steel lattice towers is the material-saving implications as well as ease of transport and construction. An important design consideration is the distribution of forces between different members of the lattice tower. The chord members generally resist tower bending moments while the web members experience loads as a result of shear and torsion (Gencturk et al., 2012). In each case, member buckling and fatigue of the joints is critical to performance. To this effect, friction grip bolts are generally used and web members are arranged as intersecting pairs instead of a triangular arrangement. This has shown to improve stability at joints as well as reduce the flexural loading of chord members due to reduced spacing of chord supports.

Despite these measures, there are still several drawbacks to the use of lattice towers. The first is the issue of maintenance – especially of the bolted connections. These connections need to be monitored throughout the structure's lifespan to ensure cyclic loading does not result in a loss of strength. Secondly, lattice towers often require large base areas in order to improve stiffness and to ensure the natural frequency of the system is adequate. This results in foundation bases either having to be larger or individual bases/piles having to be constructed at each "edg" of the structure (Hassanzadeh et al., 2012).

2.4.1.3 Reinforced Concrete and Reinforced Concrete-steel Composite Towers

The use of concrete for wind turbine towers has come to the fore in recent years. Unfortunately, concrete does not offer the benefit of steel in terms of construction efficiency and stiffness to mass relations. However, concrete does offer benefits in terms of durability, robustness and cost (Tricklebank et al., 2005). The pre-stressing of reinforced concrete also aids the tower's stiffness and ability to withstand tension and torsional loading. The issue of maintenance is significant in the process of wind turbine design, as wind turbines are generally located in remote areas and therefore materials requiring high levels of maintenance may lead projects to becoming costly and difficult. However, with the emergence of larger wind turbines the role of concrete will become important. As tubular steel towers increase in height, the thickness of the tower needs to increase in order to resist the respective loads. This poses challenges of connecting sections as well as load transfer complications. The use of concrete presents an answer to this problem, especially due to pre-stressed concrete being shown to possess good damping and stiffness characteristics and thus a pleasing dynamic loading response (Tricklebank et al., 2005).

2.4.2 Influence of Rotor Control Mechanisms on Tower Loading

Modern HAWT structures have one of three power-regulation philosophies, the mechanics of which pose an important consideration in the design of wind turbine towers and foundations. The three main methods traditionally used are: (1) passive stall, (2) active stall and (3) pitch regulation. The former two methods of power regulation are classified as stall regulated. Active stall and pitch regulation measures are deemed active, as the rotor pitch angle may be altered. The details of each method are discussed below in conjunction with Figure 2.7.

2.4.2.1 Passive Stall Regulation

Passive stall regulated machines are defined by the blade angle relative to the hub being fixed. Therefore, as the wind velocity increases, the angle of attack, α, will also increase until it reaches approximately 14°, at which point stall is induced. Drag increases as stall occurs, resulting in extreme loading on the rotor, which is in turn transferred to the tower and foundation. Furthermore, the cross-sectional area of the rotor is fixed, and hence when parked no shedding of load may occur.

2.4.2.2 Active Stall Regulation

The active stall mechanism also uses a fixed blade angle, but only until the rated power is reached. At this point the angle of the blades relative to the hub is adjusted to optimise the lift and drag forces acting on the blades. This allows the rated power to be maintained through fluctuations in wind velocity and improves the load shedding of the structure. In a parked state the blades are pitched with the trailing edge into the wind which reduces the loading on the rotor and the tower.

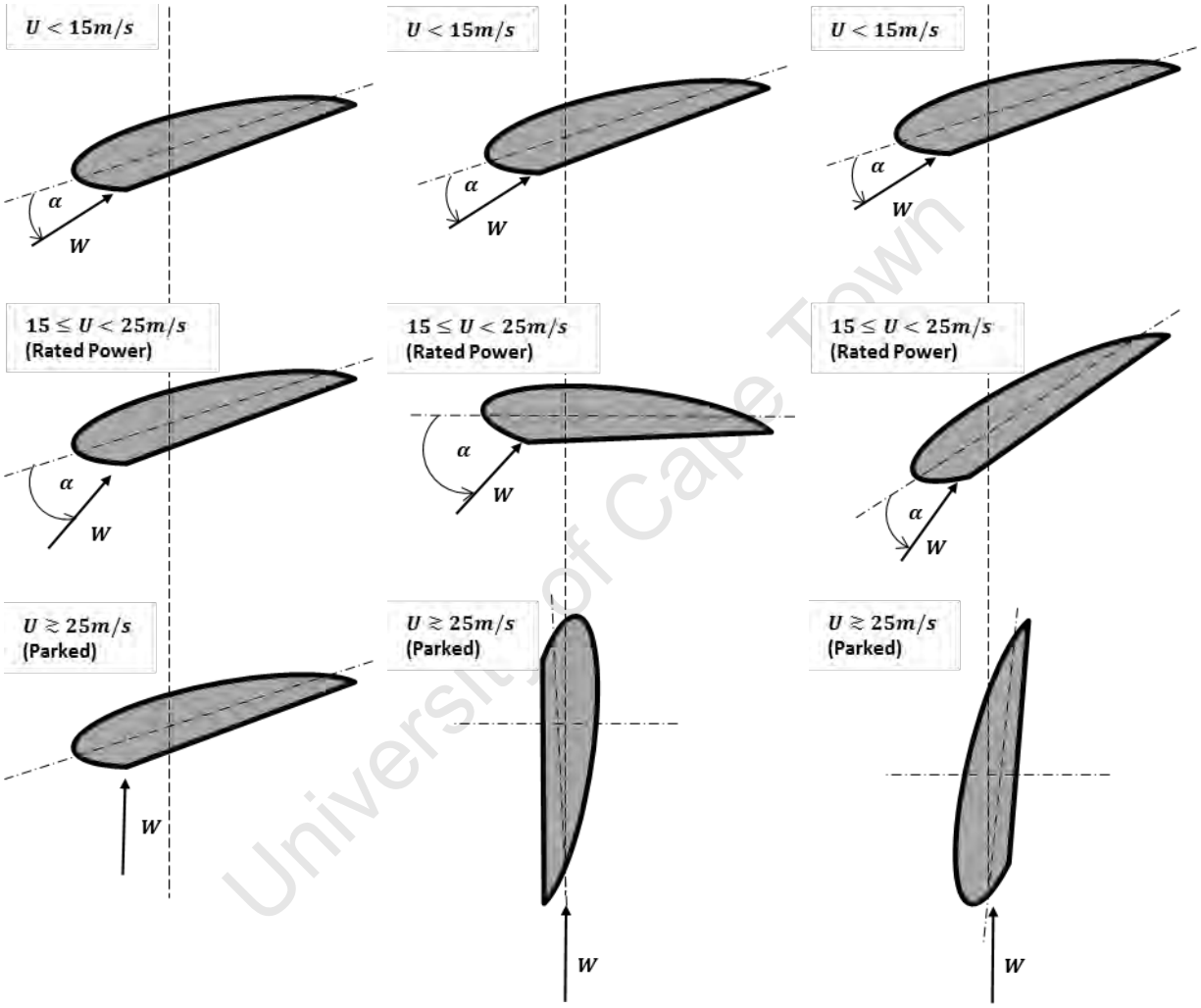

Figure 2.7 **Blade pitching for different power regulation philosophies (Bonnett, 2005): (a) passive stall, (b) active stall and (c) pitched control**

2.4.2.3 Pitch Regulation

Pitch regulated rotors are continuously controlled to reduce the angle of attack on the rotor blade and maintain the power producing capacity of the rotor by optimising the lift and drag forces. This is done by reducing lift rather than increasing drag, as in the previous cases. The consequence of this is reduced thrust loading on the rotor with increased wind velocity because the rotor sheds loads more efficiently, resulting in the thrust loading decreasing past the rated power of the turbine.

The tower base moment is directly influenced by the rotor operational mode of the turbine due to shedding, or lack thereof in the case of stall controlled machines. That is, the thrust of stall regulated machines tends to increase up to the cut out speed, opposed to the reduction in thrust associated with pitch regulated rotors after the rated power has been reached (Bonnett, 2005).

Figure 2.8 is indicative of this relationship, and shows the ability of pitch regulated machines to maintain the rated power while shedding load. The parked loading curves follow a simple squared relationship with respect to wind velocity, where the difference in magnitude between the two philosophies is based on passive regulated machines having greater cross-sectional area and drag forces when parked. Active controlled machines have a lower cross-sectional area when parked due to the pitching of the blades into the wind.

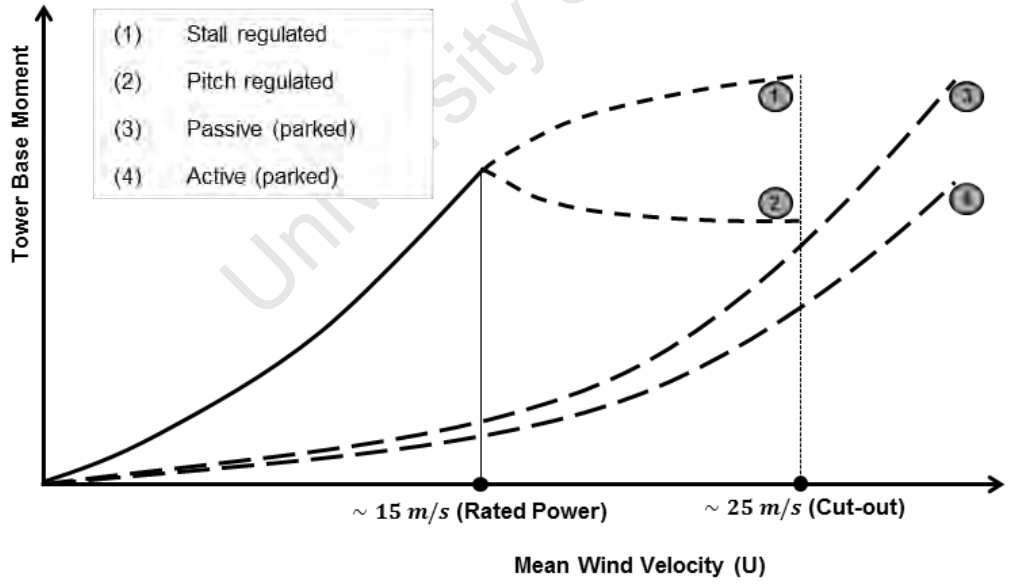

Figure 2.8 **Loading curves for stall and pith regulated machines**

These considerations culminate in two fundamental points regarding tower loading:

1. The dynamic nature of wind turbine structures results in significantly higher loading during operation than what would be expected from a static structure of equal cross-sectional area.
2. The wind turbine regulation philosophy has a significant influence on the tower and foundation loading, especially in the range between 15 m/s and 25 m/s.

These key considerations form the backbone to understanding the loading experienced by wind turbine towers as a result of the dynamic nature of the structure. The wind turbine tower may be viewed as a cantilever beam which undergoes three distinct types of loads, which include: (1) steady, (2) dynamic interactions and (3) vibration. An examination of these types of load is conducted below.

2.4.3 Steady Tower Loads

Steady tower loads are defined as the loading conditions expected under normal generation conditions, with respect to the tower height and cross-sectional area. These include:

1. A lateral load derived from the aerodynamic forces
2. A compressive load due to the weight of the rotor, nacelle and tower, $F_{ZE}(h)$.
3. A moment due to the aerodynamic forces acting on the rotor, $M_X(h)$.
4. Moments from the rotation of the rotor, $M_Y(h)$ and $M_Z(h)$.

Using a quasi-static approach with gust factor, φ, these loads may be approximated (DNV/Risø, 2002). Firstly, the lateral loading on the tower is a function of the aerodynamic drag forces acting on the nacelle and rotor, F_{YE}, and the variation of aerodynamic force with the height of the tower, $F_W(h)$.

$$F_Y(h) = F_{YE} + F_W(h) \qquad \textit{Eqn. 2.15}$$

Secondly, the axial load in the tower is the summation of the nacelle and rotor weight, F_{ZE}, and the weight of the tower as a function of tower height, H, density, ρ_t, and cross, sectional area, $A(z)$.

$$F_Z(h) = F_{ZE} + \frac{\rho_t}{2}\int_h^H A(z)dz \qquad \textit{Eqn. 2.16}$$

Effects of eccentric loads from the rotor and nacelle are accounted for in the determination of the moment, $M_X(h)$, which is also a function of the aerodynamic forces acting on the tower and nacelle at hub-height, and the deflection of the tower due to wind loading (δ_y):

$$M_X(h) = M_{XE} + F_{YE} \cdot (H - h) + M_W(h) + F_{ZE} \cdot (\delta_y(H) - \delta_y(h)) \qquad \textit{Eqn. 2.17}$$

The moments $M_Y(h)$and $M_Z(h)$ are primarily a function of the rotor torque, as discussed in the previous section.

$$M_Y(h) = M_{YE} = f(M_\zeta)$$

$$M_Z(h) = M_{ZE} = f(M_\beta, M_\zeta)$$

Eqn. 2.18

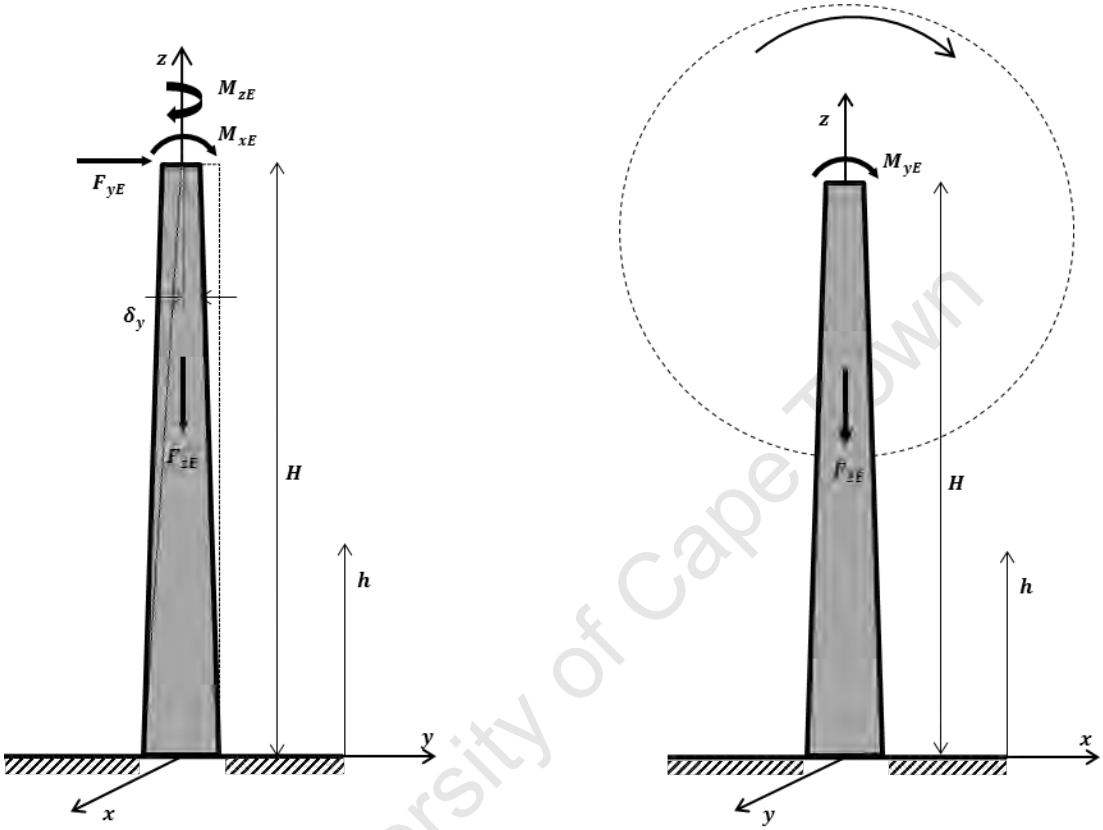

(a) **(b)**

Figure 2.9 **Free-body diagram of wind turbine tower modelled as a cantilever beam: (a) out-of-plane view and (b) in-plain view**

$M_Y(h)$, the moment arising from the rotation of the rotor, causes the nacelle to turn in the same direction, thus exerting a torque on the nacelle in the same direction as that of rotation. The nacelle must resist this torque to ensure stability of the structure. This resistance comes from the tower-foundation system, whereby the foundation applies a couple of the same magnitude as the rotor torque, but in the opposite direction to that of rotation, to resist the overturning effect of the rotor. This torque is variable as it depends on the power captured by the turbine at each instant in time.

The aerodynamic thrust, $F_W(h)$, and bending moment, $M_W(h)$, with respect to the ground level, are defined as follows:

$$F_W(h) = \frac{\rho_t}{2}\int_h^H V(z)^2 \cdot \varphi \cdot D(z) \cdot C(z)dz \qquad \textit{Eqn. 2.19}$$

$$M_W(h) = \frac{\rho_t}{2}\int_h^H (H - h - z) \cdot V(z)^2 \cdot \varphi \cdot D(z) \cdot C(z)dz \qquad \textit{Eqn. 2.20}$$

Where:

- $V(z)$: wind velocity with respect to z.
- $D(z)$: outer diameter of tower.
- $C(z)$: Form factor (usually 0.6 for tubular steel tower).

2.4.4 Tower Dynamics

Vibration is the mechanical phenomenon whereby oscillations occur about an equilibrium point, in response to a time varying load. Vibrations are a critical consideration for the tower and foundation design, due to the multitude of dynamic forces that a wind turbine tower is subject to. The two most significant sources of vibrations are (1) the dynamics of the rotor and (2) wind induced vibration.

This section firstly explores the sources of dynamic loads acting on the tower. This is followed by an assessment of vibrations using a single degree of freedom (SDOF) lumped parameter model and in so doing presents theories underpinning the response of the tower-foundation system to dynamic loading.

2.4.4.1 Rotor-tower Interaction

The previous sections (§2.3) defined the various sources of rotor loads. In terms of the tower-foundation loading, it is important to note that the rotor loads were affected by (1) the variable characteristics of the wind, which may at times be turbulent and transient in nature, and (2) the cyclic nature of the rotational forces induced in the rotor. All of which are subsequently transferred to the tower and foundation. Dynamic tower loads are the culmination of loads acting on the tower from the dynamic response of the rotor. For an ideal rigid rotor, blade moments are the main source of dynamic tower loads. Three moments for each blade – flap-wise, edge-wise and torsion – are transferred to the tower as:

$$M_x = -M_\beta cos(\psi) \qquad \textit{Eqn. 2.21}$$

$$M_y = M_\zeta \qquad \textit{Eqn. 2.22}$$

$$M_z = M_\beta sin\,(\psi) \qquad \textit{Eqn. 2.23}$$

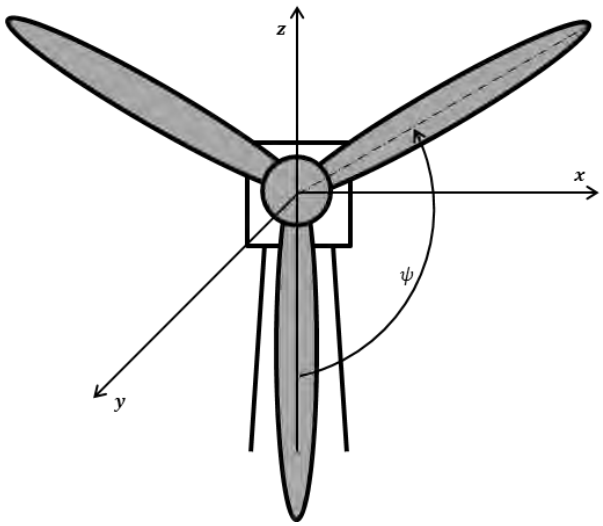

Figure 2.10 **Co-ordinate system for wind turbine rotor-tower dynamic interaction**

These moments are a function of the blade azimuth angle, ψ, the flap-wise bending moment, M_β, and the edge-wise bending moment, M_ζ. Refer to Figure 2.10 for a definition of the respective co-ordinate system which defines the above moment expressions and to § 2.3.5 for a definition of the edge-wise and flap-wise moments. Hence, given the blade rotational frequency, the loads for an instant in time may be calculated with respect to ψ, and may be modelled as harmonic (van der Tempel and Molenaar, 2002) based on the periodic nature of the loads as discussed in §2.3.4. More complex models are available which may be used to provide a closer evaluation to the actual behaviour of a wind turbine rotor and its interaction with the structure such as the *Gust Factor Approach* (Basu, 2010) and the *Flapping Blade Model* (Manwell et al., 2002).

2.4.4.2 Wind Induced Vibration: Vortex Shedding

The flow behind a long cylindrical member, such as wind turbine towers, held perpendicular to the direction of the wind, is characterised by the shedding of vortices. This develops periodic lateral forces which act on the tower, subsequently causing vibration of the structure (Liu, 1991). The process is called *vortex-shedding induced vibration*, and is caused by the generation of alternating low pressure zones on the down-wind side of the tower. This is the principle factor contributing to the vibration of wind turbine towers and is primarily controlled by the stiffness of the structure and the damping properties of the tower-foundation-soil system. However, vortex-shedding is deemed most critical during construction phases. This is because the effect of the nacelle and rotor weight under normal operation, as well as the shedding effect of the blades as they pass the windward side of the tower, reduces the effects of vortex-induced vibration on the tower.

Nevertheless, vortex-induced vibration is a critical consideration for the fatigue life of a wind turbine, as it subjects the tower to a great number of stress cycles during its service life. The wind-induced accelerations of structural components has been found to be the cause of increased downtime of wind turbine structures and the breakdown of components, including the cracking of foundation bases (Basu, 2010). The critical wind velocity that leads to maximum amplitudes of oscillation may be calculated as:

$$v_r = \frac{\omega_n D}{St} \qquad \textit{Eqn. 2.24}$$

Where, ω_n, is the natural frequency of the tower, D is the top diameter and S_t the Strouhal number. This expression may be re-arranged to characterise the excitation load, of frequency ω:

$$\omega = \frac{vD}{S_t} \qquad \textit{Eqn. 2.25}$$

Thus, when the wind velocity is such that $\omega = \omega_n$ then maximum amplitude vibrations will occur. Similarly to the tower-rotor interaction, this provides a basis upon which the wind velocity may be related to the frequency of excitation for an instant of time.

2.4.4.3 Elements of Vibration Theory

The time-varying nature of the loading emanating from the rotor and wind conditions in reality is a combination of the types of loads illustrated by Figure 2.11 (a) to (c). These may be idealised by a sinusoidal excitation force, $Q(t)$, where ω is the frequency of excitation and Q_0 the forcing amplitude:

$$Q(t) = Q_0 sin(\omega t) \qquad \textit{Eqn. 2.26}$$

The response of the structure to a time-varying load is also time-dependent. This is principally governed by the relationship between the excitation frequency, ω, and the natural frequency of the structure, ω_n, which in turn is function of the stiffness and mass.

$$\omega_n = \sqrt{\frac{k}{m}} \qquad \textit{Eqn. 2.27}$$

The most important consideration in the design of wind turbine towers is to ensure that the natural frequency of the tower avoids the blade passing frequency (3P) or a multiple thereof. The constant rotor rotational frequency (RPM or 1P frequency) must also not coincide with the natural frequency of the tower. Thus, the stiffness of the tower-foundation system is an integral component of wind turbine design, as it dictates the nature of the tower behaviour under dynamic loading.

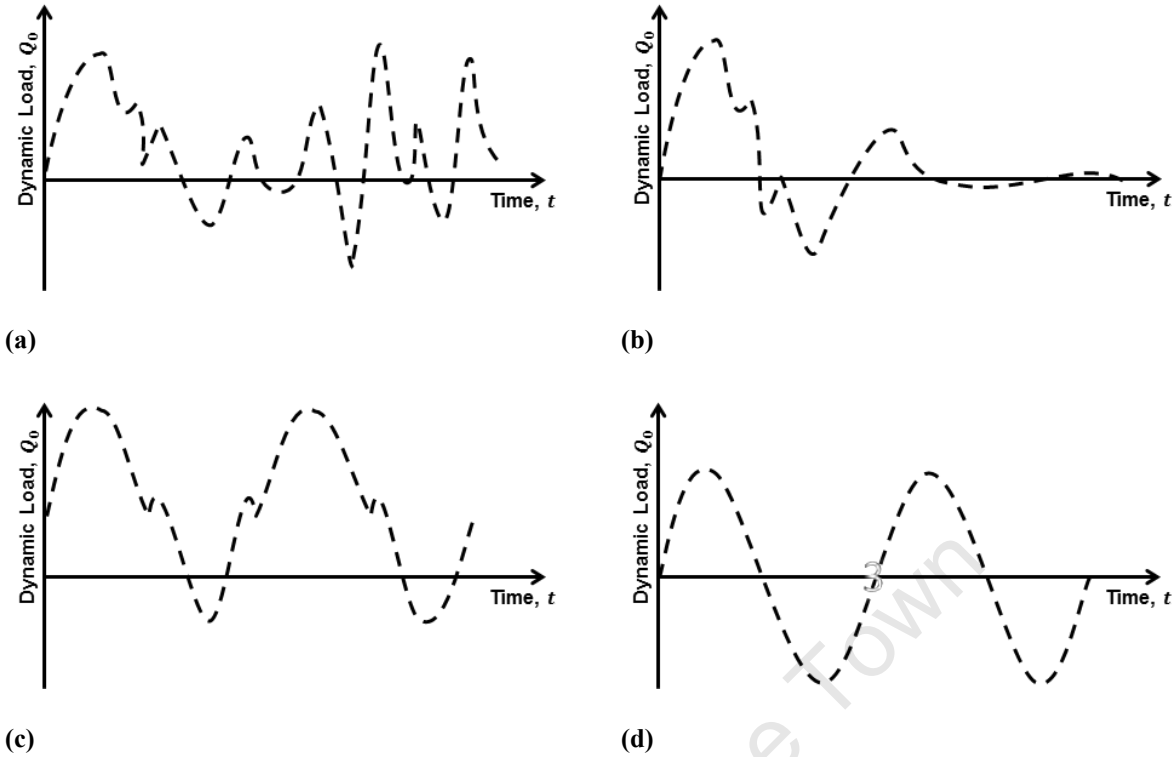

Figure 2.11 **Typical dynamic loading: (a) random, (b) transient, (c) periodic and (d) sinusoidal idealisation for (a) – (c)**

There are three distinct zones of structural behaviour that may be expected from the tower upon dynamic loading. The first is *quasi-static*. The displacement of the respective structural element in this case follows the force instantaneously. There is no phase lag between the force and the response and hence the response is similar to when a monotonic load is applied. In this case the frequency of excitation is well below the natural frequency of the system. The second case is termed *inertia dominated*. This occurs when the excitation frequency is far greater than the structure's natural frequency leading to the structure's response countering the applied force. The last case and most critical case is *resonance*, which is studied in more detail below.

2.4.4.4 Resonance Response

A system is deemed to be in resonance when the frequency of excitation is equal to the natural frequency of the system. This response is characterised by large deformations as the excitation force and phase angle are 90° apart. Thus, any frequency of excitation close to the natural frequency of the structure is to be avoided, to ensure excessive deformations do not occur under dynamic loading. This phenomenon may be described mathematically by employing the SDOF lumped parameter model. In doing so, the forces resisting the motion induced by the dynamic action are dependent on inertia ($f_I(t)$), stiffness ($f_k(t)$) and the damping of the system ($f_c(t)$).

For dynamic equilibrium, and assuming viscous damping, the relationship between these force components is:

$$m\ddot{z} + c_y\dot{y} + k_y y = Q_0\, sin(\omega t) \qquad \textit{Eqn. 2.28}$$

The critical damping coefficient and the damping ratio are defined by Eqn. 2.29 and Eqn. 2.30, respectively, so that Eqn. 2.28 may be expressed in terms of the damping ratio and natural frequency (Eqn. 2.31).

$$c_{y,c} = 2m\omega_n \qquad \textit{Eqn. 2.29}$$

$$\zeta_y = \frac{c_y}{c_{y,cr}} \qquad \textit{Eqn. 2.30}$$

$$m\ddot{y} + 2m\omega_n\zeta_y\dot{y} + k_y y = Q_0\, sin(\omega t) \qquad \textit{Eqn. 2.31}$$

The steady state response, to the differential equation defined by Eqn. 2.31, is given as follows (Clough and Penzien, 1995):

$$y(t) = A_y \cdot sin\,(\omega t - \varphi) \qquad \textit{Eqn. 2.32}$$

where A_y is the amplitude of vibration and φ the phase angle.

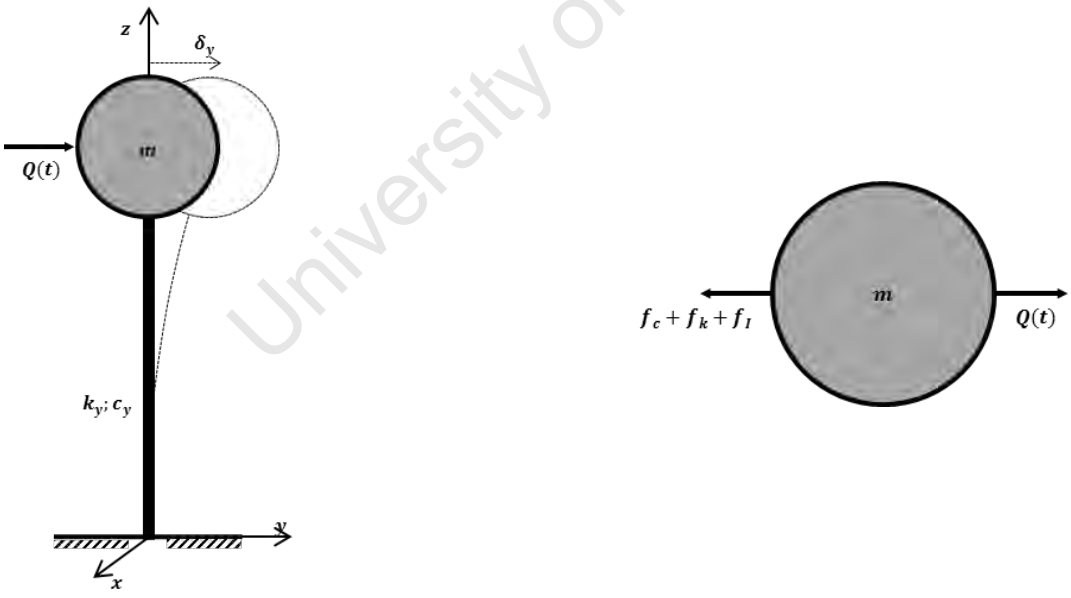

(a) **(b)**

Figure 2.12 **Lumped model: (a) SDOF tower model and (b) free body diagram**

Now, an important observation can be made during resonance response. Referring to, and substituting Eqn. 2.32 and its derivatives into the equation of motion (Eqn. 2.31) yields the following.

$$m(-Y\omega_n{}^2 \sin(\omega_n t - \theta)) + c_y(Y\omega \cos(\omega t - \theta) + k_y(Y \sin(\omega t - \theta)) = Q_0 \sin(\omega t) \quad \textit{Eqn. 2.33}$$

Therefore,

$$f_I(t) = -m\rho\omega_n{}^2 \sin(\omega_n t - \theta) \quad \textit{Eqn. 2.34}$$

$$f_c(t) = \rho\omega \cos(\omega t - \theta) \quad \textit{Eqn. 2.35}$$

$$f_k(t) = k_y(\rho \sin(\omega t - \theta)) \quad \textit{Eqn. 2.36}$$

At resonance it is evident that the only term resisting the applied harmonic loading is the damping term as shown below (note $\theta = 90°$ at resonance):

$$f_c(t) = \rho\omega \cos(\omega t - \theta) = Q_0 \sin(\omega t) \quad \textit{Eqn. 2.37}$$

The level of damping in structures is generally very low, and hence the development of resonance is to be avoided at all costs. Thus, it is imperative that the natural frequencies of wind turbine towers are tuned to ensure that the relevant rotational frequencies are avoided to ensure the safety of the structure as well as cost-efficiency. Stiffness of the tower-foundation system plays a central role in this process, as is explained in the following section.

2.4.4.5 Vibration Control of the Tower

Due to the limiting influence that damping has on controlling dynamic response, the overall stiffness of the towel-foundation system is of the utmost importance. As previously mentioned, there are three characteristic types of response from the tower-foundation system when subjected to dynamic loading: (1) quasi-static, (2) inertia-controlled and (3) resonance. Figure 2.13 conceptually illustrates the three types of dynamic response, with respect to stiffness and rotational frequency. As is customary, a $\pm 10\%$ margin has been added to the 1P and 3P frequencies as a buffer against resonance response. The behavioural states depicted here are discussed in more detail below.

(i) Soft-soft Towers

Soft-soft tower-foundation systems have a natural frequency well below the 1P frequency. This is achieved by a tower-foundation system with sufficiently low stiffness. This system is impractical as it would often lack the stiffness to resist other operational loads satisfactorily.

(ii) Stiff-stiff Towers

Stiff-stiff tower-foundation systems are at the other end of the spectrum, relative to soft-soft tower-foundation system. These structural systems have incredibly high stiffness and hence a natural frequency well above the 3P frequency. In doing so, such systems are very safe but expensive to construct due to the material requirements.

(iii) Soft-stiff Towers

Soft-stiff towers are a compromise between the two afore-mentioned cases, whereby the respective natural frequency lies between the 1P and 3P frequencies. Hence, this design option for the tower-foundation system is often resource-efficient.

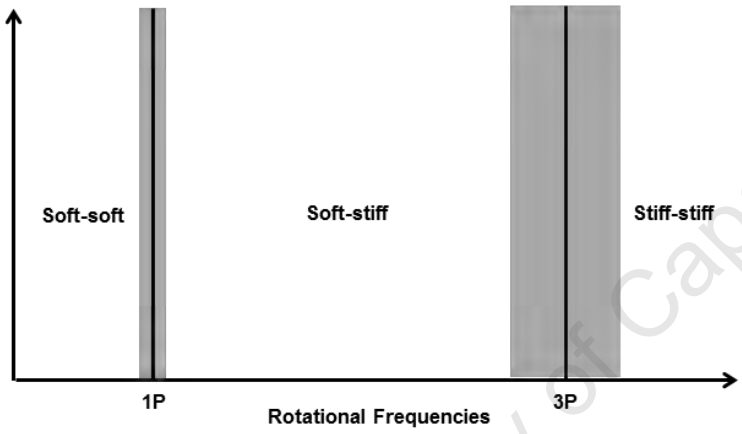

Figure 2.13 **Natural frequency control of wind turbine tower**

Accordingly, designing soft-stiff tower-foundation systems requires an intricate knowledge of the tower-foundation natural frequency to ensure it does not intercept the 1P and 3P frequency buffer ranges ($\pm 10\%$). There are varying degrees of accuracy with which the tower natural frequency may be determined. Following on from the SDOF lumped parameter model employed above, the natural cyclic frequency may be approximated by the following expression (Manwell et al., 2007; van der Tempel and Molenaar, 2002):

$$f_n = \frac{\omega_n}{2\pi} = \frac{1}{2\pi}\sqrt{\frac{3EI}{(0.23m_{tower} + m_{turbine})H^3}} \qquad \textit{Eqn. 2.38}$$

where E and I are the Young's modulus and second moment of area of the tower, respectively, H the height of the tower and m denotes mass of the respective components defined by the subscripts.

The relationship between the tower natural frequency and the excitation frequency is also fundamental in terms tower fatigue limits. It is widely accepted that the dynamic magnification factor approach be adopted to amplify the expected loads acting on the structure due to their dynamic nature. The dynamic magnification factor is derived from the steady state response of the structure, defined in the preceding section, and relates the steady state response amplitude (Y) to the equivalent static deflection that would have occurred if the respective load was static in nature (Q_0/k_y). The relationship between D and the frequency ratio $\beta = \omega/\omega_n$ is expanded upon in more detail within §7.3.

$$D = \frac{Y}{\left(\frac{Q_0}{k_y}\right)} = \frac{1}{\sqrt{\left[1 - \left(\frac{\omega}{\omega_n}\right)^2\right]^2 + \left(2\zeta_y \frac{\omega}{\omega_n}\right)^2}} \qquad \textit{Eqn. 2.39}$$

2.4.4.6 Foundation Stiffness and Vibration Control

The above discussion of tower vibration-control assumed the tower to be fixed to the foundation. That is, the foundation stiffness was not taken into account, and therefore assumed not to affect the response of the tower-rotor system, and vice-versa. This is not the case in practice. The foundation stiffness plays a central role in the dynamic response of the system; the most significant of these is the reduction in natural frequency. Figure 2.14 gives a graphical representation of this effect.

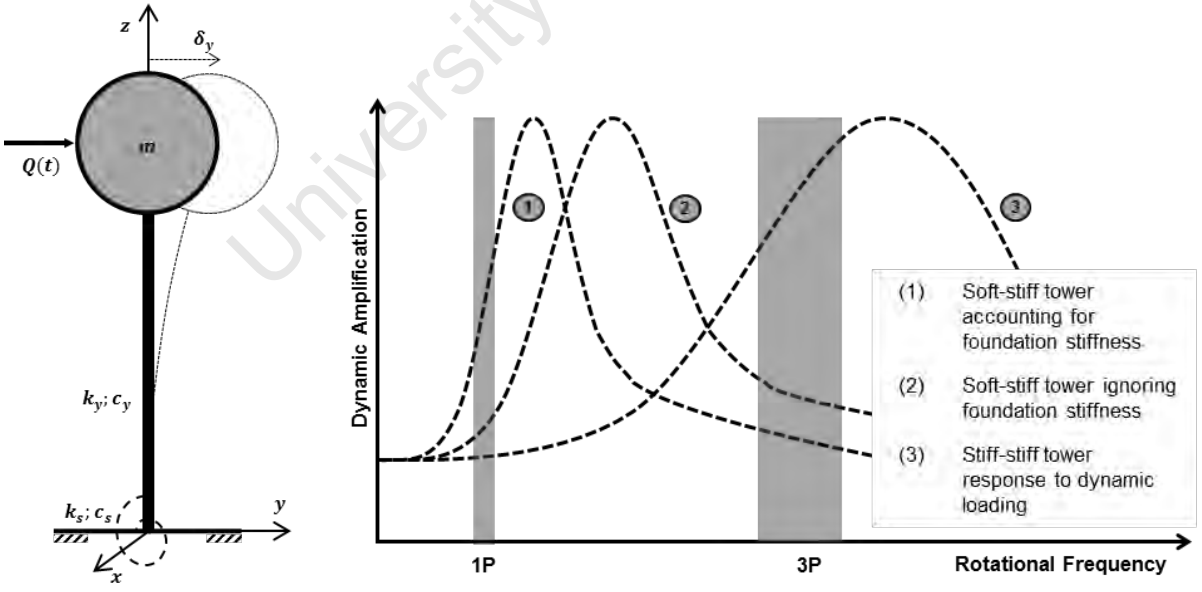

(a) **(b)**

Figure 2.14 **Effect of foundation stiffness on dynamic response of tower: (a) adjusted SDOF model and (b) schematic view of foundation stiffness effect on soft-stiff tower**

The reduction of the tower natural frequency due to the foundation stiffness may be accounted for by approximating the tower natural frequency as (Byrne, 2011):

$$f_n = \frac{\omega_n}{2\pi} = \frac{1}{2\pi}\sqrt{\frac{13EI}{m\left(\frac{H^3}{3EI} + \frac{H^2}{k_e}\right)}} \qquad \textit{Eqn. 2.40}$$

This expression was derived from the theory of a beam on an elastic foundation. Note that it is a function of the tower height, H. Also, since the tower and soil are connected in series, the equivalent stiffness coefficient, k_e, is utilised, where:

$$k_e = \frac{k_y k_s}{k_y + k_s} = \frac{k_y}{1 + \frac{k_y}{k_s}} \qquad \textit{Eqn. 2.41}$$

Observation of this equation illustrates the effect that the soil stiffness has on the overall stiffness, where, a very stiff soil renders the dynamic response dependent on the tower stiffness and a very soft foundation-soil system renders the system unstable.

More complex models, such as that proposed by Adhikari and Bhattacharya (2011) are available:

$$f_n = \frac{1}{2\pi}\sqrt{\frac{EI}{mH^4}} \cdot \sqrt{\frac{3\gamma_k}{\alpha + \gamma_m}} \qquad \textit{Eqn. 2.42}$$

Where, γ_k and γ_m denote stiffness and mass correction factors. It is important to note that the stiffness referred to in the above expressions is the rotational stiffness of the foundation. Chapter 3 provides further insight into why this is the case.

2.4.4.7 Vibration of Cantilevered Beams

The dynamic loading of cantilevered structural elements results in variable compressive and tensile stresses, thus making these structural elements particularly susceptible to fatigue damage. The *Euler Equation* of beams is most commonly used to model the vibration response of an ideal, uniform beam of constant cross-section and material properties. This method is extremely useful for determining the natural frequencies of beams under vibration, this is especially apparent when assessing different modes of vibration, as cantilever beams have several degrees of freedom, and is introduced below in enough detail for it to be applied.

The *Euler Equation*, which governs the deflection, y_i, of a uniform cantilever beam with length, l, and mode shape, i, is:

$$y_i = A\left\{cosh\left(\frac{(\beta l)_i}{l}x\right) - cos(\beta x) - \frac{sinh(\beta l)_i - sin(\beta l)_i}{cosh(\beta l)_i + cos(\beta l)_i}\left[sinh\left(\frac{(\beta l)_i}{l}x\right) - sin\left(\frac{(\beta l)_i}{l}x\right)\right]\right\} \quad \textit{Eqn. 2.43}$$

Where, the term $(\beta l)_i$ is related to each natural frequency, $\omega_{n,i}$, the density per unit length, ρ, and the flexural rigidity of the beam, EI, as follows:

$$(\beta L)_i^{\,4} = \frac{\rho {\omega_{n,i}}^2}{EIL^4} \quad \textit{Eqn. 2.44}$$

From here the natural frequencies may be solved by re-arranging Eqn. 2.44 to Eqn. 2.45 solving the frequency equation (Eqn. 2.46) for the constants $(\beta l)_i$.

$$\omega_{n,i} = \frac{(\beta l)_i^{\,2}}{L^2}\sqrt{\frac{EI}{\rho}} \quad \textit{Eqn. 2.45}$$

$$cosh(\beta l)_i cos(\beta l)_i + 1 = 0 \quad \textit{Eqn. 2.46}$$

These constants, along with Eqn. 2.44 are used to determine the natural frequencies and modes of vibration of the beam, as can be noted in texts such as that by Whitney (1999).

2.5 FATIGUE ASSESSMENT

Fatigue describes the increasing inability to withstand stress with increasing number of stress applications. The periodicity of wind turbine loads due to variations in wind velocity across the rotor-sweep area and the rotational-mass effects makes material fatigue a key consideration in wind turbine design. These effects are intensified during extreme environmental conditions due to turbulence and wind gusts, as well as during start-up and shut-down manoeuvres. Transient and stochastic loads are generated from these loading cases acting on the rotor and tower. The effect of vibrations on stability has been introduced in the previous sections where it was noted that large amplitude vibrations resulting in instability may be avoided with the control of component stiffness. However, complete cancellation of vibrations in wind turbine structures un-realistic based on the intrinsically dynamic nature of the structure and the limited role that damping can play due to cost efficiency. The number of loading cycles that a wind turbine is subjected to may be approximated as follows:

$$n_l = 60kn_{rotor}h_{operating}Y_{operating} \quad \textit{Eqn. 2.47}$$

Where k is equal to the number of blades, n_{rotor} the operating frequency (RPM) and h and Y denote the operating hours per year and the turbine service life, in years, respectively. Hence, a wind turbine structure generally experiences 10^8-10^9 stress reversals over its typical service-life of 20-30 years. This is considered extremely high, as shown by Table 2.1.

Table 2.1 **Cycle-fatigue ranges for typical structures (Göransson and Nordenmark, 2011)**

Low-cycle ($0 - 10^3$)	High-cycle ($10^3 - 10^7$)	Super-high-cycle ($10^7 - 10^9$)
Earthquake loading	Bridges	Mass transport systems
Storm loading	Airport pavements	Wind power plants
Wind loading		Offshore structures

This approximation refers to the major stress reversals (maximum amplitude) associated with the rotational frequency. However, due to mass imbalances during operation, there are a significant number of minor stress reversals between each major stress reversal stemming mainly from the flap-wise moments. Although the minor stress reversals have a significantly lower magnitude than their major counterparts, they further exemplify the importance of material fatigue in rotor and tower design. Additionally, wind turbine structures comprise various different materials, including GRPs, high strength steel and reinforced concrete, the fatigue properties of which vary considerably. Therefore, methods of fatigue assessment are introduced below in view of offering a foundation on which the fatigue life of different components may be assessed.

Fatigue assessment methods are centred on approximating a material's fatigue life. This is a complex process as the fatigue life of a material depends on the relationship between the number of load cycles, the respective amplitudes of stress, whereby the lower the amplitude of stress the greater the number of load cycles that may be withstood. The following methods of assessment are deemed appropriate for wind turbine components due to their flexibility between different materials.

2.5.2 Miner's Rule

Miner's Rule or the *cumulative damage approach* sums the damage contribution of each load cycle over a material's service life and compares this to the total number of cycles to failure. Hence, the number of load cycles of the i^{th} amplitude (n_i) are compared against the number of cycle's to failure in the respective i^{th} amplitude (N_i). The cumulative damage, D, is then defined as follows:

$$D = \sum \frac{n_i}{N_i} \qquad \textit{Eqn. 2.48}$$

2.5.3 S-N Curves

S-N curves represent the fatigue life of a structure by plotting the amplitude of cyclic stress (S) against the number of loading cycles (N) at that particular stress. The S-N curve method is popular as it has been carried out for a wide array of materials and component geometries. An endurance limit is often specified for materials which do not fail after 10^7 cycles. Thus, it is important to note that wind turbine components are often designed based on the endurance limit.

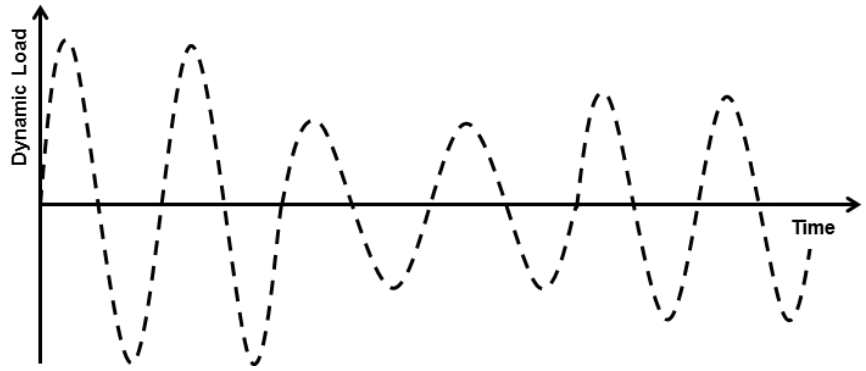

(a)

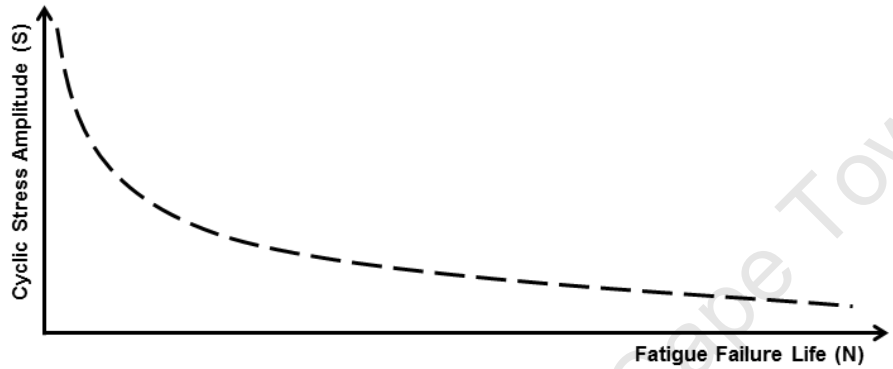

(b)

Figure 2.15 **Fatigue assessment: (a) load cycles of different amplitude and (b) typical S-N curve**

2.6 SUMMARY

1. Wind turbine structures are inherently dynamic structures. That is, the environmental conditions and state of operation dictate the nature of loading that they must withstand, and because the loading is time-dependent the structural response is also time-dependent.
2. The aerodynamic forces induce lift and drag on the rotor, causing it to rotate. The rotor must be able to withstand the aerodynamic loads which vary with the wind profile across the blade-sweep area. The periodicity of these forces is described with respect to the rotor frequency (1P).
3. Rotor blades are also subjected to periodic forces from the rotational-mass effects which refer to the changes to the weight, centrifugal and inertial forces with respect to blade azimuth angle, ψ. These forces are described by the blade passing frequency (3P).
4. When parked, the aerodynamic loads do not diminish, but rather change as there is negligible aerodynamic shedding. That is, the drag force on each blade increases as there is no lift component.

5. The loading of the tower is dependent on the rotor loading and aerodynamic forces acting on the tower. Key considerations include the interaction between the rotor and tower, the influence of the rotor control system used and aerodynamic induced vibrations, due to vortex-shedding and rotor operation.
6. All the loads imposed on a wind turbine and the loads induced by its operation are ultimately transferred to the foundation through the tower.

Critically, the above mentioned forces induce a dynamic response in the structure culminating in vibrations. To limit vibrations the tower must be designed such that the natural frequency avoids the 1P and 3P frequencies with an appropriate margin of error (usually $\mp 10\%$).A brief introduction to the importance of fatigue and appropriate methods of fatigue assessment was also presented in view of the damaging effects low-amplitude vibrations can prompt.

3. INTRODUCTION TO WIND TURBINE FOUNDATION BEHAVIOUR

3.1 INTRODUCTION

A substructure, or foundation, serves the purpose of providing a sufficiently safe connection between the ground and the superstructure, thereby acting as an interface between the superstructure and the ground. The foundation design and its response need to be understood within this context: that is, the foundation is directly affected by the loads transferred to it from the wind turbine tower and underlying soil and rock properties, which are in turn also affected by the load application.

The previous chapter dealt with key mechanical and dynamic aspects of wind turbine structures with the principle aim of providing insight into the nature of loads transmitted to the foundation as well as the factors affecting the loads. Based on the complex array of loads transferred to the foundation, several different foundation concepts have been developed over the last few decades. Modern and traditional founding concepts are studied in this chapter, which is preceded by a quantitative analysis of wind turbine foundation behaviour in response to the applicable loads previously discussed. In doing so, this chapter aims to establish a base upon which foundation design principles as well as foundation behaviour may be interpreted in the following chapters.

3.2 THE FOUNDATION DESIGN PROBLEM

In summary, wind turbine towers are slender structures, with low stiffness and a rotating mass at the free-end. It is within this context that foundation design must be understood. The nature of the structure, and hence the nature of loads transmitted to the foundation, govern the design of wind turbine foundations.

1. The vertical load transmitted to wind turbine foundations is minor in comparison to the magnitude of the overturning moment and horizontal forces imposed on the structures. This is mainly due to the slenderness and significant tower height of the structure, which results in highly eccentric loads.
2. Wind turbines are subjected to loads of a cyclic nature emanating from the environment and the rotational effect of the rotor. What makes this unusual is the fluctuation of moment and horizontal loads with time, as a result of the external conditions and operation of the wind turbine.

3. The dynamic nature of the loading leads to the time varying response of the structure: vibrations. Vibrations are an important consideration in wind turbine design as these structures are classified as *isolated columns* in foundation-engineering terms. Vibrations coupled with the cyclic nature of the overturning and horizontal actions leads to the cyclic degradation of soil stiffness over time, making differential settlement a key concern.

Given these points, wind turbine foundations may be summarised as low frequency machine loaded foundations, subjected to coupled horizontal and rocking motion. Torsional and vertical loads are also applicable but of significantly lower magnitude, which exacerbates the rocking and lateral modes. For this reason, the rotational and lateral stiffness of the foundation is of paramount importance, whereby wind turbine manufacturers usually impose specific limits, as a function of hub height, on the foundation design.

Thus, the design of wind turbine foundations is a *dynamic soil-structure interaction* problem where an understanding of the structural mechanics involved is required, due to the two facets of the system working in tandem. The crux of this is that the soil stiffness affects the response of the structure, and therefore cannot be ignored during design by assuming that the wind turbine structure has a fixed base. Furthermore, the constituents of the subgrade pose important consequences on the response, that is, the natural frequencies and modes of vibration of the structure. This means the structural response of a wind turbine underlain by soft soil will differ significantly to that of a shallow soil layer underlain by bedrock. The task of the foundation engineer is to design an economical foundation, which may be constructed time-efficiently, while accounting for the above-mentioned characteristics of wind turbine structures.

3.3 FRAMEWORK FOR EVALUATING WIND TURBINE FOUNDATIONS

3.3.1 Definition of Foundation Loading

The afore-discussed loading mechanisms relevant to wind turbines may be classified in terms of the soil response to such loads, as follows:

3.3.1.1 Monotonic Load

A monotonic load is a force or displacement path applied in a constant direction. When this force is applied over a sufficiently long time there is a negligible time dependent response. Hence it is often referred to as *static loading*. However, although monotonic loads are constant in direction and magnitude, they may induce a transient response in the underlying strata if the rate of loading is high.

3.3.1.2 Transient or Dynamic Loading

Transient loading refers to scenarios where the soil's response to loading is time dependent. Transient loading is characterised by a single impulse of short duration. Simply put, there are no loading cycles. The response of saturated soils to transient loading is a function of the rate of loading and rate of fluid flow within the soil matrix. Transient effects are also evident in the loading of dry soils where soil structure plays a vital role.

3.3.1.3 Cyclic Loading

Cyclic loads are those that involve reversals of load about a mean level and are periodic in nature. Cyclic loading may be static or transient depending on the period of loading (long or short), respectively, and nature of the soil's saturation (dry or saturated). When the number of cycles is excessively high then the soil behaviour becomes essentially fatigue related generally leading to a decrease in stiffness with loading cycles.

Dynamic and cyclic loading may be classified into three categories, in terms of the number of load cycles: (1) impulse loading, where the dynamic event is generally singular and of short duration, (2) vibration or wave propagation problems where loading is at a frequency in the range of 1 Hz to 1000 Hz and (3) fatigue related, where the number of load cycles is excessively high. Based on this classification framework, wind turbines foundations may be viewed primarily as a vibration-fatigue related problem.

3.3.2 Response of Foundations to Loading

The above discussion, coupled with the previous chapter, has highlighted the key response mechanisms associated with the respective wind turbine loads. The design of wind turbine foundations requires cognisance of this, which may be summarised within the design criteria and limit states. The ultimate and serviceability limit state design of foundations for onshore wind turbine structures should be done within the following framework (Morgan and Ntambakwa, 2008):

1. Soil-foundation strength
2. Stability
3. Soil-foundation stiffness
4. Differential settlement

Economic and durability aspects are also fundamental to wind turbine foundation design, but were omitted here as this study was centred on the geotechnical design of wind turbine foundation.

These themes were divided into monotonic and dynamic-cyclic loading, whereby strength and stability were seen as central to the ultimate limit state conditions and stiffness and settlement were deemed fundamental to serviceability constraints on the structure. Hence, Part II and Part III were divided as illustrated by Figure 3.1(a) and (b) respectively.

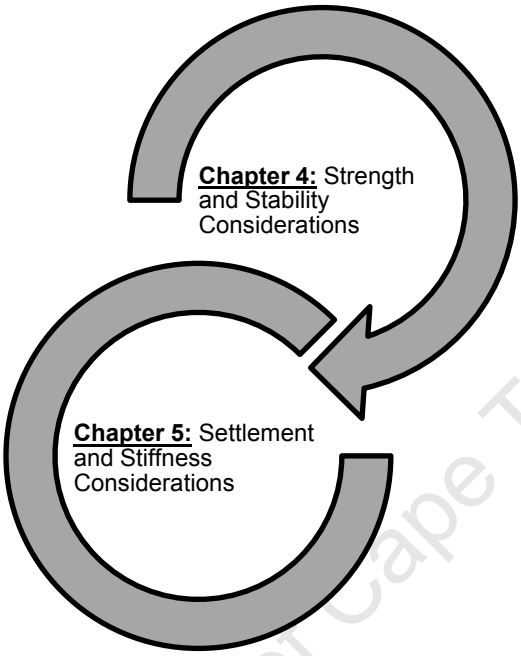

(a)

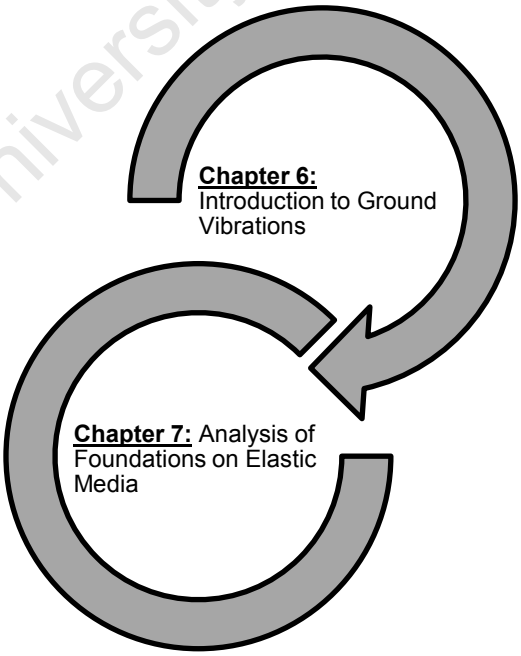

(b)

Figure 3.1 **Organisation of (a) Part II and (b) Part III**

3.3.2.1 Strength

Foundation strength refers to the structural and geotechnical design of the foundation in terms of ensuring that the respective structural and soil elements can withstand the ultimate load cases. Thus, the soil shear strength and bearing capacity as well as the structural design of the foundation are the critical components ensuring strength. The structural design of foundations does not fall within the scope of this study, but the geotechnical strength aspects - under the theory of bearing capacity - are dealt with extensively in Chapter 4.

3.3.2.2 Stability

Stability is associated closely with strength, in terms of it being directly associated with the ultimate loads. Where strength refers to the ability of the foundation materials to withstand load, stability refers mainly to the geometry of the foundation. The resistance to overturning and sliding are the foremost aspects of stability; which are dealt with alongside bearing capacity in Chapter 4.

3.3.2.3 Stiffness

Soil-foundation stiffness refers to the ability of the foundation to resist deformation under loading. One of the foremost serviceability criterion provided by wind turbine manufacturers is the minimum rotational stiffness of the foundation. This criterion controls the deflection of the foundation under the overturning moment emanating from the superstructure, which at times may be extremely high in magnitude and transient in nature. The rotational stiffness of the foundation is a key factor governing soil-structure interaction and plays an important role in resisting the rocking dominated modes of vibration prevalent in shallow foundations. It should be noted that the magnitude of vibration satisfying serviceability usually involves relatively small dynamic displacement amplitudes. As a result the soil-foundation system is often modelled as a linear elastic system for small amplitudes of strain. This assumption and other aspects of stiffness are introduced in Chapter 5 and expanded upon in Part III.

3.3.2.4 Settlement

Settlement considerations are closely related to stiffness and stability. Insufficient or differential stiffness may result in uplift at one edge of a shallow foundation. Settlement, although regarded as a serviceability criterion, may result in failure of the structure based on the nature of loads applied, as uplift at one edge of a foundation base may result in overturning under application of a transient natured overturning moment. Furthermore, the issue of settlement may affect the operation of machinery, which highlights the importance of wind turbine foundation placement in variable ground conditions.

3.4 FOUNDATION LIMIT STATES

Foundation limit states for wind turbines are stipulated below, in accordance with AWEA/ASCE (2011) and International Electrotechnical Commision (IEC) (2005).

3.4.1 Ultimate Limit State

Foundation structural elements should be proportioned and designed to have sufficient strength to resist the most critical factored load combinations to ensure structural safety of the foundation. ULS considerations include the ultimate strength of the concrete, reinforcing steel, anchor bolts, pre-stressing elements, grouting and embedment rings. From a geotechnical point of view, ULS refers to the overall stability of the structure, including bearing capacity, resistance to overturning and stability against sliding.

3.4.2 Serviceability Limit State

SLS limit states are critical in ensuring the structure may operate in a safe and efficient manner. Thus, SLS considerations include limiting foundation settlement and tilting, minimising the development of gaps between the foundation and soil, ensuring sustained soil stiffness, minimising crack propagation and foundation movement.

3.4.3 Fatigue Limit State

Due to the dynamic and cyclic nature of wind turbine loads, it is imperative that the foundation concrete, reinforcing steel, anchors and the soil-foundation system have adequate fatigue strength. It is also critical that the foundation-soil system possesses adequate stiffness to resist cyclic loading over the structure‘s lifespan with no significant reduction in load-carrying capacity.

3.5 FOUNDATION OPTIONS FOR WIND TURBINE STRUCTURES

3.5.1 Classification of Foundation Systems

Several different foundation options have emerged in view of §3.2, ranging from the conventional concepts to methods tailored for wind turbine loading. The foundation selection depends on the site-specific soil conditions and the ability of the underlying strata to provide bearing resistance and stability against overturning as well as adequate stiffness to ensure the serviceability limit states are met. As is with conventional foundation design, wind turbine foundations may be classified in terms of shallow or deep. The orthodox means of differentiation are as follows:

1. Shallow foundations: $d/B < 1$ where d is the depth of founding and B the breadth (or equivalent diameter) of the foundation.
2. Deep foundations: $d/B \geq 1$

This being said, the nature of wind turbine foundations often requires thick bases and deep founding levels in order to provide sufficient resistance to overturning and the shear forces induced from foundation bending. Thus, wind turbine foundations may be further classified in terms of the load-transferring mechanisms involved. Shallow foundations tend to resist overturning by means of the overburden and their self-weight. The axial loads are distributed over an area which ensures the force intensity is kept within the constraints of the material strength. Figure 3.2 illustrates different shallow foundation options for wind turbine structures, ranging from conventional to modern methods, the details of which are studied in the following sections.

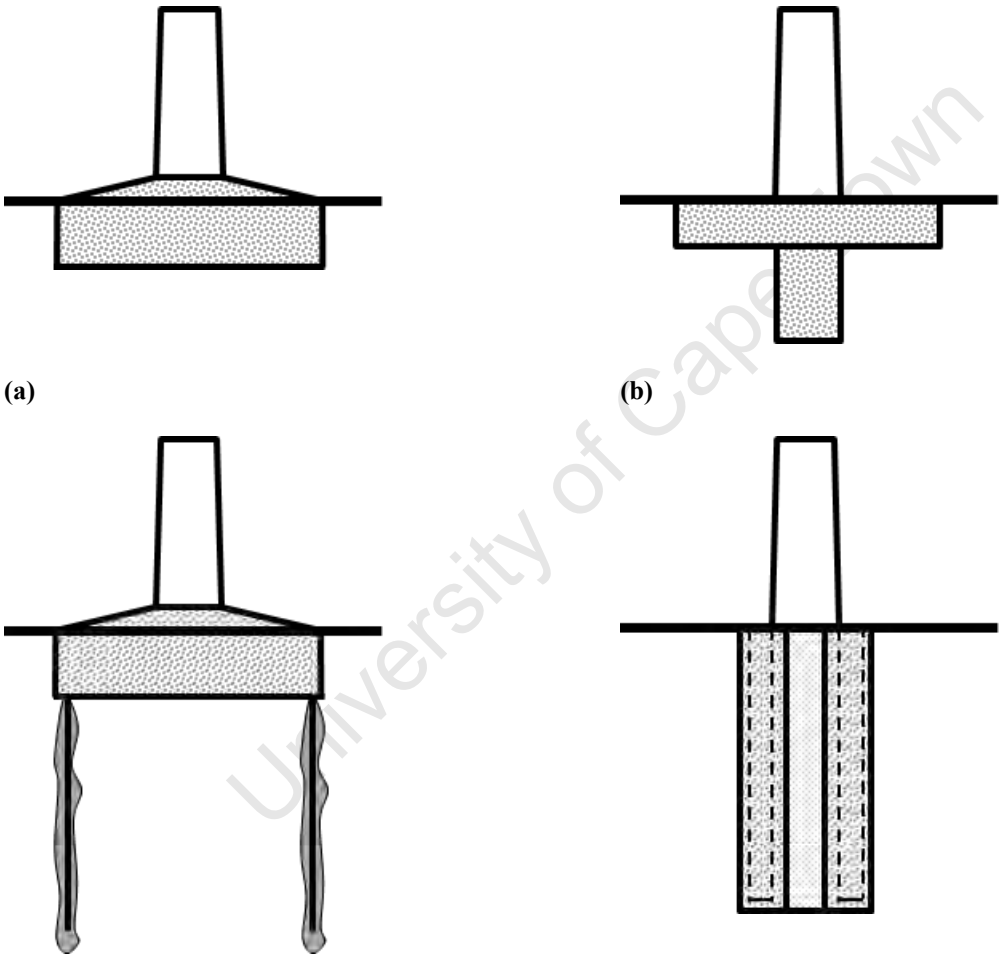

Figure 3.2 **Wind turbine shallow foundation options: (a) pad footing, (b) stiffened pad foundation, (c) anchored footing and (d) pre-stressed concrete pier**

Deep foundations tend to resist lateral loads through bending, uplift and compression, depending on the pile configuration, and the soil resistance adjacent to the foundation. Axial loads are mobilised through skin-friction and bearing resistance.

Figure 3.3 presents a schematic view of the three principal deep foundation methods for wind turbine structures. The length of embedment is dependent on a combination of the subgrade conditions, loading intensity, the method of pile construction and the mechanism of load transfer of the respective pile configuration.

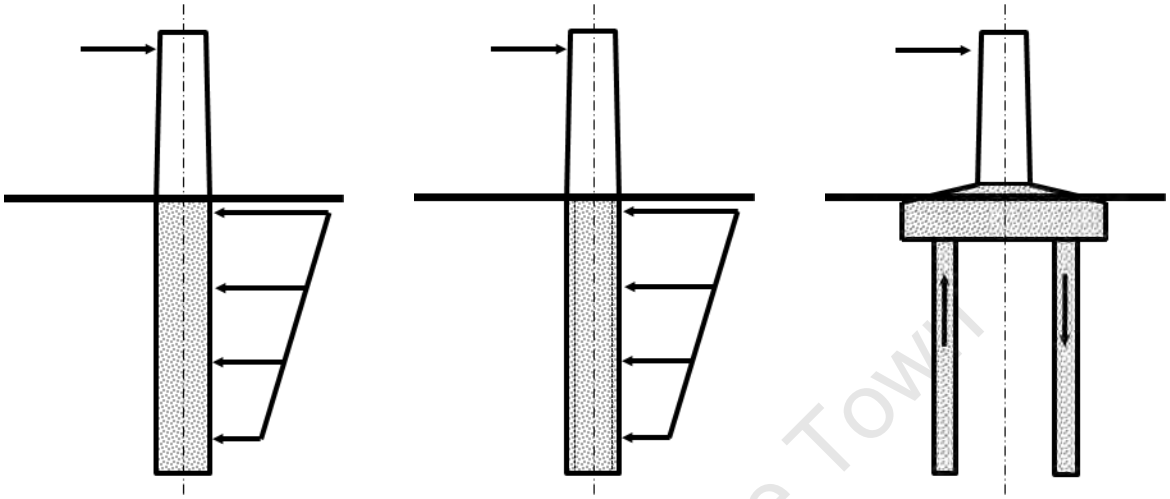

(a) **(b)** **(c)**

Figure 3.3 **Conceptual views of different deep foundation options for wind turbines: (a) solid monopile, (b) hollow monopile and (c) group and cap**

However, exploring the details of these mechanisms fell outside the scope of this study due to the following reasons:

1. Deep foundations are generally used in the offshore industry to resist considerably higher lateral loads emanating from wave loading. The use of piles onshore is only justified in extremely poor soil conditions based on the relatively minor structural benefit derived with respect to the added construction expense and time.
2. The process of deep foundation design is highly empirical and site specific as well as dependent on the construction process and experience of the operator(s). Therefore, presenting general design considerations for deep foundations here was considered superfluous.
3. The lateral capacity of piles and their behaviour under cyclic loading is a broad and complex topic which stems from the offshore gas and oil industry. The traditional methods used to design such piles are still being adapted for wind turbine structures and their characteristic loading. Reese and van Impe (2001) and Fleming et al. (2009) may be consulted for more traditional approaches to designing deep foundations for the respective loading conditions.

3.5.2 Pad Footings or Gravity Foundations

Wind turbine structures are conventionally founded on what may be classified as large pad footings. Pad foundations specific to wind turbines may be further classified as isolated footings with properties not dis-similar to raft foundations, including; large thickness to breadth ratios and bi-axial compression and tension reinforcing to ensure high foundation stiffness.

The foundation relies on its self-weight and soil over-burden to provide sufficient resistance to overturning, leading to them often being referred to as gravity foundations, and on the soil shear strength and compressibility characteristics for vertical resistance. The design methods for such foundations are also universally accepted and well understood, as well as this foundation concept being applicable to a wide range of subgrade strengths, making this the simplest and most common form of foundation for wind turbines (Morgan and Ntambakwa, 2008).

Pad footings for wind turbine structures were pioneered in the United Kingdom (UK), where early wind farm developments took place in the highlands on competent soils and rock (Bonnett, 2005). These foundations were generally rectangular, circular or octagonal in shape. Octagonal and circular footings have proved to be more suitable because at least four reinforcement layers can be provided in the bottom layers, as opposed to the two orthogonal directions provided by a rectangular footing (Maunu, 2008). This aids the moment carrying capacity of the foundation as well as construction efficiency and time. Furthermore, circular footings, approximated by an octagon or hexa-decagon, are most economical for the support of large towers where the direction of overturning moment is not fixed (Bowles, 1996). A typical octagonal wind turbine plan and sectional view is illustrated by Figure 3.4.

A critical component of pad footings is the pedestal and connection between the tower and slab. This component of the foundation is generally specified by the wind turbine manufacturer and also depends on the tower configuration. However, in general two methods have emerged, as illustrated in Figure 3.2:

1. The first is an I-beam-ring cast within the concrete. The tower is connected to the flange of the ring by pre-stressed bolts. The depth of the ring and adjacent reinforcing steel may be adjusted to better suit the applied loads and footing thickness as required.
2. The second option connects the tower to the foundation by a pre-stressed anchor bolt cage. This is done by casting a flange at the top and bottom of the slab, through which the bolts connecting the tower are pre-stressed.

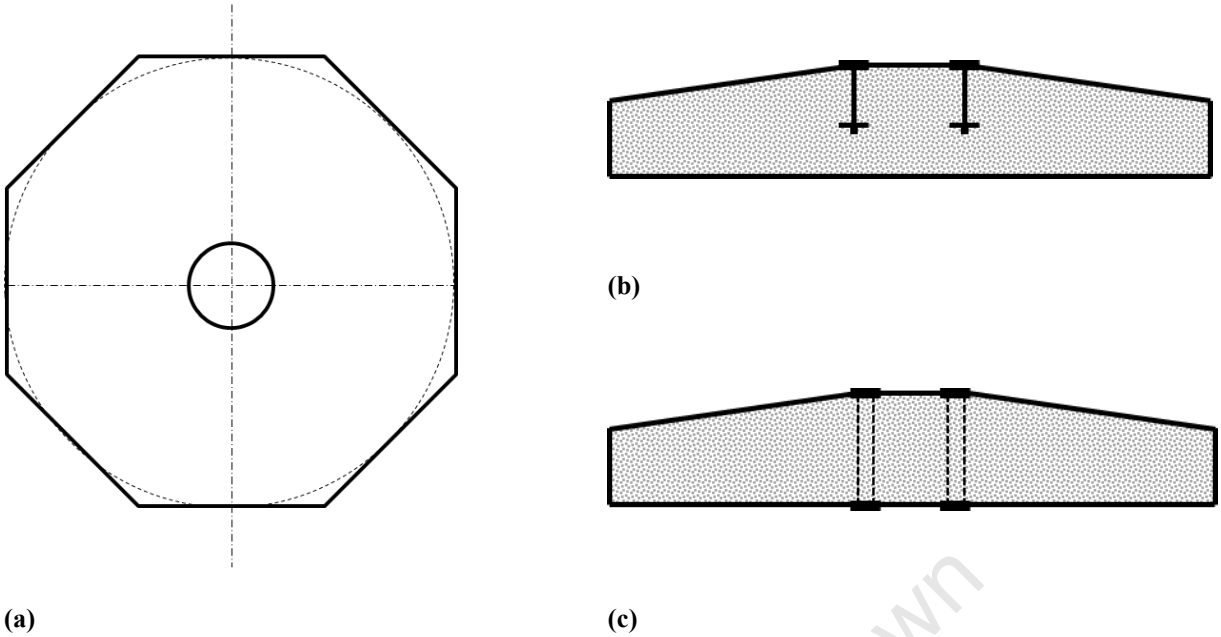

Figure 3.4 **Standard pad footing: (a) plan view, (b) section view of I-ring connection configuration and (c) the pre-stressed anchor-bolt connection**

Theory of elasticity and observations indicate that the stress distribution below a symmetrically loaded footing is not uniform, as is often assumed during pad footing design. Instead, the actual stress distribution depends on both the footing rigidity and stiffness of the founding soil. The purpose of the foundation is to distribute the applied loads to the underlying strata, and therefore, the internal stresses within the foundation are directly affected by the reaction of the subgrade. Modelling the actual soil reaction is the core of soil-structure interaction, and provides valuable insight into optimising the material requirements of foundations. Several different models have been developed to achieve this, each with varying degrees of complexity and accuracy, the details of which are addressed in §5.3.2.

This is an important consideration for wind turbine pad footings, which are required to resist large internal bending moments and shear forces based on the applied loads and geometry of the foundation. Novel wind turbine foundation concepts have been developed based on these issues of optimising material costs, a few of which are studied below.

3.5.3 Stiffened Pad Footings – The Gestamp iConkrete Wind Turbine Foundations

Gestamp iConkrete (iCK) wind turbine foundations operate similarly to pad foundations in terms of distributing the respective loads over an area which ensures the stress intensity remains safely within the bearing capacity of the soil. However, this foundation concept employs a pad of lower thickness, coupled with stiffening ribs to increase the stiffness of the system, which results in the foundation acting essentially like a series of connected T-beams.

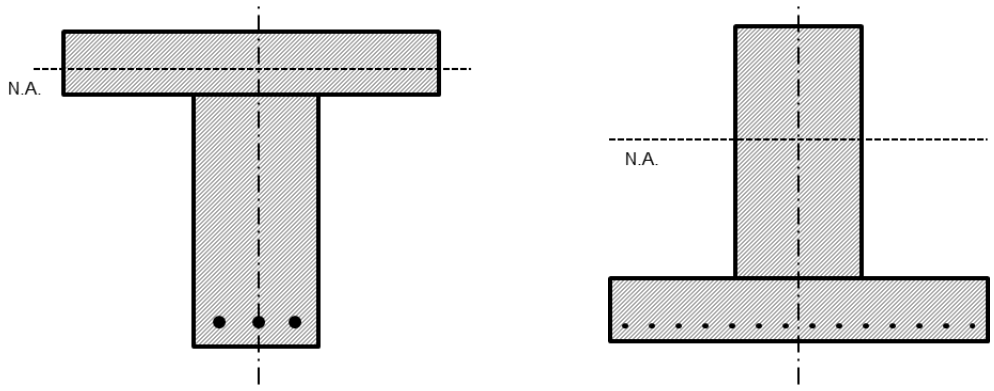

(a) **(b)**

Figure 3.5 **Elevation view of (a) iCK foundation and (b) conventional stiffened foundation**

The configuration of the iCK foundation renders the foundation more efficient – in terms of the volume of materials required – as a result of improved ductility. This is achieved by the placement if the stiffening rib on the underside of the pad footing/slab to form a T-beam configuration (Figure 3.5(a)) leading to the stiffening beam mobilising the tensile stresses induced by the overturning moment. This geometrical implication results in the neutral axis of each T-beam segment being reduced, in comparison to more conventional methods of stiffening foundations (Figure 3.5(b)). A reduction in the neutral axis leads to increased moment capacity. This arrangement of the stiffening ribs also results in improved fatigue performance and durability (Rey, 2012).

3.5.4 Rock Anchored Foundations

The use of rock bolts or micro-piles to anchor pad footings has received much attention in the field of wind turbine structures. This foundation option is especially suitable for structures founded on a shallow layer of soil underlain by bedrock (Manwell et al., 2002). Embedding an anchor in the bedrock, to sufficient depth, and connecting it to the pad footing improves the tensile stress capacity of the footing, as the anchor is used to mobilise the tensile stresses. This mechanism is significantly improved by post-tensioning of the anchor. Subsequently, a reduction in reinforcing steel and pad footing dimensions can be achieved, leading to cost optimisation of the footing.

The Patrick and Henderson (P&H) Rock Anchor Foundation is one of the novel wind turbine foundation concepts that have come to the foreground in recent years. This concept utilises a combination of a pad footing and post-tensioned anchors to improve the load carrying capacity. This is illustrated by Figure 3.6(a). This results in a saving of between 25% and 35% of costs between P&H Rock Anchor Foundations and conventional pad footings (Earth Systems Southwest, 2008).

3.5.5 Tensionless Pier Foundations

Another novel foundation concept that has emerged in the wind turbine industry is the tensionless pier. Figure 3.6(b) illustrates the P & H tensionless pier that operates as a combination of a pile and gravity foundation. A typical P & H tensionless pier has a diameter of 5 m and a depth of 10 m. These dimensions and the length of embedment generally depend on the specific loading and geotechnical site conditions. The anchor bolts which connect to the wind turbine tower are post-tensioned to ensure that the foundation remains in compression regardless of the loading scenario (Earth Systems Southwest, 2008). This ensures a high level of stiffness.

Furthermore, a deep concrete plug is cast at the bottom, the thickness of which may be varied depending on the subgrade characteristics, and the remainder of the cavity is backfilled with spoil from the foundation excavation. The level of compaction of this material is low, to aid the damping characteristics of the system. In addition, this is a pre-cast foundation which means the foundation may be constructed rapidly. This is particularly advantageous for large wind farms.

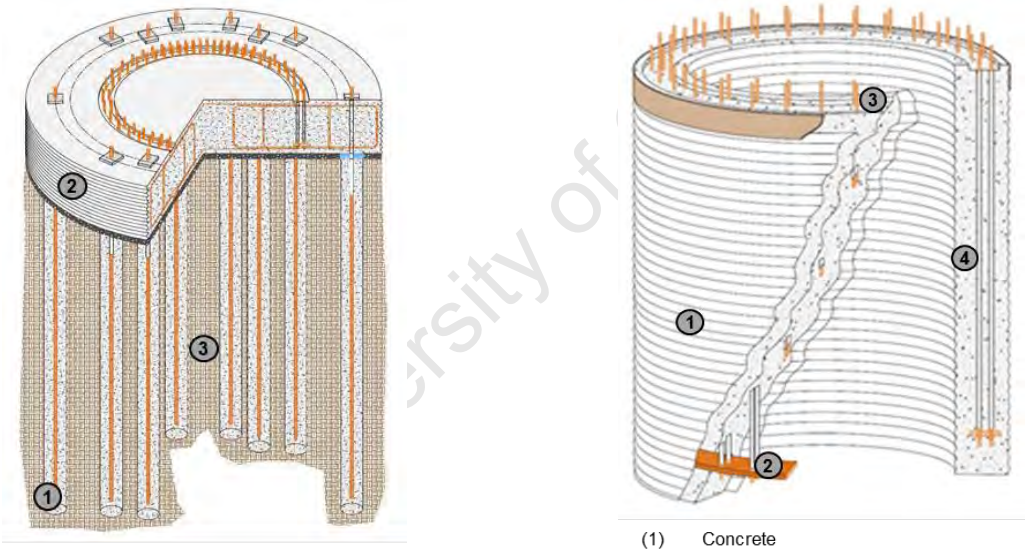

Figure 3.6 **P&H wind turbine foundations: (a) rock bolted pad footing and (b) tensionless pier footing (Earth Systems Southwest, 2008)**

Both anchored and tensionless piers are engineered systems which enhance the mechanics of the foundation, through the minimisation of tensile stresses induced by bending from the applied overturning moment. This results in a foundation which also overcomes the necessity of complex soil-structure interaction analyses as required by large footings.

3.6 SUMMARY

1. Wind turbine structures may be classified as slender cantilever elements with low stiffness and incorporating a rotating mass, the foundations of which may be viewed as machine foundations of low amplitude, dominated by rocking and translational modes of vibration.
2. Thus, wind turbine foundations present complex challenges to engineers as the disparity in overturning moment and vertical load results in extreme eccentric loading, which is dynamic in nature.
3. The design of wind turbine foundations is centred on ensuring the subgrade possess sufficient rotational stiffness to resist the dynamic and overturning nature of the respective loads.
4. Stiffness degradation upon repeated stress cycles is also an important facet of foundation design.
5. A wide array of options is available for the founding of wind turbines, the selection of which depends primarily on the site geology and groundwater conditions.
6. Due to the nature of internal loads induced in wind turbine shallow foundations, methods of increasing the foundation stiffness have been developed. These range from pre-stressed concrete to stiffening ribs.
7. Deep foundations are utilised when the soil at shallow depths is inadequate for the resistance of the applicable loads.

PART II GEOTECHNICAL DESIGN OF SHALLOW FOUNDATIONS

4. STRENGTH AND STABILITY CONSIDERATIONS

4.1 INTRODUCTION

The primary objective of a foundation is to ensure a sound connection between the superstructure and soil, and in doing so ensure the *stability* of the structure under the respective loading. The subgrade *strength* dictates the type of foundation whereas the loading regime governs the proportions of the foundation to guarantee the foundation-soil system provides sufficient stability to the structure.

Thus, strength and stability are related to the ultimate capacity of the foundation-soil system. The following chapter was centred on providing insight into aspects of the ULS design of wind turbine foundations. In view of this, the following theory was selected based on the nature of loading, and combination thereof, that wind turbine foundations are expected to withstand to satisfy the ULS, namely;

1. A significant overturning moment, often biaxial, from the torque of the rotor and aerodynamic loads;
2. Relatively low vertical load, in relation to the overturning moment and lateral load.

Firstly, bearing capacity theory was presented to provide a base upon which further aspects of foundation design may be conducted, including the assessment of foundations under combined loading. This assessment included conventional means of foundation design such as the effective area method, as well as the yield state approach, which has come to the fore in recent years.

4.2 BEARING CAPACITY

4.2.1 Definition of the Bearing Capacity Problem

The ultimate bearing capacity is a concept which allows one to evaluate the relationship between the pressure that needs to be transmitted to a soil and the pressure that the soil can withstand without failing in shear, and therefore is defined, according to Craig & Knappett (2012), as:

1. The pressure which would cause shear failure of the supporting soil immediately to or adjacent to the foundation, or,
2. The pressure that would cause a settlement which would render the serviceability limit state of the foundation to be unfulfilled.

The concept of bearing capacity was first explored by Pauker in 1850 and later by Bell and Prandtl in the early 1900s by exploring the behaviour of a metal cone passing through a metal sheet (Fellenius, 1999). It was Terzaghi who built on this research and coined the first formal bearing capacity relationship in 1943 through the analysis of rigid continuous strip footings. This was an empirical solution based on the notion that the soil would undergo a perfectly plastic failure in shear. Fundamental to Terzaghi's solution was the *Mohr-Coulomb failure criterion* which is the framework against which the shear strength (τ_f) of the material was modelled, and still is today. This is dependent on the shear strength parameters; ϕ' and c', known as the effective internal angle of friction and apparent effective cohesion, respectively:

$$\tau_f = c' + \sigma_0' tan\phi' \qquad \textit{Eqn. 4.1}$$

Thus, failure will occur in the soil mass where a critical combination of effective normal stress and shear stress develops. It is important to note that c' and ϕ' are mathematical constants defining a linear relationship between shear strength and effective normal stress.

This is one of the most common models within the field of soil mechanics – being taught universally at undergraduate-level and used extensively in engineering practice. However, the shortcomings of this model are not as universally recognised. Basing the response of a foundation on this model has important consequences, requiring engineering judgement and experience above all else. For now, this bearing capacity model originally proposed by Terzaghi, which incorporates the *Mohr Coulomb failure criterion*, and termed the *Generalised Bearing Capacity Theory* will be discussed in more detail.

4.2.2 Generalised Bearing Capacity Theory

The *Generalised Bearing Capacity Theory* assumes the soil to fail plastically under shear when the ultimate bearing capacity is reached. In doing so, the soil mass is deemed to respond with the development of three distinct zones below and adjacent to the foundation, as defined below and illustrated by Figure 4.1:

1. The first is the triangular active shear zone (I), directly below the footing.
2. The radial shear zone or transitional zone (II) is the second shear zone below and adjacent to the footing. This was derived based on the assumption, and later correlation with experimental results, that the shear zone would take the shape of a log-spiral (Strahler, 2012).
3. Lastly, the third zone is termed the *Rankine Passive Zone* (III) and develops due to the density of the material and relevant surcharge.

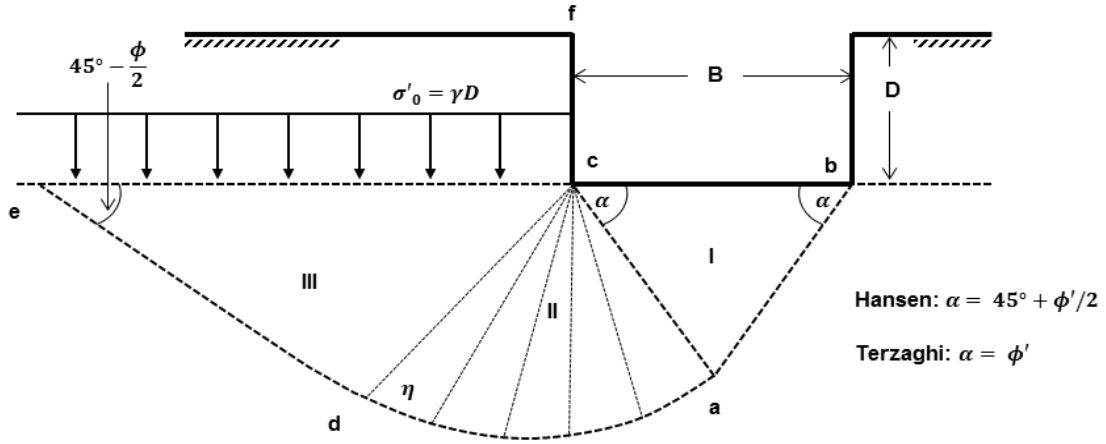

Figure 4.1 **Failure under a strip footing (adapted from (Craig, 2004))**

Figure 4.2 illustrates the comparison between three distinct bearing capacity failure modes with respect to pressure and settlement. These are (1) general shear failure, (2) local shear failure and (3) punching shear failure. The failure mode is a function of the soil density, whereby general shear failure is most likely to occur in dense or stiff strata. Local shear and punching shear failure are most likely to occur in medium loose/soft deposits and very loose/soft (collapsible/compressible) deposits, respectively.

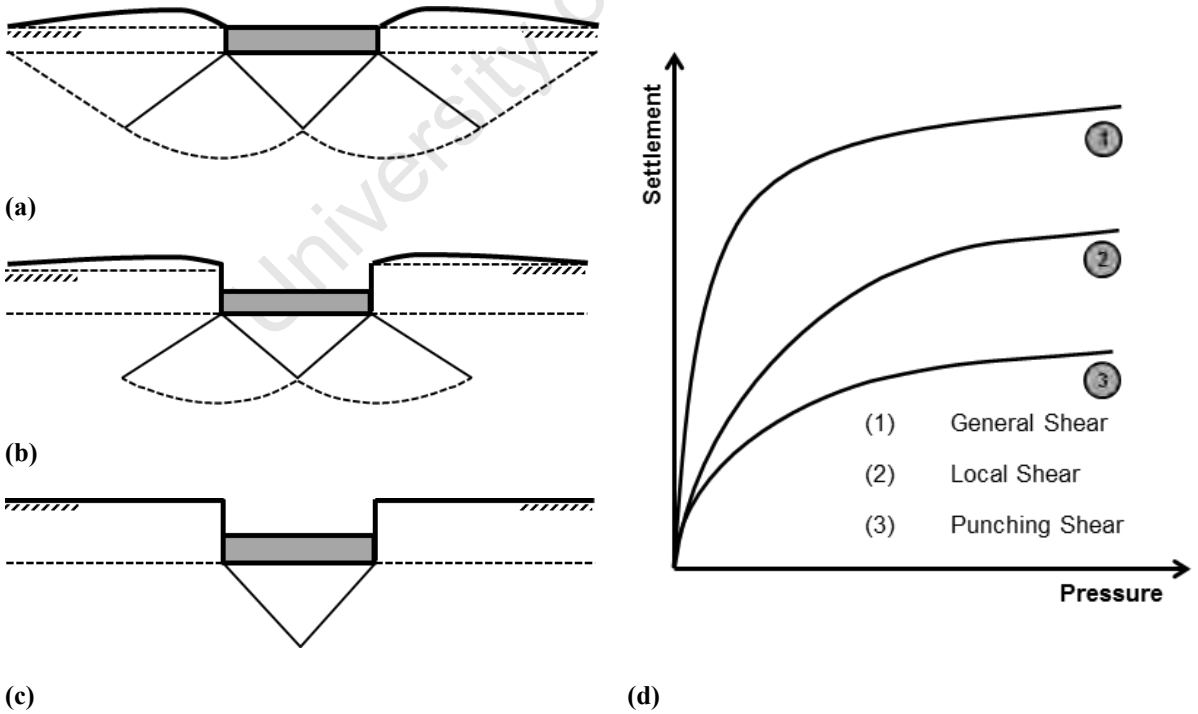

Figure 4.2 **Bearing capacity modes of failure: (a) general failure, (b) local failure, (c) punching failure and (d) pressure-settlement behaviour for each mode**

The bearing capacity formulation has received significant attention since the 1940s. This has mainly been with regard to the bearing capacity factors: N_c, N_q and N_γ, on which the solution was based. These factors are principally dependent on the shear strength parameters of the soil, and most specifically the internal angle of friction and effective stress, due to the assumption that shear failure occurs when the bearing capacity is exceeded as defined by Figure 4.1.

4.2.2.1 The Bearing Capacity Factors

The first bearing capacity factor is defined as the ratio of ultimate bearing capacity, σ_f', and the vertical effective stress in the ground on either side of the foundation at the level of founding, σ_o'. This is displayed by Eqn. 4.2, where K_p is the coefficient of passive earth pressure, given by Eqn. 4.3.

$$\frac{\sigma_f'}{\sigma_o'} = N_q = K_p e^{(\pi tan\phi')} \qquad \textit{Eqn. 4.2}$$

$$K_p = \frac{1 + sin\phi'}{1 - sin\phi'} \qquad \textit{Eqn. 4.3}$$

N_c relates the difference between the vertical total stress on the foundation at failure, σ_f, and the total vertical stress in the ground on either side of the footing, σ_o (on the founding plane) to the undrained shear stress, c_u. This term is commonly referred to as the *cohesion bearing capacity factor* and is defined by Eqn. 4.4, where σ_o is subsequently defined by Eqn. 4.5.

$$\frac{(\sigma_f - \sigma_o)}{c_u} = N_c = \frac{N_q - 1}{tan\phi'} \qquad \textit{Eqn. 4.4}$$

$$\sigma_o = \int_0^d \gamma(z)dz \qquad \textit{Eqn. 4.5}$$

The final bearing capacity factor, N_γ, accounts for the soil that takes part in the eventual failure mechanism empirically. This term accounts for the weight of the soil below the foundation level to a depth approximately equal to the breadth of the footing. Expressing it analytically has received much attention due to its dependence on the foundation-soil interface roughness as well as being a function of the foundation size due to the role that dilation plays during shearing (Craig and Knappett, 2012).

Table 4.1 in conjunction with Figure 4.3 compares several prominent bearing capacity factor theories. From this it is apparent that there is relatively little sensitivity between the Brinch Hansen (1970), Vesic (1975) and Salgado (2008) theories, especially at lower values of ϕ'. However, the sensitivity of the bearing capacity factors to changes in ϕ' should be noted, as this is one of the fundamental shortcomings of the Generalised Bearing Capacity Theory, given the inaccuracies associated with determining ϕ'.

Table 4.1 **Comparison of different empirical bearing capacity expressions for N_γ**

Theory	Bearing Capacity Factor	
Meyerhof (1963)	$N_\gamma = (N_q - 1)tan\,(1.4\phi')$	*Eqn. 4.6*
Brinch Hansen (1970)	$N_\gamma = 1.5(N_q - 1)tan\,(\phi')$	*Eqn. 4.7*
Vesic (1975)	$N_\gamma = 2(N_q + 1)tan\,(\phi')$	*Eqn. 4.8*
Salgado (2008)	$N_\gamma = (N_q - 1)tan\,(1.32\phi'$	*Eqn. 4.9*

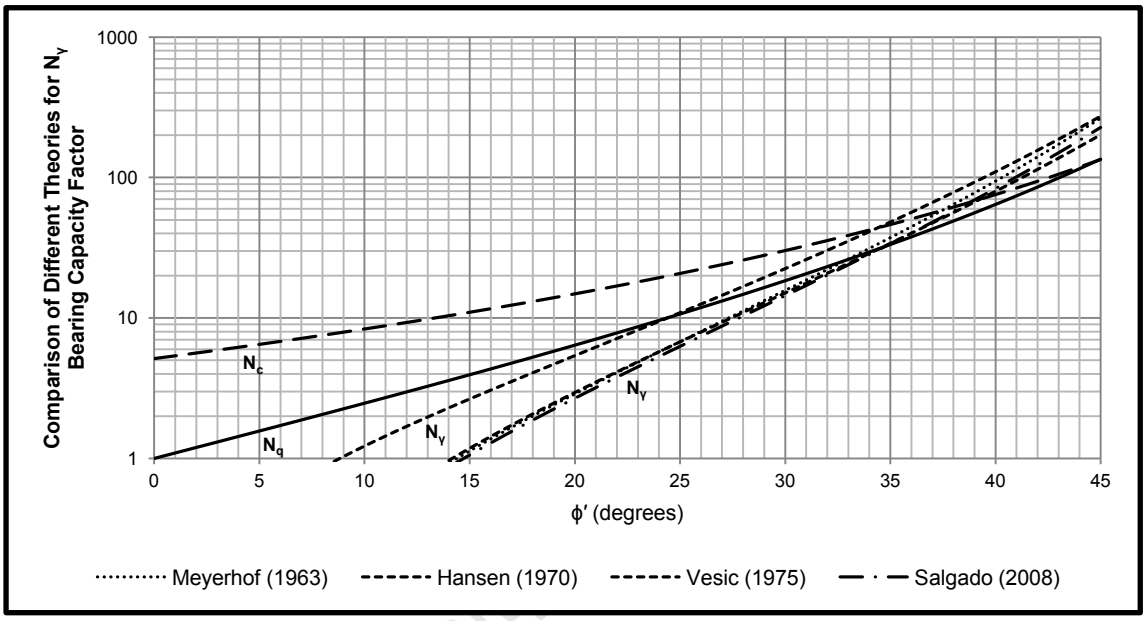

Figure 4.3 **Bearing capacity factors for shallow foundations under drained conditions**

4.2.2.2 The Effective Stress Failure Criterion

The ultimate load that can be resisted by a rigid strip footing of infinite length, V_f, is defined by Eqn. 4.10, where $A_{footing}$ is the area of the footing.

$$V_f = A_{footing}\left[N_c c + N_q \sigma_0' + N_\gamma \left(\frac{1}{2}\gamma B - \Delta u\right)\right] \qquad \textit{Eqn. 4.10}$$

There are two problems with Eqn. 4.10; when compared to the behaviour of footings in practice, (1) most foundations are not infinitely long and (2) the soil on either side of a foundation, which is modelled as a surcharge in Eqn. 4.10, possesses strength which stems from its structure. Thus, in effective stress terms, the bearing capacity equation is altered to account for the shape of the foundation and its depth.

$$V_f = A_{footing}\left[N_c s_c d_c c + N_q s_q d_q \sigma_0' + N_\gamma s_\gamma d_\gamma \left(\frac{1}{2}\gamma B - \Delta u\right)\right] \qquad \textit{Eqn. 4.11}$$

Where, in addition to the symbols already defined,

- s_c, s_q, s_γ : shape factors used to account for the fact that footings are not infinitely long;
- d_c, d_q, d_γ: depth factors which account for the reality that the soil adjacent to the foundation and above the foundation plane has some strength and does not only act as a surcharge.

Further to this, research in the mid-1960s and early 1970s yielded different empirical relationships for certain bearing capacity factors. These different relationships are discussed thoroughly in comprehensive foundation engineering texts such as Bowles (1996). The key differences between different factors, for an effective stress failure criterion, are summarised in Table 4.2.

Table 4.2 **Bearing capacity enhancement factors; effective stress failure criterion**

Parameter	Meyerhof (1963)	Brinch Hansen (1970)
Shape Factor (s_q)	$1 + 0.1K_p\left(\frac{B}{L}\right)$	$1 + \left(\frac{B}{L}\right)tan\phi'$
Depth Factor (d_q)	$1 + 0.1\sqrt{K_p\left(\frac{d}{B}\right)}$	$1 + 2tan\phi'(1 - tan\phi')k^{(1)}$
Bearing Capacity Factor (N_γ)	$(N_q - 1)\,tan(1.4\phi')$	$1.5(N_q - 1)tan\phi'$
Shape Factor (s_γ)	s_q	$1 - 0.4(B/L)^{(2)}$
Depth Factor (d_γ)	d_q	1

(1) $k = d/B$ if $d/B \leq 1.0$ else $k = tan^{-1}(d/B)$ [rad]

(2) Foundation length, L, breadth, B, and depth, d.

For the design of large bases at relatively low D/B ratios – such as the bases required to resist overturning of wind turbines – it is important to introduce another empirical factor. The reduction factor, r_γ, is used to account for the fact that the bearing capacity of footings does not increase indefinitely as the base area increases.

Eqn. 4.12 gives the definition of r_γ where $B \geq 2\ m$ and $\kappa = 2.0$.

$$r_\gamma = 1 - 0.25\left(\frac{B}{\kappa}\right) \qquad \textit{Eqn. 4.12}$$

This also applies to the undrained failure criterion, discussed below.

4.2.2.3 Undrained Failure Criterion

The bearing capacity of footings founded on clay, which are loaded rapidly is determined using a total stress analysis. This is depicted by Eqn. 4.13, and the respective enhancement factors are given in Table 4.3.

$$(\sigma_f - \sigma_o) = N_c s_s d_c c_u \qquad \textit{Eqn. 4.13}$$

Table 4.3 **Bearing capacity enhancement factors; undrained shear strength failure criterion**

Parameter	Skempton (1951)	Meyerhof (1963)
Shape Factor (s_c)	$1 + 0.2(B/L)$	$1 + 0.2(B/L)^{(1)}$
Depth Factor (d_c)	$1 + 0.23\sqrt{(d/B)}$ up to $(D/B = 4)$	$1 + 0.2(d/B)^{(1)}$

(1) Foundation length, L, breadth, B, and depth, d.

4.3 SHALLOW FOUNDATION RESPONSE TO COMBINED LOADING

4.3.1 Resistance to Overturning

4.3.1.1 The Equivalent Inclined Load Approach

The above bearing capacity formulations are applicable to vertically loaded footings. In the wind turbine industry, where wind turbines exert vertical, horizontal and moment loading on the foundation, these formulations need to be adjusted.

For a clayey undrained soil, the loads are characterised by a normal stress and shear stress, denoted by σ_f and τ_f. The modified bearing capacity equation is then defined as follows,

$$\frac{\sigma_f - \sigma_o}{c_u} = N_c = (1 + \pi - \Delta + cos\Delta) \qquad \textit{Eqn. 4.14}$$

where $\sigma_f = V/B$, $\Delta = sin^{-1}(\tau/c_u)$ and $\tau = H/B$. Similarly, the modified bearing capacity for an effective stress analysis is given by:

$$\frac{\sigma_f'}{\sigma_o'} = N_q = \frac{[1 + sin\phi' cos\,(\Delta + \delta)]}{[1 - sin\phi']} e^{(\pi - \Delta - \delta)tan\phi'} \qquad \textit{Eqn. 4.15}$$

In this case, the only undefined parameters are $sin\Delta = sin\delta/sin\phi'$ and $\delta\ tan^{-1}(\tau/\sigma_o')$. Also note that the quantity $\sigma_f' = V/B$ assumes the pore water pressure at founding level is equal to zero. These modified bearing capacity factors are applied to the respective bearing capacity equation.

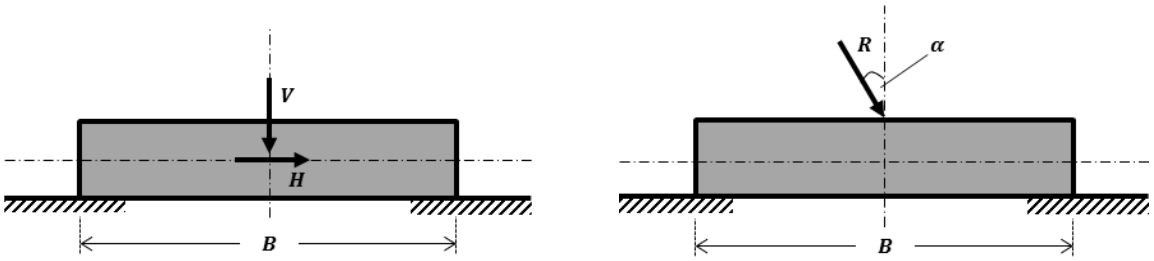

(a) **(b)**

Figure 4.4 **Statical equivalence of (a) a footing under equivalent H-V loading by (b) a central inclined load**

Alternatively, methods described by Brinch Hansen (1970) which utilised inclination factors to modify the respective bearing capacity factors. These inclination factors are defined below (Bowles, 1996):

$$i_c' = 0.5 - \sqrt{1 - \frac{H}{A_{footing} C_a}}, when\ \phi = 0° \qquad \textit{Eqn. 4.16}$$

$$i_c' = i_q - \frac{1 - i_q}{N_q - 1} \qquad \textit{Eqn. 4.17}$$

$$i_q = \left[1 - \frac{0.5H}{V + A_{footing} C_a cot\phi}\right]^{\alpha_1}, where\ 2 \leq \alpha_1 \leq 5 \qquad \textit{Eqn. 4.18}$$

$$i_\gamma = \left[1 - \frac{0.7H}{V + A_{footing} C_a cot\phi}\right]^{\alpha_2}, where\ 2 \leq \alpha_2 \leq 5 \qquad \textit{Eqn. 4.19}$$

These inclination factors are defined in terms of the equivalent horizontal load, H, and the adhesion constanc C_a and are used to account for the direction of the horizontal load by adjusting the shape factors as described by (Bowles, 1996). However, due to wind turbine bases being approximated as circular bases, by a hexa-decagon, hexagon or square, the direction of the horizontal load has negligible influence. Thus, the bearing capacity expression would become:

$$V_f = A_{footing}\left[N_c s_c d_c i'_c c + N_q s_q d_q i_q \sigma_0' + N_\gamma s_\gamma d_\gamma i_\gamma \left(\frac{1}{2}\gamma B - \Delta u\right)\right] \qquad \textit{Eqn. 4.20}$$

4.3.1.2 The Effective Area Approach

The bearing capacity theory defined in §4.2.2.2 and §4.2.2.3 are suitable for vertically loaded strip footings, where the resultant load acts through the centroid of the footing. In many cases this is not possible, which has led to the simple *effective area approach* developed by Meyerhof (1963) with contributions over the years by Brinch Hansen (1970) and Vesic (1975).

This procedure operates on the principle that a vertical load acting with an eccentricity, e, from the geometrical centre of the foundation is statically equivalent to a vertical load, V, acting at the centre, accompanied with a moment of magnitude Ve about the centre. Conversely, and more relevant to wind turbine structures, a base subjected to a moment load, M, and vertical load, V, can be made statically equivalent to a base loaded with a load V at eccentricity e. If the footing is simultaneously subjected to a horizontal load, the equivalent eccentric load becomes inclined, as discussed in the previous section. This relationship is illustrated by Figure 4.5.

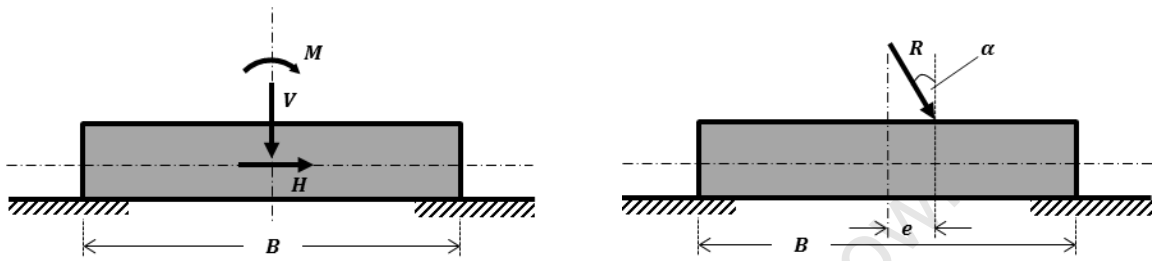

(a) **(b)**

Figure 4.5 **Statical equivalence of (a) combined vertical, horizontal and moment (V-M-H) loading by (b) an eccentric, inclined point load**

The effective area procedure is a simplified approach to dealing with foundations subjected to combined loads. In the case of rectangular bases, the base dimensions can be reduced as follows:

$$B' = B - 2e_y \qquad \textit{Eqn. 4.21}$$

$$L' = L - 2e_x \qquad \textit{Eqn. 4.22}$$

$$A' = B' \cdot L' \qquad \textit{Eqn. 4.23}$$

The effective base area, A', along with the effective footing breadth and length, $B'$and L , respectively, are used in the bearing capacity calculations that follow. This is a conservative approach which has been recommended by DNV/Risø (2002) for the design of wind turbines, given the extremely large overturning moment that wind turbines are subjected to.

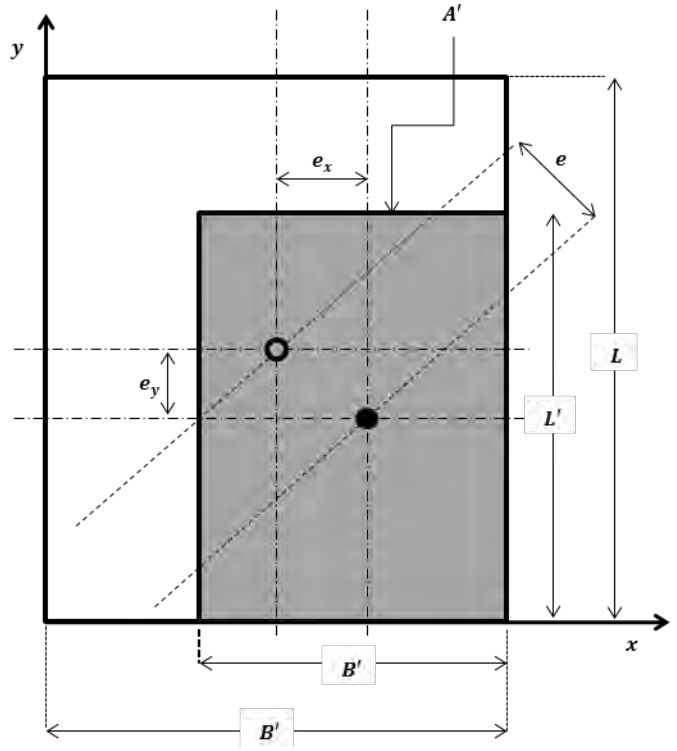

Figure 4.6 **Quadratic foundation with effective area**

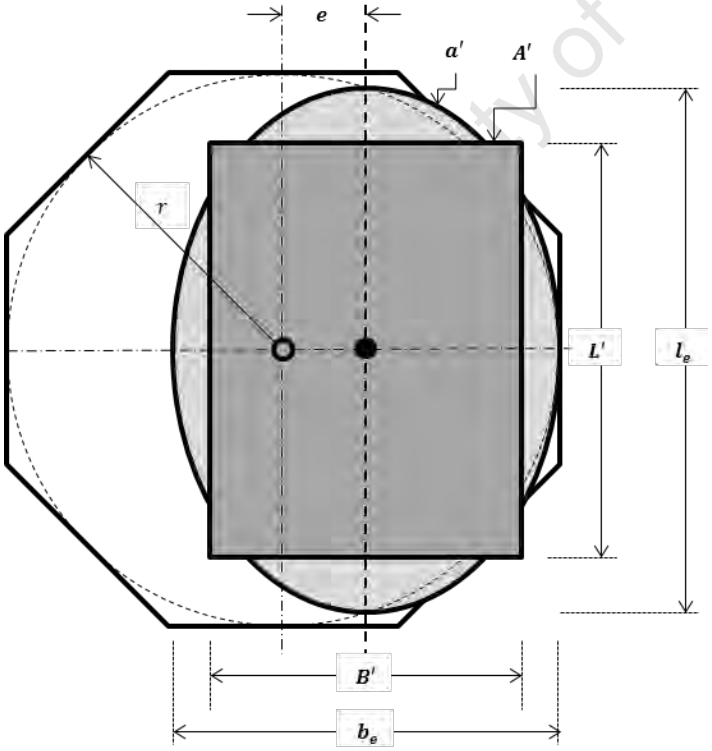

Figure 4.7 **Circular and octagonal foundation with effective elliptical and rectangular areas**

The same statical equivalence approach is used for circular footings. The octagonal footings often used for wind turbines may be approximated by a circular footing of radius r as follows. Firstly, the effective elliptical area is given by Eqn. 4.24, with major and minor elliptical axes defined by Eqn. 4.26 and Eqn. 4.25, respectively.

$$a' = 2\left[r^2 cos^{-1}\left(\frac{e}{r}\right) - e\sqrt{r^2 - e^2}\right] \quad \textit{Eqn. 4.24}$$

$$l_e = 2r\sqrt{L - \left(L - \frac{b}{2r}\right)^2} \quad \textit{Eqn. 4.25}$$

$$b_e = 2(r - e) \quad \textit{Eqn. 4.26}$$

Subsequently, the equivalent effective area of the ellipse can be approximated by a rectangle of area A', with sides B' and L'

$$B' = \frac{L'}{l_e} b_e \quad \textit{Eqn. 4.27}$$

$$L' = \sqrt{a' \frac{l_e}{b_e}} \quad \textit{Eqn. 4.28}$$

The eccentricity of loading may not exceed $B/6$ for a rectangular footing, and $0.6r$ of a circular footing (or octagonal foundation modelled as an inscribed circle). If these limits are exceeded the point of load application would fall outside the equivalent central third of the respective footing, which would lead to uplift on the edge away from the load.

The *effective area approach* is a conservative estimate, but highly efficient and widely used method in foundation engineering (DNV/Risø, 2010). However, a major limitation of this procedure, as well as the empirical bearing capacity equation defined by Eqn. 4.10, is that the respective methods only assess the ultimate load that a footing is capable of withstanding. These models do not assess the elastic and plastic deformation of the respective foundation-soil system, which may be used to predict settlements and pre-failure behaviour. Furthermore, these methods do not give a progressive view of the interaction between the different loads, nor a method of assessing the combination of maximum loads can be resisted.

These shortcomings are addressed in the sections to follow. The yield state approach may be used to address the latter of these shortcomings, namely, the combination of loads that may produce failure, and Chapter 5 provides an overview of different soil models and the theory of elasticity which may be utilised to assess the deformation behaviour of the foundation-soil system under load.

4.3.1.3 The Yield Surface Approach and Work Hardening Plasticity Theory

Wind turbine foundations are subjected to a combination of vertical (V), horizontal (H) and moment (M) loads. This occurs directly due to wind loading on the structure, coupled with the weight of the tower and nacelle, the latter of which acts eccentrically on the foundation. A work hardening plasticity model makes it possible for the foundation engineer to assess deformations as well as permissible stresses. Furthermore, this approach provides structural engineers a better representation of the foundation response. Byrne (2000) eloquently summarised the factors required to construct such a model, which include:

1. The definition of a yield surface in $\{V: M/B: H\}$ space for a strip footing of width B, or, in $\{V: M/2r: H\}$ space, for a footing of radius r. If the load state of the foundation is such that it touches or exists outside the yield surface then plastic displacements occur, otherwise the response of the foundation is elastic.
2. A hardening relationship which determines the size of the surface. This is determined by the relationship between the apex of the surface and the vertical displacement.
3. A description of the elastic behaviour of the foundation for any load combinations within the yield surface.
4. A plastic potential, which defines the direction of the incremental displacement vector upon plastic yielding. This is generally assumed to be the same as the yield surface.

Butterfield & Ticof, (1979) were amongst the first to develop an alternative approach to determining a footing‘s capacity under combined loading. This study suggested that the yield surface was —igar shaped" whereby $M/B \cdot V_{max} = 0.1$, and $H/V_{max} = 0.12$, occurring at $V/V_{max}\ of\ 0.5$. Other investigations, including recent work by Butterfield & Gottardi (1996), confirmed this relationship and also showed that the failure surface conforms to a rotated ellipse in $\{(M/B)V_{max}: H/V_{max}\}$ space. On the basis of a large number of small scale tests Butterfield & Gottardi, (1996), showed that a footing subjected to combined loads of V, H and M at failure lay on a unique three-dimensional surface when plotted in three-dimensional space with axes V, H and M/B where B was the breadth of the respective footing. An example of the postulated yield surface is illustrated by Figure 4.8.

Foundation stability may be assessed easily using a yield surface approach, where the relationship between the different loading conditions is comparable. Provided that the respective $\{V: M/2r: H\}$ loading case falls within the yield surface the foundation is deemed safe and the response thereof elastic, whereas if the loading case falls outside of the yield surface then the foundation response is plastic.

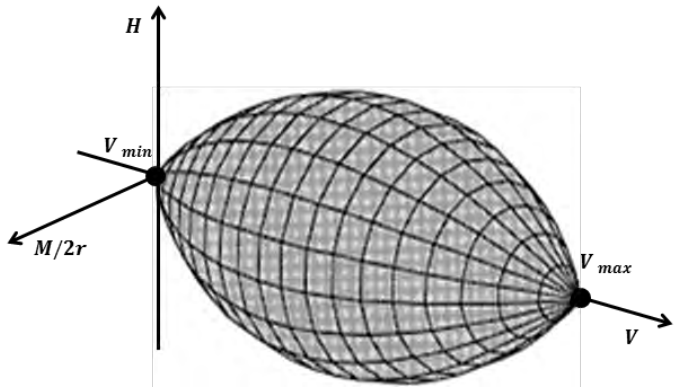

Figure 4.8 **Failure envelope for a shallow foundation – 3D view in $\{V: M/2r: H\}$ space**

The development of such a model is founded on testing and data analysis, where the construction of the yield surface is done on a theoretical and empirical level, based on the data. As illustrated in the previous discussion, this is normally conducted by normalising the V, $M/2r$ and H values by dividing through by V_{max}. V_{max} is the vertical load that would cause failure of the footing when acting on its own; effectively governing the size of the yield surface.

V_{max} is calculated on the basis that the surcharge adjacent to the footing does not exist and therefore is defined by Eqn. 4.29 (for a footing founded on soil lacking cohesion). $m_0 = (M/2r)/V$ and $h_0 = H/V$ govern the shape of the surface by controlling these relationships at the midsection, defined by $V = V_{\max}/2$.

$$V_{max} = N_\gamma s_\gamma \left[\frac{1}{2}(2r)\gamma - \Delta u\right] A_{footing} \qquad \textit{Eqn. 4.29}$$

The most important aspect to consider is fitting the respective surface, elliptical on any plane where V is constant and parabolic on planes where V is not constant, to the respective data empirically. This process is highly dependent on the pore-water characteristics of the material. In general, the three dimensional failure surface may be represented by an equation of the form (Powrie, 2012):

$$\left(\frac{\frac{H}{V_{max}}}{t_h}\right)^2 + \left(\frac{\frac{H}{2rV_{max}}}{t_m}\right)^2 - \left(\frac{2C\frac{M}{2rV_{max}}\frac{H}{V_{max}}}{t_h t_m}\right) = \left[\frac{V}{V_{max}}\left(1 - \frac{V}{V_{max}}\right)\right]^2 \qquad \textit{Eqn. 4.30}$$

Where C is a function of t_h and t_m, which are the slopes of the parabolas at the origin of the $\{V: H\}$ and $\{V: M/2r\}$ planes, respectively. V_{max} is the vertical resistance of the foundation under pure vertical loading ($H = M = 0$).

More specifically, Gourvenec (2007) presented a yield surface for the general case of $\{V:M:H\}$ loading on undrained soil where:

$$\left[\frac{1.29\frac{H}{V_{max}}}{0.25-\left(\frac{V}{V_{max}}-0.5\right)^2}\right]^2+\left[\frac{2.01\frac{M}{2rV_{max}}}{\frac{V}{V_{max}}-\left(\frac{V}{V_{max}}\right)^2}\right]^2=1 \qquad \textit{Eqn. 4.31}$$

For the general case of $\{V:M:H\}$ loading on a drained soil, Butterfield & Gottardi (1994) proposed the following relationship:

$$\frac{3.70\left(\frac{H}{V_{max}}\right)^2-2.42\left(\frac{H}{V_{max}}\right)\left(\frac{M}{2rV_{max}}\right)+8.16\left(\frac{M}{2rV_{max}}\right)^2}{\left[\frac{V}{V_{max}}\left(1-\frac{V}{V_{max}}\right)\right]^2}=1 \qquad \textit{Eqn. 4.32}$$

There are two fundamental applications of this theory to wind turbine design and the selection of a foundation system.

1. Surface footings are particularly vulnerable to horizontal and moment loading with $H \approx V_{max}/8$ or $M/2r \approx V_{max}/11$ being sufficiently high to cause failure (Butterfield and Gottardi, 1994). For this reason, foundations required to resist high lateral loads are often piled or founded at sufficient depth
2. It is practically difficult to achieve a high factor of safety for a foundation that is subjected to an increase in H or M coupled with a reduction, or low, V.

4.3.2 Resistance to Sliding

Resistance to overturning and bearing capacity govern the geometrical and structural requirements of the foundation. Centring the design of the foundation on the above-mentioned principles generally provides a sufficient safeguard against horizontal translation due to the lateral load, H. However, an analysis should still be conducted to ensure that the loading, soil properties and foundation geometry satisfy the following limits for drained and undrained cases, respectively (DNV/Risø, 2002):

$$H < A'c' + V tan\phi' \qquad \textit{Eqn. 4.33}$$

$$H < A'c_u \qquad \textit{Eqn. 4.34}$$

Note that the effective base area, A_{eff}, is utilised in the above expressions. Additionally, the ratio of horizontal to vertical loads should not exceed 0.4.

4.3.3 Correction for Torque

The transfer of a moment about the vertical axis (M_z) of the foundation may be accounted for by adjusting the horizontal load, H, applied to the foundation (DNV/Risø, 2002). The bearing capacity is then evaluated using the adjusted horizontal load, H', to account for the interaction between the torque and other loading. This is an especially important consideration during yawing of the nacelle.

$$H' = \frac{2M_z}{L'} + \sqrt{H^2 + \left(\frac{2M_z}{L'}\right)^2} \qquad \textit{Eqn. 4.35}$$

4.4 SUMMARY

This chapter explored the response of shallow foundations to loading associated with wind turbine structures. This included an analysis of soil mechanics theory pertaining to bearing capacity which formed an origin for a study of the combined loading of shallow foundations. The following key points were made:

1. The methods of assessing bearing capacity, developed by Terzaghi, and expanded by researchers such Brinch Hansen, are universally understood and utilised. For this reason these methods have become conventional. However, these methods assess the ultimate carrying capacity of the respective material which is assumed to be based on the shear strength of the material, and not the compressibility and deformation properties.
2. Furthermore, these conventional bearing capacity methods were not derived for combined loadings, and therefore methods which treat the combined loads as equivalent eccentric vertical loads have been developed. This method is deemed time-efficient but over conservative.
3. In view of this limitation the work hardening plasticity theory was introduced. This framework for assessing shallow foundations under combined loads allows the ultimate limit state of the foundation to be assessed with respect to combinations of loads. Thus critical load combinations may be assessed, where it was found that $H \approx V_{max}/8$ and $M/2r \approx V_{max}/11$ were sufficient to cause overturning (Butterfield and Gottardi, 1994).

The following chapter addresses the serviceability limit state of wind turbine foundations by assessing their deformation behaviour under working load conditions.

5. SETTLEMENT AND STIFFNESS CONSIDERATIONS

5.1 INTRODUCTION

A shallow foundation undergoes two modes of response upon loading. The first involves the initial plastic behaviour during installation and loading. This can involve significant soil compression whereby the soil and foundation establish static equilibrium. The second refers to the mechanism where, if the foundation is unloaded to a point less than the initial loading, and then reloaded, then the system responds elastically (Byrne, 2000).

This behaviour is fundamental in the assessment of shallow foundations under working loads, or serviceability conditions. Wind turbine manufacturers impose strict specifications on the serviceability conditions of wind turbines to ensure that settlements of the structure do not affect the operation of the turbine and rotor, or lead to a loss in stability due to the slender nature of wind turbine structures. Additionally, this is done to ensure a high standard of design and construction practice is upheld on an international level.

Accordingly, the following chapter is focussed on the settlement and stiffness of wind turbine foundation-soil systems. The term *foundation-soil system* is used throughout this chapter and the chapters to come. This stems from the requirement to assess the performance of foundations under working loads while accounting for both the structural behaviour of the footing, and the response of the soil to stress.

The determination of immediate settlement of granular materials is initially explored. This was in order to create a base upon which the elastic displacement theory and aspects of soil-structure interaction could be discussed, and also due to this study being focused on pedocrete materials and associated transported soils. These topics are followed by more practical issues with regard to controlling the differential settlement of wind turbine foundation-soil systems by means of adjusting the foundation and/or soil stiffness. This analysis was based on the *Winkler* model, which formulated a centre around which the dynamic behaviour of foundation-soil systems using the lumped parameter model may be addressed in Part III.

5.2 ELASTIC SETTLEMENT SOLUTIONS FOR CIRCULAR FOUNDATIONS

The preceding chapter dealt extensively with the theoretical determination, or rather, estimation of a soil's bearing capacity. This theoretical framework is taught universally at undergraduate level as the conventional means of designing foundations and is based on the *Mohr-Coulomb failure criterion*. The internal angle of friction, ϕ', was taken as the principal measure of the soil's shear strength. A fundamental problem with this theory was the sensitivity of the bearing capacity factors to changes in the internal angle of friction, coupled with the inability to determine or measure ϕ' accurately in practice (Fellenius, 1999; Strahler, 2012). Along with this, numerous methods concerning the calculation of bearing capacity factors and respective adjustments have been published over the years which often lead to one to query which method is the most suitable.

The following section addresses the notion of using settlement and stiffness as a proxy for estimating bearing capacity. This is an important consideration given the sensitivity of wind turbine foundations to settlement, and the loss of traction and overturning consequences. Instead of assuming the soil fails in a perfectly plastic manner when the ultimate shear stress is reached, a settlement analysis considers the elastic behaviour of the soil and the associated manner in which soil strength develops with displacements.

5.2.1 Definition of Settlement and its Relation to Bearing Capacity

Excessive total or differential settlement is defined as the second limit state that should be analysed during a bearing capacity analysis. This means a foundation may be rendered as unsound due to excessive settlement regardless of whether shear failure has occurred or not. From fundamental soil mechanics, the total settlement (s_t) is comprised of three components, namely; immediate (s_i), primary (s_c) and secondary (s_s).

$$s_t = s_i + s_c + s_s \qquad \textit{Eqn. 5.1}$$

Immediate settlement refers to the initial elastic deformation experienced by a soil upon loading. This is due to the (often) rapid nature of the loading rate, coupled with the stress mobilisation of the soil, and has the ability to occur in all soil types. Once yielding occurs the behaviour becomes plastic.

Primary settlement, or consolidation settlement, is a result of pore-pressure dissipation, and thus is a function of the material permeability. Thus, for saturated granular soils consolidation settlement often occurs immediately after loading (in conjunction with immediate settlement). Consolidation settlement may take months or several years to develop in saturated fine grained soils due to their inherently low permeability. Thus, this results in time-varying plastic settlements which often do not occur at the same rate across the foundation, resulting in differential settlements (Burland, 2012).

Secondary settlement, also known as creep settlement, is a less well-understood topic in soil mechanics due to its complexity and interactions with primary settlement. Creep is a well-known term in the field of civil engineering, and encapsulates the development of time-dependent shear and/or volumetric strains that occur as a result of prolonged exposure to levels of stress. Hence, for soils, creep proceeds at a rate controlled by the soil structure and is dependent on plasticity, activity and the water content of the soil (Mitchell and Soga, 2005). Complexities arise in measuring creep as the differentiation between primary and secondary settlement is blurred. However, Mitchell & Soga (2005) offered valuable insight into this behaviour, which falls outside of the scope of this section, where immediate settlement is the focus.

Upon load application to a soil, saturated or not, the material's shear strength is mobilised through the deformation of the material (Fellenius, 1999). Initially, this behaviour is elastic in nature (immediate settlement). As loading increases yielding occurs resulting in plastic deformations. It follows that if the plastic deformation response is accurately determinable then the bearing capacity of the soil may be calculated in a more rigorous manner, due to it being related to the constitutive material models, rather than the empirical solutions already presented (Strahler, 2012). This point is explored in the following sections.

5.2.2 Stress Changes beneath Circular Loaded Areas

The assessment of settlement requires the determination of vertical strains at various depths below the foundation. This requires the knowledge of two things (1) the stiffness or deformability characteristics of the soil and (2) the *change* in stress at the respective depth of analysis. The theory of elasticity is conventionally used to determine the change in stress at a particular depth, and this will be discussed below.

Stresses attenuate in a radial manner away from the loading boundary of a foundation. Foundation engineers often refer to this as a *pressure bulb*. Boussinesq's famous solution for a point load on the surface of an elastic half-space may be integrated to give the following expressions which define the change in vertical and horizontal stress, $\Delta\sigma_z$ and $\Delta\sigma_x$, respectively, for a uniformly load (q), where $q = V/\pi r^2$, which acts over a circular area of radius r, where Poisson's ratio is denoted by ν:

$$\Delta\sigma_z = q\left\{1 - \left[\frac{1}{1+\left(\frac{r}{z}\right)^2}\right]^{1.5}\right\} \qquad \textit{Eqn. 5.2}$$

$$\Delta\sigma_x = \frac{q}{2}\left\{(1+2\nu) - \frac{2(1+\nu)}{\left[1+\left(\frac{r}{z}\right)\right]^{0.5}} + \frac{1}{\left[1+\left(\frac{r}{z}\right)^2\right]^{1.5}}\right\} \qquad \textit{Eqn. 5.3}$$

These expressions are especially important for wind turbine foundations. In reality these foundations are often octagonal or hexa-decagonal, but they are modelled as equivalent circular uniformly loaded areas. From this analysis the zone of influence – or *pressure bulb* – may be defined as the contour corresponding to the ratio $\Delta\sigma_z/q = 0.2$. This is often approximated by foundation engineers as $4r$ for circular footings. The *pressure bulb* has an important bearing on the foundation design process in terms of (1) settlement considerations and (2) the materials investigation, as it defines the body of soil experiencing a significant change in stress due to the structures. For sensitive structures such a wind turbines, an investigation is required into the properties within the zone of influence and below.

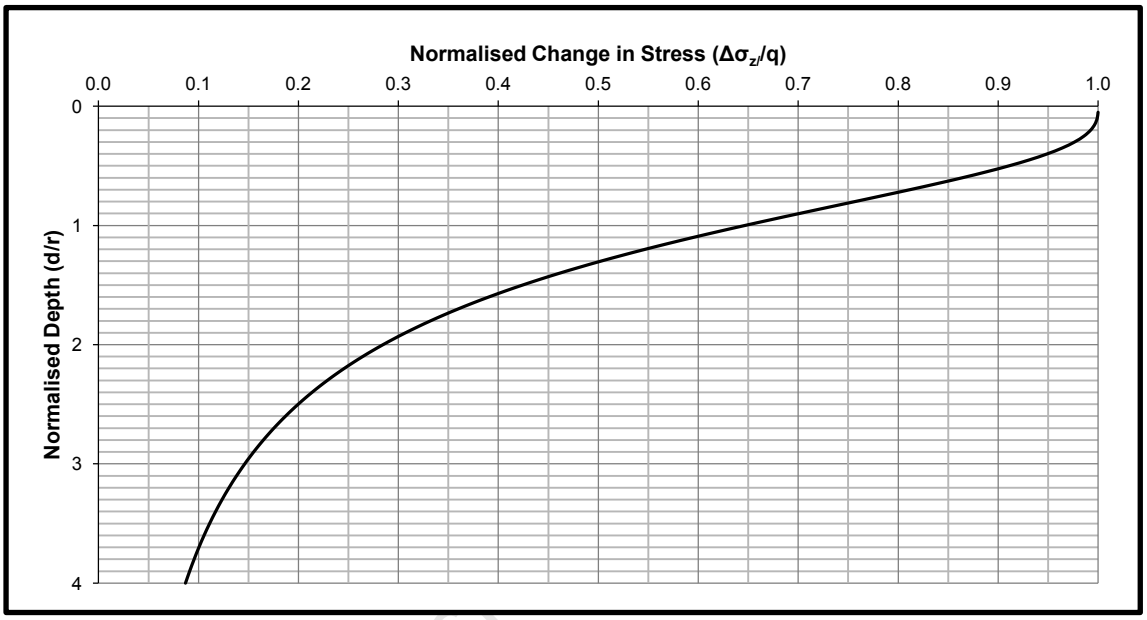

Figure 5.1 **Pressure bulb determination for circular foundation**

However, how accurate or effective are the above-mentioned relationships, given that they are based on perfectly elastic, isotropic, homogenous material characteristics, and that none of these characteristics are ever satisfied by a soil, never mind all three simultaneously? Burland (2012) adeptly presented key research in this area, the key points of which are summarised below.

5.2.2.1 Non-linear Stress-strain Behaviour

A state of the art report compiled by Burland et al. (1977) concluded that the vertical stress changes beneath a loaded area were insensitive to the non-linear stress-strain behaviour of the material. Therefore, it was shown that the Boussinesq theory correlated very closely to the actual changes in vertical stress. However, the other stresses (horizontal and shear) differed significantly.

5.2.2.2 Non-homogeneity

There is also very little deviation from the Boussinesq solution with regard to the non-homogeneity of soils. The one exception in this regard was the case when a stiff layer overlies a softer layer, which results in large errors on the conservative side when the Boussinesq theory is used (Burland, 2012).

5.2.2.3 Anisotropy

The inherent anisotropy of soils has also been documented to only have an effect in certain scenarios. In particular, the Boussinesq theory is ineffective when the effective shear modulus in the vertical plane, G_v', varies significantly with respect to the isotropic value (G).

5.2.3 Elastic Displacement Theory

The determination of settlement hinges on the calculation of vertical strains, ε_v, which is defined for an ideal isotropic elastic material and a function of the two changes in horizontal stress $\Delta\sigma_x$ and $\Delta\sigma_y$ and Poisson's ratio (Burland, 2012):

$$\varepsilon_z = \frac{1}{E}\left[\Delta\sigma_z - \nu\left(\Delta\sigma_x + \Delta\sigma_y\right)\right] \qquad \textit{Eqn. 5.4}$$

The elastic displacement follows from integrating the elastic strains over the soil body, as shown by Eqn. 5.5, but the solution to this problem is usually expressed in terms of an influence factor, I_s, which accounts for geometry, depth of founding and the rigidity of the footing, as shown by Eqn. 5.6.

$$s_i = \int_0^d \varepsilon_z dz \qquad \textit{Eqn. 5.5}$$

$$s_i = \left[\frac{VB}{E}(1-\nu^2)\right] I_s \qquad \textit{Eqn. 5.6}$$

Referring back to wind turbine structures now, it is of specific interest to note that the total settlement at the centre of a uniform circular load for a flexible and rigid footing which assume negligible and infinite rigidity, respectively, are defined below by Eqn. 5.7 and Eqn. 5.8.

$$s_i = \left[\frac{VD}{E}(1-\nu^2)\right] \qquad \textit{Eqn. 5.7}$$

$$s_i = \left[\frac{VD}{E}(1-\nu^2)\right]\frac{\pi}{4} \qquad \textit{Eqn. 5.8}$$

These expressions raise an important point: the total settlement of rigid foundations is only very slightly less than that of a flexible foundation. Thus, it may be concluded that stiffening a foundation significantly reduces differential settlement but has only a slight effect on the overall settlement of the foundation (Bowles, 1996; Burland, 2012).

This is a fundamental aspect of wind turbine design which is explored in greater detail within §**Error! eference source not found.**. The issue of foundation stiffness is also taken up in later discussions, as no foundation is infinitely rigid, as is often assumed, by the presentation of mathematical models relating the foundation stiffness to the subgrade deformation and structural response.

5.2.4 Serviceability Limit State Analysis by the Yield State Approach

The yield state approach was presented in §4.3.1.3 where it was used as an alternative method of assessing foundation stability. One of the most powerful aspects of this model is the ability to use it in the evaluation of foundation-soil performance under serviceability conditions. If the combination of $\{V: M/2r: H\}$ loading falls within the yield surface then the foundation will act elastically, and hence the yield surface approach may be used to predict deformations of the respective material (Craig and Knappett, 2012). This is an aspect which renders the approach highly valuable in the holistic design of structures subjected to general loading, such as wind turbines.

The response of the foundation to the $\{V: M/2r: H\}$ loading may be analysed with respect to the elastic stiffness of each case, given by: $K_z = V/w$ (vertical stiffness), $K_h = H/u$ (horizontal stiffness) and $K_\theta = M/\theta$ (rotational stiffness) where w, u and θ are the vertical, horizontal and rotational displacements, respectively. Accordingly, the vertical stiffness, horizontal stiffness (Barkan, 1962)and rotational stiffness (Gorbuno-Passadov and Serebrajanyi, 1961)are defined as follows:

$$K_z = \frac{V}{w} = \left(\frac{2L}{I_s}\right)\left(\frac{G}{1-\nu}\right) \qquad \textit{Eqn. 5.9}$$

$$K_x = \frac{H}{u} = 2G(1+\upsilon)F_x\sqrt{BL} \qquad \textit{Eqn. 5.10}$$

$$K_\theta = \frac{M}{\theta} = \frac{G}{1-\nu}F_\theta BL^2 \qquad \textit{Eqn. 5.11}$$

These expressions assume that there is no coupling between the different terms and utilise factors F_x and F_θ which are a function of L/B. Again, a factor I_s is utilised to account for the foundation rigidity, which in turn affects the contact pressure between the foundation and soil.

The succeeding section deals with the importance of assessing the contact pressure for optimal foundation design, because foundation rigidity, and the treatment thereof in foundation-soil system design has an important bearing on the structural response of the structure-foundation system as well as on the structural design of the actual footing. For a light single story structure founded on a competent subgrade, this approach, dubbed *rational foundation design*, may be superfluous, but for complex structures such as wind turbines it should be viewed as mandatory.

5.3 PRINCIPLES OF SOIL STRUCTURE INTERACTION FOR ELASTIC FOUNDATIONS

Soil-structure interaction (SSI) may be defined as a holistic approach to foundation design, whereby the influence of the structure-foundation system and loading regime on the subgrade reaction is studied. Simultaneously, the contact pressure and its influence on the structure-foundation system, is evaluated. This is done by constructing mathematical models to encapsulate stiffness and deformation relations between the foundation and soil. In the past this method of design has been termed *rational* foundation design based on it representing a more realistic view of how foundation-soil systems behave under load.

5.3.1 Soil-structure Interaction: Governing Equations

The problem of SSI is generally solved by developing a mathematical model which constructs links between the subgrade reaction and the structural response. Most shallow foundations may be modelled as beams (one-dimensional) or plates (two dimensional). The differential equations governing each mechanism are defined below. These models are based on the theory of elasticity, whereby the initial plastic deformation of the foundation-soil system is assumed to have already occurred, and therefore may be assessed as an elastic medium.

5.3.1.1 Beam on an Elastic Foundation

The theory of a beam resting on an elastic medium is applicable for the analysis of foundations undergoing one-dimensional loading and deformation. Hence, it has roots in several geotechnical engineering applications, the most common probably being the analysis of laterally loaded piles. The governing equation assumes no friction between the beam element and soil and is defined as follows:

$$EI\frac{d^4w}{dx^4} = V(x) - q(x) \qquad \textit{Eqn. 5.12}$$

Where EI denotes the flexural rigidity of the foundation, $\frac{dw}{dx}$ is the vertical deflection with respect to foundation length (x), $V(x)$ is the vertical force applied to the footing with respect to foundation dimension (x) and $q(x)$ denotes the subgrade reaction with respect to foundation dimension (x). The resulting structural load distributions are defined in Table 5.1.

Table 5.1 **Foundation structural design - internal foundation forces**

Parameter	Definition	
Bending Moment	$M(x) = -EI\frac{d^2w}{dx^2}$	*Eqn. 5.13*
Shear Force	$S(x) = -EI\frac{d^3w}{dx^3}$	*Eqn. 5.14*

5.3.1.2 Plates on an Elastic Foundation

The solution to plates on an elastic foundation allows for the analysis of bi-axial bending due to planar loading. Similarly to the beam on an elastic foundation, friction between the plate and soil is ignored and the plate is assumed to be sufficiently thin to allow for a plane strain analysis. The governing equation is given below, where the Laplace operator may be adjusted to account for different foundation geometries.

$$D\nabla^4\big(z(x,y)\big) + q(x,y) = V(x,y) \qquad \textit{Eqn. 5.15}$$

$$D = \frac{E_p t^3}{12(1-{\nu_p}^2)} \qquad \textit{Eqn. 5.16}$$

Where:

- D denotes the flexural rigidity of the plate
- $\nabla^4 = \nabla^2\nabla^2$ where ∇^2 is the Laplace operator
- $z(x,y)$ and $V(x,y)$ denote the deflection of the plate-soil and the vertical load in terms of the plate area, respectively
- $q(x,y)$ defines the contact pressure distribution

Note that for circular footings, the Laplace operator may be defined in terms of polar coordinates as:

$$\nabla^2 = \frac{\partial^2}{\partial r^2} + \frac{1}{r}\frac{\partial}{\partial r} + \frac{1}{r^2}\frac{\partial^2}{\partial \theta^2} \qquad \textit{Eqn. 5.17}$$

There are numerous texts which address the topic of solving these governing equations analytically, using a classical approach as well as the finite element method (FEM), such as Bowles (1996). Analysis of this falls outside the scope of this text. However, what is of primary concern is the evaluation of $q(x)$ – the contact pressure.

5.3.2 Review of Foundation-soil Models

The structural design of foundations hinges on the knowledge of the magnitude and nature of the contact pressure, as this directly affects the internal forces within the foundation element and the deformation behaviour of the soil. Conventionally, the soil pressure has been assumed to be uniform or linear/planar and although this assumption has benefits in terms of simplicity and computing time, it results in an underestimation of foundation bending moments in cohesive soils and highly conservative bending moment values in granular soils (Straughan, 1990).

This is due to the stress mobilisation mechanisms in these different soils with respect to the foundation deformation under stress:

1. It is assumed that cohesive soils behave as purely elastic media. Hence, the loading of a rigid foundation on clay results in stress concentrations at the edges and the greatest deflection occurring at the centre. The pressure distribution below a rigid footing on clay is illustrated by Figure 5.2(a). The contact pressure of a flexible foundation on clay may be approximated as uniform due to bending.
2. A granular soil‘s strength is derived from the confinement of particles. This bears important consequences for the contact pressure assessment as the soil directly below the centre of the foundation will have the greatest stiffness (assuming central loading). Thus, the settlement is greatest at the edges but the contact pressure is greatest at the centre, for rigid foundations (Figure 5.2(b)). For flexible foundations the contact pressure may again be approximated as uniform due to bending, as shown by Figure 5.2(c) (Strahler, 2012).

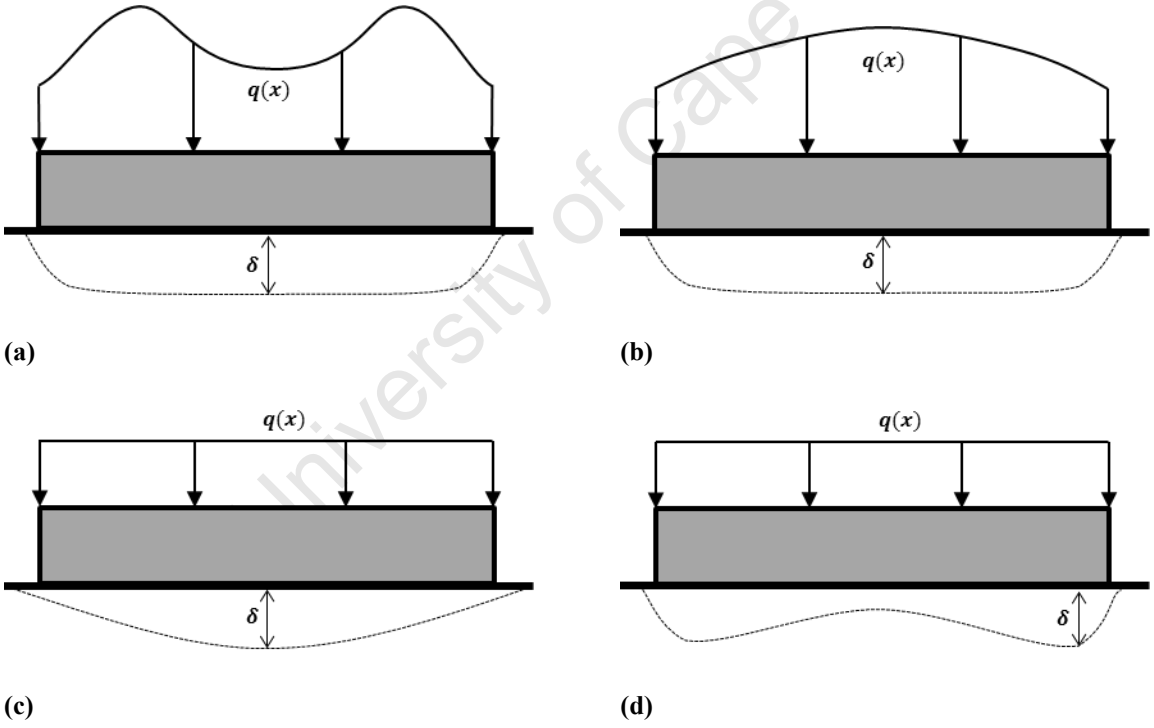

Figure 5.2 **Effects of foundation stiffness on soil reaction: (a) rigid foundation on clay, (b) rigid foundation on granular soil, (c) flexible foundation of clay and (d) flexible foundation on granular soil**

5.3.2.1 Linear or Planar Soil Pressure Distribution

As previously mentioned, the traditional method of analysis was to assume that the soil pressure beneath a rigid foundation slab varied linearly with respect to the applied loading. In doing so the soil reaction was solely a function of the external loading and foundation geometry. Thus, in essence, no-soil structure interaction exists due to each system being considered in isolation, but this is included here for illustrative purposes. Eqn. 5.18 defines such a relationship for a footing under combined loads (Kameswara Rao, 2011).

$$q(x) = \frac{V}{A_{footing}} \pm \left(\frac{M_x}{I_x} y + \frac{M_y}{I_y} x\right) \qquad \textit{Eqn. 5.18}$$

I and M donote the second moment of area and applied moment about each axis, respectively, and x and y are defined as the coordinates at which the pressure is being assessed (Figure 5.3(a)).

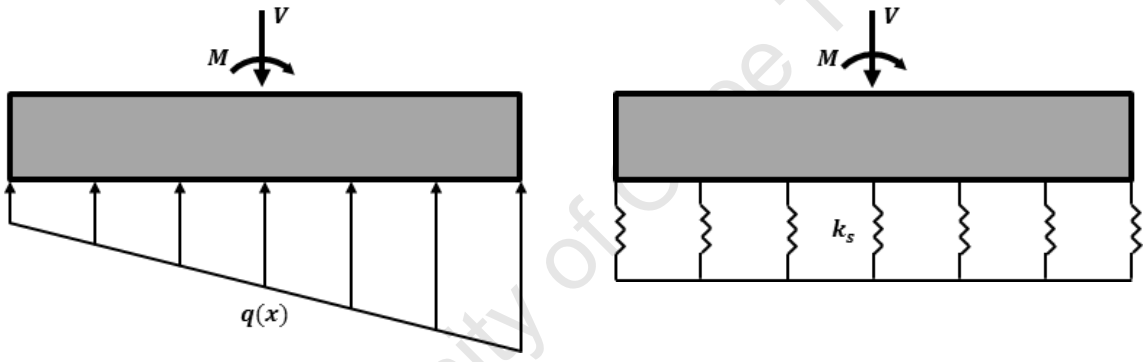

(a) **(b)**

Figure 5.3 **Soil-foundation models: (a) the linear varying soil pressure and (b) modulus of subgrade reaction**

The loading eccentricities, defined as $e_y = M_x/V$ and $e_x = M_y/V$, may be used to evaluate the loading and geometric limits of the footing. Overturning and instability is indicated by a negative contact pressure, as a result of large eccentricity.

This method has been used extensively for more traditional relatively small foundations supporting the columns of multi-story structures based on its simplicity. However, for large flexible foundations, such as those encountered in the wind energy field, this method leads to over conservative designs. This is due to the soil stress concentrations, which lead to lower internal stresses in the foundation, being neglected (Maunu, 2008).

5.3.2.2 Modulus of Subgrade Reaction or Winkler's Model

The modulus of subgrade reaction defines a relationship between the applied loading, soil stiffness and soil deformations, and is arguably the most extensively used model for assessing SSI (Kameswara Rao, 2011). This is based on its adaptability to a wide array of shallow foundation problems as well as deep foundations.

Also, selecting a SSI model is a fine balance between the degree of accuracy required and the quality of input data available. Significantly more elegant models than the modulus of subgrade reaction are available for the prediction of soil reactions, but with increased degrees of analysis and accuracy come the complications of measuring and interpreting the additional input parameters for the respective model. Hence, the main advantage of the modulus of subgrade approach is the relative low data input required and the well accepted and common material tests which it involves.

The modulus of subgrade reaction operates on the following ratio, which stemmed from *Winkler*'s hypothesis; the soil develops resistance to loading through discrete and independent elements, and therefore disregards shearing between elements and focuses primarily on the soil stiffness (Bezgin, 2010). Thus, the subgrade is modelled as a series of springs with stiffness k, often called the *Winkler* model:

$$w = \frac{q}{k} \qquad \textit{Eqn. 5.19}$$

(i) Soil-structure Interaction Equations based on the Winkler Model

Given the simplicity of the *Winkler* model and the well-established and efficient methods of obtaining the required model parameters, it is still held in high regard as the conventional means of assessing soil-structure interaction. Now, substituting the *Winkler* model contact pressure into the governing equation of soil-structure interaction yields the following expression for a beam on an elastic foundation:

$$EI\frac{d^4w(x)}{dx^4} + k\big(w(x)\big) = V(x) \qquad \textit{Eqn. 5.20}$$

where:

- EI is the flexural rigidity of the beam
- $w(x)$ is the vertical deflection of the beam with respect to footing length
- k denotes the soil spring constant in the vertical direction
- $V(x)$ is the vertical loading applied to the footing

And for plates on an elastic foundation:

$$D\nabla^4\big(w(x,y)\big) + k(w(x,y)) = V(x,y) \qquad \textit{Eqn. 5.21}$$

Note that these expressions are only valid for static analyses. Hence, k is often denoted as k_s to avoid confusion between the static and dynamic stiffness of the soil.

(ii) Limitations and Advantages of the Winkler Model

The nature of the interaction between structure and soil means that this parameter is not only a function of the soil strength, compressibility and stiffness, but also depends on the magnitude, nature and direction of loading, the geometry of the foundation and so on. The central inconsistency of this model is that it assumes a uniform-displacement of the footing regardless of the foundation loading and size of the footing, meaning that continuity is ignored. Kameswara Rao (2011) discussed much of the work, such as (Hetenyi, 1950, 1946), that has been conducted on addressing this drawback. Alternative solutions, such as the *two parameter model* and continuum methods, have been proved to model the actual foundation behaviour more accurately, but to the detriment of calculation complexities and time-inefficiency. Thus the *Winkler* model has remained the central method of assessing soil-structure interaction problems based on it being amenable to an efficient analysis. In addition, methods of assessing the value of the spring constant have improved over time with transducer and sensor technologies and improved methods of field tests. Also, the methods used to determine elastic soil moduli, upon which the Vesic (1961a, 1961b) classical correlation is based, have also received much attention:

$$k = \frac{1}{B}\left[0.65\sqrt[12]{\frac{E_s B^4}{E_f I_f}}\right]\frac{E_s}{B(1-\nu_s{}^2)} \approx \frac{E_s}{B(1-\nu_s{}^2)} \approx \frac{G(1+\nu_s)}{r(1-\nu_s{}^2)} \qquad \textit{Eqn. 5.22}$$

Possibly the most beneficial aspect of this model is its synergy with the lumped parameter model and *Lysmer's Analog* used to assess the dynamic response of footings on an *elastic half-space*. This is presented in Part III.

Another major advantage of this method of soil modelling is the ability to assess bearing capacity from load-displacement data, acquired from the plate loading test conducted to calculate k.The plate load test involves measuring the displacement of a plate, with known dimensions, under relatively rapid loading. From this load-displacement or pressure-displacement curves are plotted, as seen in Figure 4.2(d), for example. However, the non-linearity of these curves makes it difficult to assess the ultimate bearing capacity. Strahler (2012) presented a comparison of several different methods developed over time which aimed to assess this issue.

One such method, proposed by Chin, (1971), assumed that the pressure-displacement curve is hyperbolic. Hence, the Chin transformation plotted the square root of the pressure (q) - displacement (δ) ratio to the displacement. This allowed the ultimate bearing resistance to be assessed on the basis that the shear strength of the soil would be fully mobilised under failure. Hence, a linear relationship would develop, where the rate of change with respect to displacement ($\mathcal{C}$) would be inversely proportional to the ultimate bearing capacity ($\sigma_f{}'$) (Chin, 1971), *viz.*

$$\sigma_f{}' = \frac{1}{\mathcal{C}} \qquad \textit{Eqn. 5.23}$$

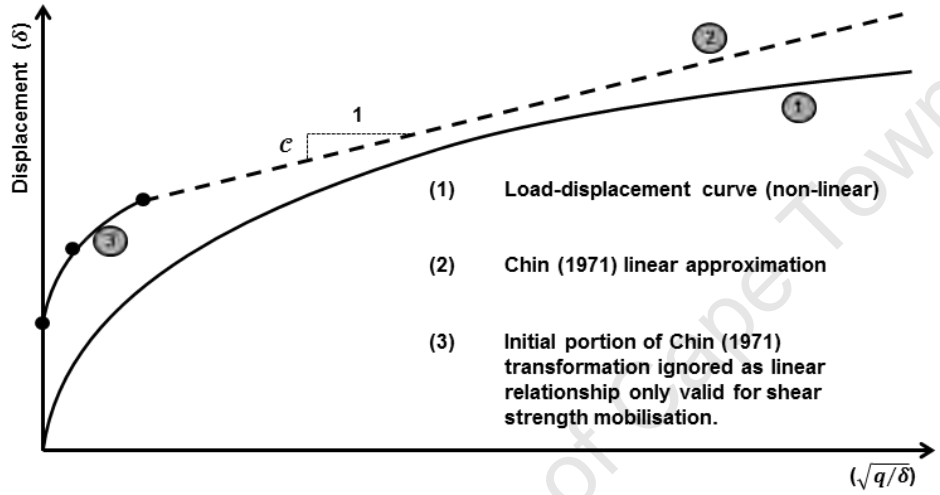

Figure 5.4 **Comparison of Chin (1971) transformation and typical pressure-displacement behaviour**

This method of assessing bearing capacity was found to produce fewer ambiguities and hence deemed more appropriate and objective than other methods of relating load-test data to bearing capacity (Elhakim, 2005).

5.3.2.3 Discrete Modelling of Soil by the Finite Element Method

Geotechnical engineering problems often involve a multitude of variables and processes which all require cognisance during a modelling process. Settlement and bearing capacity are just two in the field. FEM, coupled with growing hardware and software capabilities, has emerged as an incredibly powerful tool in this regard, as it affords engineers a time-efficient and, often, user friendly-method of determining foundation settlements. The modelling of soil-settlement by FEM hinges directly on the soil parameters, such as Young‘s modulus and Poisson‘s ratio for elastic analyses, because the soil is modelled as a continuum instead of a one-dimensional medium. Thus, non-uniform deformation behaviour may be analysed (Maunu, 2008).

This has led to shortcomings in the understanding of FEM and its capabilities. Firstly, it goes without saying that the accuracy and effectiveness of any FEM model hinges on a comprehensive and accurately executed soil investigation, as well as a sound interpretation of the results. The saying, ―rubbish in, rubbish out" is well known, but the interpretation of results is just as important. FEM models, which operate on the laws of elasticity and plasticity, are highly sensitive to parameters such as Poisson's ratio – parameters which are often not investigated. Thus, the estimation of such parameters must not be done in isolation, but rather with reference to the other investigated soil parameters to ensure continuity between input parameters and boundary conditions. Secondly, the following points were highlighted by Burland (2012b) with regard to the limitations of the FEM:

1. The principal stresses and stress changes remain vertical and horizontal within a FEM model, whereas in reality these orientations rotate.
2. Only the vertical stiffness and vertical Poisson's ratio are utilised/modelled, and hence anisotropic effects and their interactions with the orientation of the principle stresses is ignored.
3. The stress history and in-situ stresses are not modelled, which has a profound impact on the stress-strain behaviour of the soil.

5.4 MODELS OF SOIL ELASTICITY

5.4.1 Elastic Half-space Theory: Analytical Solution for Footing Displacement

Until now, the term *stiffness* has been associated with the ability of a soil to resist compression or deformation, and this was described with the modulus of subgrade reaction. However, upon closer analysis of the *Winkler* model or the modulus of subgrade reaction approach, it was noted that the modulus of subgrade reaction is dependent on the area of loading, because stiffness in this regard is defined as the ratio between applied pressure, q, and resulting deformation, δ. Thus, k is not an exclusive material property, but also rather a function of the loading and geometry of the foundation, as well as dependent on the loading characteristics (Briaud, 2001).

Therefore, evaluating the coefficient of subgrade reaction should be carried out with field tests such as the plate loading method, given the sensitivity of the parameter to the loaded area and nature of applied load. Bowles (1996) is one of many texts which present methods and correlations to perform in-situ load tests for the determination of the coefficient of subgrade modulus. The benefits of assessing stiffness from load tests was discussed above, but despite this it is deemed inappropriate for foundations such as those used for wind turbine structures. This is due to the previously discussed impracticalities, as well as the complexities and inaccuracies which arise in the scaling between plate load tests and actual wind turbine footings, which have considerable plan areas.

Rather, this study was interested in the use of analytical procedures for assessing soil stiffness, based on soil moduli, in the prediction of foundation-soil response. The analytical study conducted by Poulos and Davis (1974) is regarded as classical solution for the determination of the deflection of a circular rigid footing on the surface of an *elastic half-space*. This solution was defined in terms of the shear modulus, G, and Poisson's ratio, ν, and was later verified and expanded for embedded footings and footings on layered strata. The expressions for a three degree of freedom system are defined, with reference to Figure 5.5, as follows (Nguyen-Sy, 2005)

$$V = \left(\frac{4Gr}{1-\nu}\right)w \qquad \textit{Eqn. 5.24}$$

$$H = \left[\frac{32Gr(1-\nu)}{7-8\nu}\right]u \qquad \textit{Eqn. 5.25}$$

$$M = \left[\frac{8Gr^3}{3(1-\nu)}\right]\theta \qquad \textit{Eqn. 5.26}$$

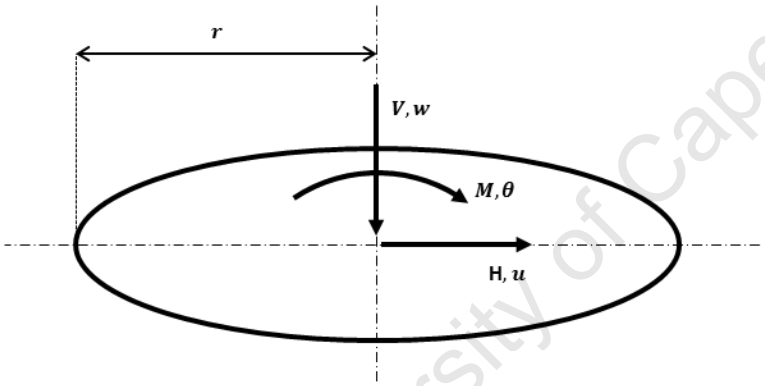

Figure 5.5 **Co-ordinate system for footing displacement (3 degrees of freedom)**

5.4.2 Introduction to Soil Moduli and Soil Models

Soil moduli are derived from the intrinsic stress-strain behaviour of soils, and may be subsequently used to assess the deformation of foundation-soil systems based on analytical models such as that presented above. However, the determination of soil moduli hinges on a wide array of factors, making this one of the most complex tasks in the field of soil mechanics. This is principally because the determination of relevant soil moduli needs to be undertaken in conditions similar to those expected for the respective structure as a wide range of loading and state factors affect soil moduli.

These factors are studied in §6.4 alongside the behaviour of soils under dynamic and cyclic loading. For now, two soil constitutive models relevant to the wind turbine structures are presented, namely, the linear-elastic model and non-linear elastic soil model. The latter of which is also expanded upon in Chapter 6, due to its close connection with the effects of cyclic loading.

5.4.2.1 Linear Elasticity

The behaviour of soil under stress varies considerably based on a wide range of variables. An idealised form of stress-strain behaviour is illustrated by **Error! Reference source not found.** The nitial region of soil behaviour, prior to yield, may be modelled as a linear-elastic constitutive model if the anticipated strain levels allow for it. The linear (isotropic) elasticity model defines a linear relationship between the shear strain and applied shear stress, the gradient of which is closely associated with the stiffness modulus, except in the situation of zero confining stress, where the gradient becomes equal to the modulus.

A linear elastic stress-strain constitutive model is governed by Hooke‘s Law, in which the strain in two-dimensions is given below, where, E is Young‘s modulus and ν denotes Poisson‘s ratio.

$$\varepsilon_x = \frac{1}{E}(\sigma_x' - \nu\sigma_z') \qquad \textit{Eqn. 5.27}$$

$$\varepsilon_z = \frac{1}{E}(\sigma_z' - \nu\sigma_x') \qquad \textit{Eqn. 5.28}$$

$$\tau_{xz} = \tau_{zx} = G\gamma_{xz} \qquad \textit{Eqn. 5.29}$$

σ' denotes the normal stress applied in the direction given by the respective subscripts. For a linear elastic isotropic material, the elastic material parameters are related as follows:

$$G = \frac{E}{2(1+\nu)} \qquad \textit{Eqn. 5.30}$$

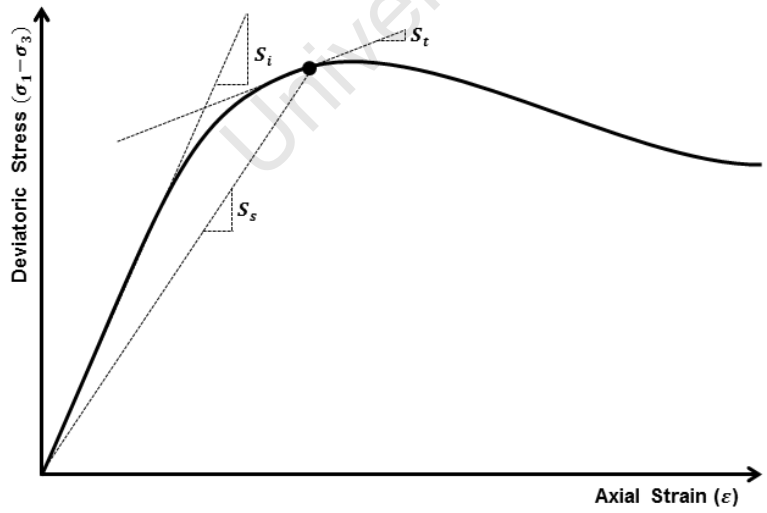

Figure 5.6 **Definition of elastic moduli**

Further elastic relationships are defined in Table 5.2. In the field of soil mechanics it is preferable to define elastic constants in terms of G and ν.

Table 5.2 **Relationship between elastic constants applicable to soil mechanics**

	$\boldsymbol{\lambda, \mu}$	$\boldsymbol{G, \nu}$	$\boldsymbol{E, \nu}$	$\boldsymbol{K, G}$
$\lambda^{(1)}$	λ	$G\frac{2\nu}{1-2\nu}$	$\frac{E}{(1+\nu)(1-2\nu)}$	$K-\frac{2}{3}G$
$\mu \equiv G$	μ	G	$\frac{E}{2(1-\nu)}$	G
$K^{(2)}$	$\frac{3\lambda+2\mu}{3}$	$G\frac{2(1+\ )}{3(1-2\nu)}$	$\frac{E}{3(1-2\nu)}$	K
E	$\frac{\mu(3\lambda+2\mu)}{\lambda+\mu}$	$2G(1-\nu)$	E	$\frac{9KG}{3K+G}$
ν	$\frac{\lambda}{2(\lambda+\mu)}$	ν	ν	$\frac{3K-2G}{2(3K+G)}$

(1) Lame's first constant
(2) Bulk modulus

Thus, the strains resulting from an applied loading of σ'_x and σ'_z may be determined by solving:

$$\begin{bmatrix}\varepsilon_x \\ \varepsilon_z \\ \gamma_{xz}\end{bmatrix} = \frac{1}{2G(1+\nu)}\begin{bmatrix}1 & -\nu & 0 \\ -\nu & 1 & 0 \\ 0 & 0 & 2(1+\nu)\end{bmatrix}\begin{bmatrix}\sigma_x' \\ \sigma_z' \\ \tau_{xz}\end{bmatrix} \qquad \textit{Eqn. 5.31}$$

Accuracy of the linear-elastic model in predicting immediate settlement may be improved by ensuring the appropriate elastic modulus is selected from the stress-strain relationship. That is, different elastic moduli are appropriate for specific loading scenarios, and thus should be selected suitably to emulate the non-linear behaviour of soils under stress. For foundation design, and the estimation of initial settlement, the secant modulus (E_s), derived from the secant slope (S_s) is generally used (Briaud, 2001). Other elastic moduli relevant to foundation loading scenarios are (Briaud, 2001)

1. The tangent modulus (E_t), derived from the slope of a tangent to the peak stress. This modulus is particularly useful in evaluating the incremental change in displacement due to a slight increase or reduction in load.
2. The initial modulus (E_i) is used to assess the immediate response of the foundation to loading, similarly to the secant modulus. However, the secant modulus has been deemed a more realistic and conservative measure of the soil response, given the non-linear behaviour of soils.

A linear-elastic, perfectly plastic model is used to assess the plastic behaviour of soils assumed to be linear elastic. This gives an estimation of the pressure at which plastic deformation occurs (q_{ult}), analogous with bearing capacity. This model has significant intrinsic errors, and when combined with the errors associated with the determination of elastic moduli, may yield significantly inaccurate results (Strahler, 2012). A schematic example of such a model is illustrated below.

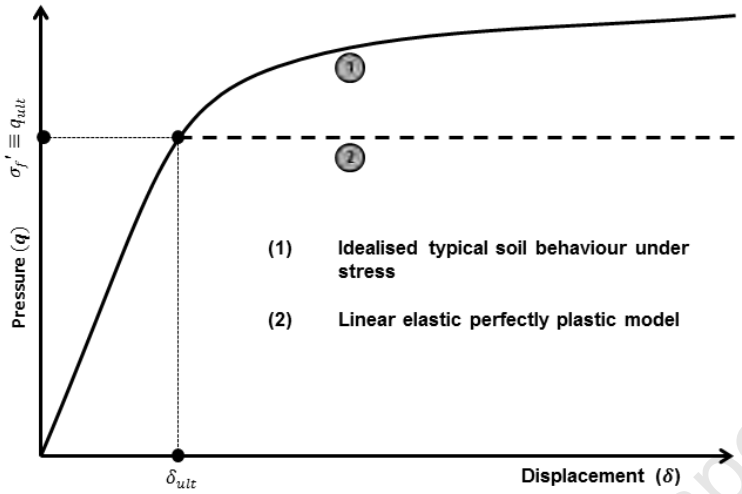

Figure 5.7 **Different elastic moduli**

5.4.2.2 Non-linear Elasticity

In reality, the strength and deformation characteristics of any geo-material are highly dependent on the level of shear strain to which the soil is subjected. Thus, the shear modulus is not a material constant, as assumed by the linear-elastic model, but rather a function of the shear stress and effective confining stress.

From this, it may be noted that the level of shear strain induced in the material dictates the nature of material response, as illustrated by Figure 5.8(a). Elastic and recoverable strains occur at low levels of shear strain, below the elastic threshold (γ_{tl}). In this range the shear modulus is independent of shear strain, and hence is denoted G_{max}. However, it is still a function of the effective confining stress ($\overline{\sigma_0}'$), the relationship of which is shown by Figure 5.8(b). σ_0' is the principal parameter affecting G_{max}, and hence soil stiffness generally increases with depth.

Once the elastic threshold is reached, stiffness degradation begins to occur, and hence the shear modulus becomes a function of the respective shear strain. Initially, the degradation is minor and the soil behaviour may be considered as non-linear elastic. Later, this will be defined as the volumetric cyclic strain threshold (γ_{tv}), but in the meantime it suffices to state that once this threshold is exceeded plastic deformation occurs.

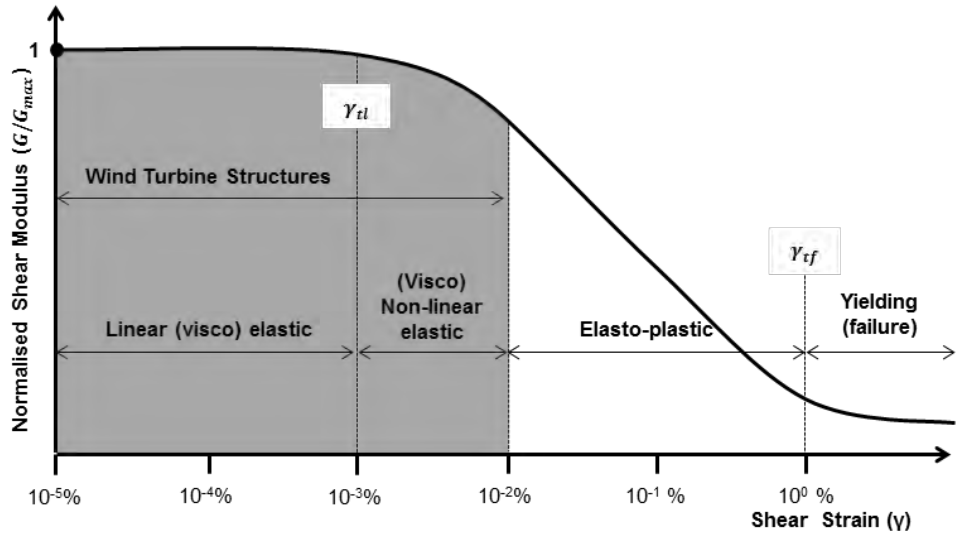

(a)

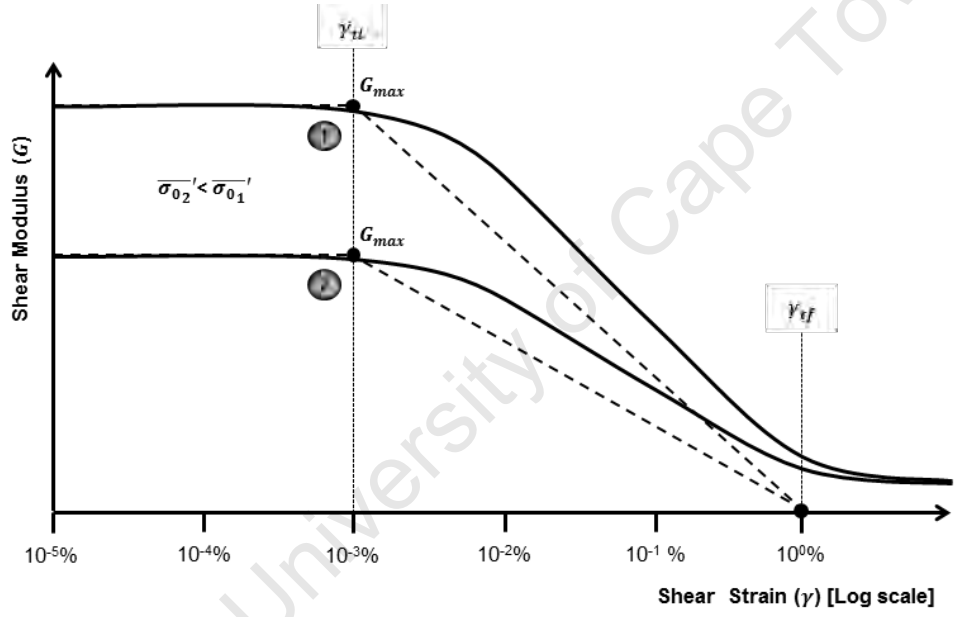

(b)

Figure 5.8 **Non-linear soil shear moduli relations**

This culminates in permanent deformations in the form of cracks and differential settlement. Fully plastic behaviour occurs thereafter, where the soil is assumed to have failed after the strains have increased with no associated increase in shear stress.

Hence, evaluating the G $-\gamma$ relationship hinges on the anticipation of the shear strain induced in the soil by the respective structure. If the elastic threshold is exceeded ($G < G_{max}$) then the full non-linear relationship of the soil is required.

One such model was presented by Atkinson (2000) where it was the use of the following relationship was deemed effective:

$$\frac{G}{G_{max}} = \frac{1-(\gamma_{tf}/\gamma)^{B}}{1-(\gamma_{tf}/\gamma_{tl})^{B}} \qquad \textit{Eqn. 5.32}$$

γ_{tf} and γ_{tl} are the failure and linear threshold, respectively, as defined in Figure 5.8(b). B is used to vary the characteristics of the stiffness degradation based on the nature of the loading (dashed lines in Figure 5.8(b)), between γ_{tl} and γ_{tf} and is typically 0.1-0.5. The $G-\gamma$ relationship may then be analysed by combining this model with a normalised G/G_{max} relationship, once G_{max} has been determined from appropriate laboratory and/or field techniques (Chapter 9).

The Hardening Soil (HS) model is constitutive relationship developed to assess the non-linear behaviour of soil more accurately by incorporating specific attributes of soil behaviour under load, including aspects such as densification, stress history and dilatancy (Obrzud, 2010). This is achieved by defining three stiffness input parameters, including, the triaxial loading stiffness, the unloading, reloading stiffness and the oedometer (one-dimensional) stiffness, as defined by Figure 5.9.

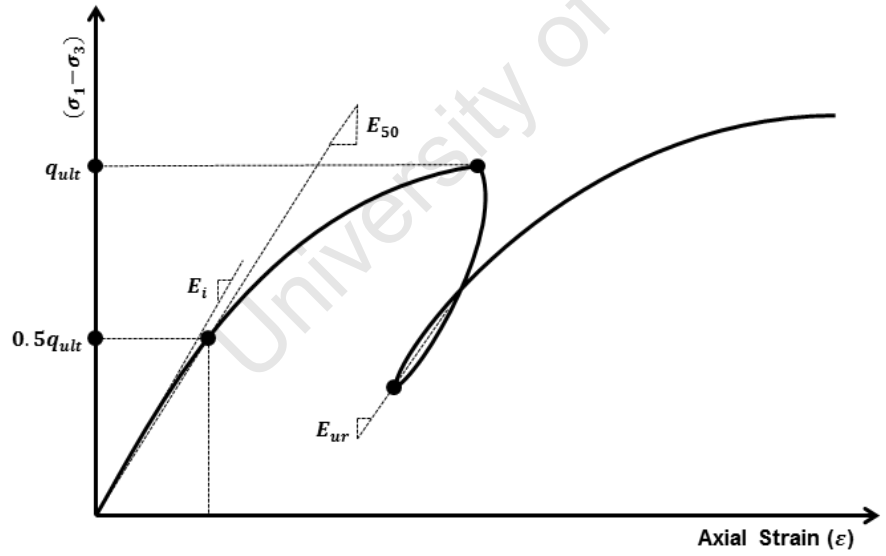

Figure 5.9 **Common definitions of soil moduli for Hardening Soil model**

The HS model accurately predicts soil deformations as it utilises a hyperbolic function to assess the non-linear nature of the stress-strain relationship. Furthermore, an enhance version of the HS model, the HS small-strain model, allows the interpretation of soil stiffness degradation due to increased strain or cyclic loading, and may also incorporate hysteretic (material) damping, which is a beneficial aspect for wind turbine foundations.

This is done by defining two parameters in addition to the HS parameters presented above:

1. The small strain, or maximum, shear modulus G_{max}
2. The shear strain level $\gamma_{0.7}$ where the secant modulus G is reduced to 70% of G_{max}

The following relationship may then be used to assess the normalised shear modulus relationship (Plaxis, 2011; Santos and Correia, 2000; Schanz et al., 2000):

$$\frac{G}{G_{max}} = \frac{1}{1 + \frac{3}{7}\left(\frac{\gamma}{\gamma_{0.7}}\right)} \qquad \textit{Eqn. 5.33}$$

Other means of assessing non-linear soil behaviour are available, such as the *mobilised shear strength* method, the non-linear perfectly plastic model and other means of correlating small strain stiffness to large strain soil characteristics (Elhakim, 2005; Strahler, 2012). However, the hyperbolic-based models presented above are beneficial here due to their synergy with aspects of soil dynamics.

5.5 CONTROL OF DIFFERENTIAL SETTLEMENT

5.5.1 Definition of Differential Settlement and Tilt

Differential settlement is the major serviceability criterion which must be met by structures with large foundation areas or which have significant spans. Wind turbine structures are particularly sensitive to differential settlement - a problem which is exacerbated by their dynamic nature. The following points are central to the foundation-soil stiffness:

1. Wind turbine manufacturers impose stringent requirements regarding differential settlement, to ensure that a high standard of foundation quality is upheld at an international level (Bonnett, 2005). These specifications are based on the susceptibility of the structure to over-turning and the potential damage of the superstructure due to foundation distortion. Differential settlement requirements are generally governed in the rotational-stiffness specifications, given its link to the dynamic response of the structure.
2. Differential settlement considerations are associated closely with the rocking and sliding modes of vibration. The foundation-soil stiffness plays an integral role in the dynamic response of the structure, that is the relation between natural frequencies, 1P, 3P and hence amplitudes of vibration. These aspects are introduced in §2.4.1 and expanded upon in in Part III.

Differential settlement may be defined as the inconsistent deformation of a foundation-soil system, which results in differences in settlement between different parts of the structure. The consideration for differential settlement is highly applicable to sites of variable soil properties, especially with respect to consistency and texture. Isolated bases, such as shallow foundations for wind turbines are generally assessed in terms of tilt, because the rigidity of the foundation, combined with the applied loading generally produces rotation of the base. Figure 5.10 defines the tilt, w^*, and differential settlement of a foundation. Furthermore, due to rotation the foundation will also undergo a translational displacement, as indicated by the deflection u in Figure 5.10.

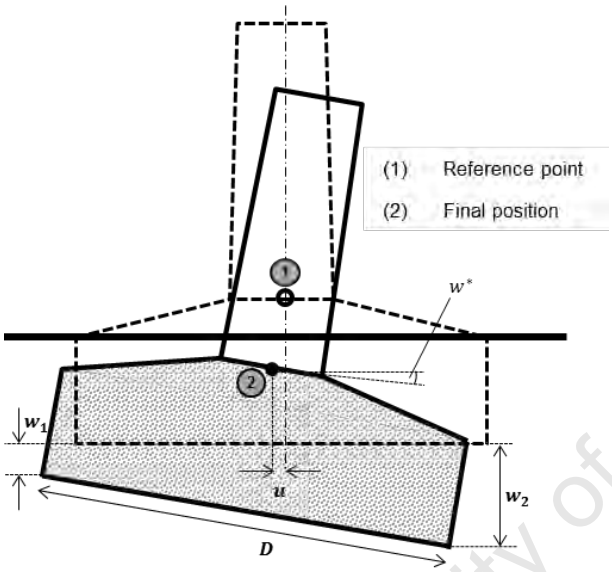

Figure 5.10 **Definition of differential settlement and tilting of foundation base**

The coupling between rotational and lateral deformation under differential settlement is generally accounted for by the specifications enforced by wind turbine manufacturers, which are generally given as the minimum lateral stiffness with respect to rotational stiffness. These stiffness limits are defined in terms of the nominal spring stiffness in order to account for the effects of dynamic loading and the influence that the foundation has on the response of the system under dynamic loading.
This was discussed in §2.4.4.5 and may be summarised by the following points:

1. The 1P and 3P frequencies are pre-determined by the wind turbine manufacturer.
2. The height of the tower, flexural rigidity, mass and damping characteristics are used to determine the natural frequency range of the tower. An interval is generally specified to account for start-up and shut-down procedures (normally $\pm 10\%$ of 1P and 3P).
3. The stiffness of the structure is a function of the tower and equivalent minimum rotational and lateral stiffness of the foundation-soil stiffness, the value of which needs to comply with the natural frequency interval determined in point 2.

5.5.2 Evaluating Foundation-soil Stiffness and Bending Moments

Building on the notion of rational foundation design by incorporating SSI, Horikoshi and Randolph (1997) presented a means of assessing soil-foundation stiffness and maximum bending moments with respect to the differential settlement of raft foundations. Technically speaking, a raft foundation is considered to be a pad footing of large breadth to thickness ratio, which is simultaneously designed for bi-axial bending (Bowles, 1996). For the purpose of this discussion, wind turbine pad footings will be assumed to act as raft foundations, based on their similarity with the respective definition of a raft foundation, and the means with which they undergo differential settlement.

The foundation-soil stiffness ratio is used to assess the relationship between the pad geometry and settlement. Horikoshi and Randolph (1997) built on research conducted by Clancy (1993) and (Brown, 1969), amongst others, to develop a foundation-soil stiffness ratio for rectangular pad foundations, which was consistent for circular foundations equivalent to square foundations of the same area. Furthermore, Poisson's ratio was incorporated, despite its relatively minor influence. These additions yielded the following expression for rectangular pads and circular pads, respectively:

$$K_{f-s} = 5.57 \frac{E_f}{E_s} \frac{1-{\nu_f}^2}{1-{\nu_s}^2} \left(\frac{B}{L}\right)^a \left(\frac{t_f}{L}\right)^3 \qquad \textit{Eqn. 5.34}$$

$$K_{f-s} = 5.57 \frac{E_f}{E_s} \frac{1-{\nu_f}^2}{1-{\nu_s}^2} \left(\frac{t_f}{D}\right)^3 \qquad \textit{Eqn. 5.35}$$

The coefficient 5.57 is equal to $\pi^{1.5}$ to create equivalence between square and circular pads. The coefficient a is selected with the notion of optimising the differential settlement with respect to the aspect ratio of the foundation. Horikoshi and Randolph (1997) determined a value of $a = 0.5$. E represents the Young's modulus of the foundation and soil, given by the subscript f and s, respectively. B, L, D and t_f are geometrical variables of the foundations, symbolizing breadth, length, diameter and thickness, respectively.

5.5.2.1 Differential Settlement – Foundation-soil Stiffness Ratio Relations

The relationship between the differential settlement and foundation-soil stiffness ratio was assessed as part of the study conducted by Horikoshi and Randolph (1997). This was done by firstly defining the normalised settlement:

$$\frac{s_{centre} - s_{perimeter}}{s_{average}} = \Delta s^* \qquad \textit{Eqn. 5.36}$$

s_{centre}, $s_{perimeter}$ and $s_{average}$ denote the settlement at the centre and the perimeter of the footing, and the gross settlement defined in §5.2.3 and $\Delta s^*$is the normalised differential settlement. For circular foundations, the approximate relationship between the normalised differential settlement and the foundation-soil stiffness is illustrated by Figure 5.11.

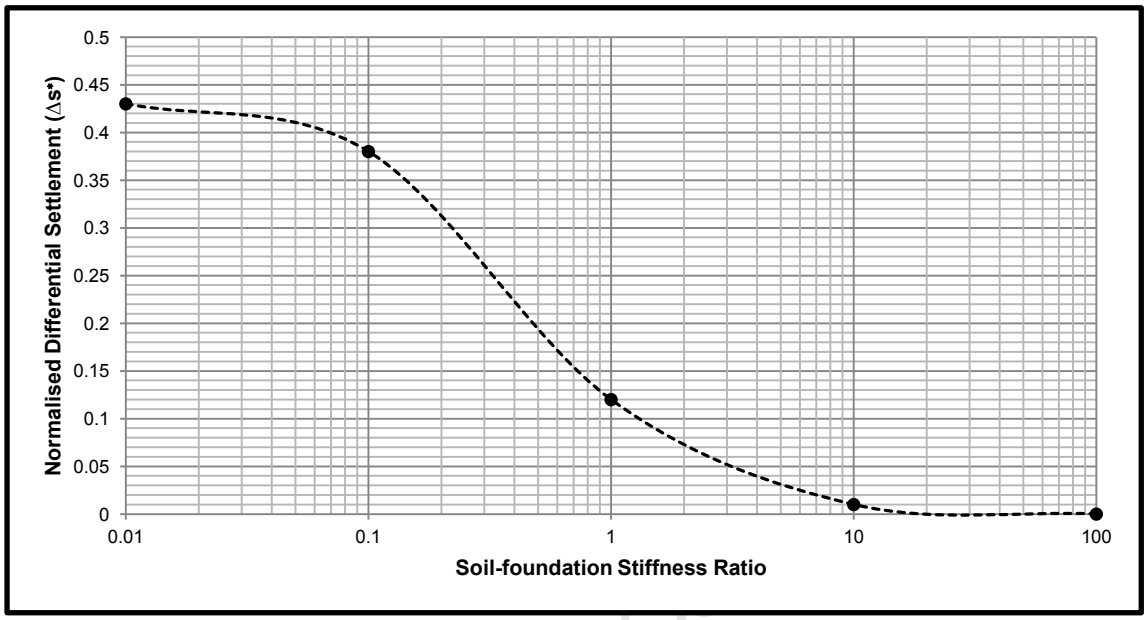

Figure 5.11 **Normalised differential settlement of foundation (Horikoshi and Randolph, 1997)**

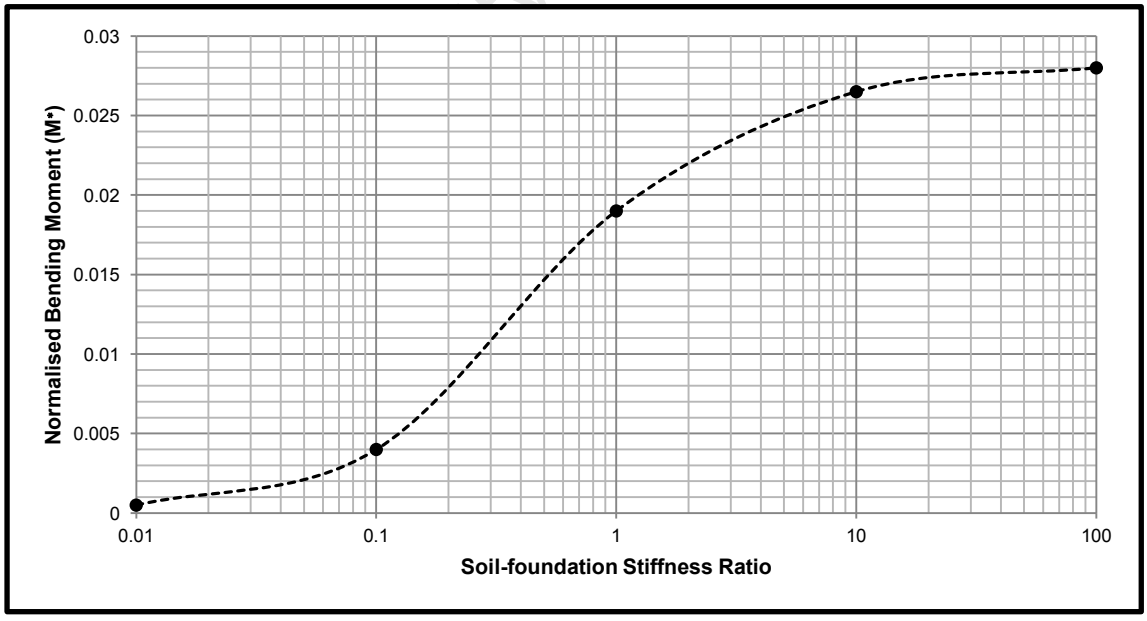

Figure 5.12 **Normalised bending moment at centre of foundation (Horikoshi and Randolph, 1997)**

5.5.2.2 Bending Moment – Foundation-soil Stiffness Ratio Relations

The maximum bending moment induced in the foundation may be expressed in terms of the soil-foundation stiffness for different foundation geometries (Horikoshi and Randolph, 1997). For the purpose of efficient structural design of the foundation, the bending moment at the centre of the foundation may be normalised by:

$$M^* = \frac{M_{max}}{VD^2} \qquad \textit{Eqn. 5.37}$$

Where M_{max} and V are the maximum bending moment and applied vertical load, respectively. The relationship between the normalised bending moment and the soil-foundation stiffness ratio is given by Figure 5.12. K_{f-s} has been normalised against the bending moment value, attained from the relationship between M^* and aspect ratio, for an aspect ratio of 1 (circular foundation).

5.5.3 Increasing Foundation Stiffness: Piling versus Flexural Rigidity

Analysis of the above-depicted relationships between the foundation-soil stiffness and the normalised differential settlement and the bending moment induced in the foundation yields useful design considerations for wind turbine foundations with respect to foundation behaviour.

These include the following:

1. As the foundation stiffness increases the differential stiffness is reduced. This principally refers to the increase in t_f which in turn increases the flexural rigidity of the foundation.
2. Simultaneously, the foundation bending moment at the centre increases as the flexural rigidity of the foundation increases.
3. These fundamental mechanisms present an important question concerning the design of wind turbine shallow foundations: at what point does it become more economical to install piles than to continue increasing the flexural rigidity of the foundation?

There are various methods of increasing K_{f-s} of the foundation at the disposal of the engineer, each one with its own advantages and disadvantages. Such methods may include increasing the foundation thickness and steel reinforcement of the foundation or employing an advanced foundation system, such as the P & H foundations (§3.5.5) or a stiffened pad footing (§3.5.3). It is well known that in some circumstances it may be more effective (and economical) to reduce the differential settlements of the foundation by installing piles underneath the foundation, rather than trying to increase K_{f-s} further. However, clearly defining a point at which this decision should be made is something which requires a dedicated parametric study in coordination with the private sector.

This is because the overall stiffness of a piled foundation (K_{p-f}) is dominated by the pile aspect ratio, L_p/D_p, the normalised pile spacing, S/D_p, number of piles, n and the geometry of the piled foundation (B/L) and may be expressed as follows (Randolph, 1983):

$$K_{p-f} = \frac{K_{pg} + K_f(1-2\alpha)}{1-\alpha^2\left(\frac{K_f}{K_{pg}}\right)} \qquad \textit{Eqn. 5.38}$$

$$\alpha = 1 - \frac{\ln\left(0.5\frac{S}{D_p}\right)}{\ln\left(2\frac{L_p}{D_p}\right)} \qquad \textit{Eqn. 5.39}$$

$$K_{pg} = n^{1-e}K_p \qquad \textit{Eqn. 5.40}$$

where:

- K_f is the vertical stiffness of foundation;
- K_{pg} denotes the vertical stiffness of the piles acting as a group;
- e_p is typically in the region of 0.5-0.6.

If the piles are considered to be rigid, circular members, then (Craig and Knappett, 2012):

$$K_p = \left[2\left(\frac{D_p}{L_p}\right) + \frac{2\pi(1-\nu)}{ln\left(2\frac{L_p}{D_p}\right)}\right]\frac{GL_p}{(1-\nu)} \qquad \textit{Eqn. 5.41}$$

$$K_f = \left[2.1\left(\frac{2r}{L_p}\right)\right]\frac{GL_p}{(1-\nu)} \qquad \textit{Eqn. 5.42}$$

($I = 0.95$ for equivalent square footings)

The total load carrying capacity of the piled foundation (Q_{p-f}) then becomes a function of the footing capacity (Q_f) and the capacity of the pile group (Q_{pg}), and pile group stiffness, such that:

$$\frac{Q_f}{Q_{p-f}} = \frac{K_f(1-\alpha)}{K_{pg} + K_f(1-2\alpha)} \qquad \textit{Eqn. 5.43}$$

$$\frac{Q_{pg}}{Q_{p-f}} = 1 - \frac{Q_f}{Q_{p-f}} \qquad \textit{Eqn. 5.44}$$

Now, using the above-defined relationships the following may be shown:

1. For small piled foundations ($2r/L_p < 1$) the stiffness of the foundation is governed by the stiffness of the grouped piles. This system essentially acts like a conventional pile group, where the pile cap has very little influence over the stiffness of the overall system (Figure 5.13(a)).
2. For large piled foundation ($2r/L_p > 1$) the stiffness of the system approaches the stiffness of the pad, such that the stiffening influence of the piles is effectively negligible, indicating an inefficient and costly design error (Figure 5.13(b)).

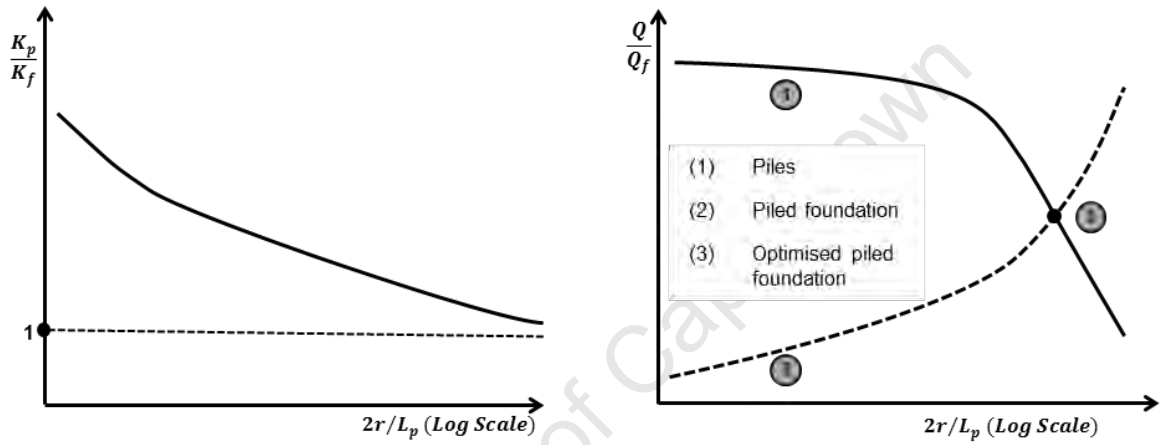

(a) **(b)**

Figure 5.13 **Conceptual relationships: (a) stiffness relations and (b) load capacity versus foundation-pile geometric relationship**

Therefore, in conclusion, a piled-foundation is effective in reducing differential settlements, but it is critical that the proportioning be done correctly with respect to the geometry of the pad and piles as well as pile spacing.

5.5.4 Increasing Subgrade Stiffness

Ground improvement refers to the controlled alteration of the state, nature or mass behaviour of geo-materials in order to achieve, in the case of wind turbines, increased shear strength and stiffness of soils underlying foundations (Gunarantne, 2006). Ground improvement is an important consideration during the wind turbine foundation selection and design process, as marginalised or remote areas are often allocated to wind farm development for reasons such as aesthetics and environmental impact mitigation.

At the same time, given the sensitivity of wind turbine structures, selecting an appropriate ground improvement method is a challenging process due to the relative lack of design theory behind such methods compared to the design of foundation elements. Furthermore, the cost and time implications of delivering equipment and materials to remote wind farms may create large cost and time implications. In addition, carrying out ground improvement techniques over the large footprints generally occupied by wind farms may not warrant such measures and hence deep foundations or advanced shallow foundations may yield more cost efficient results.

Despite these considerations, ground improvement techniques have been used to increase the underlying soil stiffness at wind turbine sites with varying degrees of success. These techniques may be classified in terms of (1) densification, (2) bonding and (3) reinforcing inclusion.

Each different class of ground improvement technique has its advantages and limitations, and most importantly, is dependent on the respective ground conditions. Table 5.3 provides an overview of these ground improvement classes and the appropriate materials. Two other important aspects govern the selection and performance of ground improvement techniques: (1) depth of influence and (2) reliability of distribution. Densification, bonding and inclusions are discussed below with respect to these aspects.

Table 5.3 **Ground improvement methods and soil suitability**

Mechanism of Improvement	Ground Improvement Method	Soil Type
Densification	Vibratory methods	Loose granular materials
	Deep dynamic compaction	Loose sand and silt
	Pre-compression	Soft clay
Bonding	Grouting	Sands and gravel
	Cement stabilisation	Sands and silt
	Lime stabilisation	Sand and silt
	Deep soil mixing	Clay, silt and sand
Reinforcing Inclusions	Stone columns	Clay, silt and sand

5.5.4.1 Densification

Densification, or compaction, methods such as vibratory rollers (Figure 5.14) and dynamic compaction have been shown to be beneficial when applied to wind turbine sites overlying loose granular soils. In theory, these processes reduce the in-situ void ratio of the respective substrata resulting in improved stiffness and settlement characteristics. A critical consideration in the application of densification methods is the consequences of disturbing the subgrade structure and fabric through compaction energies. In some cases compaction may lead to losses in stiffness due to the destruction of the natural soil fabric because the soil structure is the central characteristic that governs stiffness (Mitchell and Soga, 2005). Hence, continuous monitoring and material testing is suggested if compaction is to be carried out on a site, to ensure that the compaction process actually does improve the subgrade stiffness. Chapter 8 addresses this point in more detail, with respect to pedocrete materials.

Furthermore, compaction methods such as these may not be possible, or too costly, to carry out in the remote areas that wind turbines are often situated. Also, the depth of influence of these methods is often questionable, which may lead to degradation of foundation stiffness over time if the treated subgrade has insufficient density with respect to depth.

Figure 5.14 **Vibratory roller compacting the surface of a wind turbine footprint (Parrock, 2013)**

5.5.4.2 Bonding

Increasing the cohesion of the soil by means of binders such as cement and lime has proved to be a viable option for foundations for dynamic structures such as bridges and wind turbines, as well as being effective in reducing liquefaction potential in new and retrofit construction (Bell, 2010). There are two approaches to deep soil mixing (DSM): wet and dry grouting, which makes this method of ground improvement relatively flexible across different soil characteristics.

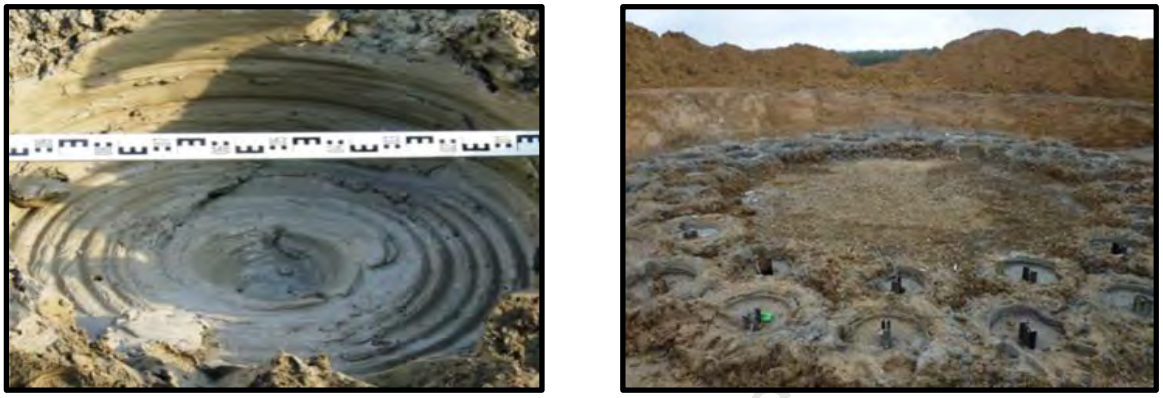

(a) **(b)**

Figure 5.15 **Wind turbine subgrade: (a) deep soil mixing column and (b) foundation subgrade post driving of I-sections to improve foundation strength (Topolnicki and Soltys, 2012)**

In terms of wind turbine foundations, DSM is particularly advantageous in that the depth of influence can be intricately controlled across the foundation footprint. The stiffness of the improved foundation may also be varied depending on the binder characteristic and density with respect to the soil properties (Topolnicki and Soltys, 2012). DSM columns may be combined with driven steel sections to further improve load-carrying capacity, as illustrated by Figure 5.15. Thus, this method offers significant cost saving opportunities and presents an alternative to stone columns, which may impose too great-a-disturbance on the structure of the respective soils.

5.5.4.3 Stone Columns and Rammed Aggregate Piers

Stone columns are defined as compacted gravel-sized particles constructed as vertical columns in the ground to improve the strength performance of the material. The performance of the subgrade is enhanced by two mechanisms; firstly the added stone improves the soil stiffness and hence strength and compressibility characteristics. The second mechanism is by means of compaction, whereby the compaction of the gravel results in densification of the surrounding soil as well. Hence, not only do the stone columns provide a stiff column of material, but also improves the stiffness of the general area with respect to depth. The magnitude of this influence depends on the nature of the materials involved. Table 5.4 provides a general guideline for different materials.

Table 5.4 **Expected performance of stone columns in different soils (Gunarantne, 2006)**

Soil Description	Densification	Reinforcement
Gravel and sand	Excellent	Very good
Sand with 10%-20% silt	Very good	Very good
Sand with >20% fines (low plasticity)	Marginal	Excellent
Clay (high plasticity)	Not applicable	Excellent

As may be noted from Table 5.4 the densification mechanics is best suited to granular soils and the reinforcement attribute is most suited to soft clay soils. Rammed aggregate pier (RAP) systems, pioneered by Geopier Foundation Company in the United States, have provided significant cost saving and improved stiffness for wind turbine foundations. Similarly to DSM, RAPs are highly desirable to wind turbine projects as the depth of reinforcement may be controlled (Fizpatrick, 2009). The process is very similar to that of stone column construction, and involves boring cavities into the respective founding soils to the required depth of reinforcement. Aggregate is then compacted within the cavity in layers by means of tampering. This induces fewer disturbances to the adjacent soils and therefore is more suited to soft cohesive soils.

5.6 SUMMARY

The assessment of differential settlement and the minimisation thereof, under monotonic working conditions, was presented by this chapter. This was based on the concepts of settlement and soil stiffness, where the following key points were made:

1. The immediate settlement of shallow foundations may be interpreted in terms of elastic displacement theory. Although this theory has shortfalls in terms of the anisotropic, inhomogeneity and non-linear behaviour of soils, if these are understood and taken into account, the immediate settlement may be calculated and used as a proxy for bearing capacity.
2. This was done by assuming the respective foundation was either perfectly flexible or rigid. It was shown that increasing foundation stiffness had negligible effect on settlement, but reduced differential settlement.
3. The rational design of footings – based on incorporating footing stiffness – was presented using the *Winkler* model to predict foundation displacement under working loads. Although useful, difficulties around determining the coefficient of subgrade reaction gave rise to an overview of soil elasticity models.

4. The linear elastic soil model and the non-linear elastic model were presented with respect to predicting the soil moduli required to evaluate analytical solutions for foundation settlement, such as those derived from the yield surface approach and the elastic half-space theory. The non-linear elastic soil models were based on hyperbolic functions, given their synergy with aspects of soil dynamic presented in the next chapter.
5. Although these relations may be considered highly simplified, based on the wind turbine strain levels remaining within the elastic threshold allows for such relationships to be used. This has important bearings on the dynamic response of footings, and hence such models are dealt with in more detail in Part III.

The differential settlement, or tilt, of wind turbine foundations was explored, where it was shown that the foundation-soil stiffness relations could be used to assess the suitability of different differential settlement mitigation measures. Hence, assessing the wind turbine foundation-soil system against a background of rational foundation design was deemed to helpful in assessing the point at which piles should be utilised over increasing the flexural rigidity of the base.

PART III DYNAMIC ASPECTS OF WIND TURBINE FOUNDATIONS

6. BEHAVIOUR OF FOUNDATION-SOIL SYSTEMS UNDER DYNAMIC AND CYCLIC LOADING

6.1 INTRODUCTION

The preceding chapters were concerned with soil strength and stiffness such that the failure state of the soil-foundation system could be defined and excessive deformation avoided. In these cases, the loads were considered static and induced strains within the soil mass from 10^{-3}% to several per cent at failure (Priest, 2012).

Wind turbines are just one of many scenarios where dynamic loads are transferred to the soil resulting in the generation of vibrations. Vibratory motion is a structural response to time-varying (dynamic) loads, whereby an elastic solid, or particles thereof, oscillate about an equilibrium position. In the case of wind turbines, the foundation vibration response originates from variable wind conditions, rotor dynamics and out-of-balance masses acting on or within the structure, respectively. It is imperative from an economical and safety point of view, that vibration of wind turbine foundations be assessed. There are three key reasons for this:

1. The cyclic loading of soils alters the natural frequency of the rotor-tower-foundation-soil system. Any change in natural frequency results in a change in bending moment and deflection characteristics at the top of the tower.
2. Strain and stress accumulation, emanating from vibrations, may lead to the densification of the respective soil leading to differential settlements and associated structural problems.
3. Fatigue effects result in damages such as reduced load capacity of the foundation and associated crack propagation, and thereby a loss of serviceability.

This chapter outlined the main attributes regarding the behaviour of soils under dynamic loading. First, the *dynamic problem* and strain dependent behaviour of soils was introduced, as these themes were deemed central to the remainder of the chapter. This was followed by the characterisation of wind turbine induced vibrations and the properties of soil under dynamic and cyclic loading. Based on this analysis, theory of wave propagation was presented. This chapter aimed to form a base upon which the concepts and methods of analysis presented in Chapter 7 may be understood.

6.2 ESSENTIAL CHARACTERISTICS OF A DYNAMIC PROBLEM

The design of foundations for the resistance of dynamic loading requires a different design approach, based on the following two factors that differentiate dynamic problems from static and quasi-static, namely, the dynamic loading of soils and the strain dependency of their response.

6.2.1 Dynamic Loading of Soils

The term *dynamic loading* may be defined as the time-varying loading of a system, which implies that the respective loads applied to the system are a function of time. To make this definition more specific, dynamic loading may be defined in terms of two attributes (1) loading frequency and (2) the number of loading cycles. The loading frequency of wind turbine foundations is relatively low; however the number of loading cycles is disproportionately high. Problems of dynamic loading may be classified in terms of the loading frequency in three categories:

1. Impulse loads, associated with singular dynamic events.
2. Vibration or wave propagation problems arising from events such as earthquakes and construction activities like pile driving. The frequency of loading typically ranges from 1-100 Hz with the number of load cycles being between 10 and 100 (Priest, 2012).
3. Fatigue related behaviour, where the soil experiences an extremely large number of load cycles.

Wind turbine foundation problems span all three cases defined above, where two major considerations may be made. The first regards the overall stability of the system when subjected to impulsive loads, associated with extreme wind events and possible faults. The second and most significant, regards the cyclic nature of wind turbine loads coupled with the extremely high number of loading cycles expected to be transferred to the subgrade of a wind turbine foundation. The resulting effects on the subgrade properties and serviceability limit state of the structure, with respect to material fatigue and stiffness, are of primary concern in this case.

The final distinction between static and dynamic loading is the generation of inertial forces within the system under loading. Inertial forces were introduced in §2.4.4, where it was shown that inertial forces resist acceleration of the respective system. The response of a structural system, or particle thereof, to a dynamic load is dependent on the nature of the load and the nature of the inertial forces resisting the acceleration induced by the dynamic load (Clough and Penzien, 1995).

6.2.2 Strain Dependent Behaviour of Soils under Cyclic Loading

The strength and deformation characteristics of any geo-material are highly dependent on the level of shear strain to which the soil is subjected. The level of shear strain dictates the nature of material response under cyclic loading, as illustrated by Figure 6.1, where specific characteristics of material behaviour may be defined. This was discussed in §5.4, and may be summarised as follows:

1. Elastic and recoverable strains occur at low levels of shear strain, below the *linear elastic threshold* (γ_{tl}).
2. Elasto-plastic behaviour is where permanent deformations occur in the form of cracks and differential settlement.
3. Minor stiffness degradation may occur as the strain exceeds the *volumetric cyclic threshold* (γ_{tv}), but will generally only become significant once the *degradation threshold* (γ_{td}) is reached and plastic behaviour begins.
4. The soil is assumed to have failed once the *failure threshold* (γ_{tf}), in the plastic range is reached. These behaviour categories are displayed below with approximate strain values.

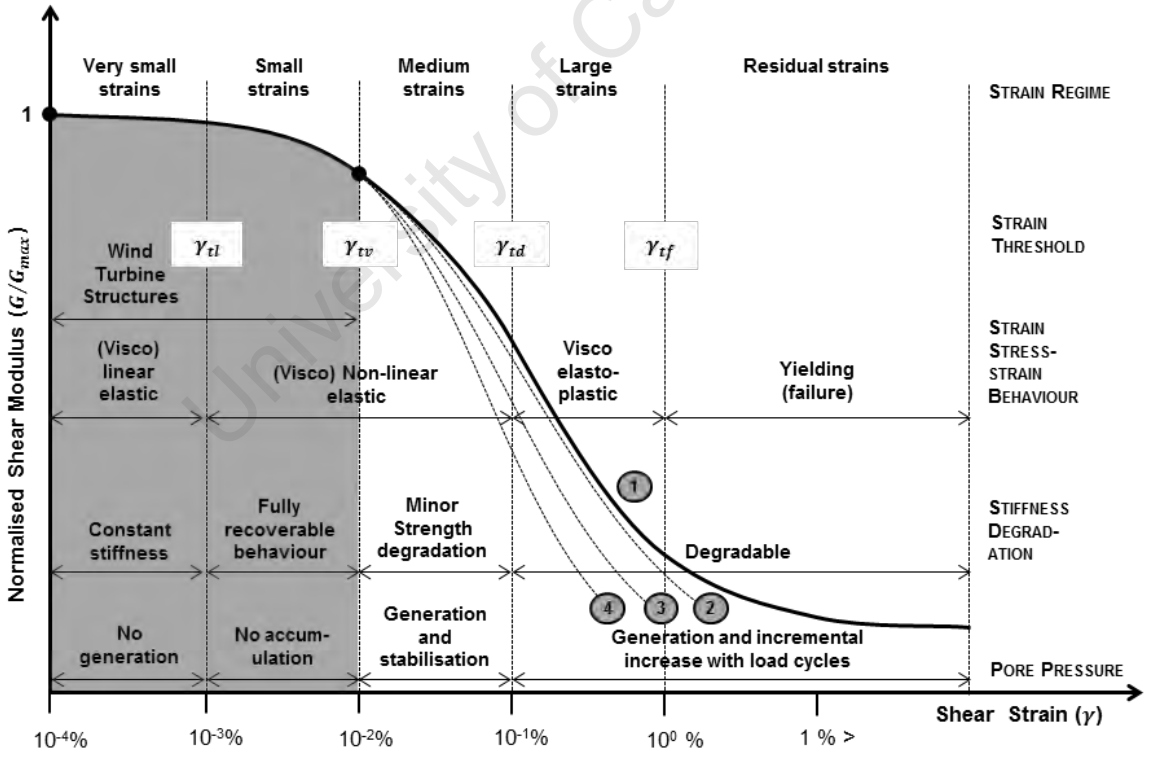

Figure 6.1 **Conceptual stress-strain behaviour of soils**

The influence of cyclic loading is fundamental to analysing and predicting the behaviour of wind turbine foundations. It has been emphasised throughout this text that wind turbines are subjected to a disproportionately high number of load cycles during their service life. Thus, fatigue considerations are of primary concern in the design of many wind turbine components. This is analogous to accounting for the stiffness degradation of foundation-soil systems under cyclic loading. A critical level of cyclic loading may be defined where, if exceeded, stiffness degradation will occur. This is termed the *degradation threshold* (γ_{td}) (Diaz-Rodriguez and Lopez-Molina, 2008).

Below this, an elastic pore pressure response and hysteretic linear equilibrium behaviour may be observed. Figure 6.1 illustrates this point, along with 4 labelled curves of stiffness degradation. It should be noted that these curves are indicative of the number of stress cycles experienced (N), where $N_4 > N_3 > N_2 > N_1$. Hence, the effect of the number of loading cycles may be viewed comparable to reducing the effective confining stress.

Another critical aspect concerning the cyclic loading of soils is the effect it has on pore water pressures. This is a function of the shear strain induced in the material, where the generation of excess pore water pressures is negligible at low strain. However, at larger strains frictional sliding and yielding at grain contacts lead to changes in soil volume producing a build-up of pore water pressures (Priest, 2012). This exacerbates the deformation as the effective confining stress is reduced. Thus, controlling the stiffness degradation of foundation-soil systems hinges on the G_{max} of the respective soil, and ensuring that adequate stiffness of the foundation-soil system is achieved.

6.2.3 Developing a Solution to the Dynamically Loaded Foundation Problem

The preceding discussion established that the dynamic and cyclic loading of soils requires a different design approach than the traditional geotechnical approach adopted for the static loading of foundations. The classic text of soil and foundation vibration by Richart, Hall, & Woods (1970) addressed this problem through four key questions which are examined below.

6.2.3.1 What Constitutes Failure?

Definition of failure criteria is a subjective process, which is based on the environment in which the foundation will operate. Therefore, if the wind turbine is to be situated close to human settlements then the controlling criteria will be based on limiting the transfer of vibrations to neighbouring structures and ensuring that the resulting vibrations are of such a frequency that they do not disturb local inhabitants. Secondly, and more critically, the design criteria for wind turbines must ensure that the foundation is designed to withstand the resulting vibrations from a material fatigue point of view. This is in order to limit the propagation of cracks in the foundations and differential settlement of the supporting soil.

6.2.3.2 How is the Applied Load Related to the Deformation of the Soil-foundation System?

This is an analytical process whereby a constitutive model is selected to describe the load-deformation behaviour of the foundation-soil system. Thus, addressing this question requires the cognisance of the strain-dependency of soils and the nature of the applied loadings. For very small shear strain amplitudes, like those to be expected from wind turbines and other machine foundations, an elastic material model suffices (DNV/Risø, 2002).

6.2.3.3 What is the most Applicable and Appropriate Design Model?

The next step in the design process is to incorporate the applied loading and material deformation relationships into an applicable and accurate model which may be solved numerically or graphically. The lumped-parameter model is probably the most widely used model in structural and soil dynamics. It operates on the notion that the system may be simplified to three components: (1) a lumped mass, incorporating the structural loads, mass of the structural component supported and the mass of the foundation, (2) a lumped spring parameter, describing the soil stiffness and (3) a lumped damping parameter defining the damping characteristics of the system. This model was constructed from the theory of a foundation supported on an elastic-half-space. Although this is a significant simplification, it allows links to be drawn between geophysical testing, wave propagation theory and foundation response, as will be picked up in subsequent chapters.

6.2.3.4 How can the Soil Parameters be Determined?

The determination of material parameters describing soil response to loading, such as G and ν, must be done under anticipated conditions. Therefore, the determination of these soil parameters for dynamic loads is different to the traditional laboratory and field techniques used to determine the same parameters under static loading.

These four key questions were addressed in the following sections and chapters within Part III and IV, the structure of which is summarised by Figure 6.2.

6.3 CHARACTERISATION OF GROUND VIBRATIONS AFFECTING WIND TURBINES

Ground vibrations are characterised in terms of their origin, duration and strain level. The type of model used to assess the relevant vibrations is a function of the vibration characteristics. This is mainly due to the strain dependent nature of soils subjected to cyclic and dynamic loading (Karg, 2008; Priest, 2012). The following discussion characterises the vibrations expected from wind turbines and provides considerations with the process of accounting for vibrational loading of foundations.

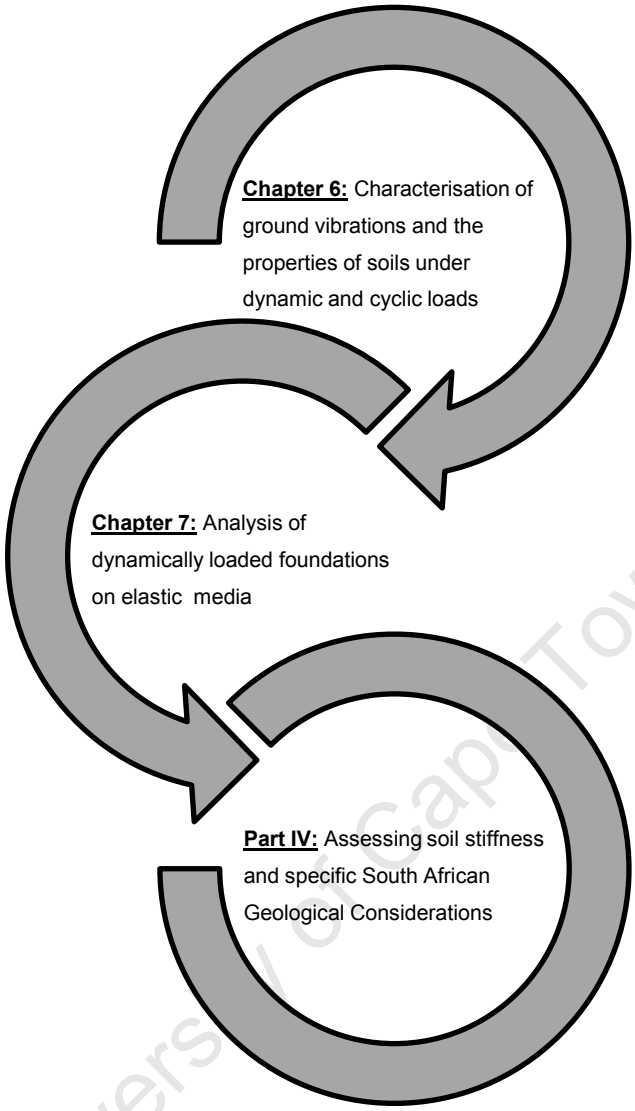

Figure 6.2 **Addressing the dynamically loaded foundation problem**

6.3.2 Source of Vibrations

The origin of vibrations is conventionally classified as man-made or natural which allows one to broadly associate a type of vibration, with respect to variation, with each origin. Man-made vibrations are considered to be easier to describe and model, as the source, duration and associate frequencies and amplitudes of vibration are generally attainable. Natural vibrations on the other hand, resulting from environmental conditions such as wind, wave and earthquake loads, are considerably more complex to describe, due to the strong variability of the strain levels. Wind turbine structures are subjected to a combination of these two sources, rendering the level of induced shear strain as the main determining factor when characterising the vibrations

6.3.3 Duration of Vibrations

The duration of vibrations is normally classified in terms of temporary or permanent. Loads emanating from events such as earthquakes, pile driving and blasting result in temporary vibrations. Temporary vibrations generally result in immediate damage but not necessarily the most extreme settlement. This is because long term vibrations, such as those experienced by the foundations of wind turbines, induce fatigue and strain accumulation within the soil. This would result in time-dependent settlement which would stabilise in time (Karg, 2008).

6.3.4 Anticipated Level of Shear Strain

The importance of soil behaviour with respect to shear strain, and the anticipation of shear strain likely to be induced in the foundation-soil system, has been emphasised. Table 6.1 gives the level of induced shear strain that can be expected to occur within the soil from the four most important sources relevant to wind turbine structures (DNV/Risø, 2002). Hence, it may be concluded that the respective loading induces low levels of shear strain within the soil, and in doing so may be modelled within the volumetric threshold which is commonly regarded as shear strains below 10^{-2}% (Diaz-Rodriguez and Lopez-Molina, 2008; Karg, 2008). Therefore, the static stiffness is commonly regarded as representative of the dynamic stiffness required in the structural analysis of wind turbine foundations.

Table 6.1 **Level of shear strain expected from common dynamic loads on soils (DNV/Risø, 2002)**

Type of Loading	Degree of Shear Strain	Approximate Magnitude (%)
Earthquakes	Large – very large	10^{-2}-10^{-1}
Ocean waves	Moderate – large	10^{-2}
Wind	Moderate	10^{-4}-10^{-2}
Rotating machines	Low – moderate	10^{-5}-10^{-3}

The important bearing of this may be summarised as follows:

1. The dynamic soil stiffness, which is frequency dependent, may be approximated by static stiffness values. Thus, methods such as the *Lysmer Analog* and lumped parameter models may be used to conduct the dynamic analysis of wind turbine foundations with sufficient accuracy. This is studied in Chapter 7.
2. Wave propagation techniques may be used to determine G_{max}, which may in turn may be used to determine the any stiffness degradation upon increased load cycles when combined with an appropriate non-linear constitutive model.

6.3.5 Damage Considerations and Reduction in Serviceability of Foundations

Two broad categories may be defined, with respect to the duration of loading and hence type of damage behaviour: (1) immediate and (2) long term. Immediate effects generally refer to the densification of a soil structure upon vibratory loading. Densification refers to the process of particle repositioning and crushing upon loading and hence the re-distribution of soil stresses and strains within a soil body. This is one of the most common serviceability issues related to the design of foundations for vibrating structures, especially when the soil conditions comprise granular materials with high void ratios. For this reason, and the focus of this study on pedocrete soils, the following chapters are primarily concerned with granular materials. Densification in this regard refers to the short-term effects of particle-repositioning, which in some cases may result in significant settlement or shear failure upon vibratory loading. However, these immediate effects are generally avoidable through thorough preparation of the subgrade.

Table 6.2 **Failure mechanisms due to vibrations in the soil**

Failure	Soil	Structure
Immediate: due to short term/singular event.	Shear Failure Liquefaction	Characteristic strength of material exceeded
Fatigue: due to long term dynamic-cyclic loading at small strain amplitudes.	Densification Strain accumulation Stress redistribution Abrasion and crushing of grains	Fatigue Stress redistribution Changes in natural frequencies

The cyclic nature of wind turbine foundation loading makes the long term damage effects of foundation subgrade the critical issue. Despite the level of shear strain induced by the external loads remaining within the elastic threshold of the material, a residual deformation may be observable with repeated load cycles, as a result of grain re-positioning, drainage and crushing effects.

This phenomenon has been termed *stiffness degradation*, or *strain accumulation*, since plastic strains accumulate in very small increments over time, despite the induced shear strain being in the elastic range. This is the most probable damage risk associated with foundation-soil systems subjected to small strain vibrations and is analogous to the material fatigue considerations for other wind turbine components.

Strain accumulation generally culminates in two forms:

1. Damage of the structure due to fatigue effects within the soil. This may include decreased load capacity, crack growth and detraction of stability with increasing number of load cycles.
2. Densification of the soil with respect to accumulated stress and strain, resulting in settlements.
3. Diminishing stiffness alters the natural frequency of the tower-foundation-soil system, resulting in a change in the structure‘s dynamic response.

The rate of strain accumulation, defined as the rate of change of accumulated strain with respect to time, depends on a multitude of factors. The first body of factors relates to the nature of the cyclic loading. The larger the cyclic stress the greater the strain accumulation rate, as more energy is transferred to the soil upon each load application (Karg, 2008). Furthermore, the higher the mean effective stress, the lower the strain accumulation rate. Secondly, the soil properties affect the strain accumulation rate. Void ratio, grain size, shape and roughness as well as the moisture content of the soil all influence the development of plastic strains within the soil body (Priest, 2012). Table 6.3 summarise the effect of these factors.

Table 6.3 **Parameters Affecting the Strain Accumulation Rate**

Influence Parameter		Strain Accumulation Rate
Number of cycles	↑	↓
Cyclic stress/strain amplitude	↑	↑
Average effective mean stress	↑	↓
Void ratio	↑	↑
Uniformity	↑	Not clear
Grain size	↑	Not clear
Moisture content	↑	Not clear

Strain accumulation is an especially difficult process to design for and quantify. On a qualitative basis the major consideration is the diminishing stiffness and change in natural frequency associated with strain accumulation. Thus, this is another reason for the stringent rotational stiffness measures stipulated by wind turbine manufacturers, because ensuring that the initial subgrade stiffness is sufficiently high is the primary mitigating factor for strain accumulation.

6.4 SOIL PROPERTIES UNDER DYNAMIC AND CYCLIC LOADING

Accounting for dynamic loads transferred to soils required an assessment of the dynamic properties of the respective soil. This requires the determination of the dynamic material parameters of soils in order to describe the behaviour of the respective material under dynamic loading. There is a wide array of dynamic soil parameters that are used to do this (Hoadley, 1984), comprising:

1. Dynamic moduli, including Young's modulus (E), shear modulus (G), bulk modulus (K). Lamé's first constant, λ, is used to link these parameters;
2. Poisson's ratio (ν);
3. Cyclic shear strain amplitude (γ_c) and shearing rate;
4. Damping ratio ( ) or attenuation factors;
5. Liquefaction factors, including cyclic shear stress ratio, cyclic deformation and pore pressure.

As defined above, wind turbine foundations are deemed to operate within two distinct domains of shear strain: (1) low ($<10^{-3}$%) where the soil is considered to act as an elastic medium and (2) intermediate (10^{-3}-10^{-2}%) which constitutes elasto-plastic behaviour with minor stiffness degradation.

An elastic constitutive model may be adopted for this range of shear strain, whereby the shear modulus, G, and Poisson's ratio, ν, are the key parameters describing the soil load-deformation behaviour, as discussed in §5.4. The relationship between G and other elastic constants were summarised in Table 5.2. Therefore, the question is whether it is necessary to devote an entire section to the analysis of these universally accepted parameters and relationships? The answer to this question is, from a geotechnical standpoint, yes, because these values adapted for these parameters are often misunderstood and abused. Reasons for this include:

1. The geotechnical testing upon which the values are based may have involved anomalies relating to calibration, testing procedure and most importantly, interpretation of the material being tested and the results obtained.
2. The data obtained may not be entirely applicable for the particular problem in the field, especially when the effects of layering and discontinuities are not accounted for.
3. There may be insufficient data or knowledge of the respective loading cases and induced strain.
4. Finally, soil is a highly heterogeneous material where the adoption of absolute parameters to describe its characteristics is flawed, but also often the only option. Thus, engineering judgement and experience is paramount.

This section defines the dynamic shear modulus and damping parameters of soils, and explores the factors upon which they are dependent. Extensive laboratory testing undertaken to determine the behaviour of soils under dynamic and cyclic loads has shown that the stiffness and damping properties of soils are influenced by a wide range of factors, the principle ones being highlighted by Eqn. 6.1 (Priest, 2012).

$$(G, \zeta) = f(\gamma_c, \overline{\sigma_0}', e, N, S, \dot{\gamma}, OCR, C_m, t) \qquad \textit{Eqn. 6.1}$$

These factors may be broadly defined in terms of, firstly, the loading characteristics, such as: the cyclic shear strain amplitude, γ_c, the number of load cycles, N, and the strain rate, $\dot{\gamma}$. Secondly, the structure of the material which is dependent on factors such as: the mean effective confining stress, $\overline{\sigma_0}'$, the void ratio, e, the over consolidation ratio, OCR, the degree of saturation, S, grain characteristics, C_m, and the geological time, t. Details of these factors are explored below.

6.4.1 Dynamic Soil Stiffness

6.4.1.1 Definition of Dynamic Moduli

The harmonic loading of a soil element, as depicted by Figure 6.3(a) results in a stress-strain relationship such as that illustrated by Figure 6.3(b). A hysteresis loop accrues for each cycle of loading. The secant shear modulus is defined as the slope of the line that connects the origin to the point of inversion between loading and unloading, and thus it decreases with each loading cycle or increase in cyclic load amplitude due to particle re-arrangement and crushing (Karg, 2008).

The shear modulus at very low strains has been found to be relatively constant and a maximum. Thus, the first loading curve, or backbone curve, is used to define the maximum dynamic shear modulus, G_{max}.

As the shear strain increases, which may be a result of an increase in the amplitude of loading, rate of loading, or number of cycles, the soil behaviour becomes elasto-plastic in nature. Elasto-plastic behaviour is also defined in terms of the shear modulus and Poisson‘s ratio. However, the stiffness of the material is deemed to reduce on repeated load applications, mainly through the slippage of particles at grain contacts (Karg, 2008). This dissipation of energy is broadly called *material damping*. It is rate-dependent and alters the nature of propagation of stress waves through the soil upon dynamic loading. For this reason it is a key parameter in determining the dynamic response of a soil and is studied in the subsequent section.

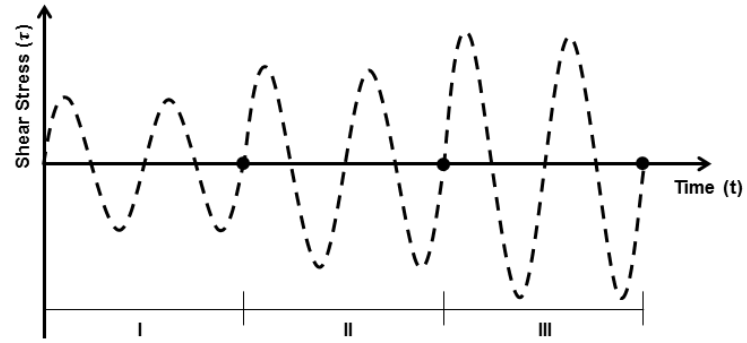

(a)

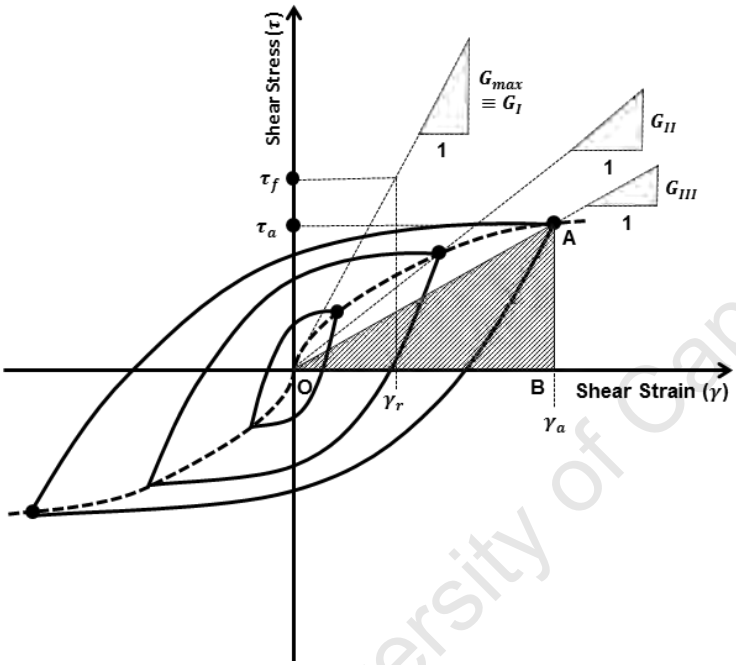

(b)

Figure 6.3 **Relationship between (a) different amplitudes of cyclic loading at constant frequency and (b) soil stress-strain response**

The two most popular constitutive models developed to describe this non-linear stress-strain behaviour of soils under dynamic and cyclic loading are the hyperbolic and Ramberg-Osgood (R-O) models, utilising two and four parameters, respectively. These models are defined below in conjunction with Figure 6.3(b).

These non-linear models are used to evaluate the deterioration of stiffness with increases in cyclic loading and strain levels in conjunction with G_{max} and the normalised shear modulus distribution. These relationships have been verified by several empirical studies, which are subsequently discussed in relation to factors affecting the stiffness of soils.

(i) Hyperbolic Model

The general form of the hyperbolic model is defined in terms of the reference strain, γ_r, and the secant shear modulus defined as the ratio between shear stress, τ_a, and strain, γ_a, at the point of inversion in the loading cycle. γ_r corresponds to the shear strength at failure under monotonic loading, and may be evaluated by the Mohr-Coulomb failure criterion.

$$\frac{G}{G_{max}} = \frac{1}{1 + \frac{\gamma_a}{\gamma_r}} \qquad \textit{Eqn. 6.2}$$

$$G = \frac{\tau_a}{\gamma_a} \qquad \textit{Eqn. 6.3}$$

(ii) Ramberg-Osgood (R-O) Model

The general form of the R-O model is given by:

$$\frac{G}{G_{max}} = \frac{1}{1 + \alpha \left[\frac{G}{G_{max}} \frac{\gamma_a}{\gamma_r}\right]^{r-1}} \qquad \textit{Eqn. 6.4}$$

Where γ_f is the shear strain at failure under monotonic loading, and τ_f is the corresponding shear stress.

$$\alpha = \frac{\gamma_f}{\gamma_r} - 1 \qquad \textit{Eqn. 6.5}$$

$$r = \frac{1 + \frac{\pi D_{min}}{2} \frac{1}{1 - (G_f / G_{max})}}{1 - \frac{\pi D_{min}}{2} \frac{1}{1 - (G_f / G_{max})}} \qquad \textit{Eqn. 6.6}$$

$$G_f = \frac{\tau_f}{\gamma_f} \qquad \textit{Eqn. 6.7}$$

α and r are determined by fitting the respective models to experimental data from triaxial or resonant column devices.

Analysis of the hyperbolic and R-O model illustrate the fact that in order to assess the dynamic behaviour of a soil under dynamic shearing the small strain shear modulus, G_{max} and ultimate shear strength, τ_f are required. It is reiterated that both of these parameters must be evaluated for the anticipated loading conditions (Richart, 1977).

6.4.1.2 Factors Influencing the Maximum Dynamic Modulus (G_{max})

Laboratory tests have yielded the most important factors affecting soil stiffness are: cyclic strain amplitude, void ratio, mean effective stress, plasticity index, OCR and number of loading cycles. The effects of these parameters are summarised in Table 6.4 (Karg, 2008). This relationship may be simplified considerably at low levels of shear strain. For granular materials the material behaviour becomes highly dependent on $\overline{\sigma_0}'$ and e, and for clayey materials the cyclic behaviour primarily becomes a function of OCR and t, the details of which are studied below.

(i) Non-cohesive Materials

The void ratio and effective confining pressure have been found to play a central role in the stiffness of geo-materials, where higher material stiffness was encountered at low void ratios and higher confining stresses (Richart et al., 1970). This behaviour may be explained in terms of the soil structure and it's relation to void ratio. The void ratio is a parameter which encapsulates key material structural attributes, such as the packing of particles and the nature of the fabric. The structure of the material plays a critical part in the resulting stiffness because of the number of grain to grain contacts, and hence the contact force per grain (Woods, 1977).

As the void ratio increases, the number of grain to grain contacts, per grain, decreases leading to higher contact forces at the grain interfaces. Higher contact forces subsequently lead to localised yielding at grain contacts, and hence lower shear modulus values. Similarly, increases in confining stress produce changes in soil fabric, resulting in lower void ratios.

Table 6.4 General influence of increasing Parameters on G_{max} (Karl, 2005)

Parameter		G_{max}
Mean effective confining stress, $\overline{\sigma_0}'$	↑	↑
Void ratio, e	↑	↓
Plasticity index, PI	↑	↑ if OCR > 1
OCR	↑	↑
Shear strain amplitude, γ	↑	↓
Cementation	↑	↑
Geological age	↑	↓

The above-mentioned material behaviour is highly dependent on the shape, roughness and angularity of the material particles under stress. These factors were summarised by Priest (2012) whereby it was shown how the elastic threshold of non-cohesive soils was higher for increasing angularity. This effect is especially apparent as the shear strain amplitude increases.

For rounded soil particles with a void ratio less than 0.8 and for angular soils Hardin and Richart (1963) presented the following relationships (in psi), respectively:

$$G_{max} = \frac{2630(2.17 - e)^2}{1 + e}\sqrt{\sigma_0'} \qquad \textit{Eqn. 6.8}$$

$$G_{max} = \frac{1230(2.97 - e)^2}{1 + e}\sqrt{\sigma_0'} \qquad \textit{Eqn. 6.9}$$

As may be observed from these relationships, the shear modulus of a granular soil is principally a function of the void ratio and effective confining stress. However, accurately evaluating the in-situ confining stress proved to be difficult in this regard.

Following the work by Hardin and Richart (1963), Seed and Idriss (1970) presented the following expression which is also fundamentally based on the mean effective stress and void ratio, but expressed in terms of a factor K_2, which is a function of the relative density (D_r).

$$G_{max} = 83.32K_2\sqrt{\sigma_0'} \qquad \textit{Eqn. 6.10}$$

$$K_2 = 0.6D_r + 16 \qquad \textit{Eqn. 6.11}$$

The use of D_r as a proxy for void ratio has made the use of the standard penetration test (SPT) for assessing D_r and hence G common. However, there are a few key consideration linked with this practice:

1. The observed SPT ‗N' value needs to be adjusted for the overburden pressure and the effects of dilation before it may be used to determined values of D_r.
2. Other corrections for SPT energy, rod length and so on also have to be accounted for depending on the specific SPT practice of the region as discussed by Abou-matar and Goble(1997) and Schmertmann and Palacios (1980).
3. This practice stemmed from the assessment of liquefaction potential, and therefore should be treated with caution when assessing the small strain amplitudes associated with machine foundations in contrast to those expected to cause liquefaction.

The saturation of coarse grained material has an effectively negligible effect on soil shear stiffness. This is a result of fluids being unable to resist shear stress, and thus only affects the shear wave velocity of the material through its influence on the material density. On the other hand, water content plays a central role in soil stiffness in much the same way as it does in the compaction of soils (Briaud, 2001). At very low water contents the rearrangement of particles is hampered by frictional resistance between grains. As moisture content increases the grain contact become lubricated aiding the closer packing of particles. If the moisture content passes an optimum value the water starts to fill voids resulting in it hindering particle re-alignment.

(ii) Cohesive Materials

The behaviour of cohesive materials under dynamic loading is also intrinsically linked to the void ratio. However, two important factors differentiate cohesive and non-cohesive dynamic material behaviour: time of confinement and stress history. An increase in the confining stress of granular materials results in a quasi-instant reduction in void ratio. The consolidation process of cohesive soils is time dependent and depends on (1) the permeability of the soil, (2) shape of the specimen and (3) the available drainage paths (Richart et al., 1970). Hence, the cohesive material behaviour resulting from an increase in confining stress depends on (1) the time of confinement and (2) the stress history of the sample, described by OCR. Therefore, the greater the time of confinement, the longer the sample has had to consolidate from the increase in stress increment and hence the higher the resulting shear modulus due to the lower void ratio.

An over-consolidated soil, that is a soil with a higher OCR, will also possess higher shear moduli values than normally consolidated materials. This is based on the irrecoverable reductions in void ratio that occur as a soil is consolidated (Priest, 2012). A relationship defined by Hardin and Drnevich (1973) encapsulated these factors as follows:

$$G_{max} = 1230\frac{(2.973 - e)^2}{(1 + e)}(OCR)^k\sqrt{\overline{\sigma_0}'} \qquad \textit{Eqn. 6.12}$$

Where k is a function of the plasticity index of the soil, given by (Chowdhury and Dasgupta, 2009):

$$k = -5 \times 10^{-8}(PI)^3 - 4 \times 10^{-5}(PI)^2 + 0.0092(PI) + 0.0025 \qquad \textit{Eqn. 6.13}$$

Considerable research has been conducted in the field of soil dynamics with respect to developing correlations between the shear modulus and other soil parameters by researchers such as Hardin, Richart, Drnevich, Seed and Idris. By no means should these correlations replace the physical measurement of soil properties by laboratory or field techniques. However, the correlations presented here have been used with success in the solving of dynamic soil-structure interaction problems.

6.4.1.3 Factors Influencing the Strain-dependent Shear Modulus (G)

As has been highlighted above, the shear modulus begins to decrease with increasing strain. The point at which this reduction is triggered is termed the *elastic threshold*, and it defines the strain at which behaviour changes from linear elastic to elasto-plastic. The behaviour of the material is then governed by the strain-dependent shear modulus (G).

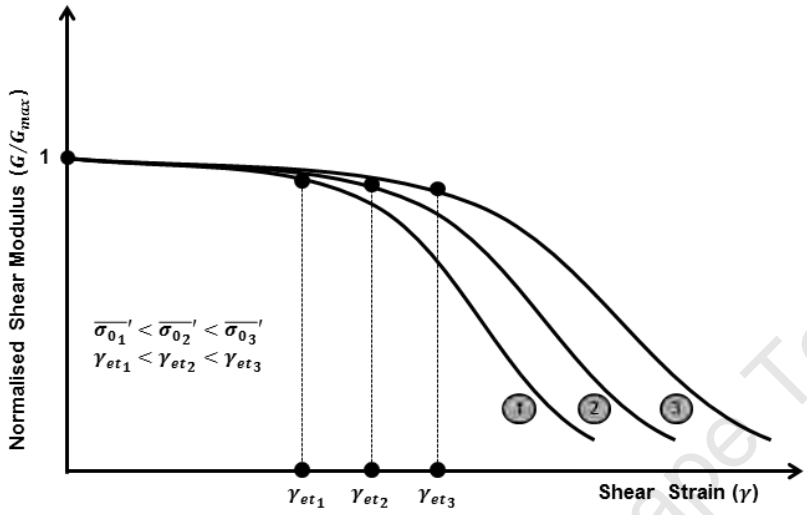

(a)

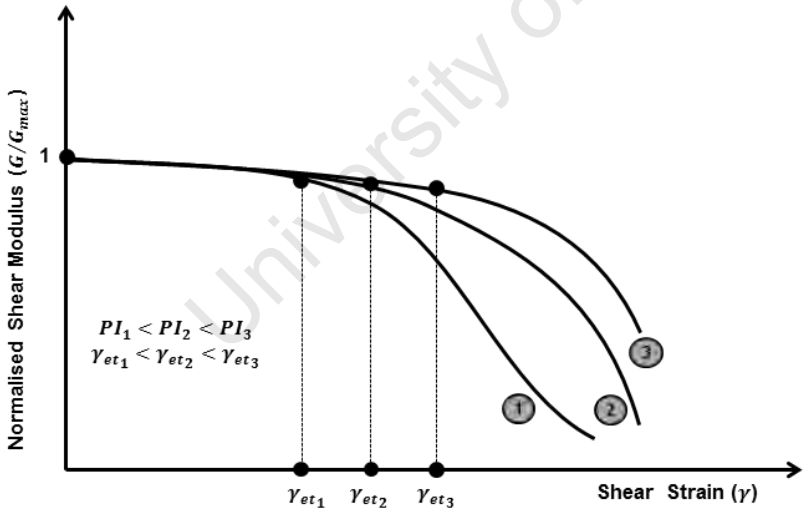

(b)

Figure 6.4 **Changes in normalised shear modulus as a function of shear strain and (a) confining stress and (b) plasticity index (PI)**

The strain-dependent shear modulus then becomes critical when strains above the *elastic threshold* (γ_{lt}) are induced in the material. Hence, it is useful to analyse the strain-dependent shear modulus in terms of factors influencing the *elastic threshold*.

Seed and Idriss (1970) presented research on this topic which illustrated a distinct relationship between the confining stress ($\overline{\sigma_0}'$) and G/G_{max} for sands. This relationship is schematically represented the normalised $G_{max} - \gamma$ relationship in Figure 6.4(a), where it may be observed that at higher confining stress the elastic threshold increases. That is, the relationship between G/G_{max} and γ_c is shifted to the right for increasing confining stress ($\overline{\sigma_0}'$).

A very similar relationship is noted for cohesive materials with regard to the plasticity index. Furthermore, the influence of the confining stress decreases with increasing plasticity for the relationship between shear modulus and shear strain. This relationship may be viewed from the schematic representation in Figure 6.4(b). Note that the behaviour of clays of low plasticity matches closely to that of non-cohesive soils in Figure 6.4(a).

6.4.2 Damping Parameters of Soils

6.4.2.1 Definition

Damping is caused by both geometric dispersion of the wave propagation away from the point source, and by internal hysteretic damping, or material damping, within the soil as it undergoes plastic deformation (Hoadley, 1984). The damping of the system is defined as the summation of the material and geometric counterparts (also known as hysteretic and radiation damping, respectively) the influences of which vary with the respective modes of vibration. Material damping plays a significant role for rocking modes of vibration and geometric damping is the major contributing factor under translation (Ambrosini, 2006). For wind turbines and other tall slender structures, the coupling of rocking and horizontal translation modes of vibration is predominant, and therefore the characteristics of geometric and material damping are important in assessing the dynamic response of the structure and the associated degradation of stiffness (Chowdhury and Dasgupta, 2009).

The area within the hysteretic loop, developed from the shear stress-strain behaviour of the respective soil under cyclic loading, represents the amount of energy absorbed by the soil during its deformation, and therefore is a measure of a soil‘s material, or internal hysteretic, damping characteristics. This is defined by Eqn. 6.14, where A_{loop} is defined as the area of the hysteresis loop and A_Δ is the area of the triangle OAB in Figure 6.3(b).

$$\zeta = \frac{A_{loop}}{4\pi A_\Delta} \qquad \textit{Eqn. 6.14}$$

At very low strain amplitudes the soil is essentially a linear elastic material, and hence the shear modulus is equal to G_{max}. At this level of shear strain (approximately 10^{-6}–10^{-3}) no material damping takes place because the elastic threshold of the material has not been exceeded. In physical terms, no

frictional losses through grain slippage, yielding or crushing have taken place (Winkler et al., 1979). Upon the application of loading cycles the strain amplitude is increased and hence the shear modulus decreases and the magnitude of hysteretic damping increases. Hence, ζ_{max} in Eqn. 6.15 denotes the maximum damping ratio which occurs when $G \approx 0$. This relationship is illustrated by Figure 6.5 and may be defined by a hyperbolic relationship as follows (Hardin and Drnevich, 1972):

$$\zeta = \zeta_{max}\left(1 - \frac{G}{G_{max}}\right) \qquad \textit{Eqn. 6.15}$$

Strain-based formulations are also available for the estimation of ζ, such as (Karl, 2005):

$$\frac{\zeta}{\zeta_{max}} = \frac{\gamma}{\gamma_r}\left(\frac{1}{1+\frac{\gamma}{\gamma_r}}\right) \qquad \textit{Eqn. 6.16}$$

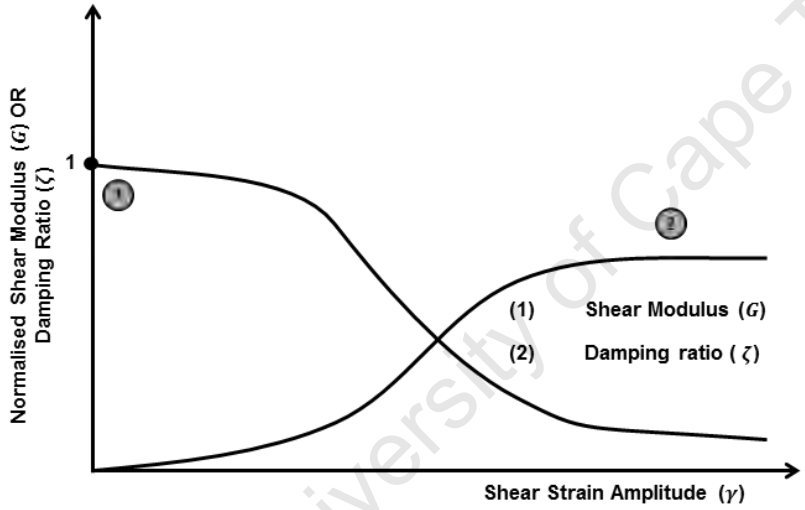

Figure 6.5 **Relationship between shear modulus and damping ratio as a function of shear strain**

6.4.2.2 Geotechnical Parameters Affecting Damping Properties

The material damping properties of a soil, in practice, are difficult to accurately determine as they depend on a wide range of parameters. For this reason, the modelling of the material damping processes such as heat generation, friction and plastic yielding, is normally done by lumping the various parameters together. According to Hoadley (1984) the key influencing parameters that govern the damping of cohesionless soils may be narrowed down to the cyclic shear strain (γ_c) and the number of loading cycles (N). Whereas, for cohesive soils the frequency of loading (f) and the mean effective principle confining stress ($\overline{\sigma_0}'$) present in the soil play the most crucial role (Priest, 2012).

The reason behind this was due to the reducing likelihood of slippage between particles as σ_0' increases, while at higher strain the shear stress between particles is higher which induces more frictional loss through crushing. Parallel to this theory is the influence of angularity on damping – increased angularity leads to reduced damping.

Table 6.5 **General Influence of Increasing Parameters on Damping Characteristics (ζ)**

Parameter		ζ
Mean effective stress, σ_0'	↑	↓
Void ratio, e	↑	↓
Plasticity index, PI	↑	↓
Strain amplitude	↑	↑
Cementation	↑	↓
Geological age	↑	↓

6.5 WAVE PROPAGATION

Based on the behaviour of wind turbine foundations being restricted to very small and small shear strain ranges, the theory of wave propagation, and the subsequent elastic relations, is relevant and especially beneficial. A time varying force applied to a soil mass induces a seismic wave within the soil. Seismic waves are defined as the transfer of energy by means of particle motion, and are characterised with respect to the type of motion induced within the medium (Lippus, 2007). The induced motion occurs under constant phase and in three-dimensions. There are two broad categories of stress waves (1) body waves and (2) surface waves. Body waves propagate in all directions and surface waves propagate along the surface of the body. Body waves are more applicable to foundation design at low-levels of shear strain, whereas surface waves involve greater amounts of energy.

6.5.1 Body Waves

6.5.1.1 Compression Waves

Compression waves are characterised by a lengthwise deformation parallel to the axis of propagation. This leads to periodic changes in the volume of the soil through compression and dilation, as illustrated by Figure 6.6(a). The compression wave is also known as the primary, or p-wave, as it has the highest velocity of the body waves. Eqn. 6.17 defines the velocity of the compression wave, v_p, which is governed by the bulk modulus, K, the shear modulus, G, and the density of the material, ρ.

$$v_p = \sqrt{\frac{K + \frac{4G}{3}}{\rho}} \qquad \textit{Eqn. 6.17}$$

The bulk modulus is a measure of a material's resistance to compression, whereas the shear modulus is synonymous with a material's ability to resist shear and therefore is indicative of rigidity. Thus, the presence of pore water distorts the actual v_p of the material due to the relative incompressibility of water.

6.5.1.2 Shear Waves

Shear waves, also known as secondary or s-waves, due to their lower velocity relative to p-waves, are defined by deformation orthogonal to the axis of stress wave propagation, as illustrated by Figure 6.6(b). Unlike p-waves, s-waves are not affected by the presence of pore water, because water cannot resist shear forces. Hence, the shear wave velocity, v_s, is a function of the soil structure alone, as defined by Eqn. 6.18.

$$v_S = \sqrt{\frac{\rho}{G_{max}}} \qquad \textit{Eqn. 6.18}$$

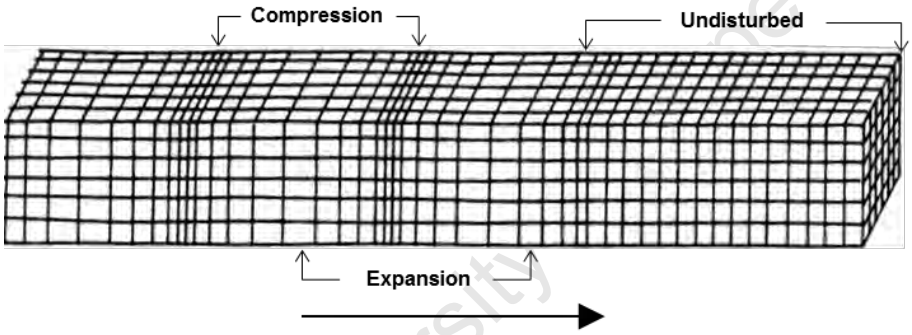

(a)

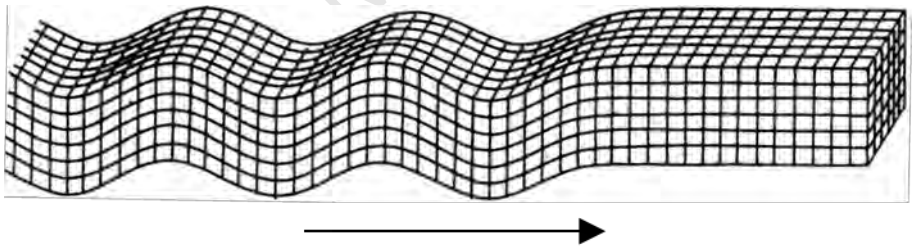

(b)

Figure 6.6 **Seismic body waves: (a) compression/primary/p-waves and (b) shear/secondary/s-waves**

6.5.2 Surface Waves

6.5.2.1 Rayleigh Waves

Rayleigh waves are a form of surface wave which involve elliptical motions in the vertical plane of the soil body as a result of the superposition of p- and vertical s-waves. This is schematically shown in Figure 6.7(a). Rayleigh waves have gained importance in recent years as their measurements can be undertaken without the need for intrusive investigations – such as those required by s- and p-wave investigations. Rayleigh waves travel slower than shear waves and attenuate at a rate of $1/\sqrt{r}$ where r is the distance from the source. These factors make Rayleigh waves particularly attractive for seismic surveys as strong distinguishable signals may be obtained.

However, there is no direct link between Rayleigh wave velocities and soil stiffness (E or G), but their velocity have been empirically linked back to the shear wave velocity, as a function of Poisson's ratio (Priest, 2012) and subsequently found to be insensitive to changes in ν (Richart et al., 1970):

$$\frac{v_R}{v_S} = \frac{0.874 + 1.117\nu}{1 + \nu} \qquad \textit{Eqn. 6.19}$$

$$v_S \approx 1.09 v_R \qquad \textit{Eqn. 6.20}$$

Therefore, Rayleigh wave velocity, v_R, may be used to give close approximations to v_s and hence G_{max}.

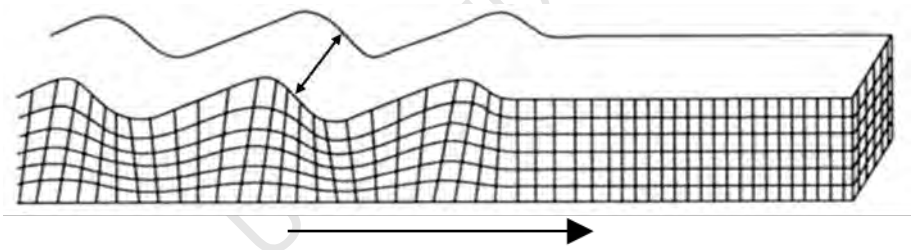

(a)

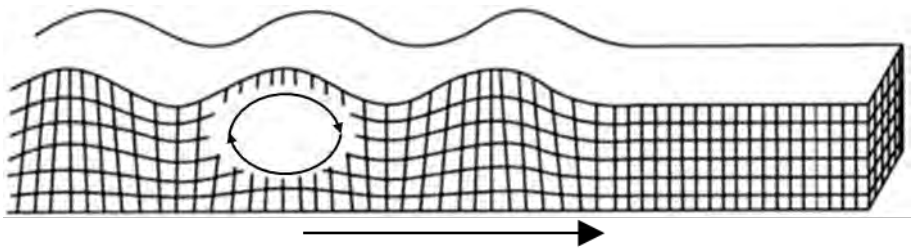

(b)

Figure 6.7 **Seismic surface waves: (a) Rayleigh waves and (b) Love waves**

6.5.2.2 Love Waves

Love waves result from the interference of two horizontal s-waves and gains its name from A. E. H. Love, who first described the phenomenon in 1908. This interference causes polarised shear waves on the surface of the media which is characterised by horizontal motion perpendicular to the direction of propagation, as depicted in Figure 6.7(b). The amplitude of motion generally reduces rapidly with depth. Furthermore, the amplitude of motion decays more slowly than body waves, with respect to the distance from the source, making Love waves the most significant contributor to earthquake damage.

Thus, the seismic design of wind turbine foundations would have to account for this type of seismic wave, and its highly non-linear characteristics.

The relationships governing the velocity of seismic waves propagating through elastic media are fundamental to the determination of G_{max}. Firstly, it is practically impossible to measure shear strain accurately at very low levels, hence wave propagation theory provides a foundation upon which elastic properties may be determined without having to measure the shear stress-strain relationship directly. Secondly, because seismic geophysical tests methods induce very low levels of shear strain, the shear wave velocity may be used to determine G_{max}, assuming an *equivalent linear model*. Hence, the following relationship is relevant:

$$G_{max} \equiv \mu_{max} = \rho {v_S}^2 \qquad \textit{Eqn. 6.21}$$

6.6 SUMMARY

The application of dynamic loads to foundation-soil systems induces strains that are generally much lower than the strains experienced from most static loads. What is critical is the frequency of loading and number of stress cycles, as these factors influence the stiffness of the system over an extended period of time. Wind turbine foundations are subjected to a range of dynamic loads, ranging from impulsive to cyclic and fatigue related. Impulse loads are generally critical to the stability of the system whereas cyclic loads are detrimental to the fatigue life of the foundation. Adverse effects of long-term ground vibrations may include differential settlement, cracking of foundation bases, redistribution of bearing stresses and changes in natural frequency. These effects are also inter-related. Thus wind turbine manufacturers specify strict limits on foundation stiffness to ensure foundation longevity.

The ground vibrations induced by wind were deemed to lie in the elastic and elasto-plastic range, meaning that the soil may be modelled as a linear elastic material. This renders the shear modulus, G, Poisson's ratio, ν, and damping ratio, ζ, the fundamental parameters describing the foundation response.

The following points regarding these parameters and their use are critical:

1. The shear modulus and damping of soils are affected principally by the shear strain amplitude. For granular soils the effective mean confining pressure, $\overline{\sigma_0}'$, and void ratio, e, play the most significant part in characterising soil stiffness. The stiffness of cohesive materials is based mainly on OCR and time of confinement, t.
2. The material damping was shown to increase with the shear strain induced in the material, due to plastic deformation. Geometric damping was not explored in this chapter due to its dependency on the stiffness-mass relationships explored in Chapter 7. Material damping was shown to be a function of σ_0' and e and was also modelled as a hyperbolic function to show its variation with the shear modulus.

Several theoretical correlations between the above-mentioned parameters, shear modulus and damping ratio have been developed. These correlations serve a useful purpose in that they display the key variables affecting each dynamic parameter, respectively, and in doing so enable parametric studies to be undertaken during the design phase. However, by no means should these correlations be used to substitute the measured values of each parameter.

Lastly, the relationship between wave propagation theory and elastic moduli was explored, where the following expression was deemed highly beneficial for the quantitative assessment of dynamic foundation response:

$$G_{max} \equiv \mu_{max} = \rho {v_S}^2$$

The following chapter applies the afore-mentioned concepts to the quantitative prediction of foundation response to dynamic loading. This is followed by the measurement of the soil stiffness and the damping properties of soils.

7. ANALYSIS OF FOUNDATIONS UNDER DYNAMIC LOADS ON ELASTIC MEDIA

7.1 INTRODUCTION

The design of foundations for dynamic loads was originally done based on increasing the mass of the foundation, or increasing the stiffness of the founding soil by means of piles. This procedure was found to work adequately, but often resulted in significant over-designs (Bowles, 1996). These early procedures also reduced the resonant frequency of the foundation and effective damping (Gazetas, 1983), both of which are undesirable consequences for wind turbine foundations. As previously shown, the natural frequency of the tower-foundation system must not intersect the relatively low 1P frequency of the turbine. Thus, the efficiency of designs for foundations under dynamic loads has been improved by the development of vibration analysis theories which occurred during the 20th century.

The study of the analysis and design of footings under dynamic loading dates back to the classic study by Lamb in the early 1900s. Lamb's paper formed the cornerstone of theoretical solutions to the displacement of an oscillator resting on the surface of a homogeneous, isotropic, elastic semi-infinite body – known as an *elastic half-space* herein. This study, termed the *dynamic Boussinesq loading*, formed a basis upon which further studies on the topic were conducted. The work of Reissner in the 1930s addressed the influence of soil properties on the response of a vertically oscillating foundation. Again, this study assumed the foundation to be placed within an elastic half-space characterised by the shear modulus, G, and Poisson's ratio, υ and the unit weight of the material, γ. Reissner's work is considered the classical solution to the foundation on an elastic half-space theory. The research by Lamb and Reissner was subsequently expanded upon.

This body of knowledge stemmed from the following expression for the vertical displacement of a circular footing on an *elastic half-space*, devised by Reissner, and later expanded upon by Quinlan and Sung:

$$z_0 = \frac{Q_0 e^{i\omega t}}{Gr}(f_1 + if_2) \qquad \textit{Eqn. 7.1}$$

where

- Q_0: amplitude of applied force,
- ω: frequency of force application,
- G: the shear modulus,
- r: the radius of foundation
- $f_1; f_2$ are Reissner's —displacement functions".

The summary of major contributions to this theory are summarised in Table 7.1.

Table 7.1 **Summary of significant contributions to the vibration analysis of foundations**

Author(s)	Year	Contribution
Lamb	1904	Solution for concentrated vertical force on surface of half space (Dynamic Boussinesq Problem).
Reissner	1936	Solution for flexible circular foundation assuming uniform load.
Quinlan	1953	Approximate solution for rigid circular foundation assuming static pressure distribution.
Sung	1953	Solutions for various assumed pressure distributions.
Bycroft	1956	Simplified solution by averaging displacements over foundation area.
Hsieh	1962	Introduced idea of frequency-dependent equivalent spring and dashpot. Obtained exact frequency-dependent spring dashpot for rigid circular foundation using computer.
Lysmer and Richart	1966	Proposed approximate frequency-independent spring and dashpot as simplified solution for engineers (*Lysmer's Analog*).
Richart and Whitman	1967	Validated *Lysmer's Analog* with field footing vibration tests.
Whitman and Richart	1967	Design procedure based on *Lysmer's Analog*.

The efforts of all these researchers cannot be ignored in the discussion of foundations under dynamic loads, as they all significantly evolved the analytical study of this problem. However, one may refer to Richart, Hall, and Woods (1970) for specific mathematical treatments and explanations, as these fall outside of the scope of this chapter. Rather, this chapter has focused on the use of the culmination of this research – the *elastic half-space analog*, otherwise known as *Lysmer's Analog*.

Before *Lysmer's Analog*, is explored, elements of vibration theory using the lumped parameter model (defined in §2.4.4.3) are introduced to form the theoretical background to the subsequent sections.

7.2 DIFFERENTIAL EQUATIONS GOVERNING VIBRATORY RESPONSE

Vibrations are time-varying the response of a system to a dynamic load, and they may take on one, or a combination, of the modes defined in Table 7.2. These six modes of vibration include translations along the x, y and z axes, as well as rotations about the x, y and z axes. Rotations about the x- and y-axes are generally accompanied by translations along the x- and y-axes, respectively.

Table 7.2 **Governing equations for vibration of foundations**

Mode of Vibration	Governing Equation	
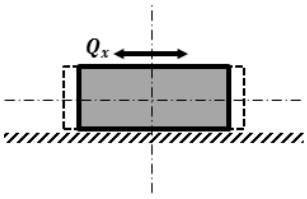	Horizontal oscillation (along x-axis) $m\ddot{x} + c_x\dot{x} + k_x x = Q(t)$	*Eqn. 7.2*
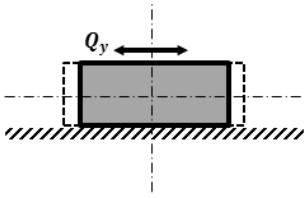	Horizontal oscillation (along y -axis): $m\ddot{y} + c_y\dot{y} + k_y y = Q(t)$	*Eqn. 7.3*
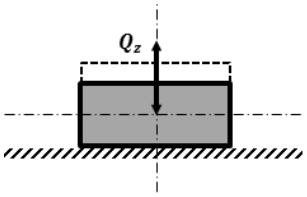	Vertical oscillation (along z-axis): $m\ddot{z} + c_z\dot{z} + k_z z = Q(t)$	*Eqn. 7.4*
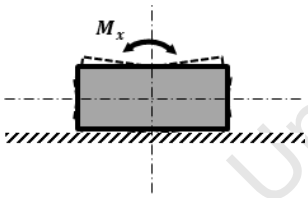	Rocking oscillation (about x-axis): $I_\varphi\ddot{\varphi} + c_{\varphi x}\dot{\varphi} + k_{\varphi x}\varphi = M_x(t)$	*Eqn. 7.5*
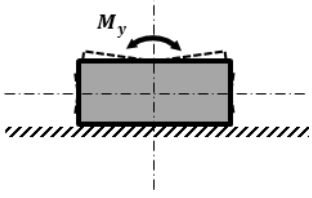	Rocking oscillation (about y-axis): $I_\varphi\ddot{\varphi} + c_{\varphi y}\dot{\varphi} + k_{\varphi y}\varphi = M_y(t)$	*Eqn. 7.6*
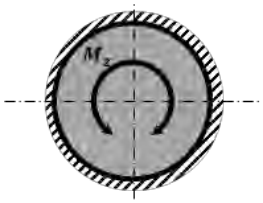	Torsional oscillation (about z-axis): $I_\psi\ddot{\psi} + c_{\psi x}\dot{\psi} + k_{\psi z}\psi = M_z(t)$	*Eqn. 7.7*

The parameters governing the vibratory response are defined as follows:

- I_ψ and I_φ denote the mass moment of inertia of the foundation about the corresponding axis of rotation;
- φ and ψ are the angles of rotation;
- c_z, c_x, c_y, $c_{\varphi x}$, $c_{\varphi y}$ and $c_{\psi x}$ are the damping coefficients for the respective modes of vibration;
- k_z, k_x, k_y, k_φ and k_ψ denote the spring constant for each mode of vibration, and;
- m is the sum of the mass of the foundation and static load transferred to the foundation.

The case of vertical oscillations is used to introduce elements of vibration theory pertinent to any vibration response. This is done with the use of a single degree of freedom (SDOF) lumped parameter model in the following section.

7.3 STEADY STATE RESPONSE TO SINUSOIDAL FORCING

7.3.1 Constant Amplitude Forcing

A lumped mass SDOF model for a footing on a soil is depicted by Figure 7.1. The soil is defined by the viscous damping coefficient, c_z, and stiffness of k_z, where the subscript z defines the properties for the z-direction only. A harmonic force $Q(t)$ is applied to the footing. This is the simplest form of dynamic loading, and is used to approximate the periodic loading generated by machinery. Q_0 denotes the amplitude of the force, ω the frequency of the force and t time. The equilibrium point about which the foundation would oscillate when subjected to a dynamic load is defined by z_s, the static deflection:

$$z_s = \frac{m}{k_z} \qquad \textit{Eqn. 7.8}$$

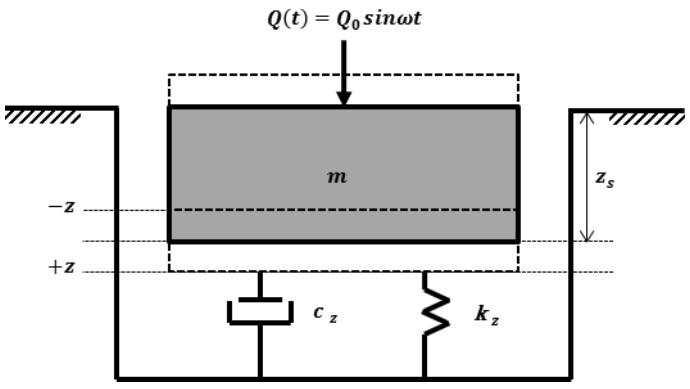

Figure 7.1 **Lumped parameter SDOF foundation model under vertical oscillation**

Now, the equation of motion governing the response to forced harmonic loading is defined as:

$$m\ddot{z} + c_z\dot{z} + k_z z = Q_0\, sin(\omega t) \qquad \textit{Eqn. 7.9}$$

Where $\dot{z}$ and $\ddot{z}$ represent the first and second derivatives of displacement with respect to time, respectively. Fundamental elements of vibration theory were defined in §2.4.4.3, including:

1. the undamped natural frequency of the system, ω_n;
2. the critical damping coefficient, $c_{z,c}$;
3. the damping ratio, ζ_z, and;
4. the frequency ratio, β.

These terms may be derived from first principles using a SDOF foundation model under free vibration, as conventionally shown in structural dynamics text books, such as, Bowles (1996), Chopra (1995), Clough & Penzien (1995) and Irvine (1986). Eqn. 7.9 may be re-written, using these relationships, as:

$$\ddot{z} + 2\zeta_z {\omega_n}^2 \dot{z} + {\omega_n}^2 z = \frac{Q_0}{m} sin(\omega t) \qquad \textit{Eqn. 7.10}$$

This is a second order differential equation, whereby the complementary and particular solutions are of the following form, respectively:

$$z_c(t) = e^{-\zeta_z \omega_n t}[C_1 cos\omega_d t + C_2 sin\omega_d t] \qquad \textit{Eqn. 7.11}$$

$$z_p(t) = C_3 cos\omega t + C_4 sin\omega t \qquad \textit{Eqn. 7.12}$$

C_i denotes constants of differentiation and ω_d is the damped natural frequency. The definition of ω_d is dependent on the relationship between the damping coefficient of the soil and the mass and stiffness properties of the system. For an underdamped system (which is almost always the case in practice) the damped natural frequency is given as:

$$\omega_d = \sqrt{-1}\sqrt{\frac{k_z}{m} - \left(\frac{c_z\omega_n}{c_{z,c}}\right)^2} = \sqrt{-1}\sqrt{\frac{k_z}{m} - \frac{{\zeta_z}^2 {k_z}^2}{m^2}} = \omega_n\sqrt{1 - {\zeta_z}^2} \qquad \textit{Eqn. 7.13}$$

This was derived from the solution to a system under free vibration, where it may be shown that distinctly different types of behaviour may occur depending on the nature of the damping present in the system.

Now, upon differentiation of $z_p(t)$ and substitution into the equation of motion, the coefficients, C_3 and C_4 may be determined:

$$C_3 = \frac{Q_0}{k_z} \cdot \frac{-2\zeta_z\beta}{(1-\beta^2)^2 + (2\zeta_z\beta)^2} \qquad \textit{Eqn. 7.14}$$

$$C_4 = \frac{Q_0}{k_z} \cdot \frac{1-\beta^2}{(1-\beta^2)^2 + (2\zeta_z\beta)^2} \qquad \textit{Eqn. 7.15}$$

These terms are used to define the steady state harmonic response of the system. Note that the complete solution to the equation of motion also includes the transient response. However, this is ignored herein due to it damping out relatively soon after load application, and hence having little effect on the overall response (Irvine, 1986). The steady state response is:

$$z(t) = A_z sin\,(\omega t - \theta) \qquad \textit{Eqn. 7.16}$$

Where, the amplitude of steady vertical vibration, A_z, and the phase angle, θ, are given by:

$$A_z = \frac{Q_0}{k_z} \cdot \frac{1}{\sqrt{(1-\beta^2)^2 + (2\zeta_z\beta)^2}} \qquad \textit{Eqn. 7.17}$$

$$\theta = arctan\left(\frac{2\zeta_z\beta}{1-\beta^2}\right) \qquad \textit{Eqn. 7.18}$$

Note that the response of a dynamically loaded damped system is out of phase with the loading frequency. This lag is given by the phase angle, which is limited to the range $0 < \theta < \pi$ (rad). Of particular interest is the ratio between the resultant harmonic response and the static dynamic displacement that a static force of magnitude Q_0 would produce. This ratio is termed the *dynamic magnification factor*, D, and is defined by Eqn. 7.19.

$$D = \frac{A_z}{Q_0/k_z} = \frac{1}{\sqrt{(1-\beta^2)^2 + (2\zeta_z\beta)^2}} \qquad \textit{Eqn. 7.19}$$

The response curves for constant-force-amplitude excitation are given by Figure 7.2. Upon close inspection of these curves it is noticeable that the maximum dynamic magnification does not occur at $\beta = 1$. That is, due to the relationship between damping, stiffness and mass the dyanamic magnification at $\beta = 1$ is not maximum, but rather defined as follows:

$$D_{\beta=1} = \frac{1}{2\zeta_z} \qquad \textit{Eqn. 7.20}$$

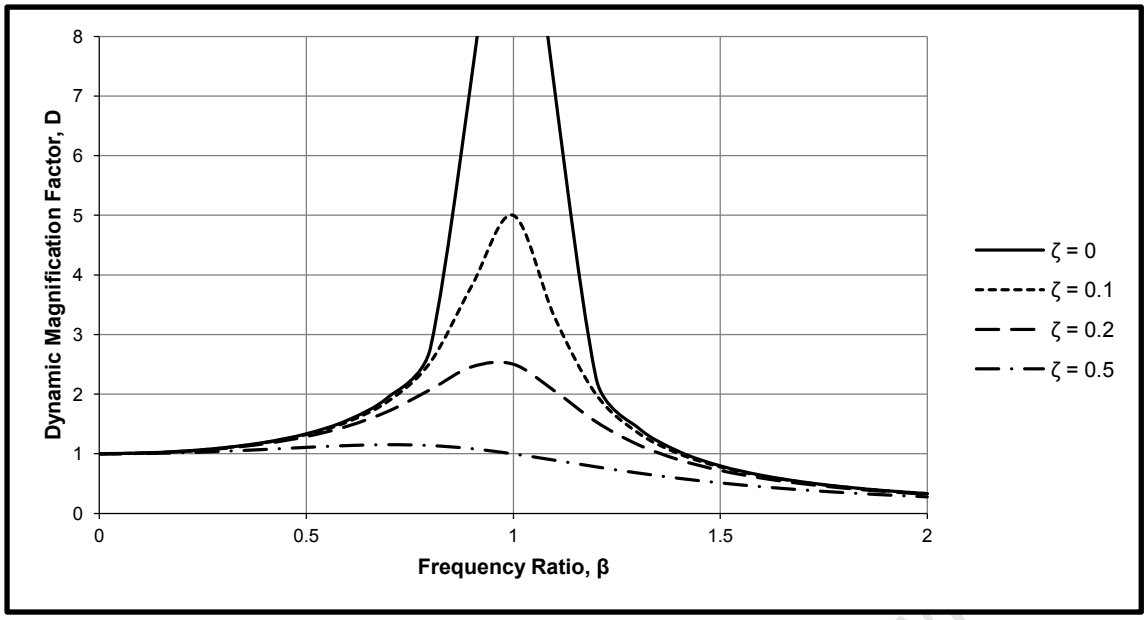

Figure 7.2 **Response of SDOF system to constant amplitude excitation force**

Now, to determine D_{max} derivative $\frac{d\beta}{dD}$ must be set equal to zero and solved in terms of β. This process yields:

$$\beta_{max} = \sqrt{1 - 2{\zeta_z}^2} \qquad \textit{Eqn. 7.21}$$

β_{max} is then substituted into Eqn. 7.19 to define the maximum dynamic magnification factor:

$$D_{max} = \frac{1}{2\zeta_z\sqrt{1 - {\zeta_z}^2}} = \frac{1}{2\zeta_z}\frac{\omega_n}{\omega_d} \qquad \textit{Eqn. 7.22}$$

The angular and cyclic frequency at which the dynamic magnification factor is a maximum are defined as, respectively, as follows (Clough and Penzien, 1995):

$$\omega_m = \omega_n\sqrt{1 - 2{\zeta_z}^2} \qquad \textit{Eqn. 7.23}$$

$$f_m = \frac{\omega_m}{2\pi} = f_n\sqrt{1 - 2{\zeta_z}^2} \qquad \textit{Eqn. 7.24}$$

The resonant frequency may be interpreted as the sinusoidal forcing frequency that produces the maximum dynamic amplification, with respect to the system stiffness, mass and damping characteristics. Therefore, this is the frequency that should be avoided during the design phase, either by tuning the forcing frequency or adjusting the stiffness, mass and damping relationships. In practical terms, the stiffness is the principal parameter that may be adjusted.

7.3.2 Rotating Mass Excitation (Frequency Dependent Amplitude Exciting Force)

Relevant to wind turbine foundation design and machine foundations in general, is the theory pertaining to rotating mass excitation. Figure 7.3 illustrates a conceptual view of the problem, whereby the lumped mass parameter, m, is attached to a rotating shaft of length $\bar{y}$. The mass M is the total mass of the system/structure, including the eccentric mass m.

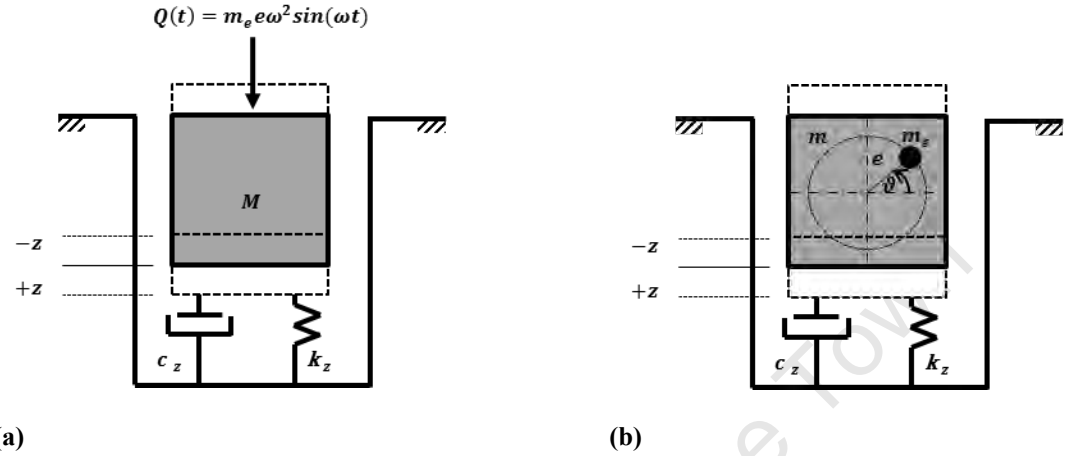

(a) **(b)**

Figure 7.3 **Lumped parameter SDOF model: (a) rotating mass and (b) equivalent SDOF system under vertical oscillation**

The position of the rotating mass at any time, t, may be defined in terms of its vertical displacement as $z(t) = esin(\vartheta) = esin(\omega t)$. Note that ω denotes the frequency at which the mass rotates. Now, taking the sum of forces in the z-direction, incorporating Newton's second law of motion yields the following:

$$(M - m)\ddot{z} + m(\ddot{z} - e\omega^2 sin(\omega t) + c\dot{z} + kz = 0 \qquad \textit{Eqn. 7.25}$$

Rearrangement of the above expression defines the equivalent excitation force to be:

$$Q(t) = me\omega^2 sin\,(\omega t) \qquad \textit{Eqn. 7.26}$$

Similar to the constant harmonic forcing excitation case, the steady state response is of primary concern, and is of the same form. The amplitude of vibration for a frequency dependent sinusoidal force is:

$$A_z = \frac{me\omega^2}{k_z}\frac{1}{\sqrt{(1-\beta^2)^2 + (2\zeta_z\beta)^2}} \qquad \textit{Eqn. 7.27}$$

The dynamic amplification factor follows on from this to be:

$$D = \frac{A_z}{Q_0/k_z} = \frac{me\omega^2}{M{\omega_n}^2} = \frac{\beta^2}{\sqrt{(1-\beta^2)^2 + (2\zeta_z\beta)^2}} \qquad \textit{Eqn. 7.28}$$

The maximum dynamic magnification factor, D_r, and the resonant frequency, $f_{m,r}$, may be defined as follows, using the same procedure as before:

$$f_{m,r} = \frac{\omega_m}{2\pi} = \frac{1}{f_n\sqrt{1-2{\zeta_z}^2}} \qquad \textit{Eqn. 7.29}$$

$$D_{r,max}(\beta_{max}) = \frac{1}{2\zeta\sqrt{1-2{\zeta_z}^2}} \qquad \textit{Eqn. 7.30}$$

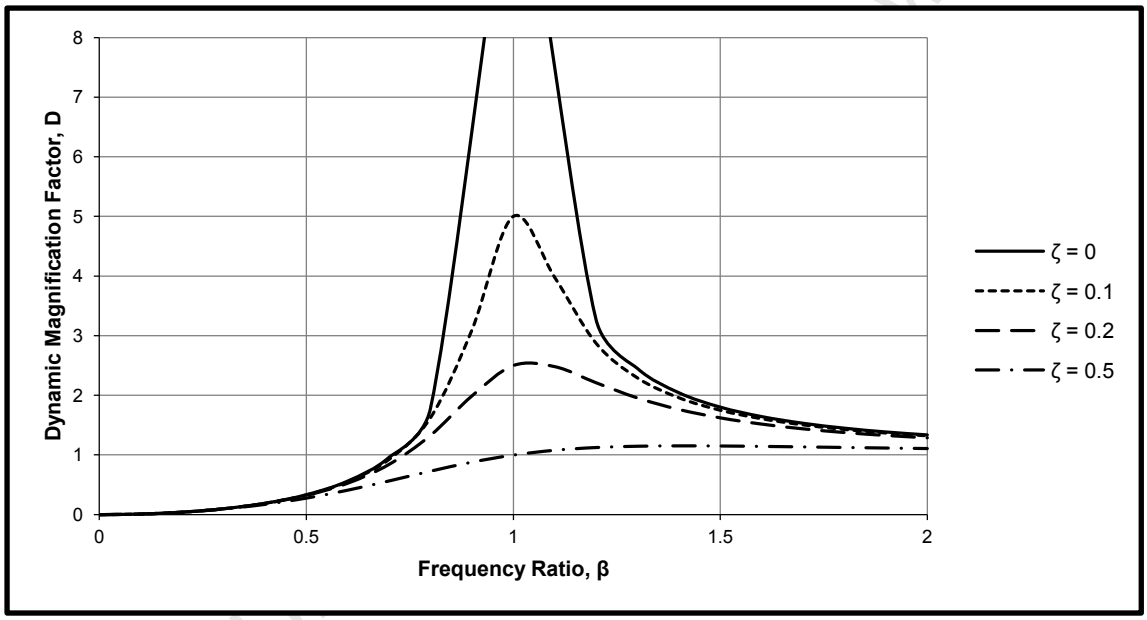

Figure 7.4 **Response of SDOF system to variable amplitude excitation force**

A key aspect to the behaviour of the relationship depicted in Figure 7.4 is that as the frequency increases the amplitude of vibration tends to $(me)/M$. That is, as $\beta \to \infty$, $D \to 1$. This behaviour is fundamental to foundation response, as it is linked to the concept that, if unrestrained, a rotating mass will rotate about its centre of gravity. Thus, it is this concept upon which mass is added to foundations which experience excitations higher than their resonant frequency (Richart et al., 1970). Also, the resonant frequency occurs above the undammed natural frequency (equivalent to $\beta = 1$), whereas the case of a constant force excitation results in the peak response being slightly below $\beta = 1$.

7.3.3 Vibration Transmission and Isolation

The preceding sections have addressed the theory pertaining to the dynamic loading of structural systems, with focus on foundations undergoing vertical vibration. The resultant force transmitted to the supports is of specific interest in foundation design. A system exhibiting a steady state response to a constant amplitude excitation transmits a force, Q_t:

$$Q_t(t) = c_z\dot{z}(t) + k_z z(t) \qquad \textit{Eqn. 7.31}$$

The steady state response was defined follows:

$$z(t) = A_z \cdot sin(\omega t - \theta) = \frac{Q_0}{k_z}\frac{1}{\sqrt{(1-\beta^2)^2 + (2\zeta_z\beta)^2}} \cdot sin(\omega t - \theta) \qquad \textit{Eqn. 7.32}$$

Hence,

$$\dot{z}(t) = \frac{\omega Q_0}{k_z}\frac{1}{\sqrt{(1-\beta^2)^2 + (2\zeta_z\beta)^2}} \cdot cos(\omega t - \theta) \qquad \textit{Eqn. 7.33}$$

Eqn. 7.32 and Eqn. 7.33 are then substituted into Eqn. 7.31 and rearranged, using trigonometric identities, to produce Eqn. 7.34. This is then expanded to form Eqn. 7.35:

$$Q_t = A_z[k_z sin(\omega t - \varphi) + c_z\omega\, cos(\omega t - \varphi)] = A_z k_z\sqrt{1 + (2\zeta_z\beta)^2} \qquad \textit{Eqn. 7.34}$$

$$Q_t = \frac{Q_0}{k_z} \cdot \frac{k_z\sqrt{1 + (2\zeta_z\beta)^2}}{\sqrt{(1-\beta^2)^2 + (2\zeta_z\beta)^2}} \qquad \textit{Eqn. 7.35}$$

The transmissibility index, T_r, is defined as the ratio of the amplitude of the transmitted force to the applied excitation amplitude, as follows:

$$T_r = \frac{Q_t}{Q_0} = \frac{\sqrt{1 + (2\zeta_z\beta)^2}}{\sqrt{(1-\beta^2)^2 + (2\zeta_z\beta)^2}} \qquad \textit{Eqn. 7.36}$$

The transmissibility index is plotted with respect to the frequency ratio in Figure 7.5. This relationship illustrates that $T_r \geq 1$ when $0 \leq \beta \leq \sqrt{2}$ and $T_r \geq 1$ when $\beta > \sqrt{2}$.

This shows that although damping reduces the vibration amplitude at all frequencies, it only reduces the force transmitted to the foundations if $\beta > \sqrt{2}$. Thus, to reduce the force transmitted to the foundation the stiffness of the foundation and hence the natural frequency, must be small enough to keep $\beta > \sqrt{2}$.

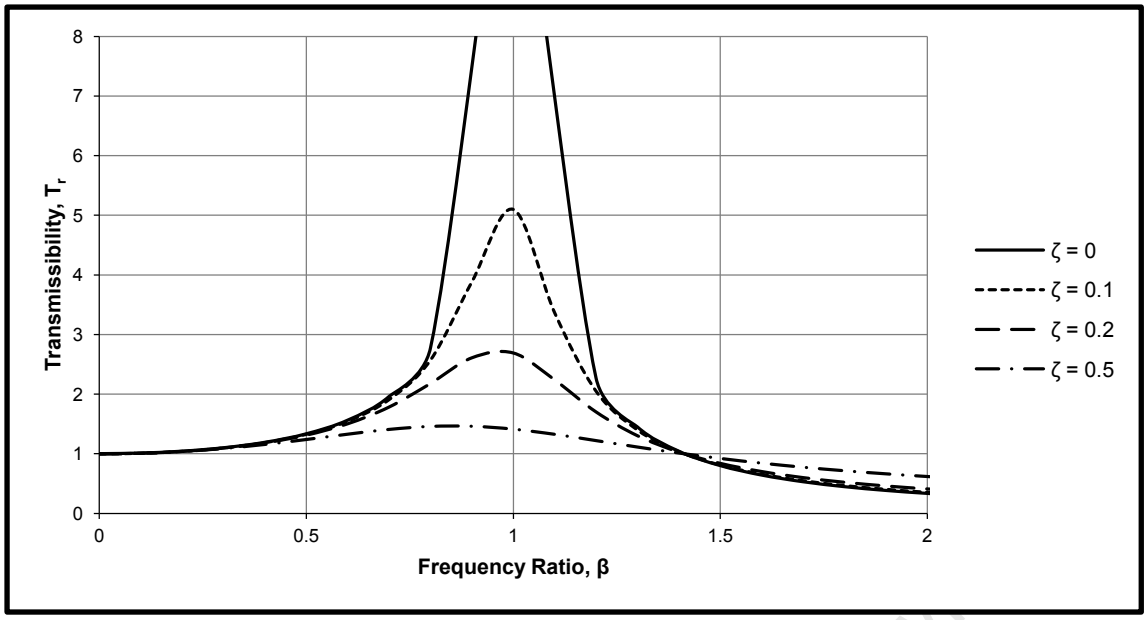

Figure 7.5 **Plot of vibration transmissibility with respect to frequency ratio**

Furthermore, minimal damping is desired in the frequency range $\beta > \sqrt{2}$, because, as illustrated by Figure 7.5, damping increases the force transmitted in this frequency range. Therefore, a compromise between a foundation of low stiffness (low natural frequency) and an acceptable static deflection is required by the designer (Chopra, 1995). If the foundation supports a rotating machine then it is critical to design the foundation to respond satisfactorily over the spectrum of frequencies expected between start-up of the machine and its operating frequency. In this case, the stiffness of the foundation must be traded off against a suitable amount of damping to suppress displacement amplitudes as the machine frequency passes through resonance, but not significant enough to increase the transmissibility at operating frequency.

7.4 ANALYSIS OF DYNAMICALLY LOADED FOUNDATIONS BY ELASTIC HALF-SPACE ANALOG

7.4.1 Vertical Mode of Oscillation

The previous section expressed the relationships between the dynamic response of a foundation and frequency of loading in terms of the parameters ζ and β. However, in practice, the damping ratio is probably the least well understood and ominously difficult to measure accurately. The mass-stiffness relations are therefore the most critical to design. Furthermore, it is a very cumbersome task to determine the exact effect of changes in mass and stiffness from $D - \beta$ curves, such as those presented in Figure 7.2 and Figure 7.4, due to the interrelatedness of mass and frequency.

Lysmer, (1965) separated the effects of mass and frequency in view of developing a more useful means of assessing dynamic response.

This was done in terms of a dimensionless frequency factor, $\bar{a}_0$ and mass factor, $\overline{\boldsymbol{B}}$, given below.

$$\bar{a}_0 = \frac{\omega}{c} \qquad \textit{Eqn. 7.37}$$

$$\overline{\boldsymbol{B}} = \frac{mk}{c^2} \qquad \textit{Eqn. 7.38}$$

The dynamic magnification factor and phase angle for a constant amplitude excitation and a frequency dependent amplitude excitation are now defined in terms of the mass factor and frequency factor:

$$D = \frac{A_z}{\left(\frac{Q_0}{k_z}\right)} = \frac{1}{\sqrt{\left(1 - \overline{\boldsymbol{B}}{\bar{a}_0}^2\right) + {\bar{a}_0}^2}} \qquad \textit{Eqn. 7.39}$$

$$D_r = \frac{A_z}{\left(\frac{Q_0}{k_z}\right)} = \frac{MA_z}{me} = \frac{\overline{\boldsymbol{B}}{\bar{a}_0}^2}{\sqrt{\left(1 - \overline{\boldsymbol{B}}{\bar{a}_0}^2\right) + {\bar{a}_0}^2}} \qquad \textit{Eqn. 7.40}$$

$$tan\varphi = \frac{a_0}{1 - \overline{\boldsymbol{B}}{\bar{a}_0}^2} \qquad \textit{Eqn. 7.41}$$

Lysmer expanded on the mathematical solution presented by Reissner in 1936 by firstly introducing a modified dimensionless mass ratio, $\boldsymbol{B_z}$, which effectively eliminated the influence of Poisson's ratio from Reissner's elastic half-space theory and hence produced a less computational intensive alternative. The fundamental stage in Lysmer's study was finding that the effective damping and spring constant parameters could be expressed as frequency independent values. When the constant expressions for c_z and k_z were substituted into the expressions for the dynamic magnification factors (Eqn. 7.39 and Eqn. 7.40) significant agreement was noted (Richart et al., 1970).

Therefore, the use of the frequency independent stiffness coefficient (Eqn. 7.42) and damping coefficient (Eqn. 7.43) was deemed to pose a negligible influence on the accuracy of the elastic half-space solution, and was rendered to be significantly more practical than the elastic half-space theory (Richart et al., 1970). In doing so, Lysmer established the bridge between half-space theory and the lumped parameter model.

$$k_z = \frac{4Gr}{1 - \nu} \qquad \textit{Eqn. 7.42}$$

$$c_z = \frac{3.4r^2}{(1 - \nu)}\sqrt{\rho G} \qquad \textit{Eqn. 7.43}$$

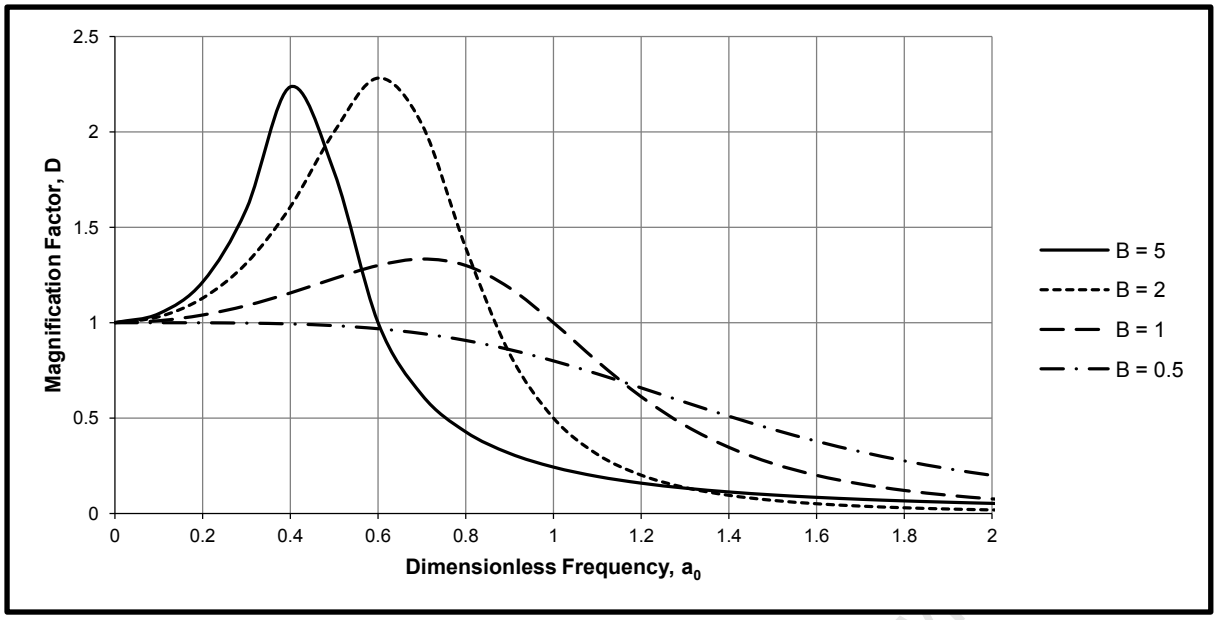

(a)

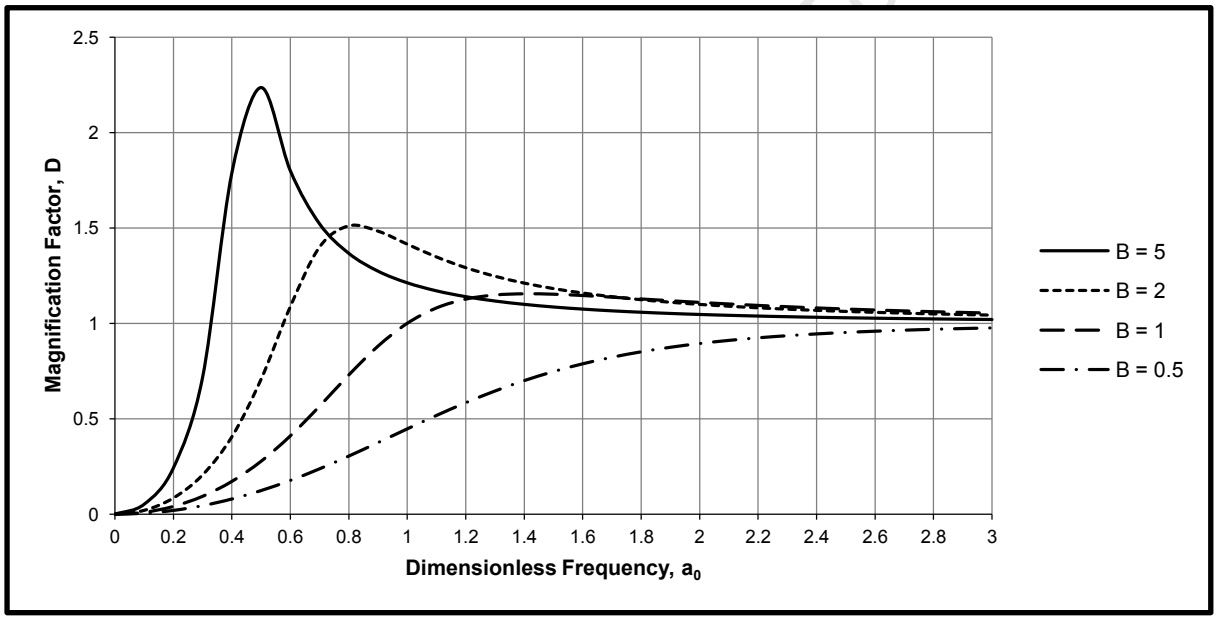

(b)

Figure 7.6 **Response curves for SDOF system with the effects of mass and frequency separated: (a) constant amplitude excitation and (b) frequency dependent amplitude excitation.**

Therefore, the equation of motion may be re-written with respect to *Lysmer's Analog* as:

$$m\ddot{z} + \frac{3.4r^{2}\dot{}}{(1-\nu)}\sqrt{\rho G}\dot{x} + \frac{4Gr}{1-\nu}x = Q(t) \qquad \textit{Eqn. 7.44}$$

The critical damping coefficient and the damping ratio may be defined using the damping coefficient defined by Lysmer:

$$c_{z,c} = 2\sqrt{km} = 2\sqrt{\frac{4Grm}{1-\nu}} \qquad \textit{Eqn. 7.45}$$

$$\zeta_z = \frac{c_z}{c_{z,c}} = \frac{0.425}{\sqrt{\boldsymbol{B_z}}} \qquad \textit{Eqn. 7.46}$$

Where, $\boldsymbol{B_z}$ denotes the modified dimensionless mass ratio:

$$\boldsymbol{B_z} = \frac{1-\nu}{4}\frac{m}{\rho r^3} \qquad \textit{Eqn. 7.47}$$

m is the lumped mass of the system, ρ denotes the density of the soil and r is the radius of the circular footing. Furthermore, $Q(t)$ may be dependent on the frequency of the applied force, such as that of rotating machinery, or of constant force amplitude. The resonant frequency for each case is defined below using the same procedures as §7.3.1 for the constant amplitude and variable amplitude forcing, respectively (Richart et al., 1970).

$$f_m = \frac{1}{2\pi}\sqrt{\frac{k_z}{m}}\sqrt{1-2\zeta_z} = \frac{1}{2\pi}\frac{v_s}{r}\frac{\sqrt{\boldsymbol{B_z}-0.36}}{\boldsymbol{B_z}} \qquad \textit{Eqn. 7.48}$$

$$f_{m,r} = \frac{v_s}{2\pi r}\sqrt{\frac{0.9}{\boldsymbol{B_z}-0.45}} \qquad \textit{Eqn. 7.49}$$

Therefore, the maximum amplitudes of vibration for each loading scenario may be found by substituting the expression for the *Lysmer Analog* damping ratio into Eqn. 7.22 and Eqn. 7.30, respectively to yield the maximum amplitude of vibration for each case:

$$A_{z,max} = \frac{Q_0(1-\nu)}{4Gr}\frac{\boldsymbol{B_z}}{0.85\sqrt{\boldsymbol{B_z}-0.18}} \qquad \textit{Eqn. 7.50}$$

$$A_{z,max,r} = \frac{me}{M}\frac{\boldsymbol{B_z}}{0.85\sqrt{\boldsymbol{B_z}-0.18}} \qquad \textit{Eqn. 7.51}$$

7.4.2 Sliding Mode of Oscillation

The sliding analysis of a circular rigid foundation under vibration is a purely mathematical analysis, as it requires the foundation to undergo translational displacement without rocking. In practice this does not occur, but the solution to this mode of vibration is an important development nonetheless. Similarly to Lysmer, Hall, (1967) defined a modified mass ratio:

$$\boldsymbol{B_x} = \frac{7-8\nu}{32(1-\nu)}\frac{m}{\rho r^3} \qquad \textit{Eqn. 7.52}$$

and in doing so, eliminated the effect of Poisson's ratio. Similarly to *Lysmer's Analog*, Hall was then able to develop frequency independent expressions for the stiffness and damping coefficients, defined as:

$$k_x = \frac{32(1-\nu)}{7-8\nu} Gr \qquad \textit{Eqn. 7.53}$$

$$c_x = \frac{18.4(1-\nu)}{7-8\nu} r^2\sqrt{\rho G} \qquad \textit{Eqn. 7.54}$$

These model constants may be used to develop the horizontal translational equation of motion in the same way as the *Lysmer Analog* was developed. For this reason, this was termed the *Hall Analog*, and like the *Lysmer Analog*, this solution presented sufficiently accurate results and a significantly more practical means of calculation, when compared to the elastic half-space theory (Richart et al., 1970). Therefore, the following parameters may be defined for *Hall's Analog*:

$$\zeta_x = \frac{c_x}{c_c} = \frac{0.288}{\sqrt{\boldsymbol{B_x}}} \qquad \textit{Eqn. 7.55}$$

Where:

$$c_c = 2\sqrt{k_x m} = 2\sqrt{\frac{32(1-\nu)m}{(7-8\nu)} Gr} \qquad \textit{Eqn. 7.56}$$

Using the same method as before, namely substituting the damping ratio for *Hall's Analog* into Eqn. 7.22 and Eqn. 7.30 to yield $D_{x,max}$ and $D_{x,max,r}$. These are subsequently used to define the maximum amplitude of vibration for constant and variable forcing, respectively (Richart et al., 1970):

$$A_{x,max} = \frac{7-8\nu}{32(1-\nu)}\frac{Q_0}{Gr} D_{x,max} \qquad \textit{Eqn. 7.57}$$

$$A_{x,max,r} = \frac{me}{M} D_{x,max,r} \qquad \textit{Eqn. 7.58}$$

7.4.3 Rocking Mode of Oscillation

Hall further developed the analog to account for the rocking mode of vibration for rigid circular foundations. Again, various parameters were defined at the onset to simplify the mathematically rigorous solutions presented by the elastic half-space theory. Firstly, a modified mass ratio was defined, and frequency independent stiffness and damping coefficients were subsequently delineated:

$$\boldsymbol{B_\varphi} = \frac{3(1-\nu)}{8}\frac{I_\varphi}{\rho r^5} \qquad \textit{Eqn. 7.59}$$

$$k_{\varphi x} = \frac{8Gr^3}{3(1-\nu)} \qquad \textit{Eqn. 7.60}$$

$$c_{\varphi x} = \frac{0.8r^4\sqrt{\rho G}}{(1-\nu)(1+\boldsymbol{B_\varphi})} \qquad \textit{Eqn. 7.61}$$

These parameters formed the centre of the *Hall Analog* for the rocking of rigid elastic foundations about the x-axis. Note that the same expressions may be applied to rocking about the y-axis. From these expressions the equation of motion and damping ratio could be expressed in terms of frequency independent stiffness and damping coefficients, respectively:

$$I_\varphi\ddot{\varphi} + \frac{0.8r^4\sqrt{\rho G}}{(1-\nu)(1+\boldsymbol{B_\varphi})}\dot{\varphi} + \frac{8Gr^3}{3(1-\nu)}\varphi = M_x(t) \qquad \textit{Eqn. 7.62}$$

$$\zeta_{\varphi x} = \frac{c_x}{c_c} = \frac{0.15}{(1+\boldsymbol{B_\varphi})\sqrt{\boldsymbol{B_\varphi}}} \qquad \textit{Eqn. 7.63}$$

Where the mass moment of inertia of the footing about the centre of rotation is designated as follows:

$$I_\varphi = \frac{\pi r^2 t_f \gamma}{g}\left(\frac{r^2}{4} + \frac{{t_f}^2}{3}\right) \qquad \textit{Eqn. 7.64}$$

The rocking mode of vibration involves relatively low levels of energy dissipation as the elastic strain energy in the supporting half-space is transferred back and forth between the two halves of the footing under rocking. Therefore, when assessing the amplitude of maximum oscillation, it is sufficient to assume very low levels of damping exist. Thus, the following expression for $D_{\varphi,max}$ assumes the effect of the damped natural frequency on the system to be negligible and the thus maximum response is defined as:

$$D_{\varphi,max} \approx \frac{1}{2\zeta_\varphi} \qquad \textit{Eqn. 7.65}$$

The amplitudes of oscillation may be defined thereafter, as done for the previous modes of vibration.

7.4.4 Torsional Mode of Oscillation

Torsional vibration is the angular vibration of an element due to a torque about the elements longitudinal axis. The technique for assessing rigid circular footings oscillating about a vertical axis was initially developed by Reissner and Sagoci, from Reissner's original elastic half-space theory with subsequent research in the 1940s. Following the same structure as the previous modes, a dimensionless mass ratio was used to eliminate the dependency on Poisson's ratio. For torsional oscillation the mass ratio is:

$$\boldsymbol{B_\psi} = \frac{I_\psi}{\rho r^5} \qquad \textit{Eqn. 7.66}$$

The frequency independent stiffness and damping coefficients were delineated and defined as a function of the torque applied, T_ψ, and angle of rotation, ψ:

$$k_\psi = \frac{T_\psi}{\psi} = \frac{16}{3} G r^3 \qquad \textit{Eqn. 7.67}$$

$$\zeta_\psi = \frac{0.5}{1 + 2\boldsymbol{B_\psi}} \qquad \textit{Eqn. 7.68}$$

Hence, the amplitudes of vibration for each type of excitation are:

$$A_{\psi,max} = \frac{3}{16}\frac{T_\psi}{Gr^3} D_{\psi,max} \qquad \textit{Eqn. 7.69}$$

$$A_{\psi,max,r} = \frac{me\bar{x}}{I_\psi} D_{\psi,max,r} \qquad \textit{Eqn. 7.70}$$

Where $\bar{x}$ denotes the lever arm of the unbalanced mass from the axis of rotation and $T_\psi = me\bar{x}\omega^2$ for rotatory excitation. Unlike the rocking-sliding modes of vibration, torsional vibration is uncoupled and hence may be treated independently of the other modes of vibration. Furthermore, this motion is not influenced by Poisson's ratio and energy is dissipated by propagation of shear waves only (Richart et al., 1970). The effect of geometric damping is very low when compared to other forms of vibration. Damping decreases rapidly with increasing B_ψ.

7.4.5 Coupled Rocking and Sliding

Solutions for the six degrees of freedom have been developed for a rigid circular surface foundation. The analysis of each degree of freedom is hardly ever carried out in practice though, because there is often insufficient information pertaining to loading regimes and material parameters to justify such an analysis, or to render the analysis accurate.

Furthermore, it is often found that vertical and torsional oscillations occur as uncoupled oscillations, whereas, sliding and rocking oscillations normally occur in coupled motion. Therefore, conducting an analysis of a foundation under rocking and sliding is generally done in practice, rather than conducting the analysis for each respective degree of freedom.

To carry out such an analysis the equation of motion must be redefined for rocking with simultaneous horizontal translation of the footing. Firstly, the translation of the base, x_b, and the horizontal force acting at the base of the footing (in terms of the translation) (Richart et al., 1970):

$$x_b = x_g - h_{0\psi} \qquad \textit{Eqn. 7.71}$$

$$P_x = -c\dot{x}_b - k_x x_b \qquad \textit{Eqn. 7.72}$$

Similarly, the expression for the resistance to rocking is given by:

$$R_\psi = -c_\psi \dot{\psi} - k_\psi \psi \qquad \textit{Eqn. 7.73}$$

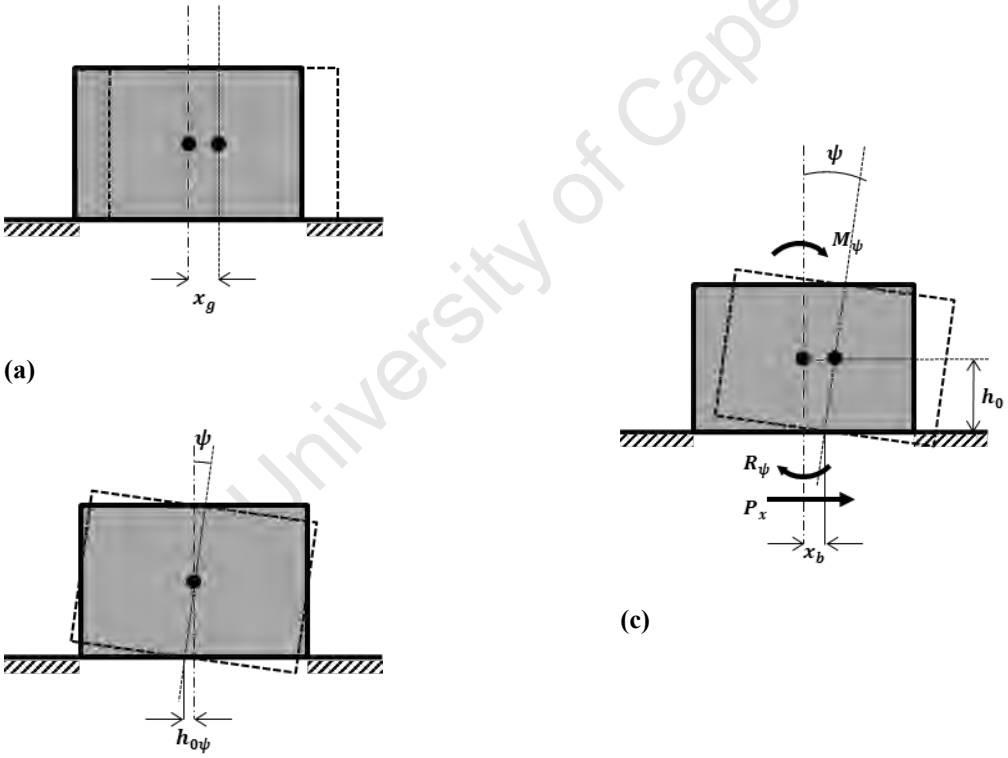

Figure 7.7 **Coupled horizontal translation and rocking oscillation: (a)rocking, (b) sliding and (c) coupled oscillation**

Now, analysing the system from the centre of gravity, one may re-write the equation of motion for horizontal translation of the centre of gravity as:

$$m\ddot{x} = P_x = -c\dot{x}_b - k_x x_b \qquad \textit{Eqn. 7.74}$$

Substituting Eqn. 7.71 into Eqn. 7.74 yields the equation of motion for translation and rotation about the centre of gravity, respectively:

$$m\ddot{x}_g = -c_x\dot{x}_g + k_x x_g - h_0 c_x\dot{\psi} - h_0 k_x\psi = 0 \qquad \textit{Eqn. 7.75}$$

$$I_g\ddot{\psi} = R_\psi + M_\psi - P_x h_0 \qquad \textit{Eqn. 7.76}$$

Now, combining Eqn. 7.72, Eqn. 7.73, Eqn. 7.74 and Eqn. 7.76, and grouping like terms, results in the final equation of motion for coupled rocking and sliding oscillation (Richart et al., 1970):

$$I_g\ddot{\psi} + \left(c_\psi + {h_0}^2 c_x\right)\dot{\psi} + \left(k_\psi + {h_0}^2 k_x\right)\psi - c_x\dot{x}_g h_0 - k_x x_g h_0 = M_\psi \qquad \textit{Eqn. 7.77}$$

A solution to this differential equation may be developed by substituting the following expressions into equations Eqn. 7.75 and Eqn. 7.77. Subsequently, the solution may be analysed with the lumped parameter model.

$$x_g = A_{x1} sin\omega t + A_{x2} cos\omega t \qquad \textit{Eqn. 7.78}$$

$$\psi = A_{\psi 1} sin\omega t + A_{\psi 2} cos\omega t \qquad \textit{Eqn. 7.79}$$

$$M_\psi = M_{\psi 0} sin\omega t \qquad \textit{Eqn. 7.80}$$

7.4.6 Effect of Foundation Embedment

There is significant research confirming that the embedment of foundations improves the soil-foundation response to dynamic loading, particularly with respect to rocking and torsional modes of vibration. However, this is an especially difficult problem to investigate analytically. Currently, FEM techniques are considered to offer the best approximation to the response of an embedded foundation, but still do not capture all the factors and interactions of the real system. Significant work was conducted by researchers such as Novak (Novak and Beredugo, 1971; Novak, 1985) in this area. The material constants developed by these analyses are summarised in Table 7.3 and Table 7.4.

The solutions are based on impedance functions, $\bar{c}$ and $\bar{s}$, which are defined as the ratio between the harmonic forcing (or moments) and the resulting displacement (or rotation), for each respective mode of vibration.

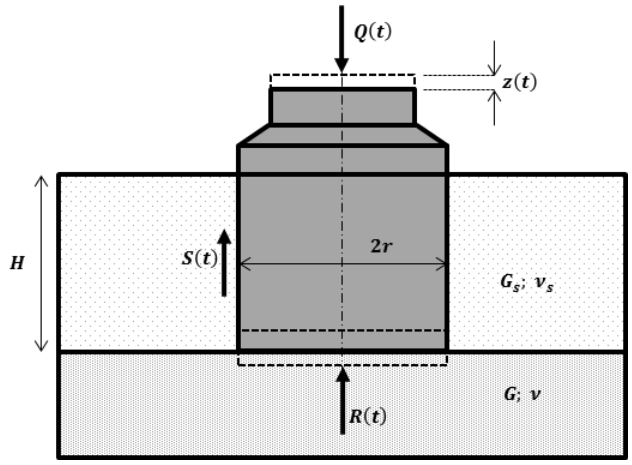

Figure 7.8 **Embedded rigid cylindrical foundation under vertical oscillation**

These factors have been defined for different ranges of a_0 with respect to ν, and may be viewed in texts such as Puri & Prakash (2006). The following stiffness and damping coefficients were developed from Novak and Beredugo's solution for a rigid cylindrical foundation undergoing vertical oscillation.

The equation of motion for this situation is defined as follows, where $R(t)$ and $S(t)$ are the dynamic base and side resistance to vibration, respectively.

$$m\ddot{z}(t) = Q(t) - R(t) - S(t) \qquad \textit{Eqn. 7.81}$$

Table 7.3 **Stiffness parameters for cylindrical embedded foundations (Puri and Prakash, 2006)**

Mode of Vibration	Soil-foundation Stiffness	
Vertical	$k_{ze} = Gr\left[\bar{c}_{z1} + \frac{G_s}{G}\frac{H}{r}\bar{s}_{z1}\right]$	*Eqn. 7.82*
Horizontal	$k_{xe} = Gr[\bar{c}_{x1} + \frac{G_s}{G}\frac{H}{r}\bar{s}_{x1}]$	*Eqn. 7.83*
Rocking	$k_{\varphi e} = Gr^3\left[\bar{c}_{\varphi 1} + \frac{G_s}{G}\frac{H}{r}\left(\bar{s}_{\varphi 1} + \frac{H^2}{3r^2}\bar{s}_{\varphi 1}\right)\right]$	*Eqn. 7.84*
Torsional	$k_{\psi e} = Gr^3\left[\bar{c}_{\psi 1} + \left(\frac{G_s}{G}\frac{H}{r}\right)\left(\bar{s}_{\psi 1}\right)\right]$	*Eqn. 7.85*

Table 7.4 **Damping coefficients for cylindrical embedded foundations (Puri and Prakash, 2006)**

Mode of Vibration	Damping Coefficient	
Vertical	$c_{ze} = r^2\sqrt{G\rho}\left[\bar{c}_{z2} + \bar{s}_{z2}\frac{H}{r}\sqrt{\frac{\rho_s}{\rho}\frac{G_s}{G}}\right]$	*Eqn. 7.86*
Horizontal	$c_{xe} = r^2\sqrt{G\rho}\left[\bar{c}_{x2} + \bar{s}_{x2}\frac{H}{r}\sqrt{\frac{\rho_s}{\rho}\frac{G_s}{G}}\right]$	*Eqn. 7.87*
Rocking	$c_{\varphi e} = r^4\sqrt{G\rho}\left[\bar{c}_{\varphi 2} + \left(\frac{H}{r}\frac{G_s}{G}\right)\bar{s}_{\varphi 2} + \left(\frac{1}{3}\frac{H^2}{r^2}\right)\bar{s}_{x2}\right]$	*Eqn. 7.88*
Torsional	$c_{\psi e} = r^4\sqrt{G\rho}\left[\bar{c}_{\psi 2} + \frac{H}{r}\bar{s}_{\psi 2}\sqrt{\frac{G_s}{G}\frac{\rho_s}{\rho}} + \left(\frac{1}{3}\frac{H^2}{r^2}\right)\bar{s}_{x2}\right]$	*Eqn. 7.89*

7.5 PARAMETERS REQUIRED FOR DYNAMIC ANALYSIS

7.5.1 Damping Constant

The preceding development of the equations describing the oscillation of foundations under dynamic loading illustrated an important point: resonance was associated with finite amplitude of motion. Resonance, by definition is the point where only damping forces restrict oscillations. Thus, the above expressions, for each degree of freedom, confirm that damping is present. However, this point conflicts with the elastic half-space theory, that assumes the material to be of a linear elastic nature and hence nullifies the presence of material damping. Thus, a differentiation between two different types of damping is required. The first form of damping is designated *material damping* and occurs due to hysteretic and viscous effects within the soil, as discussed in §6.4. The second is termed *geometric damping* and involves the dissipation of energy through the propagation of energy waves away from the foundation. Therefore, the damping noted in the previous section occurred through the transmission of elastic-wave energy radially away from the footing – geometric damping – and not through material damping which implies the soil is undergoing inelastic deformations.

Figure 7.9 illustrates the variation of geometric damping with respect to each mode of vibration and the associated mass ratios. It is valuable to note that geometric damping is relatively high for translational modes of vibration. Conversely, low levels of geometric damping are associated with the rotational and torsional modes of vibrations. This is a critical consideration for wind turbine foundations, due to their susceptibility to coupled rocking and sliding modes of vibration. Therefore, the lowest possible values of $\boldsymbol{B_\varphi}$ should be sought by the designer in order to limit rocking modes of oscillation.

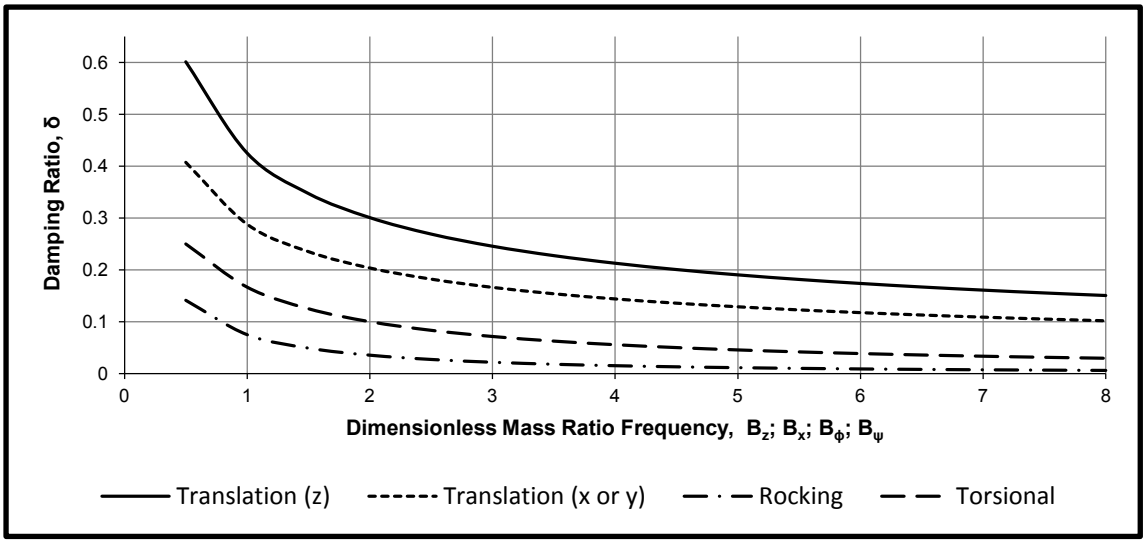

Figure 7.9 **Evaluation of geometric damping properties for different modes of vibration and mass ratios**

This emphasises the importance of optimising the radius-thickness relations to ensure the foundation has an adequate dynamic response without being over-designed. Additionally, in general the embedment of foundations reduces the amplitude of motion and increases the resonant frequency of the foundation. However, one critical case is the situation where a foundation is placed in layered soil stratum with a rigid layer at some depth below the foundation. The mathematical definitions of this situation will not be addressed, but it is important to note that the amplitudes of vibration at resonance are increased by the presence of the underlying rigid layer. This indicates that geometric damping is impeded by the rigid layer which reflects the elastic-wave energy back to the foundation (Puri and Prakash, 2006). Hence, the relationship between stiffness and internal damping in such a situation is critical.

7.5.2 Spring Constant

The spring constant, k, is the most crucial material parameter in the lumped parameter model. Firstly, it governs the static displacement of the soil-foundation system which would be developed by the application of a force equal to the amplitude, Q_0, of the dynamic force. Secondly, the spring constant plays a central role in the properties of the dynamic response. The dynamic magnification factor, D, is a function of k, because k and m are to two principle factors which control the critical damping coefficient, and hence the damping ratio. Therefore, the influence of the spring constant in the dynamic response of the foundation is twofold: it influences the amplitude of oscillation and the dynamic magnification factor. The spring constant represents a linear relationship between the applied load and resulting displacement (Richart et al., 1970). Therefore, by definition the theory of elasticity may be used to derive spring constants for footings of simple shapes for different geological conditions, as was shown in the previous sections.

However, the spring constants throughout this text were derived with respect to a homogeneous isotropic semi-infinite elastic medium. In reality, layered strata and the existence of bedrock affect the stiffness of the soil-foundation system. Furthermore, the effect of foundation embedment also positively influences the soil-foundation stiffness. Therefore, soil-foundation stiffness values for different geological conditions are defined in Table 7.5 and Table 7.6 in conjunction with Figure 7.10(a) and (b), respectively. Additionally, embedment of foundations also increases the soil resistance to motion, given that a gap does not develop between the sides of the foundation and the soil body. Therefore, it may be assumed that the spring constant increases for situations where the base is sufficiently embedded.

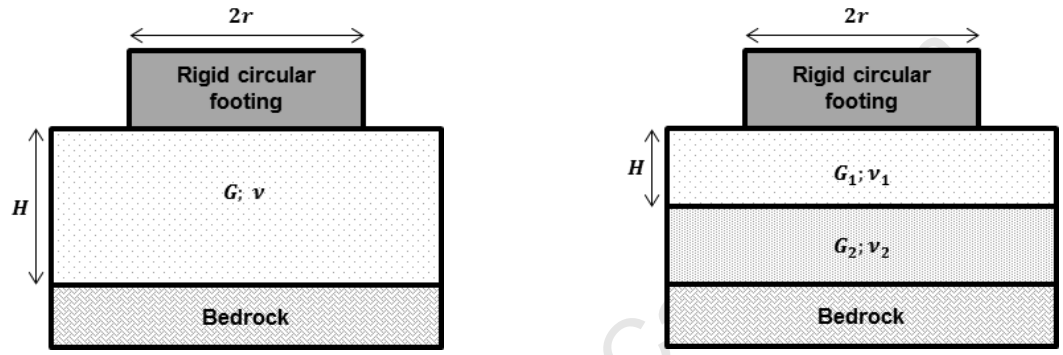

(a) **(b)**

Figure 7.10 **Rigid circular footing: (a) over bedrock and (b) underlain by layered strata and bedrock**

Table 7.5 **Soil-foundation stiffness for rigid circular footings overlaying soil with underlying bedrock (DNV/Risø, 2002)**

Mode of Vibration	Soil-foundation Stiffness	
Vertical	$k_z = \frac{4Gr}{1-\nu}\left(1 + 1.28\frac{r}{H}\right)$	*Eqn. 7.90*
Horizontal	$k_x = \frac{4Gr}{1-\nu}\left(1 + 1.28\frac{r}{H}\right)$	*Eqn. 7.91*
Rocking	$k_\varphi = \frac{8Gr^3}{3(1-\nu)}\left(1 + \frac{r}{6H}\right)$	*Eqn. 7.92*
Torsional	$k_\psi = \frac{16Gr}{3}$	*Eqn. 7.93*

Table 7.6 **Soil-foundation stiffness for rigid circular footings on layered strata (DNV/Risø, 2002)**

Mode of Vibration	Soil-foundation Stiffness	**Constraints**	
Vertical	$k_z = \frac{4G_1 r}{1-\nu_1}\left[\frac{1+1.28\frac{r}{H}}{1+1.28\frac{r}{2H}\frac{G_1}{G_2}}\right]$	$\{1 \le {}^{H}/_{r} \le 5\}$	*Eqn. 7.94*
Horizontal	$k_x = \frac{8G_1 r}{1-\nu_1}\left[\frac{\left(1+\frac{r}{2H}\right)}{\left(1+\frac{r}{2H}\frac{G_1}{G_2}\right)}\right]$	$\{1 \le {}^{H}/_{r} \le 4\}$	*Eqn. 7.95*
Rocking	$k_\varphi = \frac{8Gr^3}{3(1-\nu)}\left[\frac{\left(1+\frac{r}{6H}\right)}{\left(1+\frac{r}{6H}\frac{G_1}{G_2}\right)}\right]$	$\{0.75 \le {}^{z}/_{r} \le 2\}$	*Eqn. 7.96*

7.6 SUMMARY

Anticipating the response of foundations to dynamic loading is a complex issue. This chapter introduced the complexities surrounding this issue and settled on the classic elastic half-space theory. Theoretical relationships were then developed to illustrate the link between the lumped parameter model and the elastic half-space theory by means of *Lysmer's Analog*. Following this, the mathematical relations for different modes of vibration response were presented. This process highlighted several key points:

1. Torsional and vertical translation of the foundation tends to occur in isolation and may be treated as such. Although these modes are applicable, they are not fundamental to wind turbine structures based on the applied loading and structural characteristics.
2. The critical mode of vibration is coupled rocking and sliding. Limiting the effects of this mode of vibration requires cognisance of the mass ratio, which is dependent on the geometrical parameters of the foundation and affects the geometrical damping of the system considerably.
3. Damping comprises two parts: geometric and material, where the influence of each depends on the mode of vibration. Internal material damping is negligible at low levels of shear strain. Geometric damping is considerably reduced for foundations placed in close proximity to rigid layers as the wave energy is refracted back to the foundation.
4. The most critical parameter required for the accurate and precise determination of a foundation's dynamic response is the coefficient of subgrade reaction, or spring constant. This parameter is directly affected by the shear modulus, the determination of which is studied in Part IV, within a South Africa geological context.

PART IV CONSIDERATIONS FOR WIND TURBINES FOUNDED ON PEDOCRETES

8. FOUNDING WIND TURBINE STRUCTURES ON PEDOCRETES

8.1 INTRODUCTION

Much of the knowledge and experience of wind turbine foundation behaviour, design and construction was derived from projects in the Northern Hemisphere, due to prolific wind farm development in the UK, USA, Denmark, Germany and Netherlands. Similarly, temperate zone transported soils of the Northern Hemisphere formed the origin of modern principles of soil mechanics, soil classification and experience with regard to soil and rock behaviour. Soils of more tropical areas, that were not subjected to the glaciations of the Pleistocene, are, in contrast, characterised by deep weathering and advanced pedogenesis (Netterberg, 1994). This has resulted in the founding conditions of much of Southern Africa and other semi-arid areas of the world being characterised by variably cemented soils called *duricrusts* or *pedocretes*.

Pedocretes are common shallow formations which are developed in-situ as either weathering residues, or through cementation of pre-existing soils by various authigenic minerals precipitated from the soil or groundwater. In some cases the authigenic mineral may completely replace the parent material or mix with former cementing agents. The west coast, southern coast and northern interior of South Africa are especially suited to the formation of pedocretes. They have also been encountered in isolated areas of the Eastern Cape and KwaZulu-Natal.

Pedocretes pose unique challenges to geotechnical engineers, particularly geotechnical engineers who have little or no experience of South African geological conditions. This is due to the extreme variability of pedocretes and their engineering characteristics, which are not always accurately quantifiable with conventional classification and testing procedures.

In light of this, the following chapter aimed to provide insight into the characteristics and behaviour of pedocrete materials. The materials are firstly defined in terms of mineralogy, origin and distribution throughout South Africa. This is followed by a comparison between the engineering behaviour of pedocretes and traditional soils; where emphasis was placed on the consistency, strength and volume change attributes. Possible methods of mitigation were explored with respect to the specific loading conditions and foundation behaviour of wind turbine structures. In view of this, this chapter formed a basis upon which the challenges of founding wind turbine structures in such materials may be understood.

8.2 PEDOCRETES

8.2.1 Definition

Pedocretes are soils which have been cemented or replaced in-situ by authigenic minerals, the classification of which depends on the minerals involved. They are not sedimentary rock, although at times may resemble the similar strength and stiffness properties as sedimentary rocks. The most common authigenic minerals encountered along the southern coast of Africa are carbonates and iron oxides, silica and gypsum, yielding calcrete, ferricrete, silcrete and gypcrete, respectively (Netterberg, 1985). Manganocrete, phoscrete and mangesite are also relevant to these regions but to a lesser extent, and therefore are not discussed herein.

The classification of pedocrete materials has been done in terms of their consistency. Netterberg, (1985) defined two common states of pedocretes:

1. Indurated pedocretes may be classified as resembling sedimentary rock (hardpans) or gravel (honeycomb and nodules).
2. Non-indurated pedocretes are characterised as soft or powdery, resembling soft silt and fine sand.

There has been dispute surrounding the terminology used to describe pedocrete materials found in different areas of the world. For the sake of consistency, the terminology used throughout this chapter is defined below, and conforms to terminology frequently used throughout South Africa. Strictly speaking, a pedocrete is defined as a material consisting of more than 50% of the cementing or replacing material. The cementation or replacement by carbonates, iron-oxides or silica is defined below, respectively:

1. Calcareous pedocretes are referred to calcretes herein. This material is known as caliche in the United States of America, and surface limestone in other parts of Southern Africa. This is due to the consistency of calcretes varying between soft powdery forms and very hard rock, resembling limestone.
2. Ferricrete, or *koffieklip*, are terms used throughout South Africa to refer to indurated iron-rich materials. In the past any material of variable particle size distribution and possessing a significant silica or sesquoixide ratio was loosely termed a laterite.
3. Similarly to calcareous soils, silcretes have previously been referred to as surface quartzite, but will be denoted as silcretes hereafter.

The term *dorbank* is commonly used to refer to pedocretes which resemble hard to very hard rock, and are composed of quartz, feldspars, rock fragments and up to 15% clay. The cementing agent may vary between silica, iron-oxide and calcium carbonates, or a be a combination thereof depending on the diagenesis history (Netterberg, 1985). These materials are equivalent to the duripans of the USA and red and brown hardpans of Australia. Despite the confusion surrounding the terminology of the above materials, the differences in composition and origin implied by the above terms are not of major concern for engineers, as they do not pose a significant influence on the engineering properties of each material.

8.2.2 Formation and Distribution of Pedocretes in South Africa

Calcrete generally forms in arid and semi-arid regions where the mean annual rainfall is less than about 550 mm and where the drainage conditions result in short term seasonal water courses and pans. This is illustrated by Figure 8.1, which shows the vast distribution of calcretes throughout the arid and semi-arid regions of South Africa. The formation of calcretes may be narrowed down to two mechanisms, as discussed by (Netterberg, 1982):

1. Non-pedogenic, where the deposition of carbonates into the soil structure above a shallow water table
2. Pedogenic action, which involves the percolation of rainwater through the soil subsequently precipitating carbonates.

Due to these mechanisms, calcretes develop above the ground water table, and thus tend to trap moisture in the strata below. The origin of the carbonate may be from the in-situ weathering of the material, from the rainwater or from transported materials, the major constituents being dolomite and calcite, as shown in Table 8.1, which is also consistent with the finding that calcretes have been known to become highly silicified with time (Goudie, 1972). These mechanisms of formation generally result in calcrete horizons between 1 and 2 m thick, underlain by a much weaker, less developed horizon, also possibly affected by high moisture content over time. However, calcrete horizons of up to 30 m have been recorded (Netterberg, 1985).

Ferricretes, commonly referred to as *koffieklip* in South Africa, tend to occur in areas of higher rainfall and humidity. This is because the development of ferricretes requires the combination of seepage and a fluctuating water table. Iron oxide ions are mobilised by the percolation of water through the soil fabric, the origin of which tends to be mafic materials, resulting is iron staining as illustrated by the nodular ferricrete in Figure 8.2(a). The ions are carried to the base of the perched water table, which, upon drying, are precipitated into the soil fabric.

Ferricretes are especially prominent at gully-heads and in hill-wash sediments in the Southern Cape region, but have also been found in discontinuous layers further up the west coast.

Silcretes have been found to occupy two distinct bands in Southern Africa. The coastal band stretches for much of the Southern and Northern Cape coasts, whereas the inland region is generally confined to the northern Karoo and Kalahari Group. These materials form under similar processes to that of calcretes, but cementation occurs due to the precipitation of silica, and given the stability of silica with regard to chemical weathering, silcretes have been known to replace calcretes with time.

Duripans, which are laminar in nature and often highly fractured, are most common in the more arid areas of the Northern Cape and Namaqualand coast. The distribution of Gypcretes is not illustrated by Figure 8.1 but they are thought to occur mainly in the Namibia and the Northern Cape of South Africa. Less developed gypcretes, in the form of gypseous rich soils, have been encountered along the western coast of Africa between Angola and Cape Town. As is shown by Table 8.1 these materials are prone to develop mixtures with other authigenic minerals.

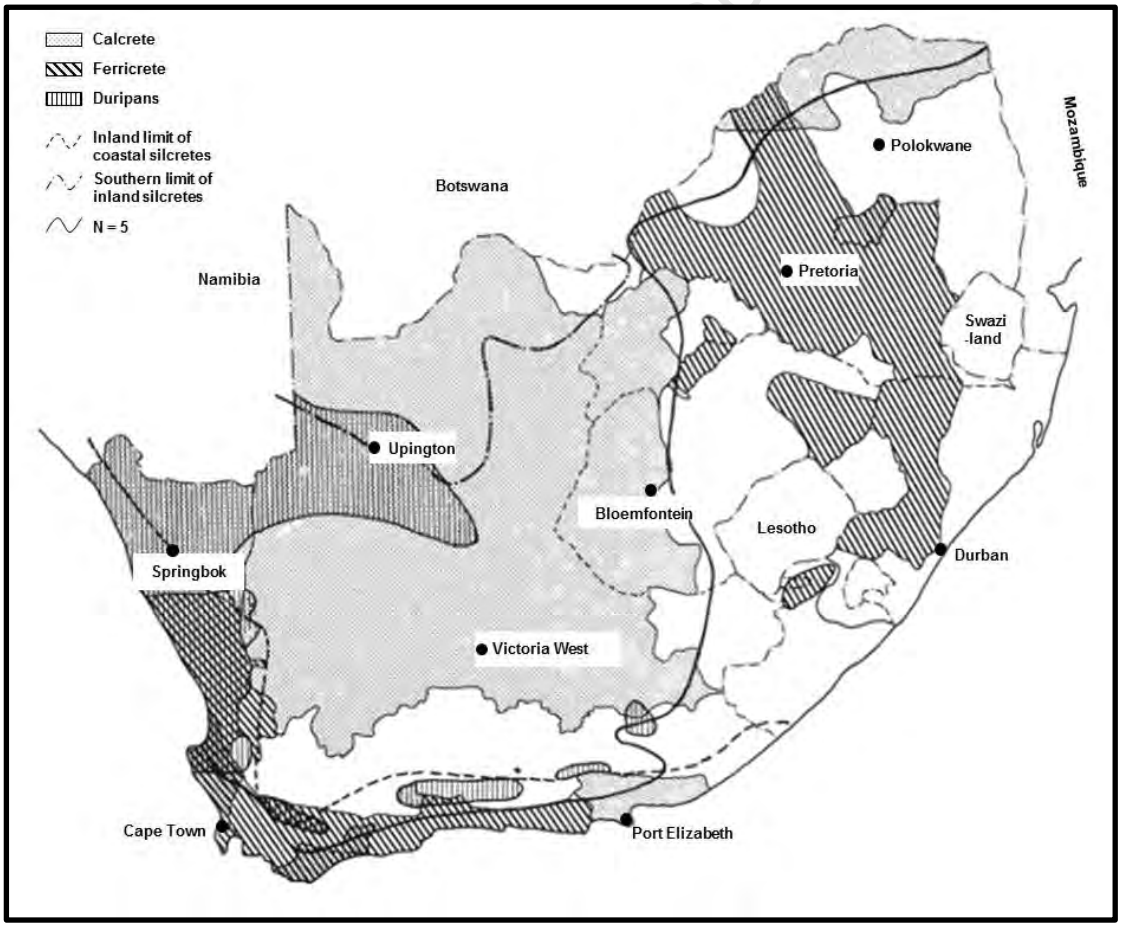

Figure 8.1 **Distribution of common pedocretes in South Africa (Netterberg, 1985)**

Table 8.1 **Typical composition of South African pedocretes (Netterberg, 1982)**

Component	Calcrete (%)	Ferricrete (%)	Silcrete (%)	Gypcrete (%)	Mineralogy
SiO_3	1-60	5-70	85-100	0-60	Quartz, feldspar, clays, opal, chaldcedony
Al_2O_3	0-5	5-35	0-5	0-60	Feldspar, clays, gibbsite
Fe_2O_3	0-5	5-70	0-10	0-60	Geothite, haematite
TiO_3	0-1	0-5	0-5	0-60	Anatase, rutile
$CaCO_3$	40-100	-	0-5	0-60	Calcite, dolomite, apatite
$Ca_3(PO_4)_3$	<0.2	0-2	0-2	-	Apatite, cellophane, dahllite
$CaSO_4.2H_2O$	0-2	0	0-2	40-90	Gypsum
H_2O	0-5	5-20	0-2	10-20	Clays, gibbsite, goethite, gypsum
Organics	0-1	0.2-2	-	-	Organic matter
$NaCl$	0-1	-	-	0-4	Halite, apatite

(a) **(b)**

Figure 8.2 **Pedocrete hardpans: (a) ferricrete (with possible cemented nodules) (Beales and Paton, 2011) and (b) calcrete (Beales, 2013)**

8.3 TYPICAL GEOTECHNICAL PROPERTIES

The engineering properties of pedocretes depend on three factors:

1. The texture and mineralogy of the parent material;
2. The stage of development (the extent to which cementation or replacement has occurred);
3. The characteristics of the authigenic agent.

These three factors are addressed below, in terms of consistency, strength and plasticity.

8.3.1 Consistency and Strength

The stage of development poses the greatest influence on the consistency of the material, and hence the geotechnical properties of pedocretes. Table 8.2 summarises the key stages of development of calcretes, ferricretes and silcretes. From this table, it may be said that the properties of a calcareous, ferruginous or silicified soil will depend principally on the engineering properties of the host soil, whereas, the indurated counterparts of each material will depend on the nature of the authigenic mineral and hence display attributes closer to those of rock (Netterberg, 1982). Pedocretes should not be classified as rock, despite the consistency of hardpan layers often resembling rock. This is because pedocretes tend to deteriorate in quality with depth, due to decreased cementation and the effect of trapped moisture below hardpan layers, whereas weathered rocks generally improve in consistency with depth, as they become less weathered.

This point is illustrated below by Figure 8.3(a) and (b), which gives a comparison between the consistencies of a calcareous sand and a hardpan calcrete, respectively.

(a) **(b)**

Figure 8.3 **Variable calcareous pedocrete consistencies: (a) calcareous sand and gravel and (b) calcrete hardpan (Beales, 2013)**

Table 8.2 **Stages of pedocrete formation, in ascending order with respect to time**

	Stage of Development	Description
Non-indurated	Calcareous/Ferruginous Soil	A soil which in texture resembles a clay, silt or sand texture and exhibits no nodular development or significant cementation. The authigenic agent is present but is not sufficient to cement the soil significantly. Variable consistency.
	Calcified/Ferruginised/Silicified Soil OR Calcified/Ferruginised/Silicified Gravel	A platy soil which has been indurated to a medium dense to dense or firm to stiff consistency. Weakly to strongly cemented gravel of medium dense to very dense consistency.
	Powder Pedocrete	A material that resembles soft silt and is generally composed of sand sized or aggregated particles of authigenic material. Soft to very stiff.
Indurated	Nodular Pedocrete	Mixture of silt to gravel sized nodules of cemented and aggregated particles. The consistency of this horizon is generally loose, but the particles themselves are in advanced stages of cementation, rendering them hard and dense.
	Honeycomb Pedocrete	The honeycomb stage is an intergrade between the hardpan and nodular stage, and consists of loose soil particles filling the voids between stiff aggregated pedocrete nodules.
	Hardpan Pedocrete	Hardpans are the final stage of development, and they are characterised by indurated and strongly cemented material of a consistency between stiff soil and very hard rock. Hardpans are generally underlain by much softer or looser material similar in nature to the powder pedocrete.
	Pedocrete Cobbles and Boulders	Discrete or partially connected cobble or boulder sized pedocrete complexes, formed by the weathering of hardpan pedocrete materials and generally very stiff to very hard.

8.3.2 Plasticity Properties of Fine Pedocrete Material

The mineralogy of the cementing agent and the clay fraction of pedocretes differs substantially from that traditionally experienced in temperate zone soils (Netterberg, 1985). This renders the behaviour of pedocrete materials as unpredictable by conventional soil classification systems. An example of this is given by Figure 8.4 where the plasticity index of calcretes and ferricretes, which indicates the compressibility and volume change tendencies of the material, is shown to lie on both sides of the Cassagrande ‗A'-line. Calcretes tend to possess higher liquid limits (LL) relative to their plasticity indices (PI). The shrinkage limit (SL) is also generally higher than the plastic limit (PL) meaning that the shrinkage indices of calcretes are often negative (Netterberg, 1982). Ferricrete materials falling below the Cassagrande ‗A'-line are potentially expansive as they are likely to contain hydrated halloysite. Furthermore, the use of pedocrete materials in road construction has been widespread throughout Southern Africa, despite the contradiction between their compaction properties, plasticity indices and poor grading characteristics as shown by Table 8.3.

There are several reasons for this behaviour of pedocrete materials (Netterberg, 1994):

1. For calcretes, this behaviour is assumed to be linked to the high particle porosity and silt content, coupled with a wide array of clay minerals and variable hydration.
2. The aggregate of traditional soils is regarded as solid and resembling rock, whereas pedocrete aggregate is often porous and consists of weakly cemented fines. This is due to the tendency of clay and silt particles to become flocculated and cemented into larger gravel-sized particles of varying porosity and strength.
3. The clay minerals of pedocretes vary widely, but mostly consist of attapulgite, in calcretes, and holloysite and/or allophane in ferricrete. This inconsistency of clay minerals is exacerbated by the inherent reactivity of pedocrete materials, especially in Southern Africa where the ground water has been found to contain higher concentrations of HCO_3 (Goudie, 1972).
4. The grading and Atterberg limits of pedocretes are sensitive to drying, mixing and working, as opposed to stable under these conditions for more conventional soils. This is due to the breakdown of the pedocrete structure as well as the tendency of porous pedocretes to retain moisture.

These findings emphasise a fundamental point related to the determination and interpretation of pedocrete geotechnical properties. Namely, that traditional methods founded on the principles of soil mechanics may in some cases be inapplicable and at best, should be interpreted with extreme caution.

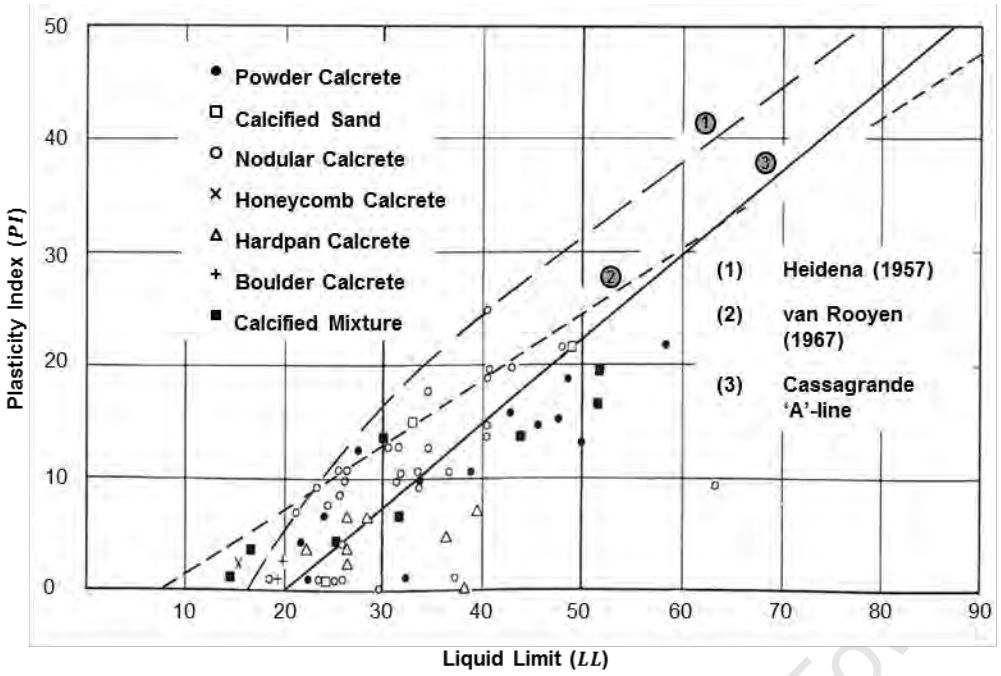

Figure 8.4 **Cassagrande plasticity chart for calcretes (Netterberg, 1982)**

Table 8.3 **Plasticity properties of calcretes (Netterberg, 1982)**

Material Type	$CaCO_3$ Content (%)	Grading Modulus (%)	PI (%)[3],[4]
Calcareous Soil	1.0-10	Varies	Varies
Calcified Sand[1]	*10*-50	*1.5-1.8*	NP-20
Calcified Gravel[1]	*10*-50	*>1.8*[5]	*<8.0*
Powder Calcrete	70-99	0.4-1.5	SP-22
Nodular Calcrete	50-75	1.5-2.3	NP-25
Honeycomb Calcrete[2]	70-90	>2.0	*SP-8.0*
Hardpan Calcrete[1]	50-99	*>1.5*	NP-7.0
Calcrete Boulders/Cobbles[1]	50-99	>2.0	NP-3.0

(1) After crushing or compaction in the case of disturbed samples
(2) Up to about 50% volume when many nodules present
(3) Without the loose soil between calcrete boulders/cobbles
(4) Conducted on the fines in the case of honeycombs/hardpans/boulders
(5) Italics denote approximate values

8.4 FOUNDING WIND TURBINES ON PEDOCRETE MATERIAL: KEY CONSIDERATIONS

Wind turbine foundation engineers need to be adaptable to the site conditions, especially with regard to pedocretes, given the material's inherent variability in terms of engineering properties, behaviour under load and spatial distribution. The problem of variability is exacerbated by the nature of loading emanating from wind turbine structures. More specifically, the dynamic nature of loading requires the soil-foundation system to be designed of high stiffness – a significant challenge in materials with such unpredictable stiffness and density. Furthermore, the variability of pedocrete materials must be encapsulated by the testing procedures used to assess the properties of the soil.

8.4.1 Variable and Deteriorating Stiffness with Depth

8.4.1.1 General Considerations

The normal weathering profile of pedocretes differs to that of rocks; that is, the consistency and strength of pedocretes generally deteriorates with depth. This is based on the pedological processes governing the formation of materials such as calcretes, which render the soils below hard pedocrete layers to be soft and compressible in nature, and possibly expansive. Hence, it is not advisable to found on pedocrete layers of unknown thickness. This point is illustrated by Figure 8.5, which shows an initial very strongly cemented laminar duripan layer, underlain by silty sand and clay. Although the materials in this image are of a very dense/stiff consistency, it is indicative of the potential variability of such underlying materials (Beales, 2013), which, more often than not, are soft and even expansive in nature.

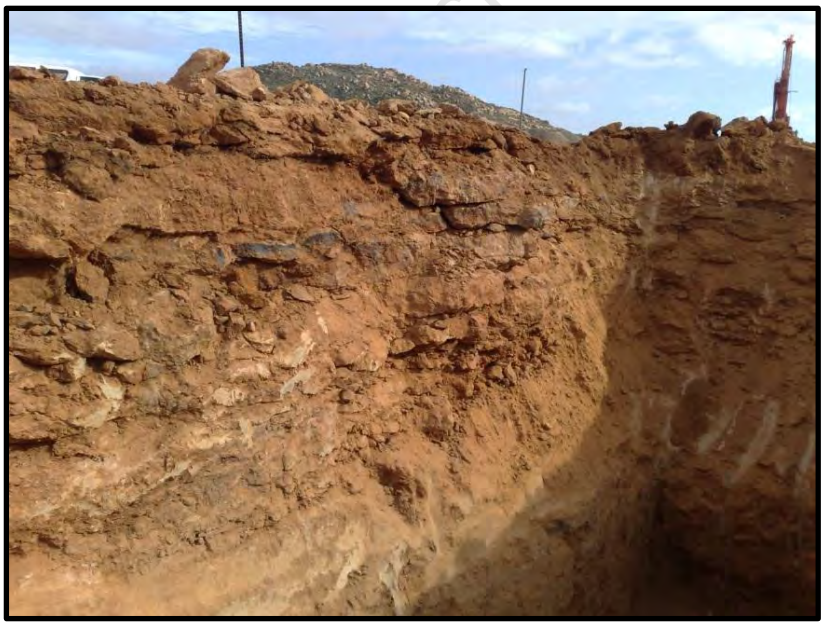

Figure 8.5 **Laminar horizon of hardpan (ferricrete and calcrete)**

Further deliberations regarding the founding of foundations on pedocretes are as follows:

1. Where thin layers are encountered at relatively shallow depths, the pedocrete hardpan layers may be removed to expose the underlying transported and residual soils. It has been reported that stabilisation by means of cement of lime has been successful in the improvement of the soft pedocrete layers below hardpans in road construction throughout south-western Africa (Netterberg, 1985).
2. The process of founding on a pedocrete layer may yield positive results due to the rafting action that may be mobilised by the underlying rigid layer, leading to further distribution of stress and minimisation of differential settlement (Netterberg, 1985). However, this is a function of the layer stiffness and consistency over the foundation footprint, as a punching failure of the pedocrete layer would result in differential settlement, and most likely failure of the structure.
3. Thick layers of pedocrete materials should be assessed thoroughly to evaluate the consistency of the soil laterally with respect to the likelihood of differential settlement. Electrical resistivity surveys or seismic methods are recommended for this purpose.

8.4.1.2 Dynamic Loading Aspects

The influence of a rigid layer on the damping and stiffness properties of a vibration foundation-soil system was studied in §7.5. Firstly, it was noted that a rigid layer close to the surface was advantageous for the foundation stiffness, but caused a reduction in geometric damping, due to it impeding the radiation away from the footing, and the partial reflection of energy back to the founding level. This was shown to result in greater amplitudes of vibration. Thus, the use of the equations and relationships defined in Chapter 7 should be used with caution given the sensitivity of geometric damping to the ground conditions. Furthermore, due to the porous nature of less-developed pedocretes and the extreme variability in density of these materials, the seismic velocity fluctuates between the different layers, as shown in Table 8.4, making the prediction of dynamic response extremely troublesome. A parametric study is suggested for this, to ensure the variability in dynamic stiffness and the role that rigid layers play in damping are accounted for.

Secondly, the existence of pedocrete layers, whether deep or shallow, gives rise to the possibility of fastening the foundation by means of micro-piles or post-tensioned anchors to the rigid layer. This may be an attractive option to the foundation engineer based on the cost benefits due to material savings. However, it is imperative that the consistency of the material and its stage of weathering are evaluated thoroughly and the weathering behaviour of the respective pedocrete is understood. Furthermore, the bond stresses of such anchors with the pedocrete material should be analysed thoroughly, advisably in conjunction with in-situ testing.

Table 8.4 **Summary of selected engineering properties of calcretes (Netterberg, 1982)**

Material Type	Consistency	Seismic Velocity (m/s)
Calcareous Soil	Variable	300-900
Calcified Sand	Med. dense to dense, or firm to stiff	600-1200
Calcified Gravel	Med. dense to very dense	1200-2450
Powder Calcrete	Soft to very stiff	400-1070
Nodular Calcrete	Med. dense to dense	600-900
Honeycomb Calcrete	Dense to very dense	900-1200
Hardpan Calcrete	Stiff to very hard	900-4500
Calcrete Boulders and Cobbles	Very stiff to very hard	Erratic

8.4.2 Lateral Variable Founding Conditions

The second major consideration facing foundation engineers looking to found on pedocrete materials is the lateral variability of pedocrete horizons. This variability is not necessarily confined to consistency, but also geotechnical behaviour. For example, certain calcrete power horizons have been found to undergo strength losses of up to 90% upon wetting (Netterberg, 1985) whereas others have been less sensitive. Furthermore, areas of the Namaqualand coast of South Africa have been found to be underlain by weathered granite outcrops. These geological features combined with pedocrete horizons have further increased the variability of such sites (Beales, 2013).

Such lateral variability presents challenges, especially with regard to rotational stiffness and associated differential settlement problems for wind turbines. The sensitivity of slender tall structures to differential settlement has been stressed in previous sections. It is therefore imperative that wind turbine structures are founded on materials of appropriate consistency and stiffness to ensure tilting does not occur. Netterberg (1985) recommended the use of trenching to evaluate the lateral variability of soils with anticipated pedocrete horizons, as opposed to the excavation of trial holes and/or auger holes for conventional foundation investigations.

More modern techniques, such as Electrical Resistivity Survey (ERS) have proved to be highly beneficial in highlighting possible lateral variability for wind turbine investigations. Figure 8.6 illustrates the results of an ERS conducted approximately 20 km inland along the Namaqualand coast, south east of Alexander Bay. These results in conjunction with standard electrical resistivity values may be used to indicate the nature of materials across the proposed footprint of the structure, with respect to depth. This technique is especially helpful in evaluating the near-surface profile of the site as they typically span a section of 100 – 150 m and to depths of around 20 m.

Table 8.5 **Typical electrical resistivity of specific pedocretes, soil and rock types (Beales, 2013)**

Soil/Rock Type	Electrical Resistivity ($\Omega.m$)
Transported Soils	20-65
Powder Pedocrete	75-150
Hardpan Pedocrete	350-600

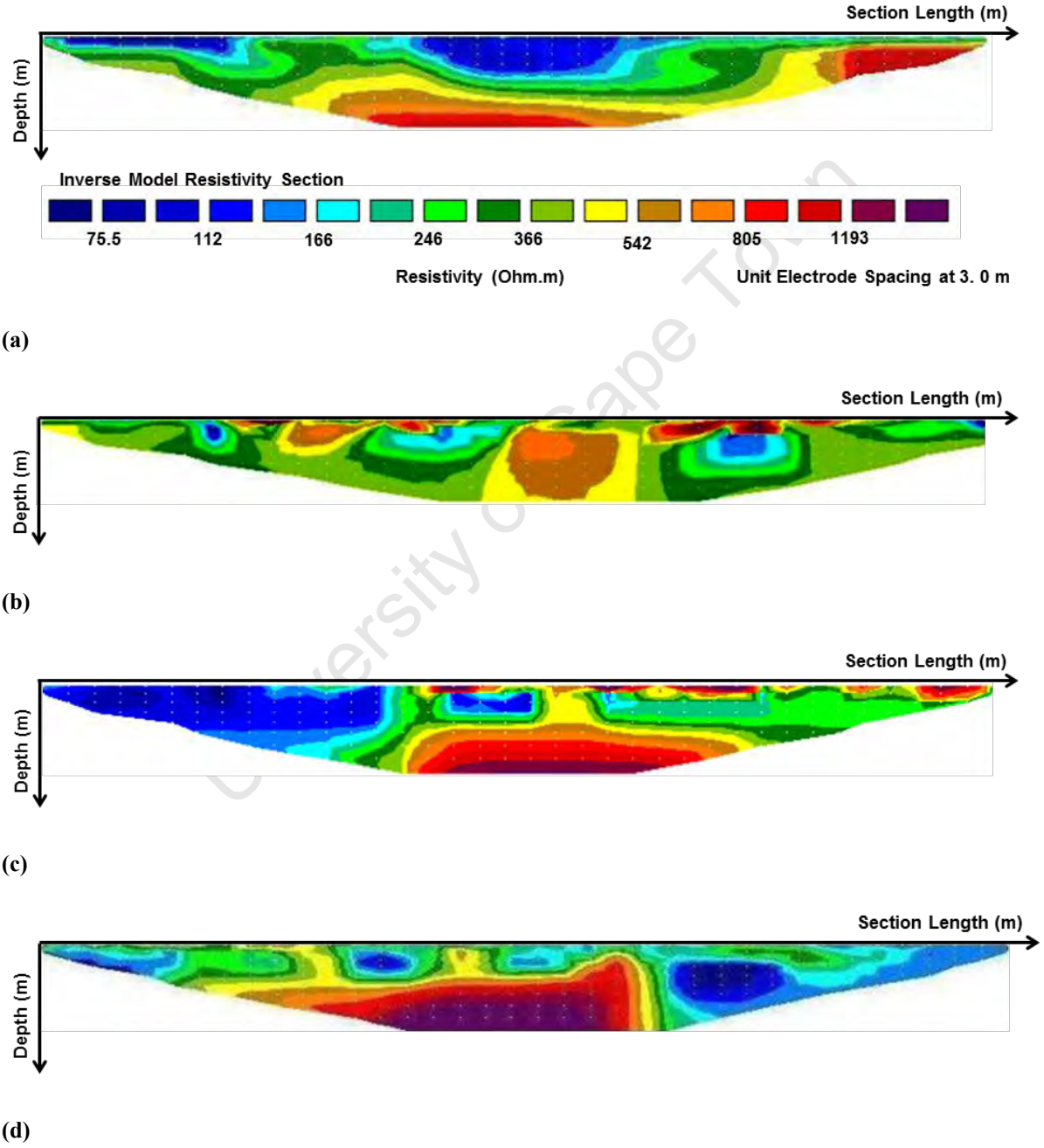

Figure 8.6 **ERS results from specific locations at a proposed wind farm in the Richtersveld (Beales, 2013): (a) possible hardpan and nodular pedocrete with loose material, (b) boulder pedocrete profile overlain by hardpan and (c & d) pedocretes of varying consistency.**

8.4.3 Founding on Collapsible Profiles

8.4.3.1 Definition and Identification of Collapsible Soils

The arid conditions of the western and northern areas of South Africa favour the formation of collapsible soils as a result of debris flows, wind blow sediments, tropical residual soils and cemented, high salt content, metastable soils. Furthermore, the decomposing granite and granitic soils of this area have also been found to have high collapse potential (Brink and Kantey, 1961). The littoral and aeolian deposits of the western and northern interior have been reported to be especially prone to collapsible behaviour (Brink and Schwartz, 1985), and when combined with calcareous, ferruginous and/or silicified soils, present a significant obstacle for foundation engineers.

A collapsible fabric is normally associated with an open textured soil with individual grains being separated by a bridging material (Brink and Schwartz, 1985). This often consists of kaolinite in the form of clay bridges, but within pedocrete horizons it is also likely to be calcium carbonates, or iron- and/or silica oxides. Thus, assessment of collapse potential (I_c) is mandatory in such areas. Traditionally, conducting a double oedometer test or a modified single odeometer test has effectively provided the collapse potential of the material. The double oedometer method involves testing two identical samples, one saturated and the other at its natural moisture content. The single oedometer test, also known as the *collapse potential test*, consolidates a sample at its natural moisture content up to 200 kPa. Upon reaching this stress the sample is fully saturated and the settlement is recorded. The collapse potential is defined below in conjunction with Figure 8.7 and Table 8.6.

$$I_c\,(\%) = \frac{\Delta e}{1 + e_0} \cdot 100 \qquad \textit{Eqn. 8.1}$$

This is a qualitative representation of the soil collapse characteristics, which may be quantified through in-situ plate load tests. However, the performance of in-situ collapse potential tests is challenging due to the three conditions of collapse settlement, and the associated challenges of evaluating the influence of each on the collapse potential. These factors were summarised by Brink and Schwartz (1985) as:

1. Partial saturation of the soil, where there has been shown to be a critical value of saturation, above which collapse cannot occur.
2. A triggering mechanism, which weakens or removes the cohesive bonds between soil particles, is required. Conventionally, the triggering mechanism was deemed to be an increase in moisture content but the transfer of vibrations to the subgrade may also act as the triggering mechanism.
3. Lastly, the soil is required to undergo a simultaneous increase in effective stress in order for collapse to be induced.

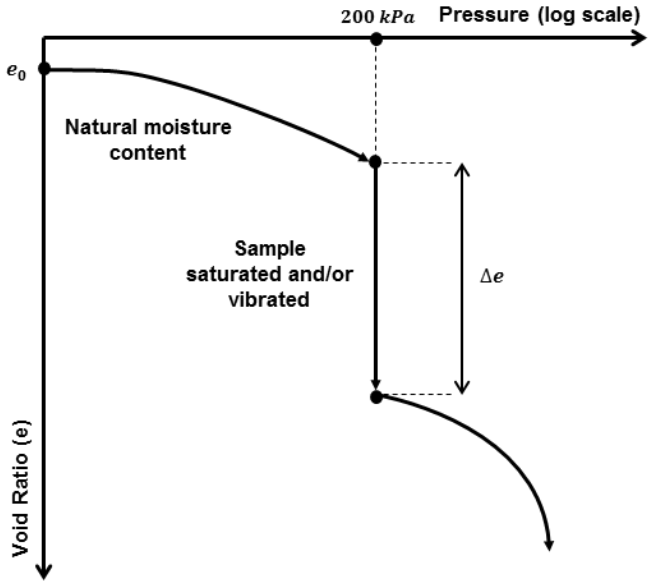

Figure 8.7 **Collapse potential assessment – typical test result**

Table 8.6 **Guidelines of collapse potential**

Collapse Potential (%)	Severity of Problem
0-1	Negligible
1-5	Moderate
5-10	Problematic
10-20	Severely problematic
>20	Very severe problem

Collapsible soils are particularly susceptible to settlement under dynamic loading owing to their highly contractive behaviour during shearing. However, assessing the dynamic settlement potential of such soils is extremely problematic. Hence, emphasis is placed on the classification of collapsible soils, which are open and spongy in nature, and once identified, a remediation process may be adopted. Remediation measures should be conservative for wind turbine structures given their dynamic nature and how vibrations exacerbate the densification problem associated with soils of a high void ratio. Three basic approaches exist when dealing with such soils:

1. Increasing foundation stiffness to minimise effects of differential settlement;
2. Bypass the collapsible layer using piles;
3. Ground improvement techniques.

8.4.3.2 Increasing Foundation Stiffness to Minimise Differential Settlement

Increasing the foundation-soil stiffness is one method that may be used to reduce the detrimental effects of collapsible soil profiles. As discussed in §**Error! Reference source not found.**, this may be one by increasing the base thickness and moment capacity, or depending on the founding conditions, it may be more efficient to adopt a piled-pad foundation.

Incorporating piles into the foundation will yield positive results provided that the pile length and base diameter are proportioned such that the foundation–soil stiffness becomes dependent on the pile stiffness. This is done by ensuring the piles are sufficiently long or are embedded into rock. Thus, adopting a piled solution poses a complex trade-off between pile length and base thickness, in terms of material and time efficiency. It is suggested that a detailed parametric study be conducted to optimise the respective dimensions.

8.4.3.3 Densification of Subgrade

An added benefit to incorporating piles into the wind turbine base is the influence of pile installation on soil stiffness. Driving piles into collapsible soil profiles reduces the void ratio by the transfer of energy through the stratum. Therefore, pile driving would reduce the collapse potential of the soil as well as the potential differential settlement of the foundation. However, this should be done with caution, as applying excessive energy to cemented soil profiles has shown to reduce stiffness through disintegration of cementation bonds, despite reduced void ratio (§8.5). Thus, other methods of ground improvement by densification, such as dynamic compaction, should be adopted with extreme caution.

The depth of influence is another critical component of densification methods, especially due to the dynamic nature of wind turbines. This means that if densification methods were to be adopted then the energy transferred to the soil would have to achieve suitable results throughout the wind turbine pressure bulb (approximate depth of $4r$) and beyond, due to the geometric radiation of energy away from dynamically loaded bases. Despite whether a sufficient amount of energy is transferred to the soil or not, the methods for evaluating the extent of densification and the resulting improvement of stiffness throughout the depth of foundation influence contain considerable assumptions and error.

Densification in pedocretes is especially hard to evaluate, given the inconsistency of the material. The energy transferred to the pedocrete material may be refracted or reflected back to the surface by one of the many possible rigid layers within the pedocrete profile. Furthermore, it should be re-iterated that fabric and structure of pedocrete materials is highly variable, and may worsen under de-structuring by means such as dynamic compaction. This may mean the disintegration of nodular pedocretes and calcareous/ferruginous gravels/sands, resulting in worse stiffness properties post-compaction.

Therefore, the use of densification methods, with the possible exception of driven piles, should only be conducted within a framework of thorough monitoring and geotechnical testing. The costs and possible consequences of error should be weighed up against the alternative method of increasing the base stiffness and/or incorporating piles.

8.4.3.4 Stabilisation by Cement or Lime

Alternatively, bonding by means of cement or lime stabilisation may be utilised to reduce collapse potential. As mentioned in §5.5.4.2, certain pedocrete materials have been found to be aggressive towards concrete and pozzolanic binders such as cement and lime. These binders are often used to improve the subgrade stiffness where loose and/or collapsible soil profiles are encountered, and given the problems associated with densification in collapsible soil profiles, the use of such binders is a feasible option for wind turbine projects.

However, it should be noted that the use of such binders may be problematic in gypseous soils and other pedocretes such a dorbanks, which are potentially saline. Gypsum rich soils pose the problem of concrete-sulphate attack and subsequent degradation of concrete stiffness or binder effectiveness.

The process of sulphate attack in gypseous soils is one which depends on a very wide array of factors, the major ones including:

1. The nature of the ground water table, where fluctuating water table, or seepage, allowing for regeneration of sulphate ions is more detrimental that a static water table.
2. The nature and concentration of gypsum in the soil.
3. The nature of the binder used. Limestone based cements are susceptible to *Thaumisite sulphate attack* (TSA), which is the reaction of the calcium silica hydrate (C-S-H) with the sulphate ion in the presence of carbonate. This reaction generally only occurs in wet environments and at low temperatures, however, it remains a key consideration where the use of limestone-based cement, potentially exposed to sulphate attack, is used.

Again, the variability of pedocrete materials renders the occurrence of this problem unpredictable, as the occurrence of gypseous rich soils may vary across a wind farm site, or even a proposed wind turbine foundation footprint. Furthermore, the nature of the problem depends on the characteristics of the gypsum involved and the groundwater conditions, both of which are key facets of the reactivity of the respective sulphate ions, concrete, and/or stabilising binder.

8.5 CASE STUDY: EASTERN CAPE WIND FARM ON A COLLAPSIBLE CALCRETE PROFILE

A case study by Parrock (2013) detailed the danger of ignoring the collapse potential of pedocrete materials during the design phase of the project. A dynamic compaction operation was undertaken to improve the subgrade stiffness after the site investigation illustrated a variable calcrete profile, ranging from hardpan calcretes to calcareous sand.

The dynamic compaction yielded negative results; that is, the compaction process worsened the soil's stiffness, which was confirmed by Continuous Surface Wave tests. Although the material underwent densification during compacting, the compaction process ruined the natural structure of the soil by destroying inter-particle bonds and possibly the pedocrete layers as well (Parrock, 2013).

This finding was aligned closely with Figure 8.7, where the slope of the curve is steeper after collapse than before, illustrating a loss in stiffness after collapse. The dynamic compaction process was beneficial from the point of view that it would have induced collapse in much of the soil body, and hence the decision to compact the soil prevented the possible sudden collapse of the proposed structure post-construction. However, this case highlights two significant points concerning the process of founding on pedocrete materials:

1. The importance of assessing collapse potential at the early stages of design is paramount to the success and cost efficiency of project.
2. A thorough parametric study should be conducted to evaluate the influence of ground improvement techniques (such as densification) versus increasing the stiffness of the proposed foundation (by increasing the flexural rigidity or installing piles) in terms of the foundation-soil system performance.

These points hinge on the central findings of the respective case study: densification methods may worsen the stiffness of a cemented soil profile, rendering further remediation measures necessary. Therefore, extensive early valuations in terms of the material and time costs of the remediation method chosen should be carried out. The adoption of a piled gravity foundation could have been more reliable and less time consuming and costly than the dynamic compaction processes conducted, however, this statement cannot be substantiated based on a lack of data.

8.6 SUMMARY

1. Pedocretes are classified as materials which have undergone cementation and/or replacement by an authigenic material, such as calcium carbonate (calcrete), iron-oxide (ferricrete) and silica-oxide (silcretes). The development of pedocretes is a function of the climatic conditions, which in turn dictates the distribution of pedocretes. The climatic conditions of western South Africa make it particularly susceptible to the formation of pedocretes.
2. The geotechnical properties of pedocretes vary considerably, based on the type of host material, nature of authigenic agent and most importantly, the stage of development. The sequential nature of pedocrete formation renders pedocrete layers as highly variable, ranging from loose calcareous/ferruginous/silicified sands and powder pedocretes to hardpan and pedocrete boulder horizons.
3. The plasticity properties of pedocrete also vary widely. Expansive material has been encountered in powder calcrete and ferricrete horizons. Also, pedocrete materials often exude negative shrinkage indices. Critically, the plasticity indices of pedocretes, and the testing thereof, are challenging because the very process of sampling, drying, grading and testing alters the natural structure of the material, rendering it to behave differently under test than in-situ.
4. Founding on pedocrete requires overcoming the challenges presented by their inherent lateral variability as well as with respect to depth. Methods of achieving this were introduced, where the following key points were noted:
    - The utilisation of hardpan layers, below foundations, to produce a rafting mechanism below foundations should be done with extreme caution, due to the lateral variability of the material and the negative influence that shallow rigid layers have on the damping properties of foundations.
    - The assessment of lateral variability and collapse potential are two fundamental aspects of mitigating differential settlement of wind turbine foundations.

This was a qualitative view of the process and challenges of founding structures on pedocrete materials. This was done in view of the proposed wind farm development along the western coast and interior of South Africa, coupled with this region‘s suitability to the formation of pedocretes. The following chapter builds on the afore-mentioned properties and behaviour of pedocretes and addresses the key issue to foundation design: assessing soil stiffness.

9. ASSESSING THE STIFFNESS OF PEDOCRETE SOILS

9.1 INTRODUCTION

Throughout the preceding chapters the terms *stiffness* and *damping* have been referred to extensively with regard to the response of the foundation-soil systems under load. Stiffness refers to a material's compressibility (or strains) at working loads, as opposed to strength which is associated with the ultimate load bearing capacity of the material (Russell, 2012). The parameters describing stiffness and damping, constitutive models, and their integral role in the elastic response of foundation-soil systems under load have also been defined in terms of the shear modulus, G, and damping ratio, ζ. However, a critical question has emerged as a result: how can these parameters be determined? Addressing this question in the context of Southern African pedocretes is challenging, given inherent variability of these materials and the inappropriateness of certain methods of assessing soil stiffness. Following discussions with practicing engineers in South Africa revealed that the state of South African geotechnical laboratories, although improving, currently lags behind those of developed nations due to a lack of equipment and funding as well as qualified and experienced personnel with the necessary skills and experience to conduct stiffness testing of soils is apparent. Factors, such as these, have led to much of the complex geotechnical testing for South African institutions being conducted overseas. This needs to be accounted for when assessing the stiffness of founding soils for wind farms in South *Africa.*

The determination of the shear modulus and damping coefficient in pedocrete materials was the focus of the following chapter, and this was done by addressing three key components upon which the stiffness of soils depend:

1. The strain dependency of soils and rate of loading;
2. The in-situ stress and drainage conditions;
3. The anticipated geological conditions.

The strain dependent nature of soils was discussed in chapters 5 and 6, where it was emphasised that the strength and deformation characteristics were dependent on the level of shear strain induced in the material and the rate of loading. Leading on from this is the importance of selecting a test method which aligns with the level of strain that the foundation will operate under. Different test procedures and their operative levels of shear strain are illustrated schematically by Figure 9.1.

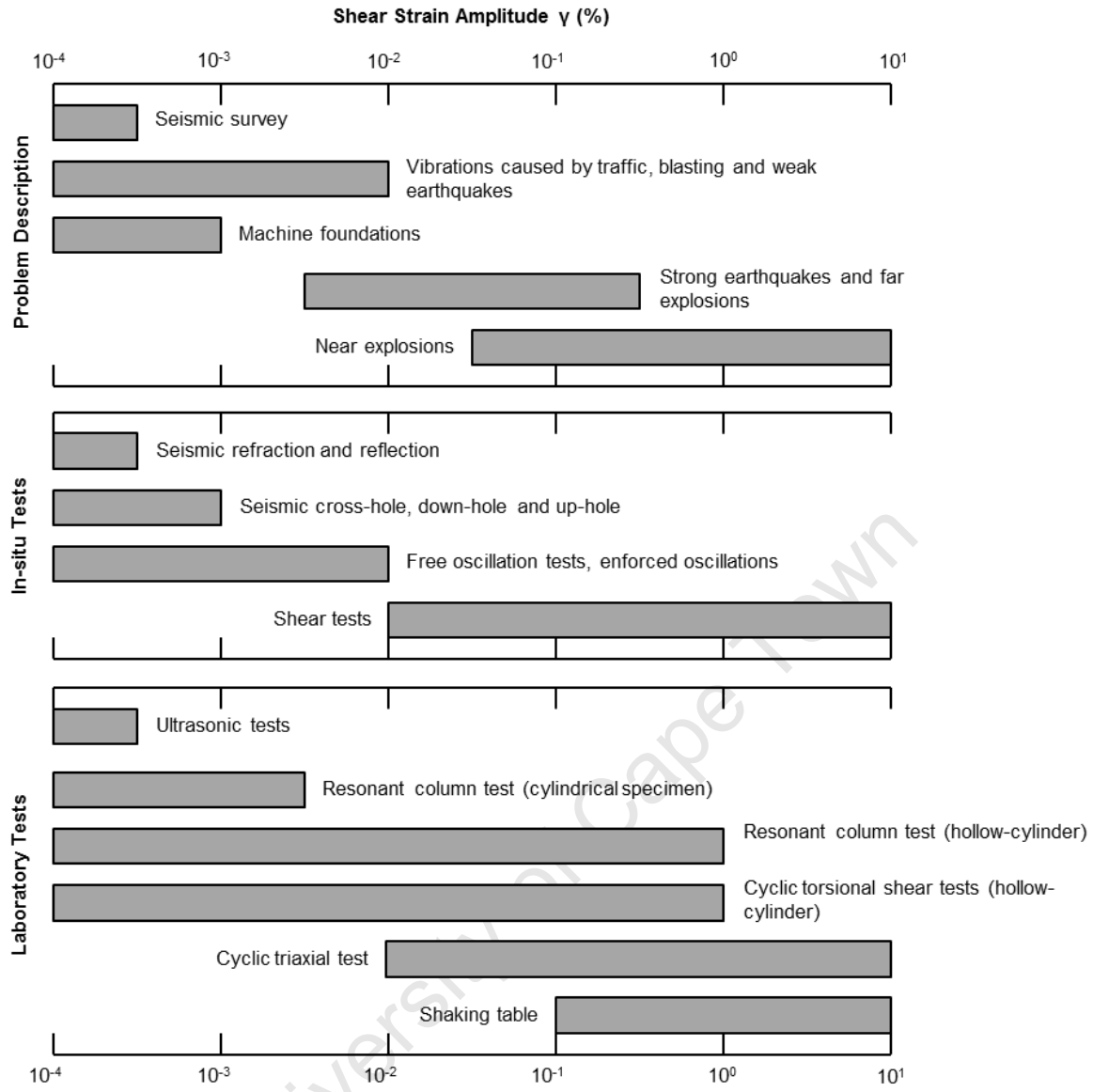

Figure 9.1 **Overview of shear strain amplitudes with respect to dynamic soil property tests (Karl, 2005)**

The constitutive model used to assess the response of the foundation-soil systems is integral to the selection of a test procedure. In the case of wind turbines, an elastic constitutive model is generally adopted based on the level of shear strain generally being constrained below the elastic threshold. Thus, the determination of G_{max}, coupled with the hyperbolic or R-O model is regarded as sufficient to assess the foundation performance, as previously discussed.

Secondly, the selected method of testing should emulate the in-situ stress conditions, as well as the nature of the drainage. Lastly, the selected method of analysis should align with the geological conditions on site.

This is a component dependent on the designer's experience with the area of investigation, and may often be a trial and error process. With this in mind, the determination of the maximum shear modulus (G_{max}) within pedocrete materials is the major focus herein, as this parameter is the most relevant to wind turbine foundations. The determination of damping properties is also alluded to.

Material constituent geotechnical parameters, which are independent of the in-situ characteristics, are also required in wind turbine foundation design. However, these are not discussed here, given the extensive experience and knowledge of the tests required for such parameters.

Fundamental geological considerations pertaining to the determination of soil stiffness are firstly presented. Following this, in-situ methods for determining the stiffness at small strains are explored, with focus on geophysical methods. Laboratory techniques are discussed last.

9.2 GEOLOGICAL CONSIDERATIONS IN THE ASSESSMENT OF SUBGRADE STIFFNESS

The principal geotechnical parameters affecting soil stiffness were included in the definition of the dynamic soil parameters in §6.4. The challenge for the practising engineer, however, is to be able to recognise specific complexities of soil and rock behaviour and to devise a computational and design strategy to overcome the conditions in a satisfactory and simple manner. This requires the translation of theoretical soil and rock mechanics parameters to physical geological processes and attributes and *vice-versa*. In doing so, one should be able to recognise the geological factors most critical in the determination and interpretation of ground stiffness, and hence the safety and economy of the project. The six most critical attributes, as defined by Clayton (1999) are explored below within the context of pedocretes and associated materials such as aeolian deposits.

9.2.1 Structure and Non-homogeneity

The development of stiffness stems directly from the respective material's depositional environment and the development of structure over time. The depositional environment of a soil is directly dependent on the climate of the region and the mode of deposition. These factors coupled with diagenesis results in structure being of key engineering significance for the following reasons:

1. Early diagenesis can result in the preservation of large void ratios, commonly known as ~~"l~~locked in pores", which may result in large strains when the material yields.
2. The stress-strain behaviour of the material is significantly different when it becomes de-structured, whether by yielding under load or by physical disturbance during sampling or construction.

The structure of pedocrete materials is highly dependent on the stage of development, and thus generally varies considerably through the soil profile. Furthermore, the effects of consolidation in typical sedimentary deposits generally results in relatively homogeneous lateral profiles. However, strength and stiffness characteristics vary considerably with depth, due to the effects of confining stress on different materials and the physical and chemical weathering of materials over time.

This latter point on variability is exacerbated in pedocretes, which have considerable lateral variability as well as deteriorating soil stiffness with depth, due to the common occurrence of powder pedocrete below and adjacent to hardpan layers and nodular pedocrete. Additionally, §8.3 detailed the influence of sampling and testing procedures on the properties of pedocrete materials, which more often than not, altered the engineering properties of the material due to the disintegration of flocculated silt and clay complexes upon sampling.

Therefore, the structure of pedocretes is highly variable laterally and with respect to depth, resulting in an extremely inhomogeneous material. A testing procedure which incorporates this variability but does not alter the structure of the material is critical.

9.2.2 Discontinuities and Anisotropy

The stiffness of soils is different in the vertical and horizontal planes mainly due to modes of deposition and variations in effective stress, whereby particle orientation plays a central role in stiffness and stress distributions. Cementation of particles further intensifies such anisotropy due to the relative inconsistency of the cementation process and varying stages of development throughout a soil body (Mitchell and Soga, 2005).

It is well known that joints and fissures are generally weaker than the adjacent intact geo-material and they occur in specific orientations. The orientations result in anisotropic effects, and hence the properties of the material need to be assessed in terms of the orientations of the discontinuities and the direction of the proposed loading. Thus, representative stiffness of jointed and fissured material can only be obtained by testing a sufficiently large specimen – usually a volume of at least 6 times the joint or fissure spacing (Clayton, 1999).

This is also true for pedocretes, such as calcrete, as the engineering properties may vary between those of calcified sand, to nodular and hardpan pedocretes over short distances. Significant anisotropy may occur, due to the cementation processes, as well as the occurrence of pedocrete in different stages of development in close proximity.

Another critical aspect relating to discontinuities such as these is ensuring that the stress conditions on the face of discontinuities are preserved during testing. This normally requires material to be tested in-situ to ensure sampling and test preparations do not alter the confining stresses which are critical to the material's compressibility characteristics and therefore stiffness.

9.2.3 Non-linear Stress-strain Behaviour and Creep

The stress-strain behaviour of soils and the importance of measuring stiffness at a strain level emulating that of the proposed serviceability and ultimate conditions have already been discussed. It is prudent to expand on this by measuring the degradation of stiffness with loading cycles and increasing strain so that this may be incorporated into the relevant models of design. Furthermore, the time-dependent deformation, or creep, of materials should be accounted for, although to date there is a lack of fundamental theory pertaining to the prediction of soil creep behaviour (Mitchell and Soga, 2005). Nonetheless, to date materials that have been recognised to undergo significant creep (such as peat) have been accounted for accurately, by providing an increased factor of safety against settlement and stiffness degradation under foundations.

The above-mentioned geological factors may be summarised as follows, with regard to the key factors which need to be considered during stiffness measurement:

1. The material should be in an undisturbed state to ensure that the in-situ structure is not altered. Changes in moisture content and effective stress should not have occurred and discontinuity surfaces should not have been opened.
2. The effects of anisotropy and discontinuities should be catered for by testing a sufficiently large volume of material. Furthermore, the number of tests conducted and their locations should be taken into account with respect to the positioning of the structure.
3. The strain levels and drainage conditions during testing should emulate, as closely as possible, those relevant to the in-situ materials.
4. The magnitude and direction of loading should align with that expected during construction and the serviceability conditions of the completed structure.

Furthermore, a significant factor to be considered when working in pedocrete materials is the existence of shallow rigid pedocrete layers, or variable pedocrete profiles with depth. These, along with the prevalence of very stiff/dense materials, boulders, granitic plutons and so on, would render conventional stiffness measurement methods, such as the Cone Penetration Test (CPT), impractical due to the excessive variability associated with such materials.

A testing approach which incorporates both laboratory and in-situ methods is recommended as they have complementary attributes in terms of considering the afore-mentioned geological factors affecting stiffness. However, such an elaborate programme is often not feasible and hence compromises need to be made depending on the material encountered on site. Table 9.1 gives an overview of the advantages and disadvantages of laboratory and field tests with respect to the above geological factors.

Table 9.1 **Attributes of in-situ and laboratory testing procedures**

	In-situ Testing	Laboratory Testing
Advantages	Tests may be carried out on materials where sampling is not possible.	Tests are carried out under controlled conditions and in a regulated environment.
	Results may be obtained quickly.	Stress and strain levels, boundary conditions, drainage and strain levels may all be intricately controlled.
	Large volumes of material may be tested at once.	Magnitudes of effective stress may be obtained easily.
	Estimates of horizontal stiffness may be made.	Effects of stress path and strain level may be studied.
		The bulk modulus may be obtained in a straightforward manner.
Disadvantages	Drainage conditions are not controlled.	Testing requires undisturbed samples.
	Stress paths and strain levels are not easily or accurately measurable.	Test results and interpretation thereof may take considerable time in some cases.
	Pore pressures are not measured meaning that the effective stress is unknown.	

9.3 IN-SITU METHODS

Recent advancements in transducer and sensor technologies have resulted in improved methods for the measurement of very small displacements of soils, and hence the direct measurement of very low shear strains (Clayton, 2011, 1999; Heymann and Clayton, 2001). However, wave propagation techniques are still employed as the conventional means of assessing the elastic properties of soils. A significant reason behind this is the links that may be drawn between wave propagation theory, geophysical testing and the elastic properties of soils (§6.5).

Furthermore, wave propagation techniques are able to give a view of the stiffness properties of the respective soil with respect to depth, even though in some cases it may be just a qualitative view. Table 9.2 gives an overview of the respective methods, which are discussed in more detail in the following sections. The next section describes popular in-situ geotechnical methods used to evaluate soil stiffness, including their applicability, practical challenges and limitations with respect to working in pedocrete materials.

Table 9.2 **Summarised attributes of geophysical methods**

Test Method	Shear strain range	Stress Wave	Depth range	Equipment
Seismic Refraction	Very low shear strain range ($\gamma < 10^{-3}\%$)	P[(1)] & S[(2)]	< 30 m	Geophones; energy source
Seismic Reflection		P & S	> 20 m	
Continuous Surface Wave		R[(3)]	Dependent on frequency. Frequency generally ranges between 5 Hz and 600 Hz	Variable frequency vibrator; geophones; amplifier
Cross-hole		S	Dependent on borehole depth	Borehole rig; energy source; geophones
Up-/Down-hole Tests		S		

(1) Primary/compression wave velocity
(2 Secondary/shear wave velocity
(3) Rayleigh wave velocity

9.3.2 Shallow Seismic Techniques

Shallow seismic techniques may be classified in terms of seismic refraction and reflection, which are based on the notion that the velocity of a seismic wave front is affected by the elastic properties of the medium through which it passes. When the wave front reaches the intersection of two materials a velocity discontinuity is encountered, leading to a portion of the energy being reflected and the remaining energy being refracted. This process is governed by Snell's law, which relates the sine of the angle of incidence (i) and the sine of the angle of the angle of refraction (r) to the respective seismic velocities of the materials involved. Hence, as i increases, r increases faster until the critical angle of incidence (i_c) is reached, which corresponds to $r = 90°$.

$$\frac{sin\ (i)}{sin\ (r)} = \frac{v_1}{v_2} = sin\, i_c \ \ if\ v_2 > v_1 \qquad \textit{Eqn. 9.1}$$

This theory forms the basis of seismic refraction and reflection techniques.

9.3.2.1 Seismic Refraction

Seismic refraction uses the critically refracted, first arrival energy only to determine the elastic properties of the respective material. An energy source generates stress waves that propagate through the medium at a velocity v_1 and an assumed critical angle of incidence, i_c. When these stress waves encounter a material boundary they are propagated along the material boundary at v_2 and refract stress waves back to the surface at the critical angle of incidence, i_c, and at a velocity, v_1.

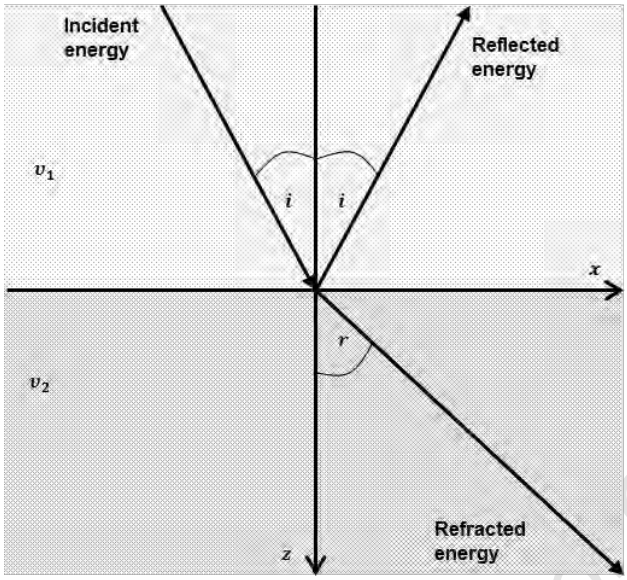

(a)

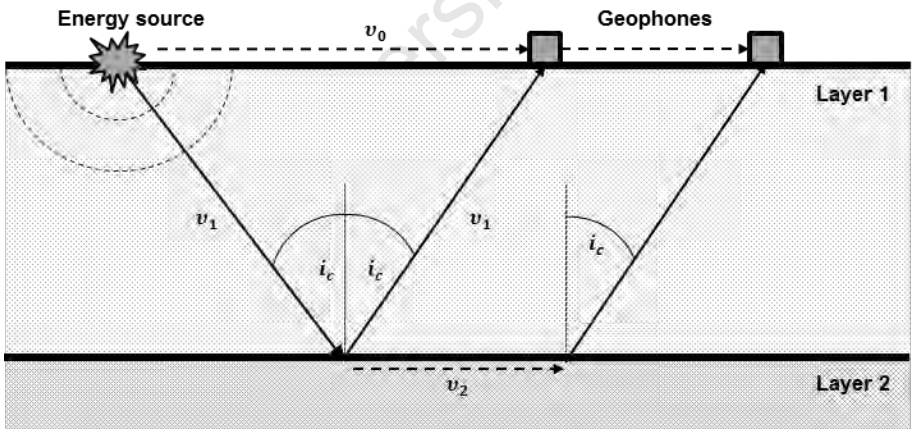

(b)

Figure 9.2 **Seismic refraction: (a) schematic view of reflection and refraction of wave energy and (b) seismic refraction test procedure**

Based on this, the depth of the layers may be determined analytically, from the travel-time and distance between geophones, to give the depth of layers. Expressions for the depth of layers 1 (h_1) is given below (Lippus, 2007).

$$h_1 = \frac{x_c}{2}\sqrt{\frac{v_2 - v_1}{v_2 + v_1}} = \frac{t_{i2} v_1}{2\cos\left[arcsin\left(\frac{v_1}{v_2}\right)\right]} \qquad \textit{Eqn. 9.2}$$

This may be expanded to determine the depth of the second layer (h_2), and subsequent layers:

$$h_2 = \frac{\left[t_{i3} - t_{i2}\frac{\cos\left[arcsin\left(\frac{v_1}{v_3}\right)\right]}{\cos\left[arcsin\left(\frac{v_1}{v_2}\right)\right]}\right] v_2}{2\cos\left[arcsin\left(\frac{v_1}{v_3}\right)\right]} + h_1 \qquad \textit{Eqn. 9.3}$$

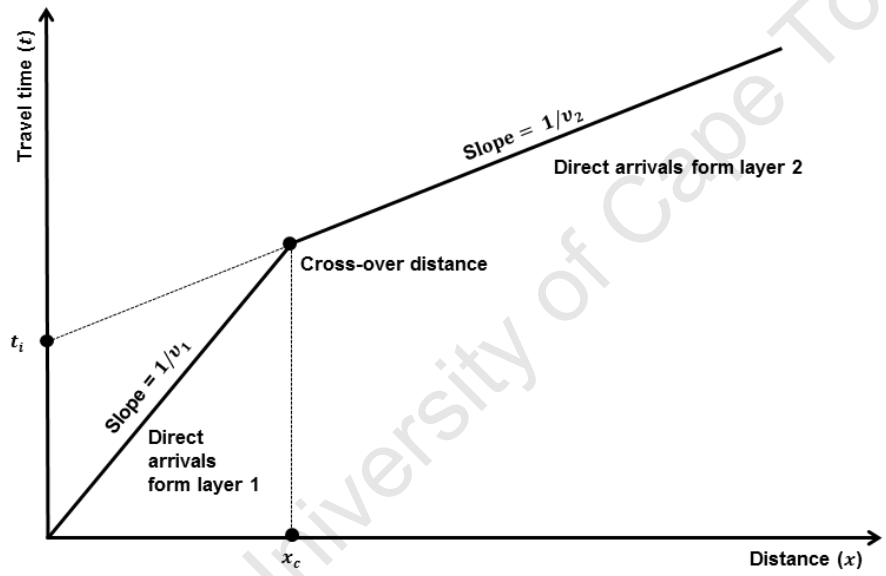

Figure 9.3 **Travel time-distance graph for seismic refraction analysis**

Seismic refraction methods are only accurate for ground conditions where the velocity of the layers increases with depth. For conditions where layers of higher velocity (e.g. saturated clay) overlay lower velocity layers (e.g. loose sand or gravel) the results will be distorted. Thus, seismic refraction may be problematic when used in areas which have variable layers of pedocrete materials. As detailed in Table 8.4, the seismic velocity of powder pedocretes is less than that of hardpans and nodular calcrete layers. Hence, pedocrete layers will generally render the seismic refraction results inaccurate or distorted, at best. Furthermore, this technique is only effective for depths up to 30 m.

Therefore, the seismic refraction method is a useful technique for assessing the general properties of the area under study and is predominantly used to determine the properties of deep transported soil deposits, depth to bedrock, faulting, disturbed zones and to assess landfilled areas and backfilled quarries (Reynolds, 2012).

9.3.2.2 Seismic Reflection

The seismic reflection testing method employs similar equipment and testing procedures to the seismic refraction method. However, the test method utilises data processing procedures which maximise the energy waves in the vertical direction. This results in near vertical stress waves being transmitted through the soil body, and reflected back to the geophones placed on the surface. The main advantage to this technique is that it can be utilised in soil deposits with layers comprising of significantly different stiffness (and hence characteristic wave velocities) and to great depths.

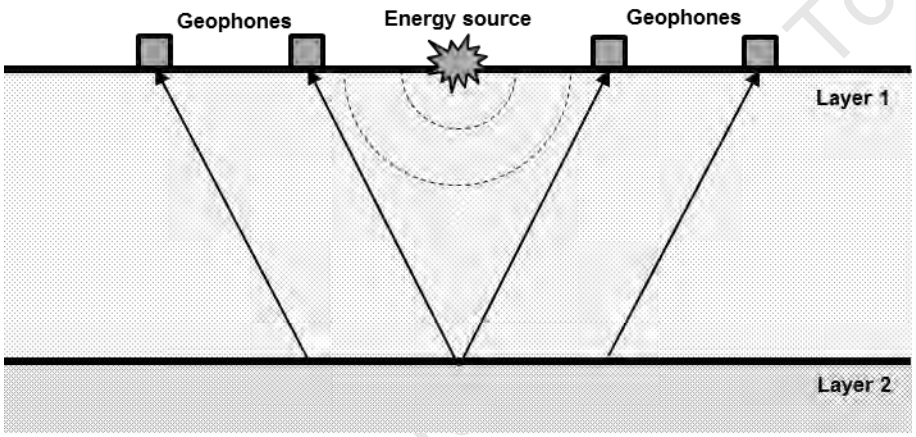

Figure 9.4 **Schematic view of seismic reflection survey**

Specific details of this method will not be studied here due to practical shortcomings which make it unsuitable for the assessment of soil stiffness for shallow foundations. These include:

1. The seismic reflection method is only feasible for the assessment of deep soil bodies (deeper than 20 m) due to the interference from surface activity (such as sound waves and vibrations from machinery) when shallow horizons are investigated.
2. Also, the reflection method is significantly more expensive than seismic refraction. Thus, the seismic reflection techniques are commonly used to determine the thickness of deep deposits of transported soils, and for other applications such as mineral prospecting and offshore applications.

Therefore, shallow seismic techniques are useful for the characterisation of the subsurface, but significant anomalies are introduced when an attempt is made to determine detailed geotechnical data from such tests. The Continuous Surface Wave test is one such method which has been developed in recent years to address this problem associated with the more traditional methods based on refraction and reflection.

9.3.2.3 Continuous Surface Wave Testing

Surface wave tests incorporate a body of methods which are centred on the generation and measurement of surface shear and Rayleigh waves. Of particular interest is the Continuous Surface Wave Test (CSW), which involves the measurement of Rayleigh wave velocity and length produced by a source of variable frequency. The wave length can be altered by controlling the frequency, f, at which waves are produced, and hence different depths of interest may be investigated to determine a dispersion curve.

This is in contrast to other surface wave techniques, such as Spectral Analysis of Surface Waves (SASW) and Multi-channel Analysis of Surface Waves (MASW), which typically use an impact source to generate the seismic waves. Thus, the frequency of stress waves produced by these methods cannot be regulated, and so the depth of analysis is relatively fixed.

The CSW test involves uses an array of geophones radiating away from the source at set intervals, d, to detect the stress waves by measuring the vertical oscillation of the ground at the surface, as illustrated below.

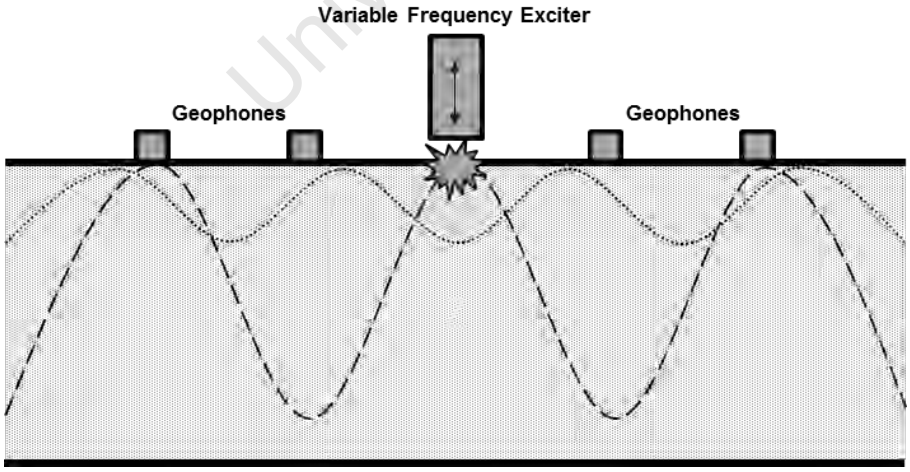

Figure 9.5 **Schematic view of CSW Testing**

The data interpretation process involves the following key steps (Heymann, 2007):

1. The first step of data analysis involves the calculation of the phase angle, ϕ, between each successive geophone using the Fast Fourier Transform algorithm (FFT).
2. Secondly, the phase angle may be used to determine the wave length, given by:

$$\lambda = \frac{d}{\left(n + \frac{\Delta\phi}{2\pi}\right)} \qquad \textit{Eqn. 9.4}$$

where n is an integer of the number of wavelengths between geophones and $\Delta\phi$ is the change in phase angle between successive geophones.

3. A dispersion curve may then be developed by relating the frequency of oscillation to certain wavelengths defined by Eqn. 9.5.

$$v_R = f\lambda \qquad \textit{Eqn. 9.5}$$

Dispersion curves may be used to relate the wave length at specific frequencies to the depth of penetration of the Rayleigh wave, which is generally assumed to be between a half and a third of the wavelength (Gazetas, 1983).

4. The final step relates to the Rayleigh wave profile (dispersion curve) to the stiffness profile of the soil body. This is done using the relationships defined in §6.5, where the shear wave velocity may be determined to be between 0.911 and 0.955 depending on the value of Poisson‘s ratio and the bulk density of the soil (Sutton and Snelling, 1998). A parametric study may be conducted to evaluate the influence of different combinations of Poisson‘s ratio and bulk density, but the influence of these parameters are generally regarded as insignificant compared to the shear wave velocity (Heymann, 2007).

The CSW test is non-intrusive and non-destructive, which makes it particularly appealing to foundation investigations and other civil engineering applications. Additionally, the test is relatively cost efficient and quick to perform, where up to 4 profiles a day may be achieved (Heymann, 2007). These positive qualities have been exemplified by the extensive use of CSW testing in South Africa for applications such as determining the liquefaction potential of tailings dams and the relationship between shear wave velocity and void ratio (Chang and Heymann, 2005).

More recently, CSW techniques have been utilised in the development of wind farms because of the relatively short time span each test takes, as well as the fact that CSW tests give an indication of stiffness variation with respect to depth (Parrock, 2013). Pequenino & Van der Merwe (2013) also showed the benefit of the CSW method through various applications throughout South Africa.

These included the use of the CSW method to confirm or supplement other site investigation results, and most importantly, assess the nature of the respective geology with respect to depth where samples could not be recovered. Furthermore, the CSW method was used to provide the stiffness profile of a highly variable alluvial profile, where sampling would have been obsolete due to the variable nature of the soil (Pequenino and van der Merwe, 2013).

Therefore, the CSW test overcomes many of the challenges presented by pedocrete soil profiles, including:

1. The highly inhomogeneous soil profile may be assessed with respect to depth without having to disturb the respective soil.
2. Large areas may be assessed and hence variability over a proposed foundation footprint determined.

Although the depth of influence may be adjusted, CSW testing is best suited for the analysis of shallow soils based on results being most accurate at high frequencies of oscillation. Furthermore, using the CSW method in circumstances of high variability, although possible, should be done with extreme caution because the relationship between wavelength and depth is incapable of identifying rapid changes in stiffness (Sutton and Snelling, 1998). For example, the stark contrast in stiffness between a nodular pedocrete, powder pedocrete and underlying transported soils may be misinterpreted by the extrapolation of the dispersion curve. Hence, pedocrete profiles may require CSW to be done in conjunction with borehole tests and/or with the aid of FEM modelling, using back analyses from the ground motions.

Seismic methods have also been shown to offer good approximations for the damping properties of soils. Haddad and Shafabakhsh (2007) illustrated how the surface attenuation coefficient, which is a function of the frequency and damping ratio, and defined as follows:

$$\zeta = \frac{\alpha V}{2\pi f} \qquad \textit{Eqn. 9.6}$$

α denotes the attenuation coefficient, v_R is the velocity of the Rayleigh wave propagation and f is the frequency of oscillation. This expression combined with inversion theory may be used to determine ζ.

Such applications of the CSW method pose thought provoking prospects in the field of soil dynamics, based on the CSW method overcoming many of the limitations of other in-situ methods, along with its ease of application and time efficiency.

9.3.3 Borehole Tests

9.3.3.1 Seismic Cross-hole Test

The seismic cross-hole test is highly effective for determining the variation of ground stiffness with depth, as the test involves the generation of shear stress waves within or at the bottom of a borehole. The waves propagate through the soil body and the travel time-distance relationship is recorded by geophones placed within a second borehole which is drilled some distance away from the energy source. Therefore, this test requires at least two boreholes to be drilled and the energy source should be rich in shearing energy to ensure that the arrival of the shear wave may be differentiated from the compression waves generated (Luna and Jadi, 2000).

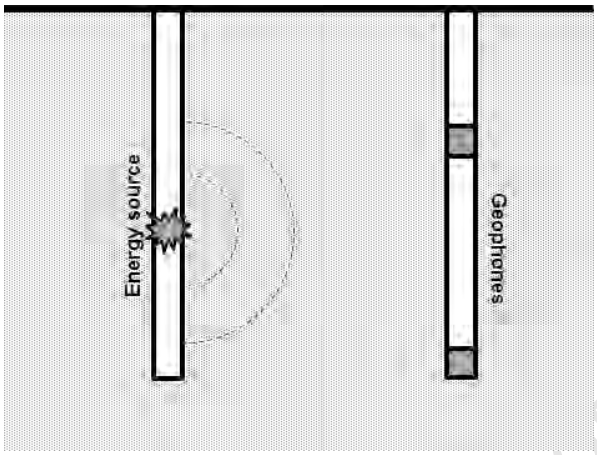

Figure 9.6 **Seismic cross-hole test**

9.3.3.2 Seismic Down-hole and Up-hole Test

The down-hole and up-hole technique is similar in principle to the cross-hole method, but more efficient as only one borehole is required. The down-hole test involves the generation of an impulse at the ground surface, the characteristics of which are then measured by geophones placed at predetermined depths within a borehole extending the depth of investigation. The up-hole method is the opposite, whereby an impulse is generated at different depths within the borehole and the time to distance relations are determined by an array of geophones placed at the ground surface. In connection with seismic borehole tests are the general benefits associated with the opportunity to log and sample the soil profile and to monitor groundwater levels. Furthermore, the use of the standard penetration test (SPT) (which is generally conducted during the drilling of boreholes in South Africa), and its relation to the shear wave velocity of the profile may be of use to the design engineer.

The root of SPT "N"-shear modulus correlations lie in the prediction of liquefaction potential, or rather, ground characterisation, as opposed to specific geotechnical parameter measurement. Considerable work has been done to improve such correlations (Akin et al., 2011; Anbazhagan et al., 2012; Bolton Seed et al., 1986; Schmertmann, 1978), however, by no means should design calculations be based on such methods. Rather, the SPT may be used as a tool to provide input to the design process, against which geophysical and laboratory tests may be compared and supplemented.

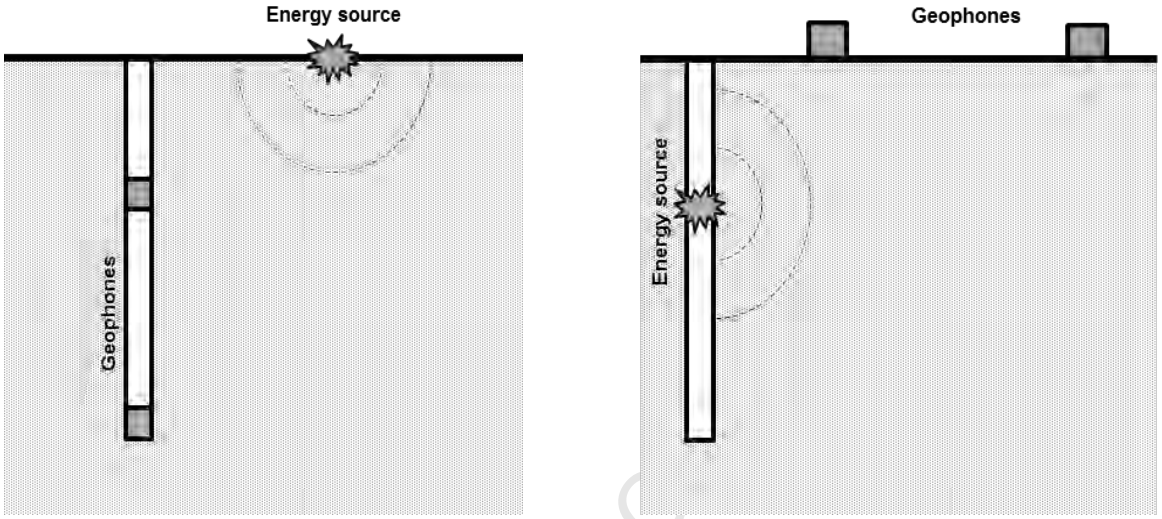

(a) **(b)**

Figure 9.7 **Comparison of borehole methods: (a) down-hole test and (b) up-hole test**

9.4 OVERVIEW OF LABORATORY METHODS

To assess stiffness in the laboratory undisturbed samples of the highest quality are required, along with specialised instrumentation and most importantly, an operator with high levels of knowledge and experience.

For these reasons, in-situ methods are generally preferred in South Africa, based on a lack of personnel capable of conducting the sophisticated tests accurately and consistently, coupled with a lack of laboratory facilities. However, this is most likely due to the suitability of in-situ tests to the highly variable materials of the arid Southern Africa, such as pedocretes. Yet, a major negative attribute of in-situ methods is their inability to directly assess the non-linear stress-strain behaviour of soils. This is because geophysical methods operate within the elastic material range. Certain circumstances may require the stiffness degradation properties of the respective subgrade to be determined directly, such as investigations into the stiffness properties of certain nodular pedocretes or cemented sands. Also, field methods are generally incapable of accurately predicting the damping properties of soils given the operating shear strain ranges.

For reasons such as these, an overview of common laboratory methods used to assess soil stiffness is given below. This was not intended as an in depth discourse on laboratory testing, but rather aimed to provide insight into common tests and their respective advantages and limitations. These tests include cyclic methods, the resonant column test and tests incorporating bender elements.

The first step in assessing laboratory test procedures is to understand the strain levels at which these tests operate. These are vastly different, as illustrated by Figure 9.8, which shows their strain level with respect to soil behaviour and wind turbine loading. Hence, laboratory methods afford the designer the option of assessing the soil behaviour under different stress-strain conditions, and may thus may provide valuable input to the design process, when combined with in-situ methods and constitutive relationships.

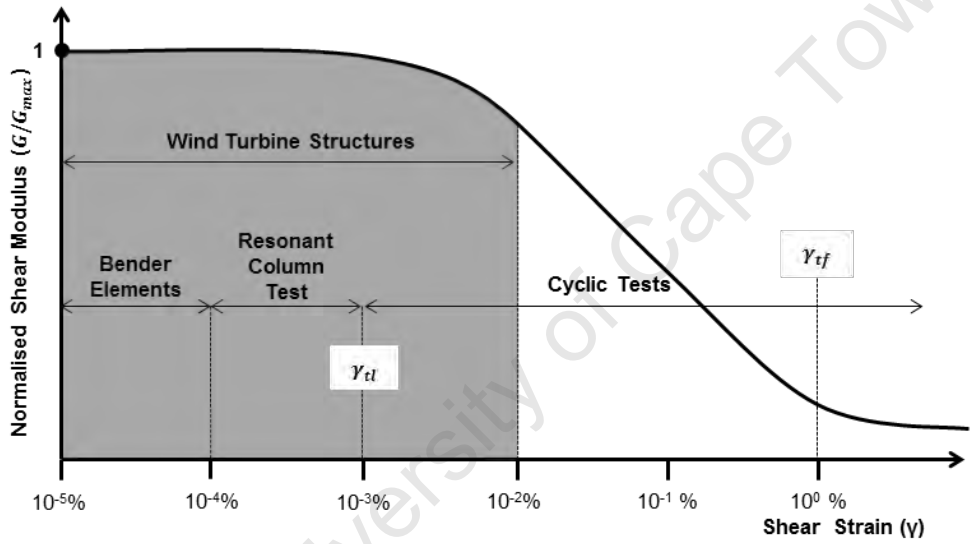

Figure 9.8 **Common strain ranges for laboratory tests with respect to soil behaviour and (Russell, 2012)**

9.4.2 Piezoelectric Bender and Compression Element Tests

Bender elements are a powerful and increasingly common method of measuring the shear wave velocity, and hence G_{max}, of an undisturbed soil sample normally done beyond the resolution of local small strain instrumentation.

Transmitter and receiver piezoelectric elements are placed at each end of a specimen to assess the stiffness by means of wave propagation. Piezoelectric materials exhibit a change in dimension when subjected to a voltage, and, similarly, produce a voltage across their faces when undergoing distortion (Karl, 2005). Thus, such elements may be used to produce stress waves through materials, where the propagation thereof may be measured by arrival time-distance relations.

Bender elements penetrate several millimetres into the specimen and oscillate laterally under changes in voltage, thus producing shear waves through the sample. Compression waves may be generated by compression elements which do not penetrate the sample.

There are several advantages to this technique, the most prominent being its simplicity and adaptability. However, there is no standard method for this technique, as interpretation of the results is often subjective with high uncertainty (Ferreira et al., 2006).

9.4.3 Resonant Column Test

The resonant column test is used to determine the shear moduli and damping characteristics of soils at very small strain amplitudes. This is based on the one dimensional wave propagation theory. An electromagnetic oscillator placed at the top of a triaxial cell applies a torsional/rotational load, of variable frequency, to the top of the sample in order to find the resonant frequency of the material at a controlled stress (Russell, 2012). A typical resonant column device is illustrated by Figure 9.9.

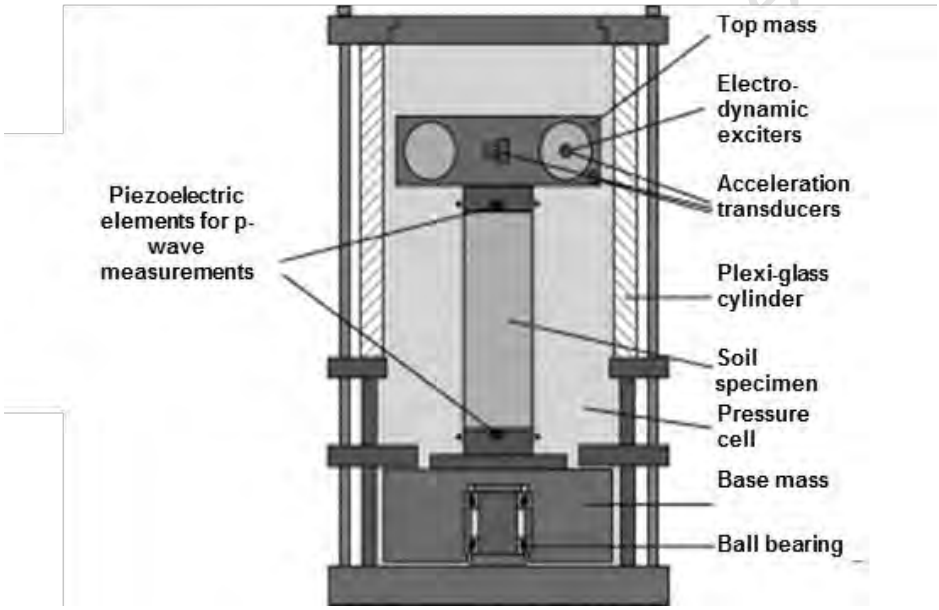

Figure 9.9 **Resonant column device**

The elastic properties of the material are then determined from the resonant frequency and one dimensional wave propagation theory, described by Eqn. 9.7 from Hoadley (1984) after Richart, Hall & Woods (1970).

$$G = 4\pi^2 \rho \left(\frac{f_r l}{F}\right) \qquad \textit{Eqn. 9.7}$$

ρ denotes the density of the material, l the length of the specimen and f_r the resonant frequency and F; which denotes a correction factor which depends on the specific apparatus used (the damping and hence resonant frequency of materials is affected by the damping properties of the apparatus used, and each testing device has different properties). Hoadley (1984) described the essential equations and processes required to perform the calibration to determine F.

The damping properties of the soil may be found upon removal of the applied loading, and the simultaneous monitoring of successive amplitudes of free vibration.

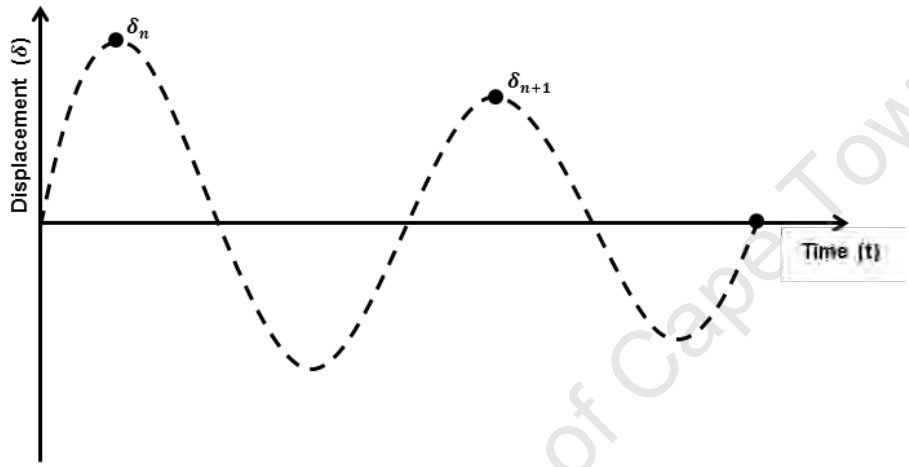

Figure 9.10 **Free vibration of soil sample**

If δ_n and δ_{n+1} are two successive amplitudes of vibration, then the logarithmic decrement may be used to determine the material damping properties of the soil using the following expression (Chowdhury and Dasgupta, 2009; Ishibashi and Zhang, 1993):

$$\zeta_m = \frac{ln\left(\frac{\delta_n}{\delta_{n+1}}\right)}{\sqrt{4\pi^2 + \left(\frac{\delta_n}{\delta_{n+1}}\right)^2}} \qquad \textit{Eqn. 9.8}$$

Note that ζ_m denotes the material damping of the system where, the total damping ratio is the sum of the material and geometric damping terms. The geometric damping ratios were studied in Chapter 7, where it was shown that the radial decay of energy away from a point source was a function of the mass and inertia of the respective system, and was critical for translational modes of vibration. The design of wind turbine structures, which are susceptible to coupled rocking and sliding, therefore require cognisance of the material damping as well as the geometric damping terms.

9.4.4 Cyclic Tests

Cyclic tests stemmed from the need to assess the liquefaction potential of soils, but subsequently proved to be useful in determining the elastic stiffness properties and damping parameters of a soil as well. The three most common cyclic tests are discussed below.

9.4.4.1 Cyclic Triaxial Test

An triaxial cell (Figure 9.11) is used to initially consolidate the material sample under an initial cell pressure, σ_a. A cyclic axial loading unit then subjects the sample to an increase in the axial stress and a simultaneous decrease in the cell stress of the same magnitude. This process induces a shearing stress in the sample but maintains a constant normal stress on the respective shear plane, as illustrated by Figure 9.12.

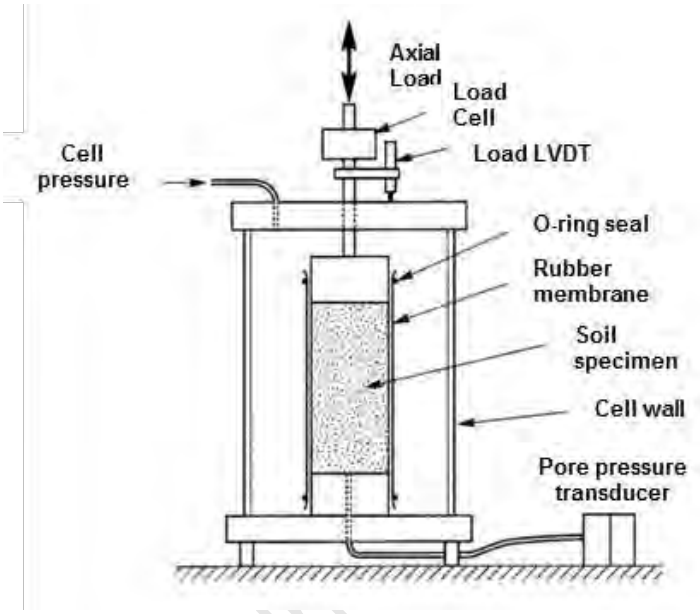

Figure 9.11 **Typical cyclic triaxial device**

The axial stress and cell stress increments are then reversed by the same magnitude, to reverse the direction of the shearing stress without altering the normal stress on the plane 45 degrees to the longitudinal axis. This allows one to determine the Young‘s modulus from the relationship between the axial stress and strain, and the shear modulus determined subsequently from elastic relations. Critically, this test affords the opportunity to analyse the pore water pressure, effective stress and deformation properties as a function of load cycles and damping characteristics are determined from the area of hysteresis loop defined by the loading. Controlling the rate of loading during the test is important. The load cycling should represent that anticipated in the field and must be, typically, in the range of 0.1 Hz to 1 Hz to ensure the results are not misleading (Russell, 2012).

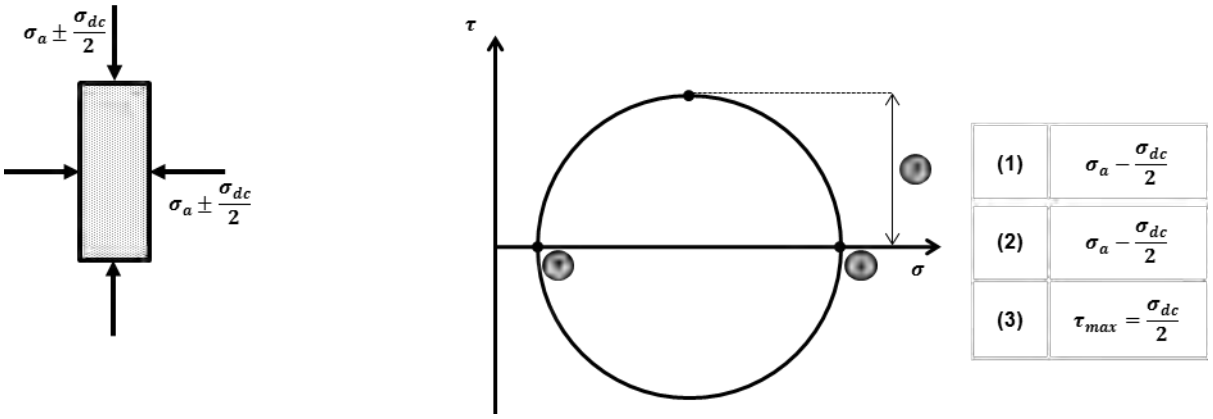

(a) **(b)**

Figure 9.12 **Cyclic triaxial test conditions (a) and corresponding Mohr's circle**

Along with this, the following limitations of the test are important:

1. Shearing strain amplitudes below 0.01% are very difficult to measure.
2. The major principle stresses change direction by 90 degrees during each load cycle.
3. The extension and compression of the loading phases yields an asymmetrical hysteresis loop which leads to further measurements and analyses being complex.
4. Stress concentrations occur at the cap and base of the specimen.
5. Void ratio redistribution occurs within the sample, which in turn affects pore water pressures and the dissipation thereof.

In conclusion, this test offers a wide range of possibilities in terms of the parameters that may be measured and the behaviour analysed. But, as will be seen with the other laboratory tests, the cyclic triaxial test requires an extremely qualified and experienced operator in order to obtain accurate and meaningful results.

9.4.4.2 Cyclic Simple Shear Test

The cyclic simple shear tests utilise a modified direct shear box. Within the device a cylindrical sample of soil is constrained within a wire-reinforced rubber membrane. The sample base is then placed on a sliding table where the sample cap is fixed. Hence the cap is restrained from horizontal motion, but is allowed to move vertically, as shown schematically in Figure 9.13. Like the shear test, a vertical load is then applied to the sample, and the sliding table is driven to produce cyclic strains in the region of 10^{-3}% to 10^{1}%. The test is conducted under constant volume conditions for a saturated specimen. Therefore, the test is conducted in two phases: (1) the consolidation phase and (2) shearing phase. Hence, the test is most applicable to conditions where the soils have consolidated fully under

the in-situ stresses, and then are subjected to changes in stress where there is insufficient time for further consolidation to occur (Russell, 2012).

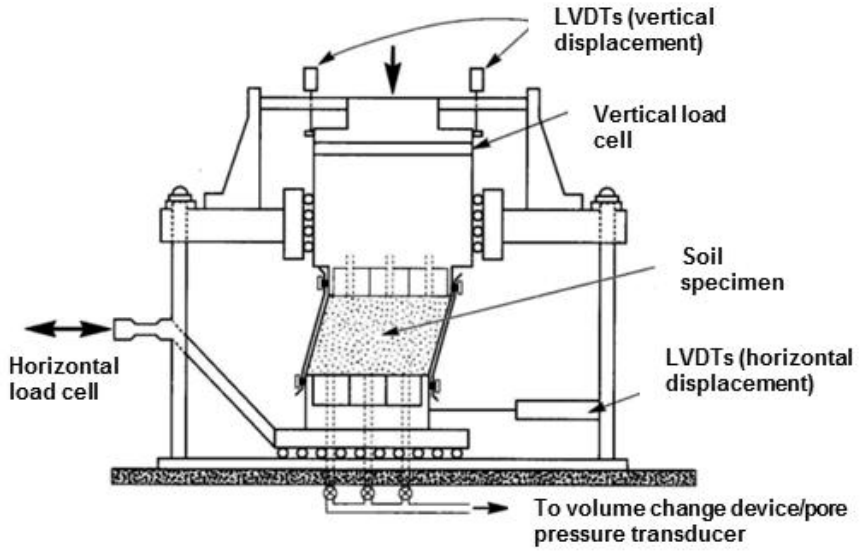

Figure 9.13 **Typical cyclic simple shear box device**

The cyclic simple shear test overcomes the limitations of the cyclic triaxial test by better defining the actual stress conditions encountered in the field when subjected to dynamic loads. However, the shear stresses are only applied at the top and bottom of the sample, due to the boundary conditions.

9.4.4.3 Cyclic Torsional Shear Test

The cyclic torsional shear test is particularly useful for evaluating the effect of the first few cycles of stress repetitions, and thereafter for assessing the effects of higher amplitude shearing strains and their influence on reductions of G from G_{max} (Hoadley, 1984). The test is performed on a hollow cylindrical sample of soil. Firstly, the sample is constrained by the application of an axial load until the desired coefficient of lateral earth pressure is reached. The sample is then sheared with an applied torque. The frequency of the axial loading and torque may be adjusted over time to represent the conditions to be expected in the field.

A test of this nature reproduces the field conditions of a dynamically loaded soil more closely because the planes of principle stress are able to vary and the whole sample is subjected to shearing. Hence, this test overcomes the drawbacks of the two previously mentioned dynamic testing methods (Karl, 2005). The cyclic torsional shear test is predominantly used in research, or for advanced numerical analyses, as the parameters derived are often superfluous in general geotechnical engineering applications.

9.5 SUMMARY

The assessment of soil stiffness may be seen as an art as much as it is a science, as it requires the consideration of a multitude of factors which need to be accounted for in the testing process, in order to yield results which are accurate and relevant to the geotechnical design. This chapter explored such considerations, by firstly assessing the strain dependency of soils in terms of methods used to evaluate soil stiffness. Secondly, geological factors influencing the stiffness of soils, and the measurement thereof were presented. These included:

1. Bonding and structure, which play a significant role in the pore characteristics of soils and the nature of particle interfaces. It was also noted that the structure of a material undergoes changes upon sampling and testing, and therefore these disturbances should be minimised to yield accurate stiffness results. This point is especially relevant to pedocretes, which undergo significant structural changes upon disturbance, as discussed in chapter 8.
2. Anisotropy and the effects of discontinuities are important considerations when determining the volume of material to be assessed, the number of samples and their respective locations. This is in view of ensuring that the variability of soils is accounted for in the testing process.
3. Lastly, the strain levels, stress conditions and drainage characteristics should be emulated by the testing procedure, as these all intricately affect soil stiffness.

Therefore, it was concluded that in-situ methods were the most appropriate means of assessing the stiffness of pedocrete materials in South Africa. Not only because of the extreme variability of these materials, but also due to the lack of advanced reliable laboratory equipment in South Africa. The following important points were noted:

1. The existence of discontinuous rigid layers rendered seismic refraction unsuitable due to Snell‘s law, as a function of the critical angle of incidence, being violated. Seismic reflection was also seen as unsuitable due to its range of influence ignoring the shallow materials and possibly yielding highly distorted results.

2. Continuous Surface Wave (CSW) testing was deemed highly suitable to applications in South Africa, with a number of known studies already conducted. Due to the ability of CSW testing to vary the depth of influence to produce stiffness profiles as a function of depth. Also the fact that CSW relatively cost and time efficient was seen as highly beneficial.
3. Borehole methods, including cross-hole, down-hole and up-hole methods were also deemed possible, but redundant, given the advances and positive attributes of CSW testing.

An overview of laboratory techniques was provided to give insight into how the strain-dependent shear modulus and damping properties of soils could be assessed. Cyclic tests, the resonant column test and stiffness determination by bender elements were all addressed. A major advantage of these tests is their ability to determine the material damping properties of soils and the stiffness degradation at higher strain levels.

Therefore, the stiffness evaluation of pedocrete materials with characteristics such as shallow rigid layers, variable density profiles with depth, the prevalence of very stiff/dense nodular/boulder materials, as well as associated materials such as collapsible aeolian sands and granitic plutons, means an holistic approach should be adopted to ensure the variability of the profile is encapsulated with minimal disturbance to the material‘s structure.

10. CONCLUSIONS

10.1 INTRODUCTION

Wind energy has been deemed an appropriate means of diversifying South Africa‘s energy mix while simultaneously addressing the deficit in electricity supply which the country faces. With this, extensive wind farm development was proposed for the Western, Northern and Eastern Capes of South Africa. Against this backdrop of imminent development, this study aimed to provide insight into the geotechnical design of wind turbine foundations under South African soil conditions. Pedocretes and associated materials, such as aeolian sands, were of specific interest, as these materials prevalent to the western and northern regions of South Africa. Importantly, these materials were deemed to poses vastly different engineering characteristics to the soils of more temperate climates, upon which much of the theory of soil mechanics and geotechnical testing is based, and from which the majority of experience on wind turbine foundation behaviour was derived.

Therefore, the site-specific design of wind turbine foundations was the major theme of this study, which has divided into four sub-themes, or parts, the key point of which are given below.

10.2 MECHANICS, DYNAMICS AND FOUNDATION BEHAVIOUR

The mechanics, dynamics and foundation behaviour of wind turbines was addressed in Part I, which aimed to define the major considerations required by the foundation designer in terms of the type and nature of the wind turbine loads, and qualitatively, how these loads affected the foundation.

Wind turbines were classified as slender members of low stiffness and with a rotating mass excitation at the free end. Due to the environmental loading of the structure, and the loads induced by its operation, wind turbine foundations were characterised as low frequency machine foundations, which are required to resist a substantial overturning moment. It is this combination of factors, coupled with the relatively low axial load of the structure, which makes conducting a thorough foundation design critical.

Fundamental to wind turbine structures and foundation design was the assessment of the dynamic response of the structure, and in doing so, ensuring that the natural frequency of the tower-foundation-soil system did not intersect the 1P or 3P frequencies of the turbine. It was shown that the foundation-soil system caused the natural frequency of the system to decrease, and hence approach the 1P frequency of the turbine, for soft-stiff towers. This was regarded as the critical case to be avoided.

Further loading considerations included the substantial overturning moment produced by the height and slenderness of the structure, coupled with its relatively minor weight and dynamic nature. It was noted that, due to the dynamic nature of the structure, that the wind turbine would experience aerodynamic loads greater than what would be expected from a static structure of equal cross-section.

To ensure stability of the structure, these loads are transferred to the foundation, the characteristics of which need to be capable of supporting the wind turbine superstructure through highly variable loading conditions for the duration of its service life. Two major themes were presented in order to achieve this: (1) strength and stability and (2) settlement and stiffness).

10.3 GEOTECHNICAL DESIGN OF WIND TURBINE FOUNDATIONS

Part II presented the geotechnical design of shallow foundations, with topics relevant to the loading and load transfer mechanisms highlighted in Part I.

10.3.1 Strength and Stability

Strength and stability considerations were centred on the generalised bearing capacity theory, which was combined with the equivalent effective area and inclined load approaches to account for the combination of monotonic loads acting on a foundation.

Plasticity theory and the yield state approach were also introduced to address the limitations of the generalised bearing capacity theory: namely, its inability to assess progressive failure and the rudimentary empirical relationships upon which it is based.

This framework for assessing shallow foundations under combined loads allows the ultimate limit state of the foundation to be assessed with respect to combinations of loads. Thus critical load combinations may be assessed, where it was found that $H \approx V_{max}/8$ and $M/2R \approx V_{max}/11$ were sufficient to cause overturning (Butterfield and Gottardi, 1994).

10.3.2 Settlement and Stiffness

The assessment of differential settlement and the minimisation thereof, under monotonic working conditions, is central to wind turbine foundation design. Tall slender structures such as wind turbines are prone to instability under differential settlement. This is exacerbated by the dynamic loading imposed on the structure. Thus, wind turbine manufacturers impose strict regulations on tilt limits for wind turbines by means of minimal rotational stiffness values.

The following key points were made:

1. The immediate settlement of shallow foundations may be interpreted in terms of elastic displacement theory. Although this theory has shortfalls in terms of the anisotropic, inhomogeneity and non-linear behaviour of soils, if these are understood and taken into account, the immediate settlement may be calculated and used as a proxy for bearing capacity.
2. The linear elastic soil model and the non-linear elastic model were presented with respect to predicting the soil moduli required to evaluate analytical solutions for foundation settlement, such as those derived from the yield surface approach and the elastic half-space theory. The non-linear elastic soil models were based on hyperbolic functions, given their synergy with aspects of soil dynamic presented in the next chapter.

Although these models are highly simplified, they were considered sufficient to emulate the behaviour of wind turbine foundation-soil systems, as the level of shear strain induced by wind turbines may be assumed to lie within the elastic range (DNV/Risø, 2002).

The foundation-soil stiffness relations were shown to be useful in the assessment of the suitability of different differential settlement mitigation measures. Critically, the relationship between foundation-soil stiffness and the improvement offered by including piles in the foundation was found to hinge on the geometrical relationships between the piles and the foundation load carrying capacity.

10.4 DYNAMIC ASPECTS OF WIND TURBINE FOUNDATIONS

Dynamic aspects of wind turbine foundation design were explored in Part III, where relationships between stiffness, mass and frequency were assessed in terms of wind turbine loading regimes.

10.4.1 The Behaviour of Foundation-Soil Systems under Dynamic and Cyclic Loading

The vibrations imposed on wind turbine foundation-soil systems were characterised as a combination of man-made and natural, of long duration within the elastic range of material response. The resulting damage considerations were then characterised in terms of immediate and long term, or fatigue-related, the latter of which was deemed the most critical. This was due to the soil stiffness degradation being proportional to the number of load cycles, as prolonged vibration cause micro-cracks, pore pressure build up, loss of bearing capacity, excessive settlement as well as other consequences not necessarily relevant to foundation design.

Therefore, the definition of the shear modulus with respect to cyclic loading was presented, as well as the respective governing factors. For granular materials there were deemed to be the confining stress

and void ratio, whereas the stiffness of cohesive material hinged mainly on the OCR and PI. The small-strain shear modulus was determined as the principle parameter governing the behaviour of wind turbine foundations. Hence it was concluded that analytical solutions applicable to the serviceability limit states under monotonic loading may be applied to the dynamic assessment of foundations. Furthermore, this fact allowed relationships between wave propagation theory and stiffness measurement to be used. Despite this, appropriate stiffness degradation models were presented to assess the non-linear response of soils under dynamic and cyclic load, accordingly.

10.4.2 The Analysis of Foundations under Dynamic Loading on Elastic media

The relationships constructed by *Lysmer's Analog* between the lumped parameter model and elastic half-space theory were utilised to assess the behaviour of foundations under dynamic loads. A few key points were noted in conjunction with the fundamental relationships summarised in Appendix A:

1. Flexible footings have higher amplitudes of vibration
2. The presence of a rigid layer below a footing increases the amplitude of vibration due to the reflection of stress waves back towards the point source.
3. Torsional and vertical translation of the foundation tends to occur in isolation and may be treated as such. The critical mode of vibration is coupled rocking and sliding. Limiting the effects of this mode of vibration requires minimisation of the mass ratio, which is dependent on the geometrical parameters of the foundation and affects the geometrical damping of the system considerably.
4. Damping comprises two parts: geometric and material, where the influence of each depends on the mode of vibration. Material damping is negligible at low levels of shear strain and plays a minor role in translatory modes of vibration, but is prominent when the foundation undergoes rocking. Geometric damping is generally associated with translator modes of vibration. Hence, wind turbines, which are susceptible to coupled rocking and sliding are dependent on both aspects of damping.

Thus the principle parameters required for the dynamic analysis of a foundation are the shear modulus and damping ratio.

10.5 CONSIDERATIONS FOR WIND TURBINES FOUNDED ON PEDOCRETES

Part IV linked the general considerations studied under the preceding themes to the engineering properties of pedocrete materials, founding considerations and the determination of soil stiffness.

10.5.1 Founding Wind Turbine Structures on Pedocretes

Pedocrete materials are characterised as highly variable in terms of their engineering properties. This is due to their process of formation and diagenesis over time, coupled with varying characteristics of authigenic minerals. Calcrete, ferricrete and silcrete were of specific interest in this study as these forms of pedocrete are prevalent in South Africa. These materials are characterised with respect to the authigenic minerals, which in this case are calcium carbonate, iron oxides and silica. The geotechnical properties of pedocretes vary considerably, based on the type of host material, nature of authigenic agent and most importantly, the stage of development. The sequential nature of pedocrete formation renders pedocrete layers as highly variable, ranging from loose calcareous/ferruginous/silicified sands and powder pedocretes to hardpan and pedocrete boulder horizons.

Furthermore, conventional geotechnical testing of pedocrete materials has concluded that their intrinsic properties are altered upon disturbance, overburden removal, drying out and sampling, making the prediction of engineering characteristics troublesome and results somewhat unreliable.

Founding on pedocrete requires overcoming the challenges presented by their inherent lateral variability as well as with respect to depth. Methods of achieving this were introduced, where the following key points were noted:

1. The utilisation of hardpan layers, below foundations, to produce a rafting mechanism below foundations should be done with extreme caution, due to the lateral variability of the material and the negative influence that shallow rigid layers have on the damping properties of foundations.
2. The assessment of lateral variability and collapse potential are two fundamental aspects of mitigating differential settlement of wind turbine foundations.

10.5.2 Assessing the Stiffness of Pedocrete Soils

The assessment of soil stiffness may be seen as an art as much as it is a science, as it requires the consideration of a multitude of factors which need to be accounted for in the testing process in order to yield results which are accurate and relevant to the geotechnical design.

The following key geological considerations were studied with respect to their influence on material stiffness and hence their influence on testing:

1. Bonding and structure; it was also noted that the structure of a material undergoes changes upon sampling and testing, and therefore these disturbances should be minimised to yield accurate stiffness results. This point is especially relevant to pedocretes, which undergo significant structural changes upon disturbance.
2. The volume of material to be assessed, the number of samples and their respective locations is governed by anisotropy and discontinuities in the material. This is in view of ensuring that the variability of soils is accounted for in the testing process.
3. Lastly, the strain levels, stress conditions and drainage characteristics should be emulated by the testing procedure, as these all intricately affect soil stiffness.

Therefore, it was concluded that in-situ methods were the most appropriate means of assessing the stiffness of pedocrete materials in South Africa. Several conventional geophysical methods were studied. Continuous Surface Wave (CSW) testing was regarded as the most viable and appropriate means of assessing the stiffness of pedocretes. Refraction and reflection surveys were deemed inappropriate due to the highly variable nature of pedocretes, and although borehole method would be applicable, they were considered redundant given the benefits of the CSW procedure.

An overview of laboratory techniques was provided to give insight into how the strain-dependent shear modulus and damping properties of soils could be assessed. Cyclic tests, the resonant column test and stiffness determination by bender elements were all addressed. A major advantage of these tests is their ability to determine the material damping properties of soils and the stiffness degradation at higher strain levels.

10.6 CLOSING REMARKS

This study has approached the site-specific design of wind turbine foundations holistically, from assessing the nature of loads, to the anticipated foundation behaviour, the application of principles from foundation engineering and soil mechanics, structural dynamics and soil dynamics, to provide a consolidated work which may be used to supplement the information prided by wind turbine design codes and manuals. Critically, this thesis related the above bodies of knowledge back to pedocrete materials in South Africa, highlighting key points to account in the design process. In doing so, the benefit bridging the gap between structural engineering and geotechnical engineering during foundation design has been stressed, especially for structures of a complex nature such as wind turbines.

GEOTECHNICAL CONSIDERATIONS FOR ONSHORE WIND TURBINES	
Mechanics, Dynamics and Foundation Behaviour	1) Tower-foundation-soil system must be design such that the natural frequency does not intersect the 1P or 3P frequencies. 2) The dynamic nature of wind turbine structures renders the overturning moment substantially larger than what would be expected from a static structure of equal cross-sectional area.
Geotechnical Design of Shallow Foundations	3) Strength and stability analyses need to ensure the foundation provides a competent connection with the ground, and in doing so the combination of critical loads needs to be assessed. 4) Stiffness and settlement may be assessed based on the theories of elasticity. 5) Increasing foundation stiffness has negligible effect on total settlement, but minimises differential settlement. 6) This may be done by incorporating piles into the foundation (the geometrical proportioning of which is critical to ensure optimisation between load capacity and cost), or by ground improvement (which should be aligned closely with the respective subgrade properties to ensure a reduction in stiffness is not caused).
Dynamic Aspects of Wind Turbine Foundations	7) Wind turbine structures are particularly susceptible to coupled rocking and sliding modes of vibration. Minimisation of this requires minimising the mass ratio. 8) Rigid layers below the foundation impede geometric damping. 9) High foundation stiffness is preferred to reduce amplitudes of vibration. This corresponds to differential settlement considerations.
Considerations for Wind Turbines Founded on Pedocretes	10) The performance of wind turbine foundation hinges on the respective subgrade properties. 11) Pedocrete materials pose specific foundation challenges, including: • Lateral and vertical variability, exacerbating differential settlement problems. • Collapsible soil fabrics, the collapse potential of which should be a mandatory procedure. • The existence of discontinuous and rigid layers poses may be beneficial or detrimental to foundation performance. 12) The testing of pedocrete materials should be done so using in-situ methods to incorporate their extreme variability, stress and drainage conditions. 13) Also, sampling and disturbance of pedocrete soils has adverse effects on their soil properties and induces inaccuracies in the test results.

REFERENCES

Abou-matar, H., Goble, G.G., 1997. SPT Dynamic Analysis and Measurements. ASCE J. Geotech. Geoenvironmental Eng. 123, 921–928.

Adhikari, S., Bhattacharya, S., 2011. Vibrations of Wind Turbines Considering Soil-structure Interaction. Wind Struct. 14, 85–112.

Akin, M.K., Kramer, S.L., Topal, T., 2011. Empirical Correlations of Shear Wave Velocity and Penetration Resistance for Different Soils in an Earthquake-prone Area (Erbaa-Turkey). Eng. Geol. 119, 1–17.

Ambrosini, R.D., 2006. Material Damping vs. Radiation Damping in Soil-structure Interaction Analysis. Comput. Geotech. 33, 86–92.

Anbazhagan, P., Parihar, A., Rashmi, H.N., 2012. Review of Correlations Between SPT N and Shear Modulus: A New Correlation Applicable to Any Region. Soil Dyn. Earthq. Eng. 36, 52–69.

AWEA/ASCE, 2011. Recommended Practice for Compliance of Large Onshore Wind Turbine Support Structures.

Barkan, D.D., 1962. Dynamic Bases and Foundations. McGraw-Hill, New York.

Basu, B., 2010. Tower Design and Analysis, in: Tong, W. (Ed.), Wind Power Generation and Wind Turbine Design. WIT Press, Boston, pp. 527–557.

Beales, P., 2013. Report on Geotechnical Investigations for Richtersveld Wind Farm. Cape Town.

Beales, P., Paton, I., 2011. Klawer Wind Farm Geotechnical Report. Cape Town.

Bell, A.L., 2010. Geotechnical Grouting and Soil Mixing, in: Burland, J., Chapman, T., Skinner, H., Brown, M. (Eds.), ICE Manual of Geotechnical Engineering - Volume II - Geotechnical Design, Construction and Verification. ICE Publishing, London, pp. 1323–1340.

Bezgin, O., 2010. An Insight into the Theoretical Background of: Soil Structure Interactin Analysis of Deep Foundations. Istanbul.

Bolton Seed, H., Tokimatsu, K., Harder, L.F., Chung, R.M., 1986. Influence of SPT Procedures in Soil Liquefaction Resistance Evaluations. ASCE J. Geotech. Eng. 1425–1445.

Bonnett, D., 2005. Wind Turbine Foundations – Loading, Dynamics and Design. Struct. Eng. 3, 41–45.

Bowles, J.E., 1996. Foundation Analysis and Design, 5th ed. McGraw-Hill Companies, Inc., Peoria, Illinois.

Briaud, J., 2001. Introduction to Soil Moduli. Geotech. News.

Brinch Hansen, J., 1970. A Revised and Extended Formula for Bearing Capacity. Copenhagen.

Brink, A.B.A., Kantey, B.A., 1961. Collapsible Grain Structure in Residual Granite Soils in Southern Africa, in: 5th International Conference on Soil Mechanics and Foundation Engineering. Paris, France, pp. 611–614.

Brink, A.B.A., Schwartz, K., 1985. Aeolian Deposits, in: Engineering Geology of Southern Africa - Post Gondwana Deposits. Building Publications, Pretoria, pp. 174–184.

Brown, P.T., 1969. Numerical Analysis of Uniformly Loaded Circular Rafts on Elastic Layers of Finite Depth. Geotechnique 19, 301–306.

Burland, J., 2012. Settlement and Stress Distributions, in: Burland, J., Chapman, T., Skinner, H., Brown, M. (Eds.), ICE Manual of Geotechnical Engineering - Volume I - Geotechnical Engineering Principles, Problematic Soils and Site Investigation.

Institute of Civil Engineers Publishing, London, pp. 207–220.

Burland, J., Broms, B., de Mello, V., 1977. Behaviour of Foundations and Structures, in: Sixth European Conference of Soil Mechanics and Foundation Engineering. Vienna, pp. 495–545.

Burton, T., Sharpe, D., Jenkins, N., Bossanyi, E., 2008. Wind Energy Handbook, 1st ed. John Wiley & Sons, Chichester.

Butterfield, R., Gottardi, G., 1994. A Complete Three-dimensional Failure Envelope for Shallow Footings on Sand. Geotechnique 44, 181–184.

Butterfield, R., Gottardi, G., 1996. Simplified Failure-Load Envelopes for Shallow Foundation on Dense Sand. Int. J. Offshore Polar Eng. 6.

Butterfield, R., Ticof, J., 1979. Design Parameters for Granular Soils, in: 7th Int Conference on Soil Mechanics and Foundation Engineering. Brighton, pp. 259–261.

Byrne, B., 2011. Foundation Design for Offshore Wind Turbines, in: Géotechnique Lecture 2011. Géotechnique, London.

Byrne, B.W., 2000. Investigations of Suction Caissons in Dense Sand. Oxford University.

Byrne, B.W., Houlsby, G.T., 2003. Foundations for Offshore Wind Turbines. Philos. Trans. R. Soc. A (Mathematical, Phys. Eng. Sci. 361, 2909–30.

Chang, H.P.N., Heymann, G., 2005. Shear Wave Velocity of Gold Tailings. South African Inst. Civ. Eng. J. 47, 15–20.

Chin, F., 1971. Estimation of the Ultimate Load of Piles from Tests not Carried to Failure. University of Singapore.

Chopra, A.K., 1995. Dynamics of Structures - Theory and Applications to Earthquake Engineering. Pretence-Hall, Inc., New Jersey.

Chowdhury, I., Dasgupta, S.P., 2009. Dynamics of Structure and Foundation – A Unified Approach, 1st ed. Taylor & Francis, Chennai.

Clancy, P., 1993. Numerical Analysis of Piled Raft Foundations. University of Western Australia.

Clayton, C.R.I., 1999. Assessing the Stiffness of Soils and Weak Rocks, in: Wardle, G.R., Blight, G.E., Fourie, A.B. (Eds.), Geotechnics for Developing Africa. A. A. Balkema, Rotterdam, pp. 303–315.

Clayton, C.R.I., 2011. Stiffness at Small Strain: Research and Practice. Geotechnique 61, 5–37.

Clough, R.W., Penzien, J., 1995. Dynamics of Structures, 3rd ed. Computers & Structures, Inc., Berkeley.

Craig, R.F., 2004. Craig‘s Soil Mechanics, 7th ed. Spon Press, Dundee.

Craig, R.F., Knappett, J.A., 2012. Craig‘s Soil Mechanics, 8th ed. Spon Press, Abingdon.

Diaz-Rodriguez, J.A., Lopez-Molina, J.A., 2008. Strain Thresholds in Soil Dynamics, in: The 14th World Conference on Earthquake Engineering. Beijing, China.

DNV/Risø, 2002. Guidelines for Design of Wind Turbines, 2nd ed. Det Norske Veritas (DNV) & Risø National Laboratory, Copenhagen.

DNV/Risø, 2010. Design of Offshore Wind Turbine Structures. Det Norske Veritas (DNV) & Risø National Laboratory, Copenhagen.

Duguay, P.M., 2011. Wind Power to the People: Overcoming Legal, Policy and Social Barriers to Wind Energy Development in South Africa. J. World Energy Law Bus. 4, 1–31.

Earth Systems Southwest, 2008. P & H Foundations for Wind Turbine Support. 5586417.

Elhakim, A.F., 2005. Evaluation of Shallow Foundation Displacements using Small-strain Stiffness. Georgia Institute of Technology.

Fellenius, B.H., 1999. Bearing Capacity of Footings and Piles — A Delusion? Dearborn, Michigan.

Ferreira, C., Viana da Fonseca, A., Santos, J.A., 2006. Comparison of Simultaneous Bender Elements and Resonant Column Tests on Porto Residual Soil, in: Soil Stress-Strain Behaviour: Measurements, Modeling and Analysis Geotechnical Symposium. Roma.

Fizpatrick, B., 2009. Innovative Turbine Foundation Solutions. Davidson.

Fleming, W.G.K., Weltman, A.J., Randolph, M.F., Elson, W.K., 2009. Piling Engineering, Taylor & F. ed. Oxford.

Gazetas, G., 1983. Analysis of Machine Foundation Vibrations: State of the Art. Int. J. Soil Dyn. Earthq. Eng. 2, 2–42.

Gencturk, B., Attar, A., Tort, C., 2012. Optimal Design of Lattice Wind Turbine Towers, in: WCEE. Lisboa.

Gestamp, 2013. GRI Hybrid Towers [WWW Document]. URL http://www.gestamprenind.com/en/business/gestamp-hybrid-towers (accessed 4.16.13).

Göransson, F., Nordenmark, A., 2011. Fatigue Assessment of Concrete Foundations for Wind Power Plants.

Gorbuno-Passadov, M.I., Serebrajanyi, R. V., 1961. Design of Structures upon Elastic Foundations, in: 5th International Conference on Soil Mechanics and Foundation Engineering1. Paris, France, pp. 643–648.

Goudie, A., 1972. The Chemistry of World Calcrete Deposits. J. Geol. 80, 449–463.

Gunarantne, M., 2006. Foundation Engineering Handbook, 1st ed. Taylor & Francis, Tampa.

Haddad, A., Shafabakhsh, G., 2007. Non-invasive Continuous Surface Wave Measurements for In Situ Damping Ratio Profiling of Soils. Int. Jounral Civ. Eng. 5, 93–103.

Hall, J.R., 1967. Coupled Rocking and Sliding Oscillations of Rigid Circular Footings, in: International Symposium on Wave Propagation and Dynamic Properties of Earth Materials. Albuquerque, New Mexico.

Hardin, B.O., Drnevich, V.P., 1972. Shear Modulus and Damping in Soils: Measurement and Parameter Effects. J. Soil Mech. Found. Div. ASCE 98, 603–624.

Hardin, B.O., Drnevich, V.P., 1973. Shear Modulus and Damping in Soils - Design Equations and Curves. J. Soil Mech. Found. Eng. ASCE 98.

Hardin, B.O., Richart, F.E., 1963. Elastic Wave Velocities in Granular Media. J. Soil Mech. Found. Eng. ASCE 89.

Hartdegen, P., 2011. 88 Wind Farms for the Cape [WWW Document]. Prop. 24. URL http://www.property24.com/articles/88-wind-farms-for-the-cape/13668

Hassanzadeh, M., Thor, S., Stalin, T., Berglund, H., Sandros, D., Jokiranta, T., Lundstrom, R., Ronnholm, R., Bjoorck, A., 2012. Cracks in Onshore Wind Power Foundations - Causes and Consequences. Stockholm.

Hemami, A., 2011. Wind Turbine Technology, 1st ed. Cenage Learning, Montreal.

Hetenyi, M., 1946. Beams on Elastic Foundation, 1st ed. University of Michigan Press, Ann Arbor.

Hetenyi, M., 1950. A General Solution for the Bending of Beams on an Elastic Foundation of Arbitrary Continuity. J. Appl. Phys. 21, 55–58.

Heymann, G., 2007. Ground Stiffness Measurement by the Continuous Surface Wave Test. South African Inst. Civ. Eng. J. 49, 25–31.

Heymann, G., Clayton, C.R.I., 2001. Stiffness of Geomaterials at Very Small Strains. Geotechnique 51, 245–255.

Hoadley, P.J., 1984. Measurement of Dynamic Soil Properties, in: Moore, P.J. (Ed.), Analysis and Design of Foundations for Vibrations. A. A. Balkema, Rotterdam.

Horikoshi, K., Randolph, M.F., 1997. On the Definition of Raft-soil Stiffness Ratio for Rectangular Rafts. Geotechnique 47, 1055–1061.

International Electrotechnical Commision (IEC), 2005. IEC 61400-1 International Standard. Geneva.

Irvine, H.M., 1986. Structural Dynamics for the Practising Engineer, 1st ed. Allen & Unwin, London.

Ishibashi, I., Zhang, X., 1993. Unified Dynamic Shear Moduli and Damping Ratios of Sand and Clay. Soils Found. 33, 182–191.

Kameswara Rao, N.S. V., 2011. Foundation Design: Theory and Practice, 1st ed. John Wiley & Sons, Singapore.

Karg, C., 2008. Modelling of Strain Accumulation Due to Low Level Vibrations in Granular Soils. Ghent University, Ghent.

Karl, L., 2005. Dynamic Soil Properties Out of SCPT and Bender Element Tests with Emphasis on Material Damping. Ghent University.

Kassimali, A., 2005. Structural Analysis, 3rd ed. Thomson, Carbondale.

Lippus, C., 2007. Fundamentals of Seismic Refraction - Theory, Acquisition and Interpretation. San Jose.

Liu, H., 1991. Wind Engineering - A Handbook for Structural Engineers, 1st ed. Pretence-Hall Inc., Englewood Cliffs.

Luna, R., Jadi, H., 2000. Determination of Dynamic Soil Properties Using Geophysical Methods, in: Proceedings of the First International Conference on the Application of Geophysical and NDT Methodologies to Transportation Facilities and Infrastructure. St Louis, pp. 1–15.

Lysmer, J., 1965. Vertical Motion of Rigid Footings. University of Michigan.

Manwell, J.F., Elkinton, C.N., Rogers, A.L., McGowan, J.G., 2007. Review of Design Conditions Applicable to Offshore Wind Energy Systems in the United States. Renew. Sustain. Energy Rev. 11, 210–234.

Manwell, J.F., McGowan, J.G., Rogers, A.L., 2002. Wind Energy Explained, 1st ed. John Wiley & Sons, Chichester.

Maunu, P., 2008. Design of Wind Turbine Foundation Slabs. Lulea University.

Meyerhof, G.G., 1963. Some Recent Research on the Bearing Capacity of Foundations. Can. Geotech. J. 1, 16–26.

Mitchell, J.K., Soga, K., 2005. Fundamentals of Soil Behaviour, 3rd ed. John Wiley & Sons, New Jersey.

Morgan, K., Ntambakwa, E., 2008. Wind Turbine Foundation Behavior and Design Considerations, in: AWEA Windpower Conference. AWEA, Houston, pp. 1–14.

Netterberg, F., 1982. Geotechnical Properties and Behaviour of Calcretes in South and South West Africa, in: Demars, K.R., Chaney, R.C. (Eds.), Geotechnical Properties, Behaviour and Performance of Calcareous Soils - ASTM Special Publication No. 777. ASTM, Philadelphia, pp. 269–309.

Netterberg, F., 1985. Pedocretes, in: A., B.A.B. (Ed.), Engineering Geology of Southern Africa - Post Gondwana Deposits. Building Publications, Pretoria, pp. 286–312.

Netterberg, F., 1994. Engineering Geology of Pedocretes abd Other Residual Soils, in: Keynote Paper for the 7th IAEG Congress. Lisbon, Portugal.

Nguyen-Sy, L., 2005. The Theoretical Modelling of Circular Shallow Foundations for Offshore Wind Turbines. Oxford.

Novak, M., 1985. Experiments with Shallow and Deep foundations, in: Symposium on Vibration Problems in Geotechnical Engineering, ACSE Annual. Convention. ACSE New York, Detroit, pp. 1–26.

Novak, M., Beredugo, Y.O., 1971. Effect of Embedment on Footing Vibrations, in: Anual Conference on Earthquake Engineering. Con. Soc. Eq. Engg., Vancouver, pp. 111–125.

Obrzud, R.F., 2010. On the Use of the Hardening Soil Small-strain Model in Geotechnical Practice, in: Zimmermann, T., Truty, A., Podles, K. (Eds.), Numerics in Geotechnics and Structures. Elmpress International.

Parrock, A., 2013. Geotechnical Aspects of an Eastern Cape Wind Farm. South African Inst. Civ. Eng. Mag. 20–25.

Pequenino, F., van der Merwe, F., 2013. Some Practical Applications of CSW Testing in South Africa. South African Inst. Civ. Eng. Mag. 26–30.

Plaxis, 2011. Material Models Manual.

Poulos, H.G., Davis, E.H., 1974. Elastic Solutions for Soil and Rock Mechanics. John Wiley & Sons, New York.

Powrie, W., 2012. Bearing Capacity Theory, in: Burland, J., Chapman, T., Skinner, H., Brown, M. (Eds.), ICE Manual of Geotechnical Engineering - Volume I - Geotechnical Engineering Principles, Problematic Soils and Site Investigation. ICE Publishing, Southampton, pp. 227–230.

Priest, J., 2012. Dynamic and Seismic Loading of Soils, in: Burland, J., Chapman, T., Skinner, H., Brown, M. (Eds.), ICE Manual of Geotechnical Engineering - Volume I - Geotechnical Engineering Principles, Problematic Soils and Site Investigation. London, pp. 259–270.

Puri, V.K., Prakash, S., 2006. Foundations for Vibrating Machines. Struct. Eng. SERC, Madras.

Randolph, M.F., 1983. Design of Piled Raft Foundations, in: International Symposium on Recent Developments in Laboratory and Field Tests and Analysis of Geotechnical Problems. Bangkok, pp. 525–537.

Reese, L.C., van Impe, W.F., 2001. Single Piles and Pile Groups under Lateral Loading, 1st ed. A. A. Balkema, Leiden.

Rey, J.F., 2012. iCK Foundation - Analysis and Design. Madrid.

Reynolds, J.M., 2012. Geophysical Exploration and Remote Sensing, in: Burland, J., Chapman, T., Skinner, H., Brown, M. (Eds.), ICE Manual of Geotechnical Engineering - Volume I - Geotechnical Engineering Principles, Problematic Soils and Site Investigation2. London, pp. 601–618.

Richart, F.E., 1977. Field and Laboratory Measurements of Dynamic Soil Properties, in: Prange, B. (Ed.), Dynamical Methods in Soil and Rock Mechanics. A. A. Balkema, Karlsruhe.

Richart, F.E., Hall, J.R., Woods, R.D., 1970. Vibrations of Soils and Foundations, 1st ed. Pretence-Hall Inc., Englewood Cliffs.

Russell, C.S., 2012. Sampling and Laboratory Testing, in: Burland, J., Chapman, T., Skinner, H., Brown, M. (Eds.), ICE Manual of Geotechnical Engineering - Volume I - Geotechnical Engineering Principles, Problematic Soils and Site Investigation. ICE Publishing, London, pp. 667–686.

Ruukki, 2013. Tower for Wind Turbine [WWW Document]. URL http://www.archiexpo.com/prod/ruukki-uk-ltd/towers-for-wind-turbine-70187-889020.html (accessed 4.16.13).

Santos, J.A., Correia, A.G., 2000. Shear Modulus of Soils under Cyclic Loading at Small and Medium Strain Level, in: 12th World Conference on Earthquake Engineering. Auckland.

Schanz, T., Vermeer, P.A., Bonnier, P.G., 2000. The Hardening Soil Model: Formulation and Verification, in: Beyond 2000 in Computational Geotechnics. A. A. Balkema, Rotterdam.

Schmertmann, J.H., 1978. Use of the SPT to Measure Dynamic Soil Properties - Yes, But...! Dyamic Geotech. Testing, ASTM STP 654 Am. Soc. Test. Mater. 341–355.

Schmertmann, J.H., Palacios, A., 1980. Energy Dynamics of SPT. J. Geotech. Eng. Div. 105, 909–926.

Seed, H.B., Idriss, I.M., 1970. Soil Moduli and Damping Factor for Dynamic Response Analysis. Berkeley, USA: University of California.

Seimens, 2012. Wind Turbine Nacelle [WWW Document]. URL http://www.siemens.com/press/en/presspicture/?press=/en/presspicture/2009/renewable_energy/ere20050601.htm (accessed 4.17.13).

Stoddard, F.S., 1978. Structural Dynamics, Stability And Control of High Aspect Ratio Wind Turbines. Amherst.

Strahler, A.W., 2012. Bearing Capacity and Immediate Settlement of Shallow Foundations on Clay. Oregon State University.

Straughan, W.T., 1990. Analysis of Plates on Elastic Foundations. Texas Tech University.

Sutton, J.A., Snelling, K., 1998. Assessment of Grounf Improvement using the CSW Method, in: 4th Meeting of the Environment

and Engineering Geophysical Society. Barcelona, Spain.

Szewczuk, S., Prinsloo, E., 2010. Wind Atlas for South Africa (WASA): project overview and current status, in: Science Real and Relevant Conference. CSIR, Pretoria.

Thresher, R.W., Mirandy, L.P., Carne, T.G., Lobitz, D.W., James, G.H., 2009. Structural Dynamic Behaviour of Wind Turbines, in: Spera, D. (Ed.), Wind Turbine Technology: Fundamental Concepts in Wind Turbine Engineering. ASME, pp. 607–665.

Topolnicki, M., Soltys, G., 2012. Novel Application of Wet Deep Soil Mixing for Foundation of Modern Wind Turbines, in: 4th International Conference on Grouting and Deep Mixing. New Orleans.

Tricklebank, A.H., Halberstadt, P.H., Magee, B.J., Bromage, A., 2005. Concrete Towers for Onshore and Offshore Wind Farms, Foundations.

Van der Tempel, J., Molenaar, D.P., 2002. Wind Turbine Structural Dynamics – A Review of the Principles for Modern Power Generation , Onshore and Offshore. Wind Eng. 26, 211–220.

Vesic, A.S., 1961a. Bending of beams Resting on Isotropic Elastic Solid. Eng. Mech. Div. ASCE 87, 35–53.

Vesic, A.S., 1961b. Beams on Elastic Subgrade and the Winkler‘s Hypothesis, in: 5th International Conference on Soil Mechanics and Foundation Engineering. Paris, France, pp. 845–850.

Vesic, A.S., 1975. Bearing Capacity of Shallow Foundations, in: Winterkorn, H.F., Fang, H.Y. (Eds.), Foundation Engineering Handbook. Van Nostrand, New York, pp. 121–147.

Warrenski, 2010. Darling Wind Farm [WWW Document]. URL http://www.flickr.com/photos/warrenski/2529220364/ (accessed 4.17.13).

Whitney, S., 1999. Vibrations of Cantilever Beams: Deflection, Frequency, and Research Uses. Lincoln.

Wilkinson, J., 2008. Klipheuwel Wind Energy Facility [WWW Document]. URL http://www.flickr.com/photos/johnwilkie/3263501401/ (accessed 4.17.13).

Winkler, K., Nur, A., Galdwin, M., 1979. Friction and Seismic Attenuation on Rocks. Nature 227, 528–531.

Wolf, J., Song, C., 2002. Some Cornerstones of Dynamic Soil-structure Interaction 24, 13–28.

Woods, R.D., 1977. Parameters Affecting Elastic Properties, in: Prange, B. (Ed.), Dynamical Methods in Soil and Rock Mechanics. A. A. Balkema, Karlsruhe, pp. 37–61.

APPENDIX

1A Elements of vibration theory

Dynamic Parameter	Expression
Natural Frequency	$\omega_n = \sqrt{\frac{k}{m}}$
Critical Damping Coefficient	$c_{z,c} = 2\sqrt{km}$
Damped Natural Frequency	$\omega_d = \omega_n\sqrt{1-{\zeta_z}^2}$
Static Displacement	$z_s = \frac{Q_0}{k_z}$
Steady State Dynamic Displacement	$z(t) = A_z sin\,(\omega t - \theta)$
Amplitude of Vibration	$A_z = \frac{Q_0}{k_z}\frac{1}{\sqrt{(1-\beta^2)^2 + 2(\zeta_z\beta)^2}}$
Dynamic Magnification Factor	$D = \frac{A_z}{\frac{Q_0}{k_z}} = \frac{1}{\sqrt{(1-\beta^2)^2 + 2(\zeta_z\beta)^2}}$

Constant Force Excitation (Q_0)	**Rotating-mass Excitation ($Q_0 = m_e e\omega^2$)**
Amplitude at Frequency f	
$A_z = \frac{Q_0}{k_z}m$	$A_{z,r} = \frac{m_e e}{m}\left(\frac{f}{f_n}\right)$
Maximum Amplitude of Vibration	
$A_{z,max} = \frac{Q_0}{k_z}\cdot\frac{1}{2\zeta_z\sqrt{1-{\zeta_z}^2}}$	$A_{z,r,max} = \frac{m_e e}{m}\cdot\frac{1}{2\zeta_z\sqrt{1-{\zeta_z}^2}}$
Frequency of Maximum Amplitude	
$f_m = f_n\sqrt{1-2{\zeta_z}^2}$	$f_{m,r} = f_n\frac{1}{\sqrt{1-2{\zeta_z}^2}}$

2A **Spring constants for circular rigid footing resting on elastic half-space**

Mode of Vibration	Equivalent Stiffness
Vertical Translation	$k_z = \frac{4Gr}{1-\nu}$
Horizontal Translation	$k_x = \frac{32(1-\nu)Gr}{7-8\nu}$
Rocking	$k_\varphi = \frac{8Gr^3}{3(1-\nu)}$
Torsional	$k_\psi = \frac{16}{3}Gr^3$

3A **Equivalent damping ratios**

Mode of Vibration	Mass Ratio	Equivalent Damping Ratio
Vertical Translation	$\boldsymbol{B_z} = \frac{(1-\nu)}{4}\frac{m}{\rho r^3}$	$\zeta_z = \frac{0.425}{\sqrt{\boldsymbol{B_z}}}$
Horizontal Translation	$\boldsymbol{B_x} = \frac{(7-8\nu)}{32(1-\nu)}\frac{m}{\rho r^3}$	$\zeta_x = \frac{0.288}{\sqrt{\boldsymbol{B_x}}}$
Rocking	$\boldsymbol{B_\varphi} = \frac{3(1-\nu)}{8}\frac{I_\varphi}{\rho r^3}$	$\zeta_\varphi = \frac{0.15}{(1+\boldsymbol{B_\varphi})\sqrt{\boldsymbol{B_\varphi}}}$
Torsional	$\boldsymbol{B_\psi} = \frac{I_\psi}{\rho r^3}$	$\zeta_\psi = \frac{0.50}{1+2\boldsymbol{B_\psi}}$